UNIVERSITY
OF TASMANIA

Mixed anion lithium complexes - models for superbases

by

Bryce James Lockhart-Gillett, B. Sc. (Hons)

Submitted in fulfilment

of the requirements for the degree of

Doctor of Philosophy

School of Chemistry,

University of Tasmania

March 2011

This thesis contains no material which has been accepted for a degree or diploma by the University or any other institution, except by way of background information and duly acknowledged in the thesis, and to the best of my knowledge and belief no material previously published or written by another person except where due reference is made in the text of the thesis, nor does the thesis contain any material that infringes copyright.

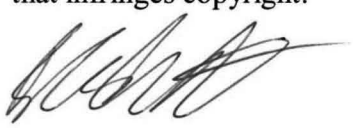

Bryce Lockhart-Gillett

March 2011

Bryce Lockhart-Gillett

March 2011

ABSTRACT

The work reported in this thesis describes the synthesis, characterisation, and reactivity of several mixed anion lithium complexes.

Chapter 2 is concerned with the design, synthesis, and characterisation of the mixed phenol/amine containing ligands, which serve as the backbone for mixed O/N anion lithium complexes also described. *N*-phenylsalicylaldamine, ($ONPhH_2$), *N*-2,6-diisopropylsalicylaldamine ($ONDIPPH_2$), and *N*-*t*-butylsalicylaldamine ($ONtBuPhH_2$), were prepared from their corresponding imine precursors, which were themselves prepared via imine condensation of the appropriate primary amines with salicylaldehyde. Solid state structures were obtained for the amine compounds, which display intermolecular H-bonding networks.

Chapter 2 also details the synthesis, and characterisation of mono- and some dilithiated complexes of the O/N ligands. The monolithiated complexes were observed to exclusively form tetrameric species. The two complexes $[\{Li(ONPhH)\}_4]$ and $[\{Li(ONDIPPH)\}_4]$ were prepared by lithiation of the corresponding amine ligands with *n*-BuLi in 40-60 °C petroleum spirits. The dilithiated complexes were observed to preferentially form dimers in the solid state. Two dimeric dilithiated complexes $[\{Li_2(ONPh)\}_2(THF)_6]$ and $[\{Li_2(ONDIPP)\}_2(THF)_4]$ were prepared by lithiation of the amine ligands with *n*-BuLi in THF. Several of the lithiated complexes underwent various solvent exchange reactions yielding related complexes; the THF solvated monolithiated tetrameric complex $[\{Li(ONPhH)\}_4(THF)_3]$ was obtained by exposing $[\{Li(ONPhH)\}_4]$ to THF, and the dilithiated complexes $[\{Li_2(ONPh)\}_2(TMEDA)_3]$,

$[\{Li_2(ONDIPP)\}_2(TMEDA)_2]$, $[\{Li(ONPh)\}_2(DME)_2(THF)_2]$, and $[\{Li_2(ONDIPP)\}_2(DME)_2]$ were prepared by exposing the dilithiated THF complexes to TMEDA and DME respectively. (TMEDA = *N,N,N',N'*-tetramethylethylenediamine, DME = 1,2-dimethoxyethane). A related tetrameric dilithiated complex $[\{Li_2(ONPh)\}_4(THF)_4]$ was obtained from $[\{Li_2(ONPh)\}_2(THF)_6]$ by heating in benzene.

Chapter 3 describes further solvent exchanged dilithiated complexes. The complexes $[\{Li_2(ONPh)\}_2(MeOCH_2CH_2O\textit{t}\text{-Bu})_2(THF)_2]$, $[\{Li_2(ONDIPP)\}_2(MeOCH_2CH_2O\textit{t}\text{-Bu})_2]$, and $([\{Li_2(ONDIPP)\}_2(dioxane)(THF)])_\infty$ were obtained by exposing the dilithiated THF complexes to $MeOCH_2CH_2O\textit{t}$-Bu and dioxane respectively. This chapter also describes the reactivity of some of the dilithiated complexes towards ether type substrates. Cleavage of both aliphatic and aromatic ether molecules was observed, with predictable stereospecificity correlated to the observed geometry of the dilithiated complex. From this reactivity a further monolithiated complex containing a modified *N*-methylated ligand was obtained $[\{Li(ON(Me)PhH)\}_4]$.

Chapter 4 reports the synthesis and characterisation of mixed amide/alkoxide ligands and their complexes. The ligands *N*-phenyl(2-trimethylsilylmethyl)benzyl amine ($NCPhH_2$) and *N*-2,6-diisopropylphenyl(2-trimethylsilylmethyl)benzyl amine ($NCDIPPH_2$) were prepared, and lithiated with *n*-BuLi to yield the monolithiated complexes $[(\{Li(NCPhH)\}_2(NCPhH))_2]$ and [(*N*-TMS 2,6-diisopropyllithiumamide)$(THF)_3$].

Chapter 5 is a compilation of some serendipitous compounds that were isolated from reactions described in Chapter 2 and Chapter 3. Each compound contains unexpected

and serendipitous inclusion of molecular fragments, either into the aggregated complex as in the complex [{Li(ON*t*Bu)}$_3$Li(OEt)(Et$_2$O)$_3$], or a portion of silicon grease incorporated into the dilithiated ligand backbone as in [{Li$_2$OODIPPSi$_2$}(DME)$_2$], [{Li$_2$(OODIPPSi)}$_2$(TMEDA)$_2$] and [K$_2${Li$_2$(OODIPPSi)}$_2${Li(ONDIPPH)}$_2${LiOSi(Me)$_2$O}$_2$(DME)$_4$]. The complex [{Li$_2$(OODIPPSi)}$_2${Li(OEt)}$_2$(Et$_2$O)$_2$] was also observed, which contains both a molecular fragment as well as a modified ligand.

Some theoretical work was undertaken to investigate the preference of the dimeric complexes in Chapter 2 towards particular core geometries observed in the solid state. In addition, a possible reaction pathway for the cleavage of DME was modelled in Chapter 3, and supports the observed stereospecificity of the reaction.

ACKNOWLEDGEMENTS

I would firstly like to thank my principle supervisor Dr Michael Gardiner for his tuition throughout my candidature. His guidance and encouragement has been essential to the completion of this work, and I am sincerely grateful for his assistance. I am also thankful for the assistance from my co-supervisor Prof. Brian Yates, whose support and guidance through the theoretical component of my project has been of great assistance.

Thankyou to Dr Craig Forsyth, Monash University, for X-ray crystallography services. Thanks also to Dr Noel Davies, Dr Thomas Rodemann and Dr James Horne, Central Science Laboratory, University of Tasmania for GC-MS studies, elemental analysis and NMR studies, respectively. Thanks are also extended to Dr Alireza Ariafard and Dr Nigel Brookes for their assistance with the computational investigations.

I would also like to thank my co-workers from the Gardiner group throughout my candidature, particularly Mr Adam James, Dr Damien Stringer, and Dr Sam Karpiniec whose friendship yielded many of the fond memories I will take away with me. Thanks are also extended to Mr Adam James for his assistance with X-ray crystallography studies.

The completion of this project would not have been possible without the support of my family and friends, and I am eternally grateful for their support and encouragement throughout my studies. I would like to extend particular thanks to the following people, in no particular order; Mum and Dad, Elizabeth Davies, Stephen Pinkus, Elysia Chase, Renee Kelly, Trina Collins, Kat Scott, Kara Martin, Grandma Pat, Zoe Gardam, and the Swing dancing community.

TABLE OF CONTENTS

ABBREVIATIONS

Å	Ångström, 10^{-10} meters
Anal.	elemental analysis
Ar	aromatic, aryl
bm	broad multiplet
br	broad
B3LYP	Becke 3-Parameter (Exchange), Lee, Yang and Parr
n-Bu	normal-butyl
t-Bu	tertiary-butyl
CIPE	Complex Induced Proximity Effect
DFT	Density Functional Theory
DIPP	2,6-diisopropylphenyl
DME	1,2-dimethoxyethane
DMF	dimethylformamide
Et	ethyl
Et_2O	diethyl ether
GC-MS	gas chromatography-mass spectrometry
gCOSY	gradient correlation spectroscopy
gHMBC	gradient heteronuclear multiple bond correlation
gHMQC	gradient heteronuclear multiple quantum correlation

gHSQC	gradient heteronuclear single quantum correlation
HRMS	high resolution mass spectrometry
IR	infra-red
L	ligand
m	multiplet
M	metal
$M^{+\cdot}$	molecular ion peak
Me	methyl
NMR	nuclear magnetic resonance
PMDETA	*N,N,N',N'',N''*-pentamethyldiethylenediamine
ppm	parts per million
pt	pseudo triplet
R	alkyl, aryl
s	singlet
t	triplet
TEEDA	*N,N,N',N'*-tetraethylethylenediamine
THF	tetrahydrofuran
TMEDA	*N,N,N',N'*-tetramethylethylenediamine
TMS	trimethylsilyl
δ	chemical shift (ppm)
ν	frequency

Chapter 1

Introduction

1.1. Organolithium chemistry

Organolithium reagents are today perhaps some of the most widely recognised and utilised organometallic compounds in the field of synthetic chemistry.[1-3] They have become established as standard reagents in both organic and organometallic laboratories. Organolithium compounds are a specific subset of a larger class of compounds, the organoalkali metal compounds. The discovery of organoalkali metal compounds came somewhat later than other corresponding main group organometallic compounds. In 1849 Edward Franklin discovered dimethylzinc as the first main group organometallic compound, [4] but it wasn't until 1914 that the pioneering work of William Schlenk yielded the first organoalkali metal compounds.[5] For a recent review on the development of the synthetic methods for their preparation, see Seyferth.[6, 7]

The chemistry of organolithium compounds is governed by the same distinguishing feature of all organometallic compounds; a metal-organic bond with the metal being more electropositive than the organic bonding partner. Thus, the organic fragment displays anionic characteristics and is nucleophilic. In the heavier organoalkali metal compounds, the metal is so electropositive that the metal-organic bond is considered essentially ionic. In contrast, organolithium compounds retain a degree of covalency in their metal-organic bond.[8]

The reactivity of organolithium compounds can be exploited in a number of ways; the metathesis, or salt elimination reaction, allows for the preparation of

organometallic compounds of less electropositive metals, as illustrated in Equation 1-1.

LiR + MX → MR + LiX

(where M is a less electropositive metal, and X is often a halide).

Equation 1-1

The most common use of organolithium reagents, however, is in the Schorigin reaction;[9] commonly referred to now as a 'metallation reaction'. As shown in Equation 1-2, organolithium complexes, and in particular alkyllithium complexes, are strong enough bases to render the protons of many organic compounds 'acidic' enough to undergo a metal-hydrogen exchange with them, including ones that lack any functionalisation.

R-H + LiR' → R-Li + H-R'

Equation 1-2

In reality this metallation is an equilibrium process, however if the difference in acidities between the two conjugate acids is greater that *ca.* 10 pH units the reaction is essentially quantitative. For *n*-BuLi this means that it has a limiting pK_a of ~35 for effective reactivity. The metallation reaction is of central importance to synthetic chemistry because it allows for the formation of a new functional group at the site of metallation simply by 'quenching' the organolithium with a nucleophilic substrate, as shown in Equation 1-3.

R-Li + R'-X → R-R' + LiX

(where X is often a halide).

Equation 1-3

It is evident that alkyllithium compounds are some of the strongest organolithium reagents in terms of the metallation reaction, as their corresponding alkane conjugate acids are amongst the weakest. Because of this, they are widely utilised in synthetic

chemistry and several of the simple alkyllithiums are commercially available; e.g., *n*-BuLi is available in a variety of aliphatic solvents in concentrations up to 10 M. MeLi, *sec*-BuLi, and *t*-BuLi are also widely available. In addition to these alkyllithium reagents, a variety of other organolithium compounds have become utilised synthetically such as amide derivatives including lithium diisopropylamide (LDA), lithium bis(trimethylsilyl)amide and lithium diethylamide, and consequently these are also available commercially.[2] While being weaker bases, these amide derivatives offer alternative advantages such as being non-nucleophilic if sufficiently bulky and able to undergo proton abstractions with high regio- and stereoselectivity.[10]

The intrinsic reactivity of alkyllithium reagents in the metallation reaction was observed to be markedly increased with the use of Lewis basic donor solvents, and more recently by using auxiliary coordinating ligands such as *N,N,N',N'',N''*-pentamethyldiethylenediamine (TMEDA).[11-13] This modulation of the intrinsic properties of alkyllithium reagents by incorporation of Lewis bases such as TMEDA is now understood in terms of the deaggregation effect they have, which is discussed further in the following section. Lewes bases are routinely used to enhance or modify the behaviour of alkyllithiums to influence the regioselectivity of metallation reactions.[1, 14, 15] The increased reactivity afforded by incorporation of Lewis bases helped to further expand the synthetic applicability of organolithium compounds, yet for a long time there was minimal understanding of the structure and bonding of many of these compounds. This lack of understanding is to an extent still overlooked, perhaps in part because of the way in which organolithium reagents are typically used synthetically; that is without isolation of the reactive organolithium intermediate and described to a sufficient degree in terms of a simple carbanion transfer.[16] However, where it has been possible to establish the structure property

relationship between the organolithium compounds and the complexes they form with their substrates, much progress has been made towards achieving targeted metallation reactions of organic substrates. Wheatley provides a relatively recent example of a review of directed lithiation reactions, focusing on the mechanism by which the organolithium complex that is formed in the reaction with the substrate molecule governs the outcome of the reaction.[17] It is now well established that the effect of aggregation of the reagent on the synthetic outcome of metallation reactions is of the upmost importance and has been extensively demonstrated.[18] Much new chemistry has resulted from the increased understanding of the way organolithium reagents interact with their substrate molecules. Included are highly specific, unique selectivities that are unlikely to have ever been developed without the systematic knowledge that has been generated through detailed structural studies of organolithium complexes. The best understood systems are still, however, those based on simple organolithium lithium reagents, and much more remains to be investigated in systems that are more complex.

An illustrative example of the influence of the structure of organolithium compounds on their corresponding reactivity is the metallation of toluene with *n*-BuLi. If toluene is reacted with *n*-BuLi in hexane, no reaction occurs. If however, the reaction is repeated with equimolar amounts of *n*-BuLi and TMEDA, toluene is metallated as expected,[19] and benzyl lithium is produced as shown in Figure 1-1.

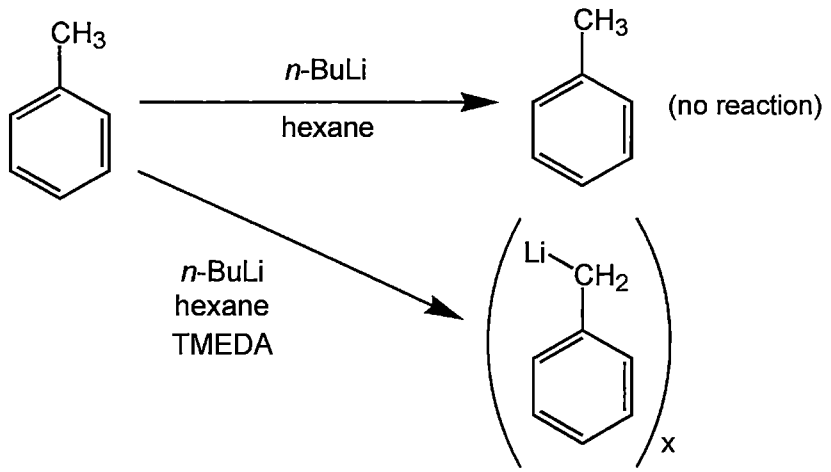

Figure 1-1: Reactivity of toluene towards metallation with *n*-BuLi with and without TMEDA.

If the *n*-BuLi is regarded as simply a carbanion transfer agent, this alteration of the reaction outcome by the addition of TMEDA, which itself is only a mild, non-reactive Brønsted-Lowry base, cannot be rationalised. Results such as this helped prompt researchers to seek out a better understanding of the fundamental processes occurring when organolithium compounds interact with organic substrates, and indeed the processes occurring within solutions of the organolithium reagents with and without Lewis basic additives. This work was aided greatly in the 1960's with the first solid state X-ray crystal structure determination an organolithium compound, $[(EtLi)_4]$.[20] This allowed researchers to glimpse the discrete chemical nature of these compounds, and in some cases their complexes with substrate molecules.[11] Furthermore, they could begin to formulate the structure property principles by which they could rationalise the observed changes in behaviours of organolithium compounds.[18] Upon these, they could base their predictions for new reactions and wider applications. These structure property relationships are of central importance to the continuing development of organolithium compounds as synthetic tools for chemical research. Whilst the focus of this thesis is on the structural rationalisation of organolithium complexes, it is worth making mention of some of

the synthetic uses to which these and related organometallic bases have been put. Naphthalene and the biphenyl dianion have been used to selectively metalate poly haloalkynes,[21] as well as carbolithiate terminal and strained internal alkenes.[22] In the area of arene synthetic manipulations, Rummel reports on the accelerated alkylation of naphthalene and toluene,[23] and Schlosser has written an extensive review titled "regiochemically exhaustive functionalisation" which incorporates various methodologies and organometallic reagents.[24] An important class of organolithium reagents utilised for synthetic chemistry are chiral amidolithiums. Their uses include, but are certainly not limited to asymmetric deprotonation of chiral epoxides and unsaturated ketones, as well as prepare chiral organometallic reagents. They have also been used for chiral epoxide opening and can undergo Michael type reactions.[15, 25-34] There has also been significant development in the area of regiochemical control of pyridine functionalisation. Investigations into *n*-BuLi/lithium aminoalkoxide aggregates by Fort have helped develop new powerful reagents for selective functionalisation of pyridines.[35-40]

1.2. Structure and bonding of alkyllithium complexes

Organolithium complexes display a huge array of bonding modes in the solid state.[41] The work presented in this thesis is primarily concerned with the aggregation of alkyl-, alkoxido- and amidolithium compounds, which have been shown to be largely governed by the concepts of ring stacking and laddering established by Mulvey and Snaith.[2, 3]

It is common to depict alkyllithium reagents as discrete monomeric molecular entities for simplicity. Simple monomeric alkyllithium complexes are, however,

under coordinated. Due to this, as well as the fact that they are hard Lewis acids, they have strong tendencies to aggregate to increase the number of Lewis basic interactions. Several of the simple alkyllithium complexes have been structurally characterised in the solid state and the arrangement of the ions within the aggregated complex were discovered to follow commonly occurring trends in how they were arranged. Many of the alkyllithium compounds aggregate with cores that display an aggregation mode that has been called 'stacking'.[42] The two most common stacking modes are the tetramer, as shown in Figure 1-2a, and the hexamer, as shown in Figure 1-2b. In both of these cases the alkyl anions cap three lithium centres in electron deficient two electron - four centre bonding arrangements.

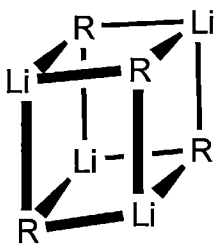

Figure 1-2a: Structure of a tetrameric lithium alkyl aggregate.

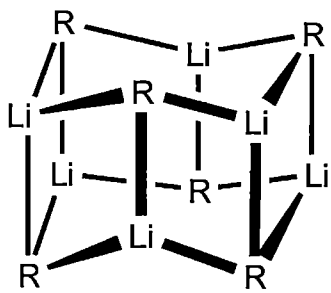

Figure 1-2b: Structure of a hexameric lithium alkyl aggregate.

Aggregation of simple alkyllithium complexes is still observed in solution, and dynamic processes are common.[43-45] Aggregates of different sizes are observed for many systems. In these aggregates the lithium atoms are still relatively exposed and readily accommodate further Lewis basic interactions. These Lewis basic interactions can either be in the form of solvation by a Lewis basic solvent, or they can arise from coordination of a Lewis basic donor group contained within the organic fragment. Further self-aggregation of alkyllithiums is prevented from occurring in the case of the tetrameric and hexameric arrangements by the fact that incorporation of a further alkyl group would require a further lithium atom also to

maintain a balanced charge on the aggregate. Thus, the self-aggregation process is limited to these oligomers, as the additional lithium centre cannot effectively satisfy its coordination sphere in turn. For a recent review on the structure and reactivity of alkyllithium compounds see Strohmann *et al.*[1]

As noted in the previous section, Lewis bases have been intimately involved in the development of alkyllithium compounds as synthetic reagents. In the presence of Lewis bases the tetrameric and hexameric aggregates will often tend to break up into smaller units. This is due to the competitive complexation of the lithium atoms via electron precise (two electron – two centre) interactions with the typically hard Lewis basic donor atoms (N, O, etc.) of the solvent which out competes the electron deficient interactions of the μ_3-bridging carbon centred alkyl anions. The resulting aggregation type adopted upon the addition of a Lewis base to an alkyllithium system is difficult to predict, but are usually able to be rationalised once known and tend to exhibit recurring trends. The degree of dissociation of the Lewis base solvated aggregates can vary from one extreme to the other; the addition of TMEDA to a solution of MeLi results in the TMEDA adduct leaving the $[(MeLi)_4]$ unit unchanged,[46] forming $[((MeLi)_4(TMEDA)_2)_\infty]$, **I** as shown in Figure 1-3a. Where as a monomeric species is observed for the *N,N,N',N'',N''* pentamethyldiethylenediamine (PMDETA) containing complex $[\{(Me_3Si)_2HC\}Li(PMDETA)]$,[47] **II** as shown in Figure 1-3b.

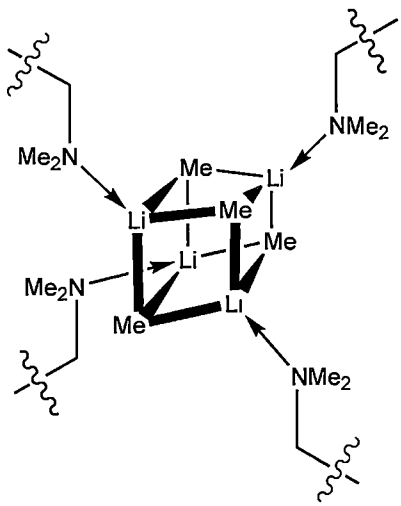

(I)

Figure 1-3a: Tetrameric MeLi solvated by TMEDA.

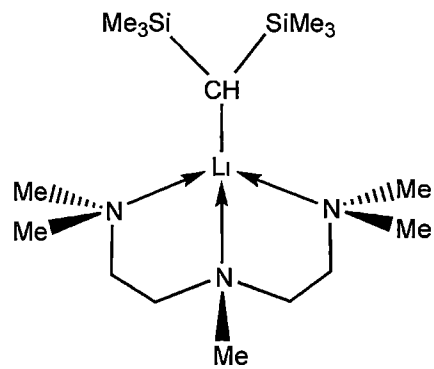

(II)

Figure 1-3b: Monomeric organolithium complex solvated by PMDETA.

1.3. Amidolithium chemistry

While alkyllithium compounds are the subset of the organolithium compounds characterised by a C-Li bond, the amidolithium compounds are distinguished by an N-Li bond and formally, amidolithium chemistry is a subclass of these inorganic compounds. Despite this formal distinction between these two classes of compound, there are many overlapping characteristics and amidolithium chemistry is hence generally accepted as part of organometallic chemistry and will be described within this thesis under the term organolithium compound.[2]

Amidolithium chemistry significantly predates alkyllithium chemistry. Amidolithium compounds were in fact the first amido-metal compounds to be discovered. In 1809 amidosodium and amidopotassium, MNH_2, M = Na and K, respectively, were prepared by reaction of the alkali metal with ammonia gas at elevated temperatures.[48] As happened within organometallic chemistry, it wasn't until much later that the corresponding amidolithium compound was prepared in 1894.[49]

Amidolithium compounds are used synthetically today in a similar fashion to alkyllithium compounds as strong Brønsted-Lowry bases. In particular, bulky amidolithium reagents such as LDA and lithium 2,2,6,6-tetramethylpiperidide are very poor nucleophiles and are able to remove relatively non-acidic organic protons without undergoing further reaction.[2, 50] Amidolithium compounds are able to be prepared via a variety of ways, however the bulkier dialkylamido- and disilylamido-complexes tend to be prepared via metallation reactions of the parent secondary amine with an alkyl lithium reagent as shown in Equation 1-4.

$$R_2NH + LiR' \rightarrow R_2NLi + HR'$$

Equation 1-4

As for alkyllithium compounds, amidolithium compounds display a huge variety of bonding modes.[51] Many of the 'simple' amidolithium complexes have been characterised in the solid state as a result of the ongoing effort by the groups of Mulvey, Snaith, Schleyer, and others. This has allowed the establishment of the ground rules for their aggregation. As mentioned in the previous section, the work presented in this thesis is primarily concerned with the concepts of ring stacking and laddering established by Mulvey and Snaith.[2, 3]

Like alkyllithium compounds, amidolithium compounds have a tendency to aggregate to increase the total number of Lewis basic interactions. In the case where the nitrogen centre is sp^3 hybridised, there is a lone pair available to participate in further Lewis base interactions through electron precise bridging. Where this occurs the distinction between the original metal-amido interaction and the subsequent Lewis basic interaction is lost. This process is illustrated in Figure 1-4.

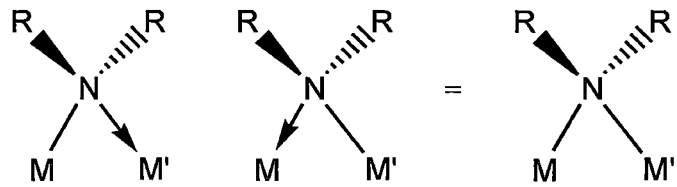

Figure 1-4: Symmetrical binding of an amide bridging two metal centres.

As well as having a lone pair, amidolithium compounds differ from alkyllithium compounds in their geometric arrangement of their substituents, which affects the way that they undergo ring aggregation. While alkyllithiums are able to stack, amidolithiums are prevented from stacking by the fixed projection of their substituents above and below the plane of the Li_2N_2 ring formed upon dimerisation, as shown in Figure 1-5.

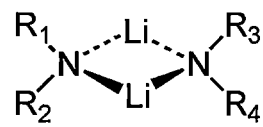

Figure 1-5: Amidolithium Li_2N_2 ring formation upon dimerisation.

Amidolithiums consequently tend to aggregate in a 'laddering' fashion with rings joining edge-to-edge. This tendency makes amidolithium compounds the exception amongst the majority of organolithiums. The difference between ring stacking and ring laddering is illustrated in Figure 1-6. The concept of ring aggregation is discussed in detail for amidolithiums, as well as many other possible lithiated systems in the reviews by Mulvey and Snaith.[2, 3]

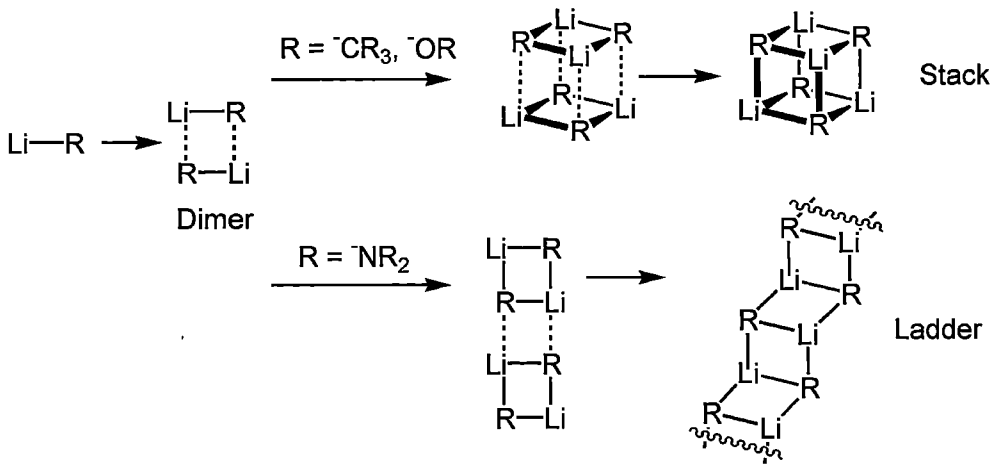

Figure 1-6: Aggregation trends of organolithium fragments, showing face-to-face association of rings for alkyl and alkoxide anions, and edge-to-edge association for amide anions.

It is evident that due to the difference in how the dimeric rings of lithium amides aggregate, that they are not limited to tetrameric and hexameric structures, as the laddering can in principle continue indefinitely. It was long suspected that many amidolithium systems contained these infinite polymeric ladders, but it was some time before they were confirmed crystallographically. The first polymeric lithium amide structure to be reported was for the important reagent LDA in 1991.[50] It adopts a helical structure rather than laddered dimeric rings, as shown in Figure 1-7 .

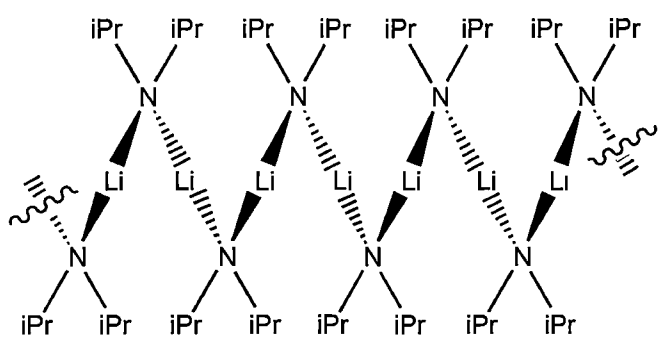

(III)

Figure 1-7: Helical polymeric structure of LDA in the solid state.

Though a 'pure' (solvent free) infinite amide ladder remains elusive, there have been a number infinite polymeric amide ladders, characterised.[52-55] There have also been a handful of successfully characterised ladder fragments; the preparation of lithium pyrrolide in the presence of TMEDA and PMDETA results in the isolation of two

such ladder fragment complexes $[\{LiN(CH_2)_4\}_4(TMEDA)_2]$, **IV** and $[\{LiN(CH_2)_4\}_6(PMDETA)_2]$, **V**.[56, 57] Their structures are illustrated in Figure 1-8. Preparation of lithium piperidide using limited *n*-BuLi (2:1 piperidine:*n*-BuLi) results in a similar ladder fragment complex $[\{Li[N(CH_2)_5](HN(CH_2)_5)\}_4]$ **VI**.[58] This time, however, the terminal lithium centres are solvated by the neutral piperidine remaining in the reaction mixture. The structure of **VI** is shown in Figure 1-9.

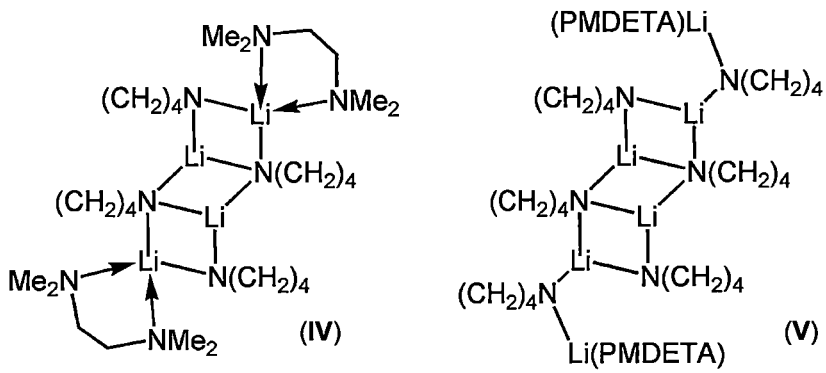

Figure 1-8: Short amidolithium ladder-segment complexes of lithium pyrrolide.

The core of the ladder fragments **IV**, **V** and **VI** are essentially flat and are only distorted at the terminal lithium centres due to the influence of the Lewis basic solvents. As discussed in the previous section, the influence of Lewis basic solvents on the aggregated structure of organolithium complexes is often to break up larger aggregates in to smaller units. In the case of amidolithium complexes, the Lewis basic ligands act to break up the unsolvated infinite lithium amide ladder complex into the smaller fragments shown here.

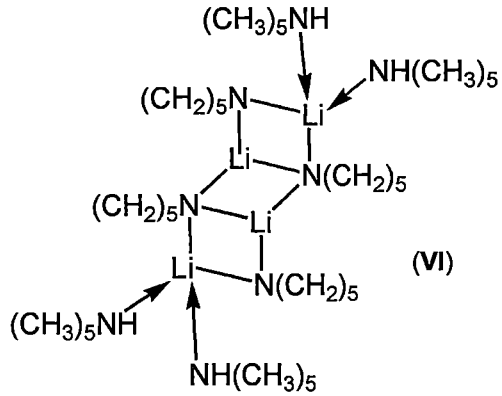

Figure 1-9: Short amidolithium ladder-segment complex of lithium piperidide.

In some cases, the unsolvated structure of the lithium amide is not infinite. In the case where the Li_2N_2 rings fuse together in a non-planar way the junctions can be either cisoid or transoid. In the structure of $[\{t\text{BuN(H)Li}\}_8]$[55], **VII** these junctions are exclusively cisoid, resulting in a cyclic octameric ladder complex. The structure of **VII** is shown in Figure 1-10.

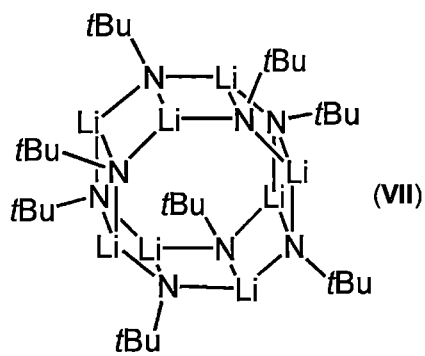

Figure 1-10: Cyclic unsolvated amidolithium ladder complex.

The concept of ring stacking and laddering has now been extended to organic chemistry, in particular in the area of secondary ammonium halides. Two papers by Bond provide a good coverage of how the developments of structural analysis of amidolithium and alkyllithium compounds has helped allow a similar rationalisation of the structural motifs observed in this area.[59, 60]

1.4. 'Superbase' systems

The term superbase has been used to refer to a variety of different systems. The earliest reports of the term appeared in 1975.[61, 62] What are now referred to as 'classical' superbases are associated with Lochmann and Schlosser and are a mixture of an alkyllithium reagent and a heavier alkali metal alkoxide ('LiCKOR' reagents as they are sometimes called). These were the focus of the Lochmann's extensive investigations and were determined to be the strongest systems with regard to deprotonation ability. It is now accepted, however, that any mixture of bases that interact in a synergistic way to yield a mixture that exhibits properties different to either base in isolation can be referred to as a 'superbase' system.[63] Caubere makes it abundantly clear in his review article that the generalised concept of a 'superbase' reagent is widely applicable and, furthermore, has impact extending far beyond merely proton abstraction as the term 'base' implies. This is true for the more reactive, and more extensively studied heteroalkali metal super bases, but also true for the more synthetically manageable homometallic lithium superbases.

Of particular interest to the work presented in this thesis are the 'superbase' systems that have mixed alkali metals and/or mixed anions. In the literature there are multiple claims made of the origins of hetero-alkali metal chemistry; Wittig's report of 'diphenyllithium sodium' in 1955[64] is reported as the beginning of hetero-alkali metal chemistry.[65] However, while this work was undoubtedly a significant development, the first account of hetero-alkali metal chemistry was reported by Morton nearly a decade earlier.[66] Morton was working on using alkysodium reagents as initiators for polymerisation reactions and discovered that the addition of isopropyl alcohol to the existing *n*-amylsodium based initiating mixture yielded a very potent polymerisation initiator.[66] From this observation he further noted that

the addition of either sodium or potassium alkoxide to a suspension of *n*-amylsodium in alkane medium increased the rate and yield of the metallation reaction.[67]

Perhaps because it was observed for sodium, rather than lithium, the work of Morton was overlooked by the three groups that rediscovered the alkoxide effect in alkyllithium chemistry 20 years later. Wofford and Schlosser were also working on polymerisation initiation, and discovered that the addition of one molar equivalent of potassium or sodium alkoxide to alkyllithium reagents had the effect of 'activating' the alkyllithium.[7]

Much of the work carried out by Lochmann's group focussed specifically on determining the composition of the mixture arising from the individual components comprising a 'superbase' when they combined together to form the active species. This resulted in many failed attempts to isolate a species from the reaction mixture that was not simply the product of a metal exchange reaction, as shown in Equation 1-5.

$$R_1Li + R_2OM \rightarrow R_1M + R_2OLi$$

(M = Na, K, Rb, Cs)

Equation 1-5

In general, the products from the reaction between an organolithium reagent and a heavier alkali metal alkoxide have been found to be the result of a metal exchange reaction.[68] This process, as well as the tendency for autoaggregation of the constituent reagents, greatly limited the ability to gain mechanistic understanding of the reactions between organolithium reagents and the substrates. Although these early results yielded little about the active species involved, they were important in the development of the synthesis of heavier alkali metal compounds and led to

improved methods of preparation of many organosodium and organopotassium compounds.[7, 69-71]

More success was had in determining the aggregation behaviour of these mixtures via solution studies. Using thermometric titration and infrared spectroscopy Lochmann determined that a 1:1 complex was formed between *t*-BuOLi and *n*-BuLi, *t*-BuLi, and *i*-PrLi.[72] The mixture of *n*-BuLi and *t*-BuOLi was shown the following year to be a tetramer in benzene solution.[73] It was over a decade until this was confirmed crystallographically. The structure of $[(n\text{-BuLi})_2(t\text{-BuOLi})_4(n\text{-BuLi})_2]$, **VIII** is shown in Figure 1-11.[74]

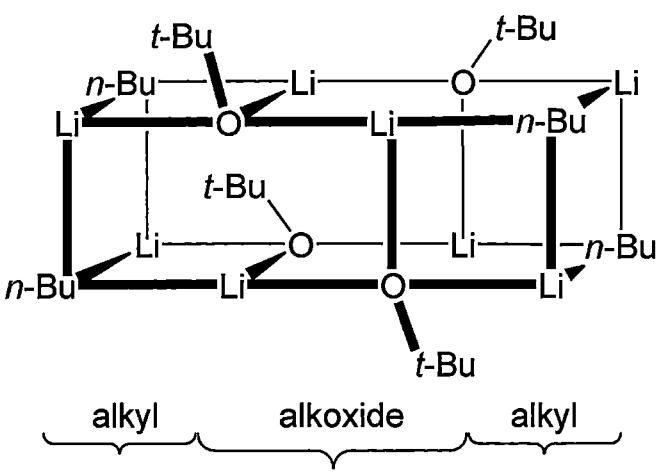

(VIII)

Figure 1-11: Solid state structure of $[(n\text{-BuLi})_2(t\text{-BuOLi})_4(n\text{-BuLi})_2]$, **VIII** showing segregation of anion types.

The structure of **VIII** illustrates the ring stacking principle that is characteristic of both the anion types comprising it. The structure can be described as a partially opened tri-cube stack, with the opening of the stack occurring at each of the sites of the *t*-butoxide anion incorporation. It is noteworthy that whilst both anions are involved in this structure there is a segregation of the different anion centre types. The *t*-butoxide anions form the inner pseudo cube of the structure. Whereas the

n-butyl anions form the outermost faces of the cube stack, adopting geometries very similar to that observed for tetrameric *n*-BuLi itself.

Another rare example of a solid state structure of a mixed anion species is from Snaith's group, shown in Figure 1-12.[75] This compound was prepared serendipitously when diphenylamine was treated with a large excess of *n*-BuLi. Remarkably, the unexpected product **IX** was able to be isolated. The complex comprises a mixture of the expected metallated amine (Ph_2NLi) and *n*-BuLi, as well as a dimetallated amine of the type Ph(*o*-C_6H_4Li)NLi. This dimetallated amine has arisen from a second lithiation occurring in the *ortho*-position of one of the phenyl substituents on the parent lithium amide. In hindsight, this reaction was able to be carried out using the correct stoichiometry and resulted in an improved yield of approximately 75 %.

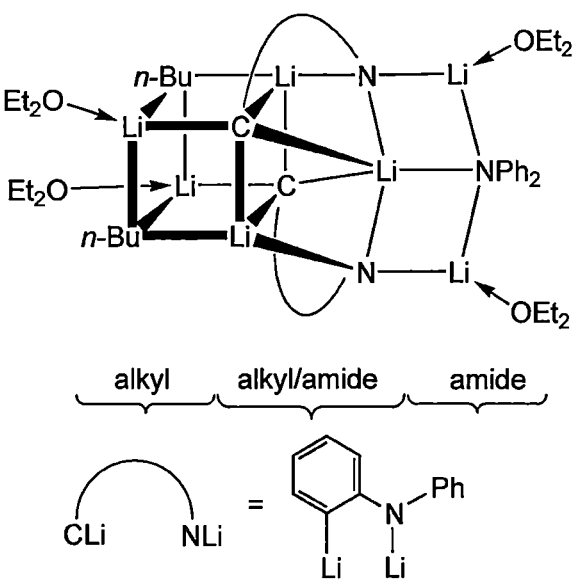

(IX)

Figure 1-12: Mixed alkyl/amide aggregated lithium complex illustrating segregation of anion types.

The structure of **IX** again illustrates the tendency for particular anion types to adopt certain aggregated arrangements. The structure is comprised of three sections,

corresponding to the nature of the anions involved within them. The left hand side of the structure is similar to that observed in **VIII**; a pseudo cube arrangement of two *n*-BuLi units attached on the interior of the molecule to the carbon atoms from the dilithiated amide units. The right hand side displays ring laddering with a single amide unit forming the exterior of the middle rung of the ladder. The middle section is comprised of two dilithiated amide units with the carbon anions forming the inner portion of the cube motif and the nitrogen anions forming the interior ends of the top and bottom rungs of the ladder portion.

This remarkable compound provides a rare glimpse of the type of structures that may occur in many multilithiation reactions as well as the mixed anion aggregation that occurs during all lithiations. It is particularly remarkable also as it displays incorporation of different aggregation tendencies within the one molecule; ring stacking in the left hand portion and ring laddering in the right hand portion. Though a mixture of anion types are incorporated in complex **IX**, it is evident that the anions have tended to homoaggregate, and remain segregated as indicated in Figure 1-12. This observation is significant because although heteroaggregation is accepted to be a general phenomenon occurring during lithiation reactions, there are comparatively few structurally authenticated complexes incorporating a mixture of anions, and most of these reported structures are not part of a systematically varying investigation. Thus, it remains that the possible alterations to the chemical properties of the aggregated anions are poorly understood.

The preceding two examples represent the area of homometallic heteroanion mixed organoalkali chemistry. Equally valuable have been the developments in the area of heterobimetallic organoalkali containing systems. Rummel has recently reported on the synergistic acceleration of alkylation of aromatic substrates with ethene using

mixtures of alkali metals.[23] In the area of amidoalkali metal complexes, in particular, several structurally characterised compounds have been reported that include a mixture of alkali metals. [55, 76-79] These complexes have structures that mirror the structural trends identified in the homolithium complexes, with particular variances in some circumstances. These complexes represent a significant achievement in the investigation of organoalkali compounds, as the most potent and selective reagents fall into this category. An understanding of the relationship between structure and property is essential to developing new systems with specific selectivities for organic synthesis.

A more recent advance in the field of 'superbase' chemistry comes from the area of 'ate' chemistry. Following on from the work of Kondo and Uchiyama investigating new organozincates,[80-82] this area of heterobimetallic systems offers some remarkable new synthetic possibilities.[83, 84] These systems take advantage of the alteration of the effect of metallating reagents not solely towards their strength, but also to their selectivity. A remarkable example of this is the selective deprotonation of toluene in the meta position reported by Mulvey's group. Deprotonation in the meta position is in direct contrast to the observed behaviour of toluene towards *n*-BuLi as discussed in Section 1.1. Mulvey's group were able to isolate and characterise the resulting heterobimetallic complex **X** which is shown in Figure 1-13.[85]

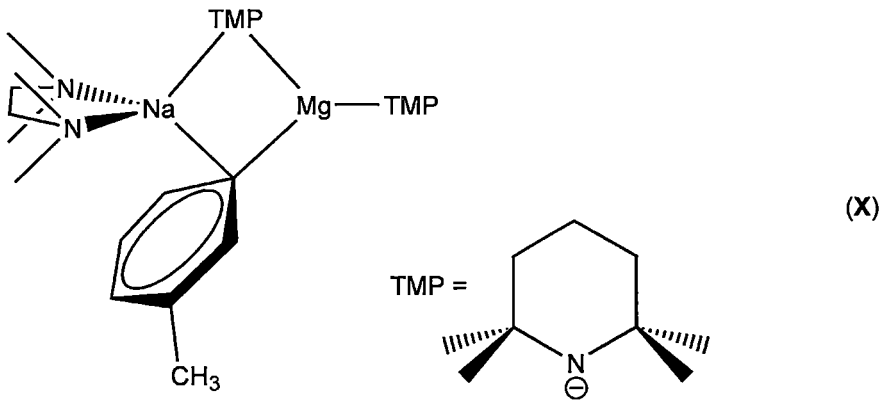

(X)

Figure 1-13: Mixed sodium-magnesium complex achieving selective metallation of toluene at the *meta* position.

This metallation outcome and some other remarkable results have been achieved using these new mixed metal systems.[85-87] Frequently, these new results indicate enhanced selectivities rather than increased 'strength'. Consequently, there is now a move away from the all alkali metal systems into systems incorporating magnesium and zinc, as noted above, and most recently incorporating new metals such as copper and cadmium to achieve novel selectivities for organic transformations.[88-90] These new systems have been dubbed 'alkali metal mediated' metallation reagents,[91, 92] as it is frequently the less electropositive metal that is found to metalate the organic substrate. The alkali metal component is in some way modulating the properties of these normally mild metal reagents. A recent review on 'alkali metal mediated metallation' has been published by Mulvey.[93] These developments demonstrate resoundingly that much can be achieved (more than is conventionally believed) when synergistic behaviour can be harnessed.

1.5. General research aim

Organolithium reagents are key reagents in synthetic chemistry. Despite a predominant lack of understanding of the structure and bonding in many

organolithium systems they are extensively utilised.[94] Described in this chapter in particular are the areas of organolithium chemistry encompassing mixed metal systems, as well as homometallic mixed-anion systems and how they offer exciting potential as new synthetic tools. It has been established that the phenomenon of mixed anion aggregates forming in solution is widely applicable.[3, 41, 63, 95] and implicit to both the areas of mixed metal systems and homometallic mixed-anion systems is the concept of alteration of chemical behaviour due to aggregation of multiple anion types. As put by Mulvey,[65] "Placing Na^+ near Li^+ could open the way to realising new structures/unconventional coordination modes in organolithium compounds, which, in turn, could have a profound effect on the reactivity and selectivity of organolithium reagents."

Although much has been learnt about the structural chemistry of organolithium compounds as pure reagents, much remains to understand regarding their behaviour throughout the process of a reaction. It is important to note that during the course of any metallation reaction there must exist a mixture of the reagent and the metallated product. These mixtures may themselves form mixed anion species that have behaviour different to that expected of the reagent itself.

The intended aim of the work presented in this thesis was to undertake a systematic investigation into the synthesis and characterisation of some closely related mixed anion lithium complexes. The intention was to prepare a variety of closely related homometallic mixed anion lithium complexes and compare their reactivities as well as their structure and bonding to allow a formulation of some structure property relationships governing these important systems.

The focus of the research presented in this thesis is on homometallic lithium systems, which in part act as a model system for the classical 'LICKOR' superbase systems,

but are also of interest in their own right. This was done to simplify the chemistry by eliminating the possibility of isolating the product of a metal exchange reaction, as discussed in Section 1.4, as well as to allow the possibility of multinuclear NMR spectroscopic solution structure studies. The ligand system(s) was/were designed and synthesised to incorporate two anion types within the single molecule and hence eliminate the possibility of isolating autoaggregated single anion type complexes. This was anticipated to improve the likelihood of isolating a complete array of systematically varied mixed anion systems.

Chapter 2

Mixed anion O/N ligands and their lithiated complexes

2.1. Introduction

The great majority of the work done on the structural studies of organolithium complexes has focussed on the nature in which a single component metallated species aggregates and how this aggregation is affected by Lewis basic solvation. From this, the generalised observations that phenoxide anions tend to form stacked arrangements and amide anions tend to form laddered arrangements has been made, as shown in Figure 1-6. Following on from the observations of Morton, and later Schlosser, Lochmann and Wofford, that the 'strength' of these lithiated compounds towards proton abstraction can be increased by the addition of chelating ligands such as TMEDA, as well as the addition of a heavier alkali metal alkoxide. Efforts have been made to better understand the structure property relationships occurring within these reaction mixtures to their observed altered properties.

Significant progress has been made into understanding the effect of TMEDA and other coordinating solvents. It is now understood that they can act to break up the aggregated lithium complex as well as enhancing the nucleophilicity of the anionic centre. It is worth noting, however, while decreasing the degree of aggregation of organolithium reagents can result in higher reactivity, the most reactive species may not be the monomeric organolithium unit, and evidence is emerging to suggest that dimers are amongst the most reactive aggregation states that exist in solution.[44, 96-98]

It is of particular significance then, that much less success has been achieved in understanding the effect of the mixing of anion types. Caubere presented an

extensive review of the experimental findings regarding mixed anion superbase systems available in the early 1990's, concluding essentially that it is an area worth investigating in a systematic way to further the understanding of this ubiquitous and potentially very useful chemical phenomena.[63]

A relatively small number of solid state organolithium structures containing multiple organic derived anion types exist; two such examples were discussed in Section 1.4. An interesting example of a mixed anion complex containing a rare structural motif was obtained by Donkervoort from the reaction of 1,3-bis[1-(dimethylamino)propyl]benzene with *n*-BuLi.[99] The work was focussed on synthesising chiral ligands based on monoanionic terdentate aryldiamino ligands for stereoselective addition reactions. The lithiated complex is a 2:2 complex incorporating *n*-BuLi in the core of the complex. Complex **XI** has an 8 atom Li_4C_4 core, which is arranged in what has been called a 'ladder' arrangement. The authors note that such an arrangement for the core of their complex is unusual as this aggregation is more familiar for amide anions as illustrated in Figure 1-6.

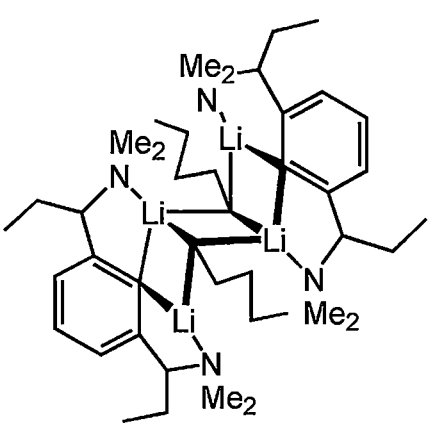

(**XI**)

Figure 2-1: Mixed anion organolithium complex with a ladder core.

Each ligand in **XI** contains two Lewis basic donor atoms, which help to stabilise this complex in the absence of any coordinating solvent molecules.

Another example of a structurally authenticated mixed anion complex is the dimeric complex of a lithiated methyl ketone containing a siloxy group, co-crystallised with LDA.[100] Williard *et al.* were investigating the effect of aggregation on the lithiation of ketones and isolated **XII** from the reaction mixture. The structure of **XII** is shown in Figure 2-2.

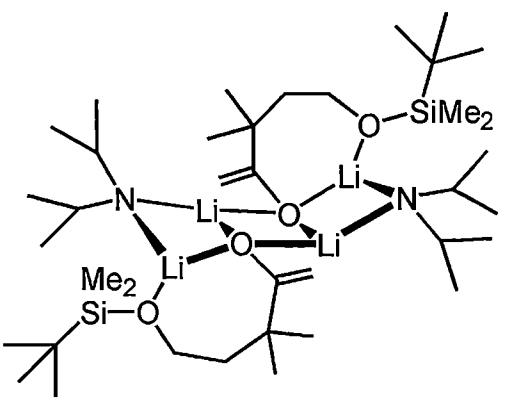

(**XII**)

Figure 2-2: Mixed organolithium complex with a ladder core.

The complex **XII** contains two Li_2ON rings, which are fused together along the O-Li edges, forming a central Li_2O_2 ring. Together the three rings have a similar appearance to complex **XI**, that of a ladder core. As noted previously, the inclusion of an intramolecular Lewis basic donor atom from one of the anions is likely to be a stabilising influence in the complex, and may contribute to the restriction of the aggregation to a dimer. Each of the lithium centres is only three coordinate; two coordinating to three anions (O_2N) and two coordinating to two anions and the neutral silyl ether group (O_2N). As noted in Chapter 1 in the structures of **VIII** and **IX**, here in the complex **XII** there is segregation of the anion types. The alkoxide anions form the inner ring and the amide anions are incorporated in the outer part of the ladder core aggregation.

The structures **XI** and **XII** are examples of serendipitous inclusion of the organolithium reagent with the lithiated substrate, and consequently provide valuable

insight into the possible effects, such as stereoselective induction, that aggregation may have on a lithiation reaction. It is not typically possible with such aggregated systems, however, to perform a systematic investigation into the effects that the aggregation may have on a reaction. A way to help overcome this problem is to tether the two anions of interest together into a single molecule.

Two particularly interesting examples of lithium complexes where the two anions contributing to the larger aggregate are tethered together into the same molecule are described by Chen.[101] Chen's groups' dilithiated ligands are symmetric, each containing two secondary amine groups. They have varied the ligand moieties in several ways: the separation between the ligands (in the length of the aliphatic chain between them), the nature of the spacer between the two anions, as well as the bulk adjacent to the anions. Interestingly, the lithiated ligands both form dimeric aggregates with aggregated cores similar to **XI** and **XII**. The structures of these dimers, **XIII** and **XIV** are shown in Figure 2-3.

One of the major differences between the two complexes **XIII** and **XIV** and the earlier two complexes incorporating the organolithium reagent, is the nature in which the ligand is involved in the structure of the aggregated core of the complex. Note that in the mixed anion complexes **XI** and **XII** the anions are distinct and separate molecules and each core of the complexes is defined by the eight ions comprising it (Li_4C_4, and $Li_4O_2N_2$ respectively). In the complexes **XIII** and **XIV** however, there is distinct difference between the ladder cores as **XIII** is comprised of six ions, Li_4N_2, and two neutral silicon atoms, as the ligand backbone itself contributes three of the four atoms in each outer LiN_2Si ring of the core. While the complex **XIV**, containing the diamide anions has a ladder core of eight ions as noted earlier. Noting that the ligand backbone in **XIV** straps along the ladder edge, it is evident that this will influence the flexibility of the complex to conformational change. The effect of this

strapping arrangement of the ligand is noted by the authors, and is particularly evident when the core is viewed in isolation as shown in Figure 2-4.

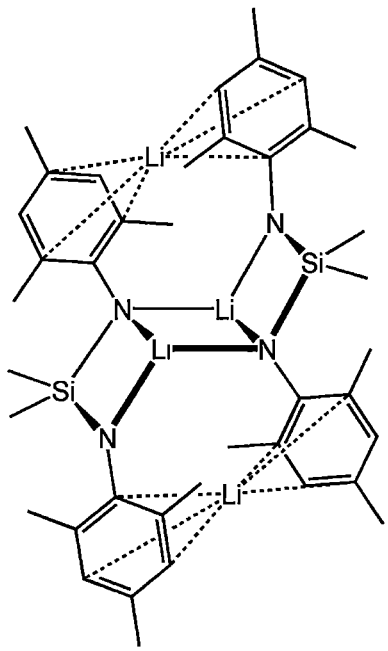

(XIII)

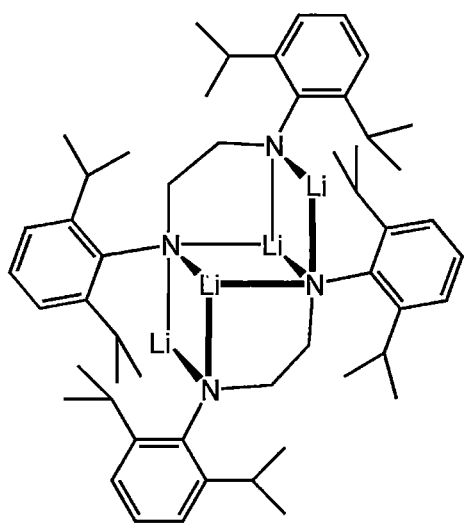

(XIV)

Figure 2-3: Tethered multi-anion complex with a ladder core.

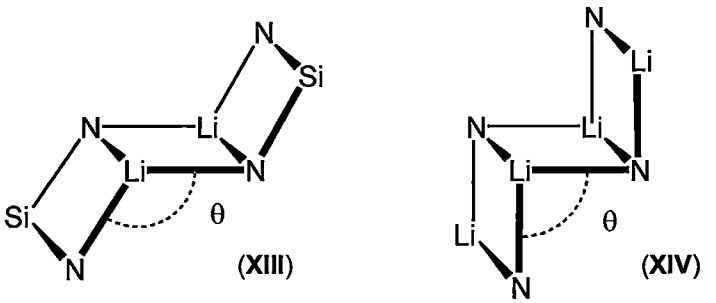

Figure 2-4: Illustration of the change in interplanar angles of a ladder core induced by the restricted length of the ligand backbone for a tethered multi-anion complex.

The interplanar angles (θ) calculated for each structure along the ladder are 129.6 ° and 107.5 ° for **XIII** and **XIV**, respectively. In particular, θ in **XIV** is markedly smaller than in polymeric lithium amide complexes, including ones of similar length such as $[\{LiN(CH_2)_4\}_4(TMEDA)_2]$ **IV** and $[\{LiN(CH_2)_4\}_6(PMDETA)_2]$ **V** shown in Chapter 1, in which the three rings are essentially planar.[56, 57]

For the work presented in the following chapters it is relevant to expand and clarify the different ways in which the ligand backbone's interaction with the core of the aggregated complex will be described. Whether a complex is comprised of stacked rings, or laddered rings, the following two distinct ways in which a ligand backbone can be involved are 'edge strapping' or 'face bridging'. These are illustrated in Figure 2-5.

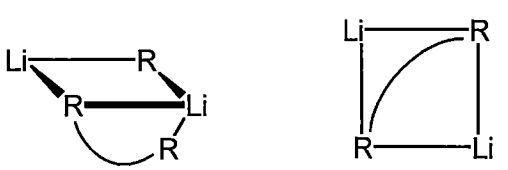

'edge strapping' 'face bridging'

Figure 2-5: Illustration of two possible modes of multi-anion ligand incorporation within an aggregated complex relative to the Li_2R_2 ring that they comprise.

Further to this for complexes incorporating more than one ring fused together, there are different distances that an edge strapping ligand can span, in terms of the number

of 'rungs' between the atoms of the ligand incorporated into the core. This is illustrated in Figure 2-6.

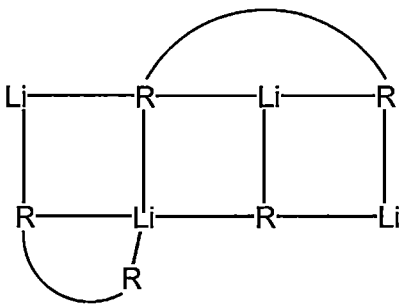

Figure 2-6: Illustration of different lengths of edge strapping possible for a ligand within a ladder complex.

Figure 2-6 is of a four-rung core, with a ligand arranged in a '3-rung' strapping position on the top side, and a different ligand arranged in a '2-rung' strapping position. From this it is clear that, although the anions present in a reaction mixture may have preferred tendencies, the ability of those tendencies to be fulfilled in the aggregated complex will depend on the ligand backbone; in particular the distance and flexibility between the anions.

An important aspect of the work undertaken lay in the design of a suitable organic ligand. A generalised ligand model allowing variability of the different structural features of the aggregated complex is illustrated in Figure 2-7a.

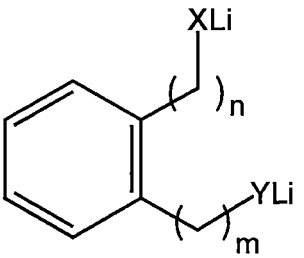

n, m = 0, 1, 2...,

X, Y = anion (alkyl, amide, alkoxide)

Figure 2-7a: Generalised multi-anion ligand scaffold.

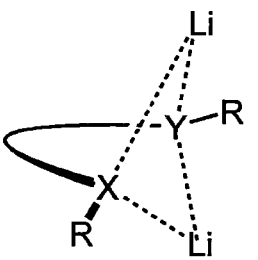

Figure 2-7b: 'Double-butterfly' binding mode of lithium.

This ligand scaffold is primarily based on an *o*-disubstituted benzene moiety; the inclusion of this rigid backbone would serve to limit the separation of the anions, X and Y, to the extent permitted within the ligand scaffold design and would help to prevent the often observed 'double-butterfly' aggregation mode for lithium complexes for shorter tethers between the metallated heteroatoms, as shown in Figure 2-7b. In the general case, the ligand incorporates two anions of different type, one on each arm extending from the *o*-phenylene backbone. Combinations of anions of particular interest are those that would be likely to introduce both ring stacking and ring laddering tendencies, e.g. alkyl- and amido- (N/C mixed anion) or alkoxido- and amido- (O/N mixed anion).

For a particular anion combination two other important variable parameters exist: proximity of the anions (alternatively viewed as the separation of the anions) as well as the bulk around each anion (in the case of alkyl- and amido- anions). By altering the length of the spacer between the *o*-phenylene ring and the anion the effect of the geometric constraint on the anion, as well as the effect on the aggregation of the

dilithiated monomers could be systematically investigated. Similarly, by altering the bulk adjacent to the anions the effect of this on the aggregation could be investigated.

Schiff bases containing hydroxylated aromatic ring substituents are an example of a particular class of compounds that contain multiple Lewis basic functionalities, and have been widely used as ligands.[102, 103] The general formula for a *Schiff* base is shown in Figure 2-8.

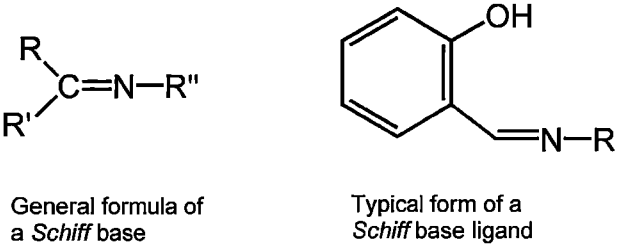

General formula of a *Schiff* base

Typical form of a *Schiff* base ligand

Figure 2-8

There are many examples in the literature where additional functionalities to increase their denticity have also been incorporated.[104, 105] In particular, the *N*-substituted salicylideneimine molecules shown on the right in Figure 2-8 have been investigated as ligands to facilitate catalytic hydrogenation[106] and precursors to chiral catalysts.[107] The intramolecular hydrogen bond that can occur in these molecules has also been investigated with relevance to understanding biological processes.[108]

Schiff bases are a good starting point for accessing a particular mixed anion ligand system based on the general case illustrated in Figure 2-7 as they readily introduce a desirable combination of potential anions, as well as facilitating easily variable bulk surrounding the amido anionic centre. Their development and synthesis is discussed in Section 2.3.1.

2.2. Research aim

The synthetic variability of the imine condensation reaction was to be exploited to allow the production of a variety of ligands based on the amide/alkoxide pairing of potential anion centres with different substituents at the nitrogen atom. It was expected that the imine could potentially either be reduced to the corresponding amine and subsequently deprotonate the two heteroatoms using an alkyllithium reagent, or alternatively there was the potential to carbolithiate across the double bond of the imine intermediate and directly form a related *C*-alkylated O/N dianionic complex from the *Schiff* base.

Following this, it was intended to explore the aggregation modes of these mixed O/N anion ligand scaffolds once lithiated. The intention was to investigate how systematic variations to the system affected the aggregation of the anions and the corresponding structure of the aggregates. Initially the difference between the aggregation of the monoanion ligand scaffold and the dianionic ligand scaffold were to be investigated; it was predicted that the monoanionic compounds would have a strong tendency to form phenoxide based stacked aggregates, however it was unknown what effect solvation might play on altering this aggregation. Further to this, the effect that altering the bulk of the substituent attached to the nitrogen anion (or atom in the monoanion cases) had on the structure and aggregation was to be investigated.

The intention was also to extensively investigate the effect Lewis basic solvation had on the observed structures, in order to observe how changing the denticity of the coordinating solvent affected which aggregation modes were accessible and whether the observed aggregation tendencies were more influential in determining the structure of the aggregates than the solvation effects.

It was unknown what degree of aggregation would be favoured, or what structural compromises would be observed with the inclusion of the two different anion types within the same ligand scaffold molecule.

2.3. Results and discussion

2.3.1. Ligand synthesis

The precursor *N*-phenyl, ON=PhH **1**, *N*-2,6-diisopropylphenyl, ON=DIPPH **2**, and ON=*t*BuH **3**, substituted *o*-hydroxyphenylene derived imines were prepared using a modified literature method.[106] They were synthesised via condensation reactions in methanol between salicylaldehyde and aniline, 2,6-diisopropylaniline, and *t*-butylamine, respectively, as shown in Scheme 2-1. Following this, each of the imines were reduced using sodium borohydride in methanol to yield the corresponding O/N mixed ligands ONPhH$_2$ **4**, ONDIPPH$_2$ **5** and ON*t*BuH$_2$ **6** respectively as shown in Scheme 2-1.

The salicylaldehyde and the amines were used without prior distillation despite the anilines being noticeably dark in colour. In each case the aldehyde and the amine were stirred together at room temperature in equimolar amounts. In the case of the aromatic amine reactions the solid imine product may be observed to begin precipitating out of solution as yellow or green crystals. After stirring together overnight the solution volume may be reduced to afford the intermediate imine complex ON=PhH **1** as a yellow/green crystalline solid, ON=DIPPH **2** as a yellow crystalline solid, or ON=*t*BuH **3** as a yellow oil. In all cases it was possible to perform the reduction of the imine *in situ* by adding sodium borohydride directly to the reaction mixture, as shown in Scheme 2-1. As the reduction reaction takes place

the yellow colour of the solution is observed to disappear as the amine product is formed. The progress of the reaction is easily monitored by TLC and confirmed as complete by NMR spectroscopy as the imine proton has a characteristic chemical shift downfield from the aromatic protons in all cases.

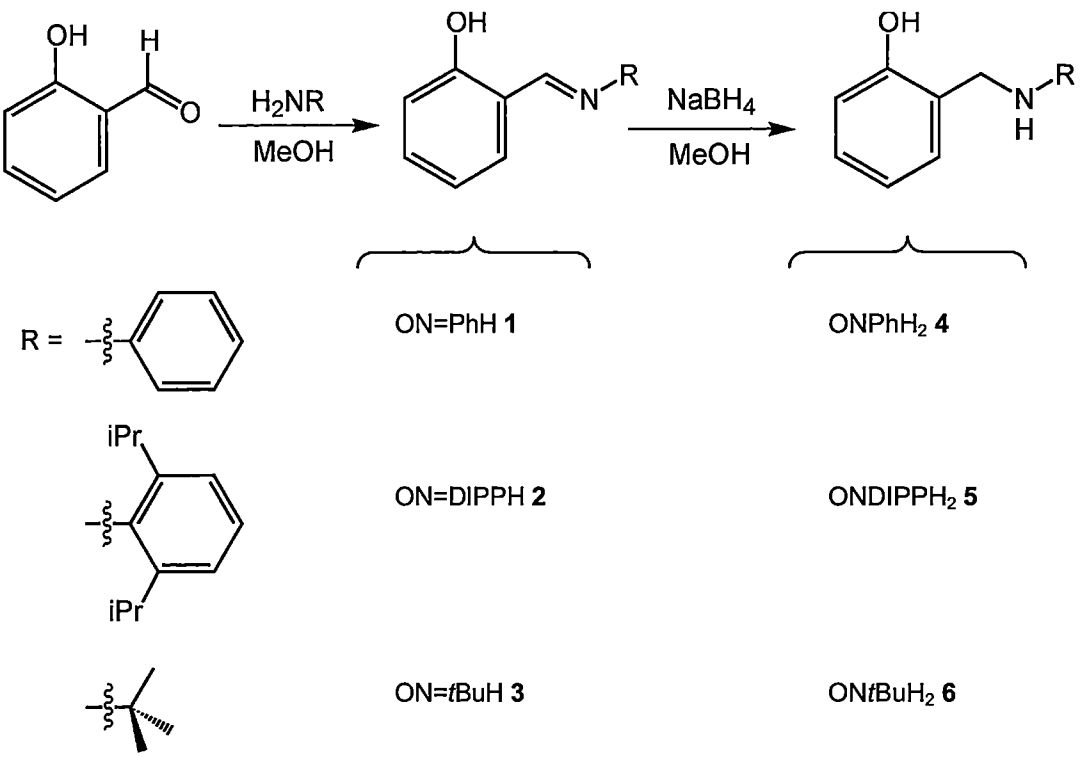

Scheme 2-1: Synthesis for the mixed O/N ligands with abbreviated formulae shown.

After reduction of the imine intermediates the amine ligand products *N*-phenylsalicylaldamine, $ONPhH_2$ **4**, *N*-2,6-diisopropylsalicylaldamine, $ONDIPPH_2$ **5**, and *N*-*t*-butylsalicylaldamine, $ONtBuH_2$ **6**, can be obtained as reasonably pure whitish solid material after work-up in 87, 95, and 55 % overall yields, respectively. In the cases of $ONPhH_2$ **4**, and $ONDIPPH_2$ **5**, it was relatively easy to purify the compound by recrystallisation. Single crystals suitable for X-ray crystal structure determination were grown for compounds $ONPhH_2$ **4**, $ONtBuH_2$ **6**, and with some difficulty $ONDIPPH_2$ **5**.

During the preparation of suitable crystals for X-ray crystal structure determination of $ONDIPPPH_2$ **5**, two different crystal types were observed. The main product was the reported compound that crystallised out as a thin fibrous crystalline material. There were also, however, prismatic crystals evident. Structural determination of the latter form identified them as a tertiary amine that has formed from the addition of a second salicylaldehyde unit onto the existing ligand system, *N,N*-di-(2-hydroxybenzyl)-2,6-diisopropylphenylamine. There was no evidence to suggest that this material was present in the bulk samples of $ONDIPPPH_2$ **5** prepared. The material used to prepare suitable crystals of the ligand was from of a sample of the ligand **5** that was recovered from larger lithiation reactions, and consequently it is uncertain how the impurity may have been formed and consequently it was not investigated further. The structure of this by-product is shown in Figure 2-9.

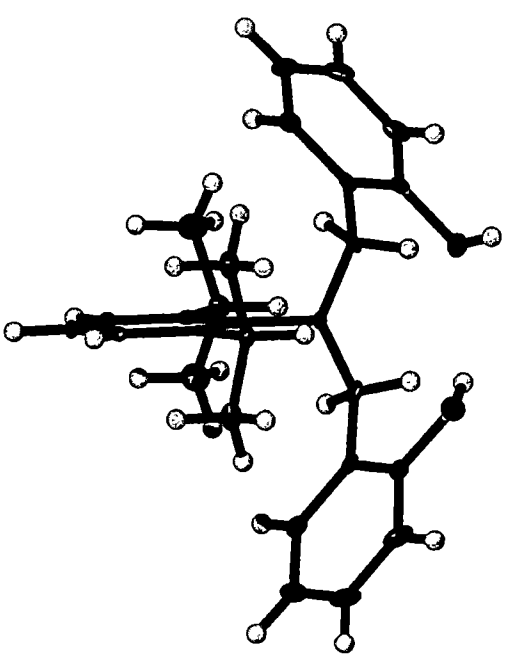

Figure 2-9: Molecular structure of $(HOC_6H_4CH_2)_2NDIPP$, with thermal ellipsoids drawn at the level of 50 % probability.

The *d*-chloroform ^1H NMR spectra of the amine ligands $ONPhH_2$ **4**, $ONDIPPPH_2$ **5**, and $ONtBuH_2$ **6** do not display any abnormal characteristics. The aromatic

resonances in $ONPhH_2$ **4** display non-first order coupling and appears as overlapping multiplets. In $ONDIPPH_2$ **5** the three aromatic protons on the aniline derived portion of the molecule appear as a single resonance, while the remaining 4 protons from the salicylaldehyde derived ring are resolved into doublets and pseudo triplets. In $ONtBuH_2$ **6** the same four salicylaldehyde ring protons are not as well resolved, with only one doublet and pseudo triplet visible while the other two resonances overlap to give a multiplet. The exact appearance of the aromatic region in all cases was somewhat dependent on the concentration of the sample and in many cases the resolution of the peaks was reduced. This is consistent with the H-bonding capabilities of the compounds.

The methylene protons for the three amine ligands **4-6**, display a moderate amount of deshielding from the neighbouring aromatic ring and at room temperature are equivalent and appear as singlets. The methylene proton resonance(s) turned out to be a good diagnostic handle for determining the degree of lithiation of the compounds. When dilithiated the resonance remained as a singlet, however in the monolithiated compounds it typically appeared as a triplet. This is discussed further in Section 2.3.3.

In each of the amine ligands **4-6**, both of the heteroatom attached proton resonances display broad resonances in *d*-chloroform. Of the six different heteroatoms only two appeared as discernable resonances; they are centred approximately at 6.2 ppm and most likely correspond to the amine proton in $ONPhH_2$ **4** and $ONtBuH_2$ **6**. The appearance of these heteroatom attached protons in the ^1H NMR spectrum of **4** in *d*-chloroform is markedly different to their appearance in d_6-DMSO. In d_6-DMSO all of the proton signals appear as sharp resonances; the phenol protons appear furthest downfield at 9.49 ppm and the amine proton displays first order triplet coupling to

the methylene protons ($^3J_{HH}$= 5.7 Hz). This NMR experiment was conducted early on in the research to help confirm the identity of the broad resonance observed and was not repeated for remaining compounds.

In the majority of cases throughout this thesis the aromatic resonances have not been fully assigned as it was often impractical to undertake the assignment and of limited value. What was noted were significant aromatic proton resonance differences between the monolithiated compounds and the dilithiated compounds that became a useful diagnostic handle for investigating the protonation of the dilithiated compounds, as discussed further in Section 2.3.3.

2.3.2. Molecular structures

Off-white crystals of $ONPhH_2$ **4** suitable for X-ray crystal structure determination were grown from a hot solution of **4** in toluene. The crystals belong to the triclinic space group $P\bar{1}$ (No. 2), $a = 5.611(4)$, $b = 7.950(3)$, $c = 11.815(2)$ Å, $\alpha = 90.69(2)$, $\beta = 92.09(3)$, $\gamma = 90.08(4)$ °, with two molecules in the unit cell and the asymmetric unit consisting of one molecule of $ONPhH_2$ **4**. The molecular structure of **4** is shown in Figure 2-10.

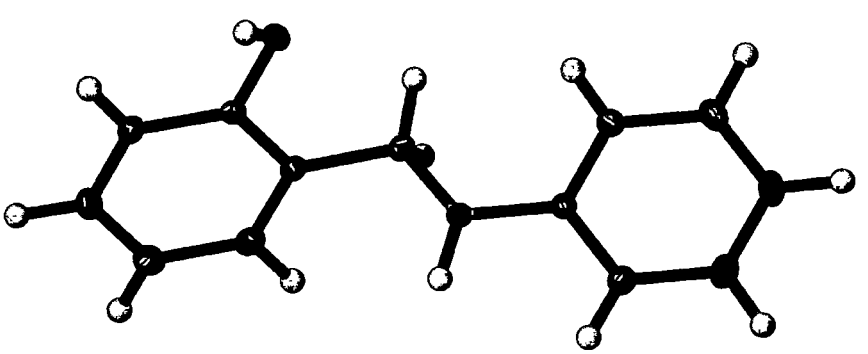

Figure 2-10: Molecular structure of ONPhH2 4 with thermal ellipsoids drawn at the level of 20 % probability.

Off-white crystals of ONDIPPPH$_2$ **5** suitable for X-ray crystal structure determination using the PX1 beam line at the Australian Synchrotron were grown with difficulty by evaporation of a concentrated solution of **5** in acetone. The crystals belong to the monoclinic space group $P2_1/c$ (No. 14), a = 12.406(8), b = 15.113(8), c = 8.925(5) Å, β = 105.40(4) °, with four molecules in the unit cell and the asymmetric unit consisting of 1 molecule of ONDIPPPH$_2$ **5**. The molecular structure of **5** is shown in Figure 2-11.

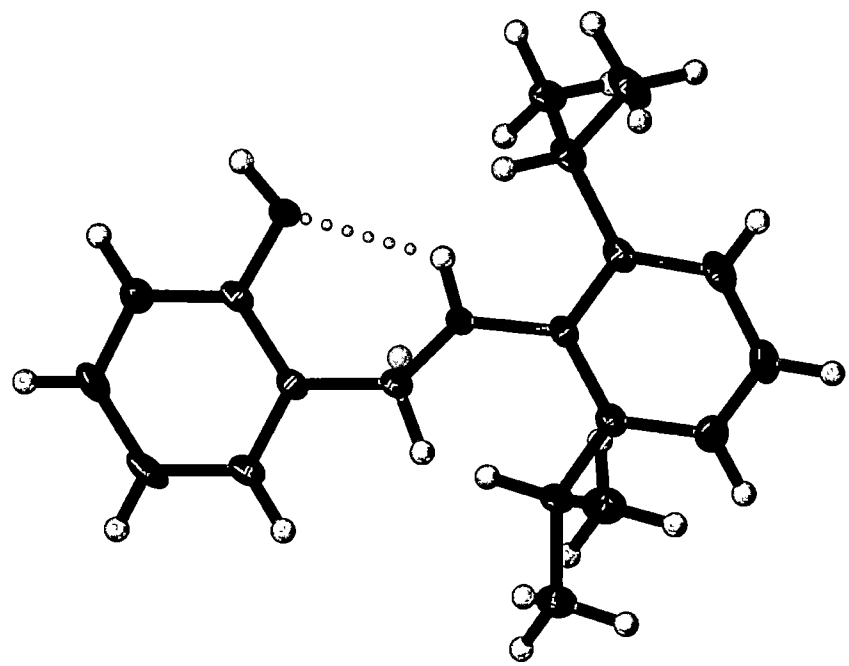

Figure 2-11: Molecular structure of ONDIPPPH$_2$ **5** with thermal ellipsoids drawn at the level of 50 % probability.

Off-white crystals of ON*t*BuH$_2$ **6** suitable for X-ray crystal structure determination using the PX1 beam line at the Australian Synchrotron were grown with difficulty by evaporation of a concentrated solution of **6** in 40-60 °C petroleum spirits. The crystals belong to the monoclinic space group $P2_1/c$ (No. 14), a = 10.8080(16), b = 10.0970(13), c = 9.733(4) Å, β = 96.864(8) °, with 4 molecules in the unit cell and the asymmetric unit consisting of 1 molecule of ON*t*BuH$_2$ **6**. The molecular structure of **6** is shown in Figure 2-12.

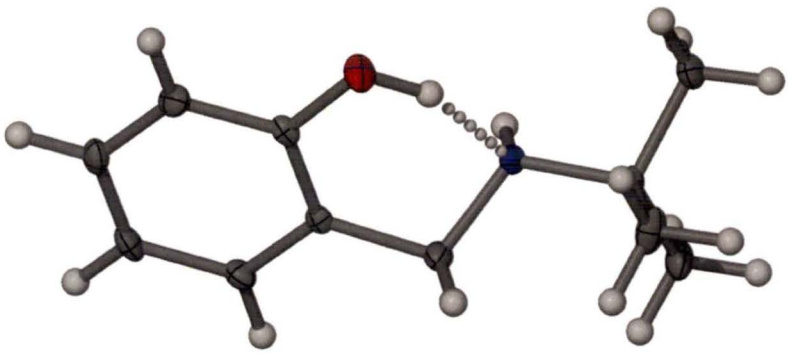

Figure 2-12: Molecular structure of ON*t*BuH$_2$ **6** with thermal ellipsoids drawn at the level of 50 % probability.

The structures of the *N*-phenyl imine and amine ligands ON=PhH **1** and ONPhH$_2$ **4** have been published previously.[109, 110]

The three amine ligands form an extended hydrogen bonded structure in the solid state. For compounds ONDIPPH$_2$ **5** and ON*t*BuH$_2$ **6** this H-bonding interaction is in addition to an intramolecular hydrogen bond, as shown in Figure 2-11 and Figure 2-12. The extended solid state structure of each ligand is similar, forming a zigzag sheet. The extended structure of ligand **4** is two zigzag layers thick, with each zigzag H-bonding to each other as shown in Figure 2-13. The other ligands **5** and **6** form a zigzag only a single layer thick, as shown in Figure 2-14 and Figure 2-15. The ligands **5** and **6** do not alternate orientation within their H-bonding sheets, and are arranged head-to-head, this is also true of the ligand ONPhH$_2$ **4** within each zigzag layer, however the two connected layers are connected in a head-to-tail fashion. Portions of each of the extended H-bonded structures of the ligands are shown in Figure 2-13, Figure 2-14 and Figure 2-15.

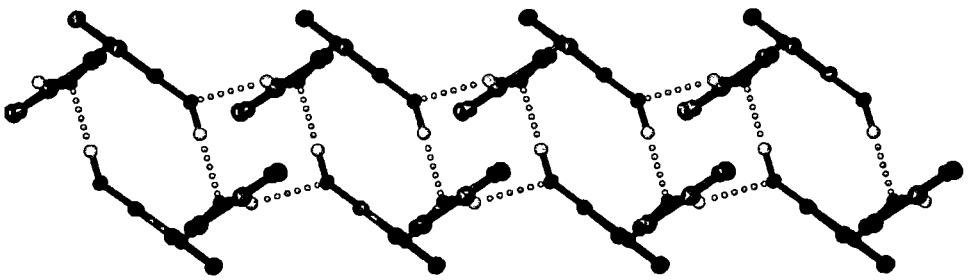

Figure 2-13: H-bonded structure of $ONPhH_2$ **4**. Thermal ellipsoids drawn at the level of 20 % probability.

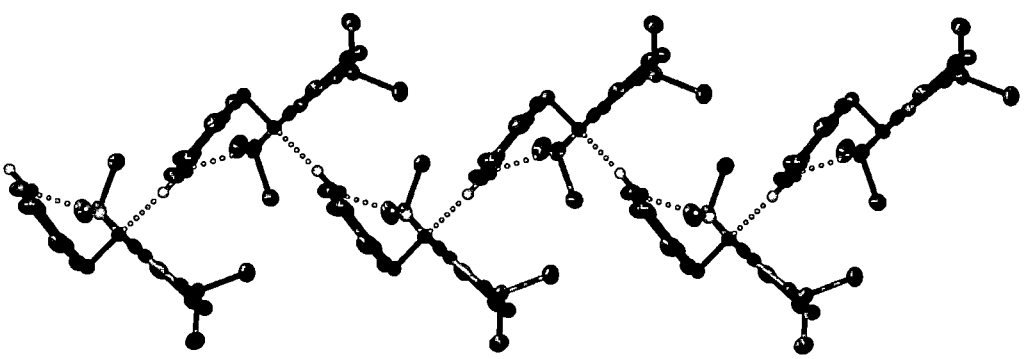

Figure 2-14: H-bonded structure of $ONDIPPH_2$ **5**. Thermal ellipsoids drawn at the level of 50 % probability.

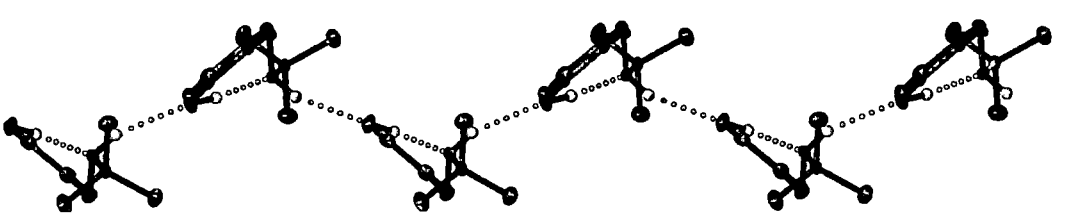

Figure 2-15: H-bonded structure of $ONtBuH_2$ **6**. Thermal ellipsoids drawn at the level of 50 % probability.

The two aromatic rings in $ONPhH_2$ **4** are quite offset, and the torsion angle between them is approximately 120 °. This is more than the observed torsion angle in the precursor imine compound ON=PhH **1**, which is closer to planar with a torsion angle between the rings of approximately 55 °. In the more bulky substituted

N-2,6-diisopropylphenyl amine ligand **5** the arene rings are nearly co-planar (within 5 °). One may expect that the imine compound would exist much closer to planar across the molecule due the extended π-delocalised system that can extends the length of the molecule. However, it is known that there are two photochromic polymorphs observed where the rings are not co-planar, as well a planar polymorph.[109, 111] As the imine compounds were not investigated extensively in this work, the occurrence or impact of this was not looked into any further.

2.3.3. Monolithiated O/N complexes

Each of the two ligands $ONPhH_2$ **4** and $ONDIPPH_2$ **5** were treated, respectively, with *n*-BuLi in 1:1 reactions in petroleum spirits to yield the complexes $[\{Li(ONPhH)\}_4]$ **7** and $[\{Li(ONDIPPH)\}_4]$ **9** in 93 and 76 % yield, respectively, as shown in Scheme 2-2.

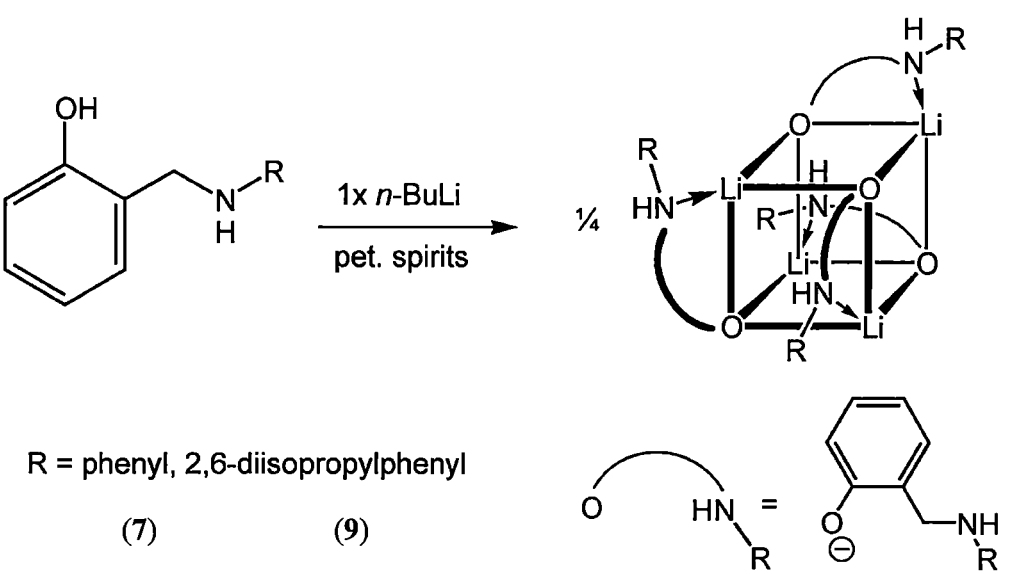

Scheme 2-2: Synthesis of unsolvated monolithiated O/N complexes $[\{Li(ONPhH)\}_4]$ **7** and $[\{Li(ONDIPPH)\}_4]$ **9**.

The reaction mixtures were stirred at room temperature for two hours and one hour, respectively. This was observed to be sufficient reaction time upon characterisation

of the reaction product in both cases. The products formed as insoluble, finely crystalline white material, isolable via filtration of the mother liquor away from the reaction solution.

Complexes **7** and **9** were characterised by X-ray crystal structure determination, and elemental analysis. Complex **9** was also characterised by ^{1}H and ^{13}C, gCOSY, and gHMQC NMR spectroscopy. Complex **7** was not characterised by NMR spectroscopy as it is insoluble in benzene. It is worth noting that when the attempted sample was run no free protonated ligand was evident in the NMR spectrum.

Both of the unsolvated monolithiated complexes **7** and **9** aggregate as tetramers in the solid state, with the phenoxide anions stacking together to form a Li_4O_4 cubic core. For less bulky anions of this type it is possible to observe either tetramers or hexamers as described in Chapter 1.[1] It is possible that the presence of the internal coordinating Lewis base within each monolithiated ligand helps to limit the size of these aggregates, and thus tetramers are exclusively observed for the monolithiated complexes. There are several previous reports of similar amino alkoxide complexes comprising both phenoxide and alkoxide anions to give a cubic Li_4O_4 core.[112-119] In both of the unsolvated monolithiated complexes **7** and **9** the ligands arrange themselves the same way around the Li_4O_4 core, with two orthogonal pairs of ligand straps shown in Scheme 2-2. This ligand arrangement is typical for these complexes.

Both of the complexes are insoluble in petroleum spirits but dissolve in THF giving colourless solutions. The monolithiated complex formed from the bulkier ligand, [{Li(ONDIPPH)}$_4$] **9** is isolated from THF free from solvating THF molecules, whereas the less bulky complex [{Li(ONPhH)}$_4$] **7** is isolated as the THF solvated complex, [{Li(ONPhH)}$_4$(THF)$_3$] **8** in 97 % yield, as shown in Scheme 2-3.

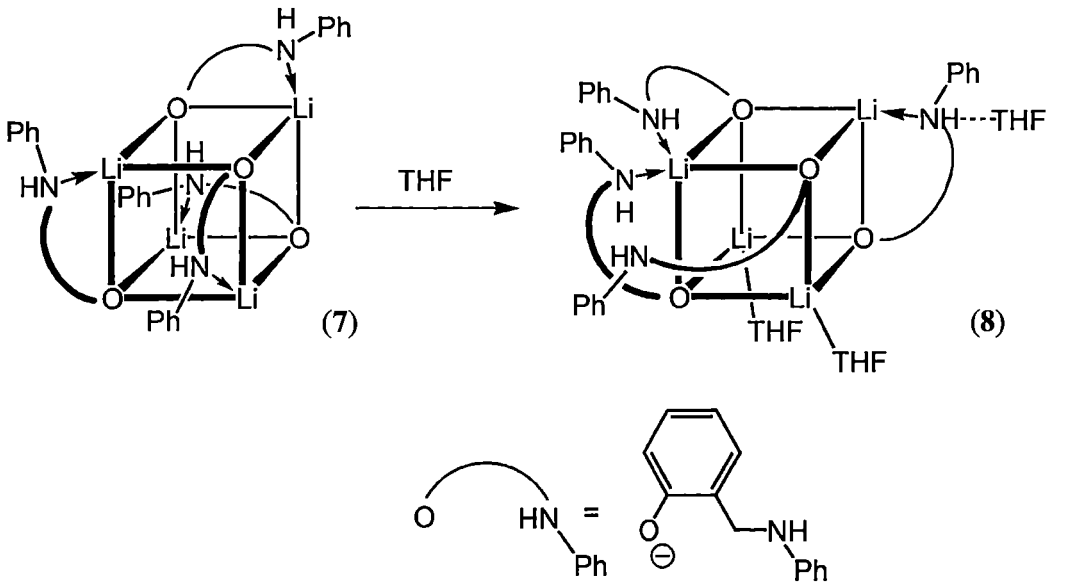

Scheme 2-3: THF solvation of the unsolvated monolithiated complex [{Li(ONPhH)}$_4$] **7** to give [{Li(ONPhH)}$_4$(THF)$_3$] **8**.

The THF solvated monolithiated complex [{Li(ONPhH)}$_4$(THF)$_3$] **8** was characterised by X-ray crystal structure determination, ^{1}H, ^{13}C, gCOSY, gHMQC, and gHMBC NMR spectroscopy, and elemental analysis. This monolithiated complex is also a tetramer based around the cubic stack of the phenoxide anions. However, the ligands are arranged in a different way to that observed in the unsolvated monolithiated complexes, showing a complete lack of symmetry. Rather than each amine group acting as an intramolecular Lewis base to unique lithium centres as for the unsolvated monolithiated complexes, in the THF solvated complex [{Li(ONPhH)}$_4$(THF)$_3$] **8** two of the nitrogen atoms are coordinated to one of the lithium centres, forming a five coordinate (3O, 2N) centre. One of the remaining nitrogen atoms is coordinated to the lithium centre on the same face of the Li_4O_4 core as the five coordinate (3O, 2N) lithium centre, and the remaining monolithiated ligand is not acting as an internal Lewis base but is positioned above the five coordinate lithium centre. Variability of the coordination of the nitrogen donor atoms within amino alkoxide complexes has been observed previously to produce an

interesting chiral arrangement of the ligands.[120] The arrangement of the ligands around the Li_4O_4 core of complex **8** is shown in Scheme 2-3.

It is worth noting that each of the ligands $ONPhH_2$ **4**and $ONDIPPH_2$ **5** will only undergo single lithiations when reacted with *n*-BuLi in 40-60 °C petroleum spirits. The first attempts to obtain the dilithiated complexes were carried out in 40-60 °C petroleum spirits, as this would have yielded the unsolvated complexes. However, in each case only the monolithiated complex was isolated. This is not surprising as the monolithiated complexes are both insoluble in 40-60 °C petroleum spirits, and the *n*-BuLi is not as activated by any Lewis basic donors.

Both of the monolithiated complexes $[\{Li(ONPhH)\}_4]$ **7** and $[\{Li(ONPhH)\}_4(THF)_3]$ **8** containing the less bulky *N*-phenyl substituents are insoluble in benzene. NMR data for $[\{Li(ONPhH)\}_4(THF)_3]$ **8** was obtained by the addition of a small amount of d_8-THF to a C_6D_6 NMR sample. Despite the asymmetric solid state structure observed for **8**, the ^1H NMR spectrum shows a single ligand type present in solution, suggesting that the structure is fluxional. All of the resonances in the ^1H NMR spectrum of $[\{Li(ONPhH)\}_4(THF)_3]$ **8** were partially assigned. The aromatic region is discernable as resonances arising from pseudo first order coupling of the protons on the *N*-phenyl and phenylene rings and appears between 6.33 and 7.21 ppm. The resonances arising from THF and the methylene linker between the two aromatic rings appear as multiplet and doublet resonances at 1.44, 3.55, and 3.88 ppm, respectively. The *N*-H resonance is visible as a broadened triplet at 3.36 ppm.

The bulkier complex $[\{Li(ONDIPPH)\}_4]$ **9** is soluble in benzene. The methyl groups of the 2,6-diisopropylphenyl substituents appear as a broad multiplet in the ^1H NMR spectrum between 0.77 and 1.11 ppm. The aromatic region displays partial

resolution, with two doublets centred at 6.47 and 6.83 ppm, respectively, and two pseudo triplets centred at 6.37 and 6.61 ppm, respectively, visible in the upfield portion. These four resonances correspond to the four protons of the phenylene ring of the salicylaldehyde derived portion of the monolithiated ligand. The remaining three aromatic protons on the amine substituent ring appear as a narrow multiplet centred at 7.00 ppm. The remaining aliphatic protons however, are each inequivalent, and display unique resonances. One of the methylene proton resonances appears as a pseudo triplet centred at 4.90 ppm while the other resonance appears at 3.22 ppm, overlapping with the methine resonances. The methine resonances form part of a multiplet between 3.04 and 3.39 ppm. There is a broad resonance centred at approximately 2.3 ppm, which was tentatively assigned as the *N*-H resonance. The inequivalence observed in the methylene and methine proton resonances may indicate that the observed intramolecularly solvated tetrameric solid state structure is maintained in solution. The orientation of the *N*-2,6-diisopropylphenyl substituent in each monolithiated ligand within the tetramer gives rise to different chemical environments for each 'side' of the *N*-aryl ring with respect to being closer or further from the Li_4O_4 core. The separation of the aliphatic protons from within their respective sets was observed to be maintained at 60 °C, with a methylene proton resonance corresponding to a single proton still clearly visible as a pseudo triplet at 4.90 ppm.

In the early stages of this work the feasibility of establishing the degree of lithiation (mono- or dilithiated ligands) by checking for the N-H stretching band in the IR spectrum was trialled. This initially appeared to have successful results with the dilithiated complex **11** in Section 2.3.5 showing no N-H stretching absorption band, while the corresponding monolithiated complex **8** and neutral ligand **4** did show one. Further to this, when the dilithiated sample was exposed to air for a short time and

visibly observed to change from a white material to yellow material as it underwent hydrolysis, the appearance of an N-H stretching band in the IR spectrum resulted. However it was observed that the results were variable between samples and in some cases false negatives were obtained, i.e., samples of monolithiated complex showed no N-H absorption band. Consequently, this approach was abandoned and as a result some of the compounds have the IR data reported in the experimental section while others do not.

In later work, ^{1}H NMR spectra were predominantly used to help identify the presence or absence of monolithiated complexes. The regions of interest for this distinction were the shape and chemical shift of the resonance arising from the methylene proton resonance and the chemical shifts of the aromatic resonances. In the *N*-2,6-diisopropylphenyl substituted monolithiated complex the methylene resonance appearing near 5 ppm appears as a pseudo triplet, whereas in the dilithiated complexes the resonance appears as either a singlet or multiplet arising from two overlapping singlet resonances. In addition, in the monolithiated complexes the aromatic resonance region extends further upfield than in the dilithiated complexes by approximately 0.1 ppm.

2.3.4. Molecular structures

Throughout this thesis all metallated complexes are depicted using thicker grey bonds for the covalent interactions within each ligand and solvent molecule. Thinner gold bonds are used to indicate the metal containing interactions comprising the core, as well as all Lewis basic interactions within the complex.

Small colourless crystals of the monolithiated complex [{Li(ONPhH)}$_4$] **7** suitable for X-ray crystal structure determination using the PX1 beam line at the Australian Synchrotron were grown by heating the material in benzene to 100 °C overnight in a sealed NMR tube fitted with a Young's tap. The crystals belong to the tetragonal space group $I4_1/a$ (No. 88), $a = 19.592(3)$, $b = 19.592(3)$, $c = 12.841(3)$ Å, with 4 Li_4O_4 molecules in the unit cell and the asymmetric unit consisting of ¼ molecule of [{Li(ONPhH)}$_4$] **7**. The complex is a tetramer and shows crystallographic S_4 symmetry. The molecular structure of **7** is shown in Figure 2-16.

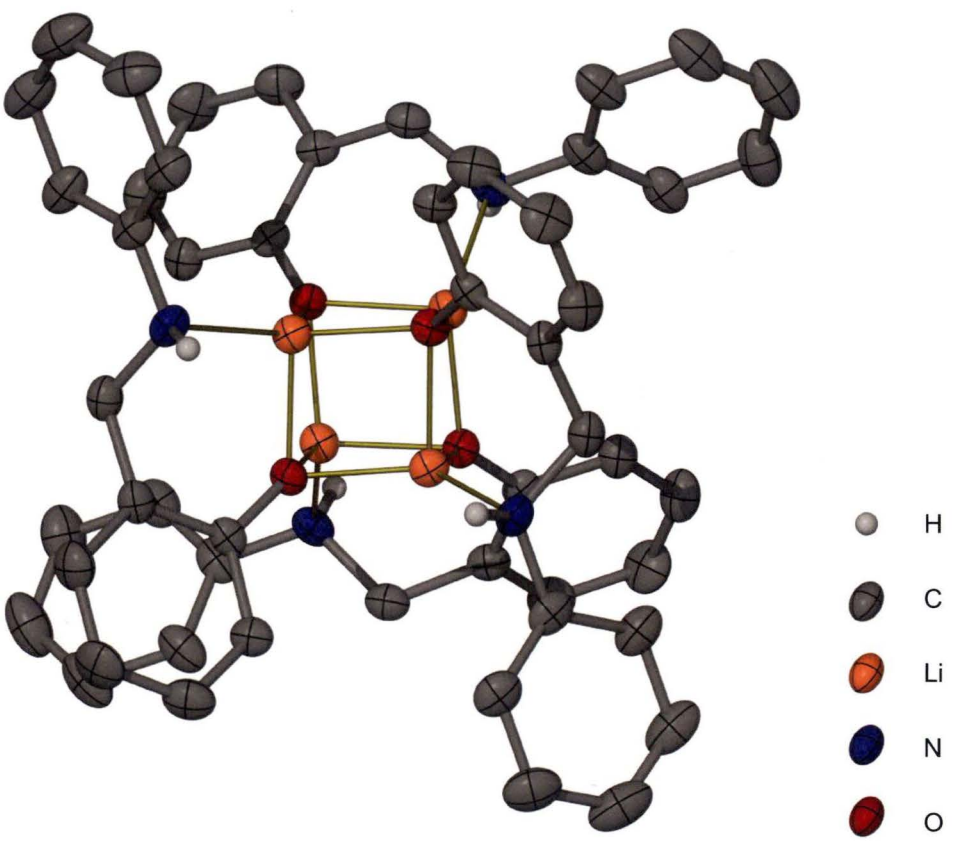

Figure 2-16: Molecular structure of [{Li(ONPhH)}$_4$] **7** with thermal ellipsoids drawn at the level of 50 % probability. Hydrogen atoms other than *N*-H removed for clarity.

Colourless crystals of the monolithiated complex [{Li(ONDIPPH)}$_4$] **9** suitable for X-ray crystal structure determination were grown from a concentrated solution of **9** in THF left standing at room temperature overnight. The crystals belong to the monoclinic space group $P2_1/c$ (No. 14), $a = 20.838(9)$, $b = 13.678(15)$,

c = 29.858(10) Å, β = 98.01(3) °, with 4 Li_4O_4 molecules in the unit cell and the asymmetric unit consisting of 1 molecule of [{Li(ONDIPPH)}$_4$] **9** processing C_1 crystallographic symmetry. X-ray crystal structure determination of the complex [{Li(ONDIPPH)}$_4$] **9** was carried out on crystals obtained from a variety of solvents. These polymorphs and different solvates are discussed in Section 3.5.5. The molecular structure of the monolithiated complex **9** was observed to be the same in all the cases where it was isolated (unsolvated). The structure of the above polymorph ($P2_1/c$) is shown in Figure 2-17.

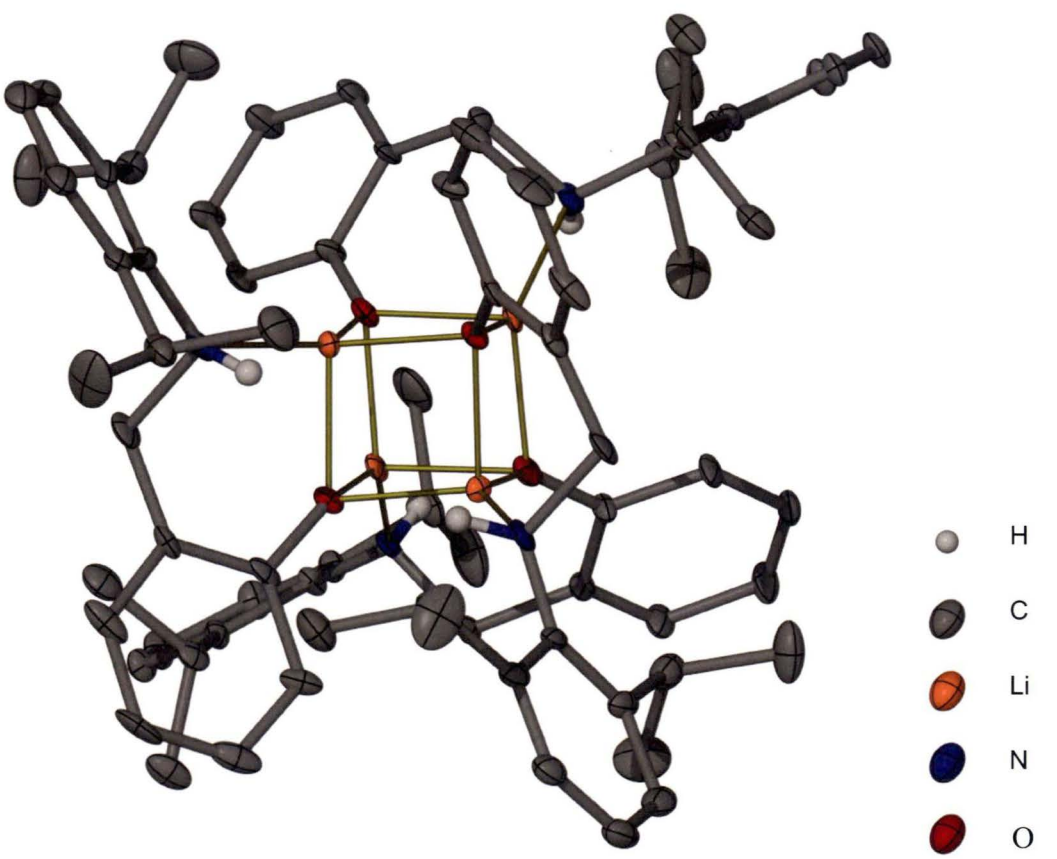

Figure 2-17: Molecular structure of [{Li(ONDIPPH)}$_4$] **9** with thermal ellipsoids drawn at the level of 20 % probability. Hydrogen atoms other than *N*-H removed for clarity.

As outlined in Chapter 1, phenoxide anions fall in to the category of anions that tend to aggregate in stacked arrangements. Specifically, the Li_4O_4 cubic core or a Li_6O_6 hexagonal prismatic core. The monolithiated complexes **7-9** aggregate as the smaller

tetrameric Li_4O_4 complexes in preference to hexameric Li_6O_6 aggregates. This is likely to be due to the presence of the internal Lewis basic amine donor groups within the lithiated ligand. Because the amine groups are tethered to the phenoxide anion within each of the lithiated ligands, once the smaller tetrameric aggregate is formed it will be rapidly stabilised by those Lewis basic interactions, which will tend to prevent further aggregation of additional lithiated ligands.

The Li_4O_4 cubic cores of complexes [{Li(ONPhH)}$_4$] **7** and [{Li(ONDIPPH)}$_4$] **9** are composed of alternating lithium and oxygen atom vertices; they consist of four lithium-phenoxide pairs of atoms, giving rise to the tetrameric complexes. The Li-O distances are typical and range in length from 1.918(4)-1.957(4) Å in [{Li(ONPhH)}$_4$] **7** and from 1.90(1)-1.99(1) Å in [{Li(ONDIPPH)}$_4$] **9**. In both monolithiated complexes **7** and **9** the amine groups within in the monolithiated ligands act as internal Lewis basic donors to unique lithium centres (N-Li 2.08(1)-2.09(2) Å) making each lithium centre four coordinate (O3, N) with approximate tetrahedral geometry. The monolithiated ligands each adopt an edge strapping arrangement around the core and are orientated in two pairs. Each pair is orthogonal to each other on opposite faces of the cube, as shown in Scheme 2-2.

There are minor differences in the twist angles of the *N*-aryl rings between the two complexes; however, the most significant difference is the degree of steric congestion around the Li_4O_4 core from the different sized amine substituents. In the less bulky complex [{Li(ONPhH)}$_4$] **7** there is much more room surrounding the core and, consequently, when exposed to THF a THF adduct is obtained. Conversely, for the bulkier substituents, [{Li(ONDIPPH)}$_4$] **9** shows a nearly complete steric saturation of ligand atoms surrounding the Li_4O_4 core of the complex. It is clear looking at the space filling representation in Figure 2-18 that there is no room for additional interactions of the core with solvating THF molecules. Potential

decoordination of the amine centres of ONDIPPH groups would unlikely allow sufficient room for the THF molecules to coordinate to the lithium centres, as they remain tethered to the core.

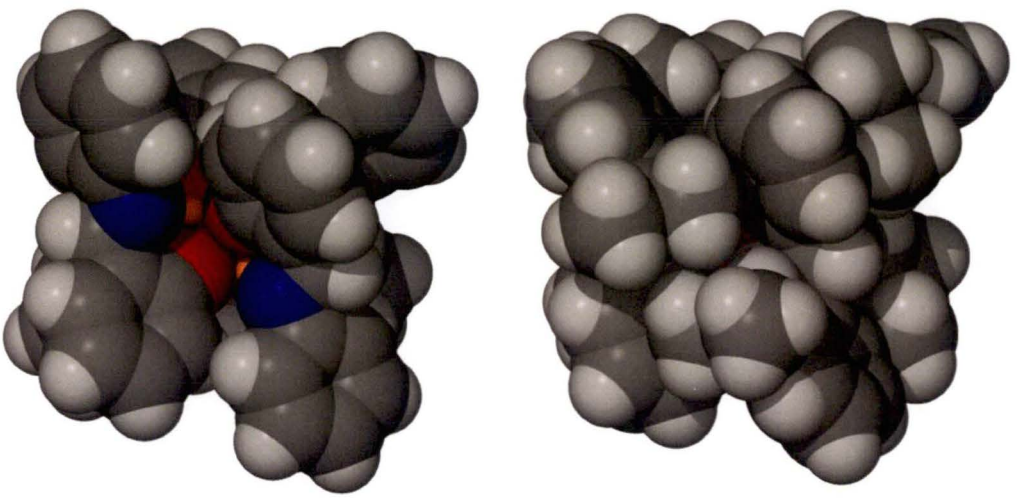

(a) (b)

Figure 2-18: Space filling representations of the molecular structure of the complexes (a) [{Li(ONPhH)}$_4$] **7** and (b) [{Li(ONDIPPH)}$_4$] **9**

Colourless crystals of the THF solvated monolithiated complex [{Li(ONPhH)}$_4$(THF)$_3$] **8** suitable for X-ray crystal structure determination were grown from a concentrated solution of **8** in THF allowed to stand at room temperature overnight. The crystals belong to the monoclinic space group $P2_1/c$ (No. 14), $a = 11.907(11)$, $b = 17.932(4)$, $c = 29.440(8)$ Å, $\beta = 91.78(5)$ °, with 4 Li_4O_4 molecules in the unit cell and the asymmetric unit consisting of one molecule of [{Li(ONPhH)}$_4$(THF)$_3$] **8**. The complex is C_1 symmetric. The molecular structure of **8** is shown in Figure 2-19.

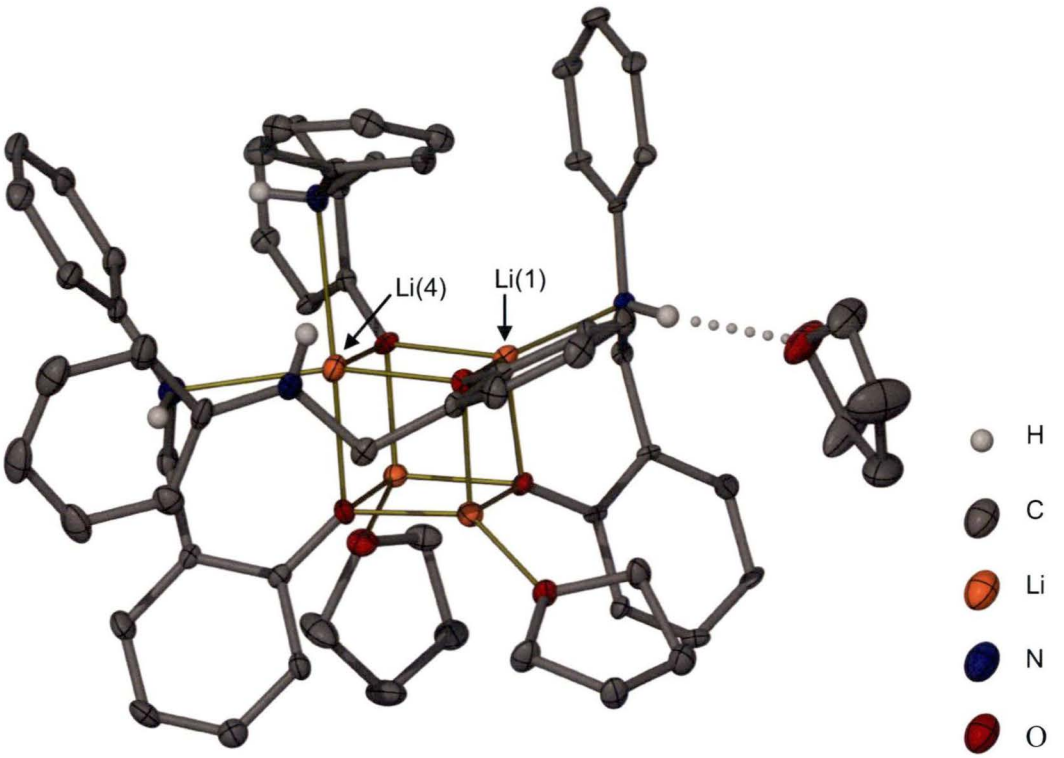

Figure 2-19: Molecular structure of [{Li(ONPhH)}$_4$(THF)$_3$] **8** with thermal ellipsoids drawn at the level of 20 % probability. Hydrogen atoms other than *N*-H removed for clarity.

In the solid state the incorporation of THF molecules around the core of the complex [{Li(ONPhH)}$_4$] **7** causes it to lose its symmetrical ligand arrangement. The core of the complex remains as a Li_4O_4 tetramer analogous to the unsolvated complexes [{Li(ONPhH)}$_4$] **7** and [{Li(ONDIPPH)}$_4$] **9**. The arrangement of the ligands in [{Li(ONPhH)}$_4$(THF)$_3$] **8** is not what one would expect given the symmetric nature of the core or the other monolithiated complexes. As described in Section 2.3.3 the complex has two of the amine groups from the monolithiated ligands acting as Lewis basic donors to a single lithium centre, Li(4) in Figure 2-19, (N-Li 2.418(7) Å and 2.497(8) Å). This gives rise to a five coordinate (O3,N2) centre, with a single amine group from a third monolithiated ligand acting as a Lewis basic donor to the lithium centre adjacent to the five coordinate lithium centre, Li(1) in Figure 2-19, (N-Li 2.100(7) Å), forming a four coordinate (O3, N) centre. The remaining amine group is positioned above the five coordinate lithium centre, Li(4), in the solid state structure,

however it is not interacting with either the lithium centre or the other amine groups via H-bonding. The remaining two lithium centres are solvated by THF molecules (O-Li 1.922(8) Å and 1.928(8) Å), forming four coordinate (O4) lithium centres. A third THF molecule incorporated in the complex is hydrogen bonded to the *N*-H proton of the amine group incorporated within the four coordinate (O3, N) lithium centre (O···H 2.214(4) Å).

There is noticeable steric congestion around the five coordinate (O3,N2) lithium centre, Li(4), in [{Li(ONPhH)}$_4$(THF)$_3$] **8**; the two N-Li distances are 0.3 Å and 0.4 Å longer, respectively, than the N-Li distances observed for both the four coordinate lithium centre in [{Li(ONPhH)}$_4$(THF)$_3$] **8** and the centres in the unsolvated complexes [{Li(ONPhH)}$_4$] **7** and [{Li(ONDIPPH)}$_4$] **9**. The asymmetry in the ligand arrangement also has a noticeable effect on the core of the complex, and the cube is distorted compared to the core of the unsolvated complex [{Li(ONPhH)}$_4$] **7** with the Li-O distances from the five coordinate lithium centre, Li(4), ranging between 2.026(7)-2.1123(8) Å. These distances are all longer than the Li-O bonds observed in the unsolvated complexes.

A further monolithiated complex of the imine ligand ON=DIPPH **2** was obtained as a small yielding by-product from one of the reactions discussed in Chapter 3. The colourless crystals of [{Li(ON=DIPPH)}$_4$] **10** belong to the monoclinic space group $P2_1/n$ (No. 14), $a = 12.743(3)$ Å, $b = 21.441(5)$ Å, $c = 25.816(5)$ Å, $\beta = 103.975(19)$ ° with 4 Li_4O_4 molecules in the unit cell and the asymmetric unit consisting of one molecule of [{Li(ON=DIPPH)}$_4$] **10** with approximate, non-crystallographic S_4 symmetry. The molecular structure of **10** is shown in Figure 2-20 and Figure 2-21.

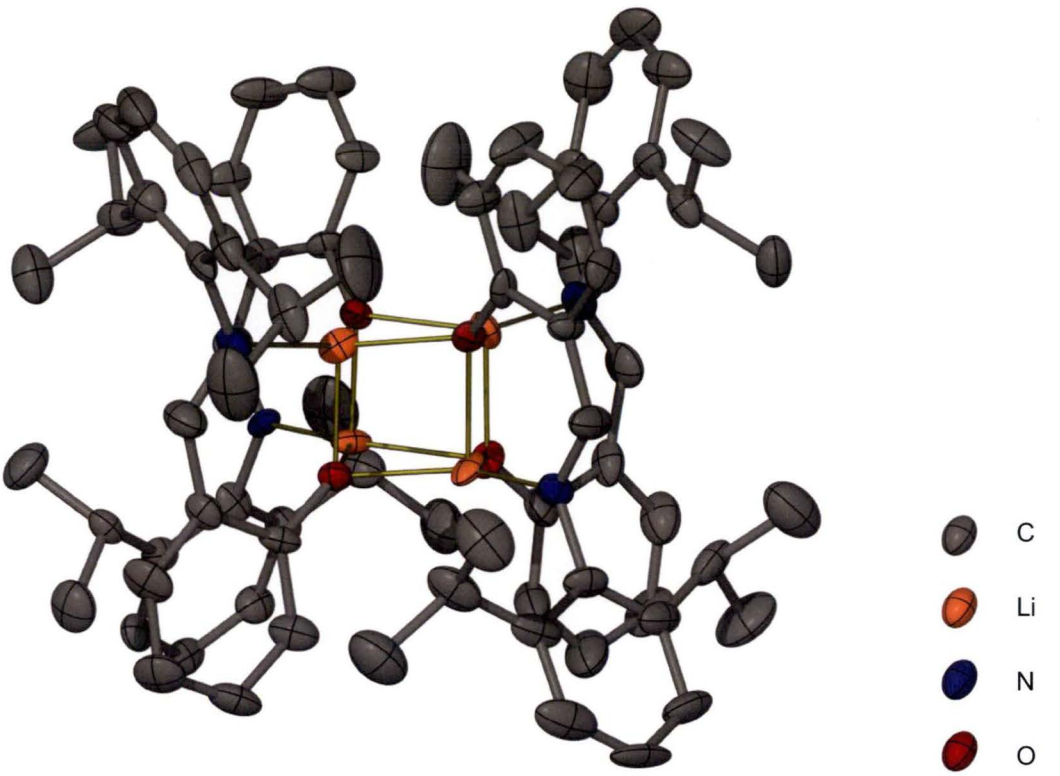

Figure 2-20: Molecular structure of [{Li(ON=DIPPH)}$_4$] **10** with thermal ellipsoids drawn at the level of 50 % probability. Hydrogen atoms removed for clarity.

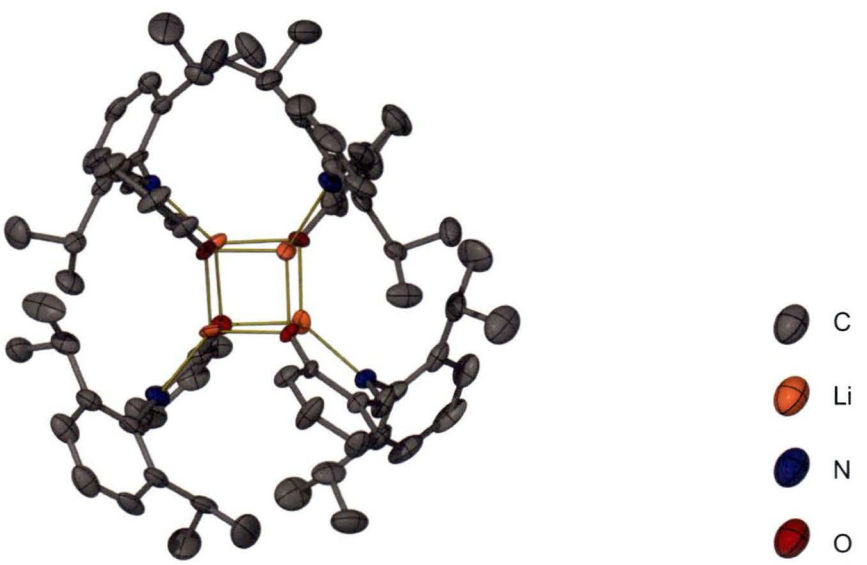

Figure 2-21: Top down view of the molecular structure of [{Li(ON=DIPPH)}$_4$] **10** with thermal ellipsoids drawn at the level of 50 % probability. Hydrogen atoms removed for clarity.

Complex **10** is a tetramer of the monolithiated imine ligand ON=DIPPH **2**. The four phenoxide anions form an analogous Li_4O_4 cubic core to the earlier reported monolithiated complexes. The range of Li-O distances within **10** is just wider than those of the monolithiated complex of the amine, [{Li(ONDIPPH)}$_4$] **9** at 1.87(1)-2.03(1) Å, also, the distances between the lithium atoms and the internal Lewis basic imine donor atoms in **10** are shorter than observed in **7** and **9** at 2.01(2)-2.07(1) Å. This is consistent with a reduction in coordination number of the nitrogen centres from four to three between the imine nitrogen centres within the ligands comprising complex **10**, and the amine nitrogen centres within the ligands comprising complexes **7** and **9**. The ligands in the tetrameric complex **10** are arranged in a unique way for the complexes reported within this thesis; they are all still edge strapping, however, they are arranged parallel to each other, alternating head-to-tail around the central rotation axis of the cubic core. Such an arrangement of the ligands is possible within complex **10** as the ligand backbone is flat, and the nitrogen centre is trigonal planar as it is sp^2 hybridised. Together, these allow the *N*-2,6-diisopropylphenyl substituents on each ligand to orientate themselves perpendicular to the phenylene rings, and consequently they are positioned symmetrically above the Li vertices of the cubic core as shown in Figure 2-21. This symmetrical positioning of the *N*-2,6-diisopropyl substituents in complex **10** allows two pairs of aggregated lithiated ligands to dimerise to form the tetramer with the ligands alternating in the head-to-tail way as observed. This head-to-tail arrangement of the lithiated ligands is prevented in complexes **7** and **9** as the nitrogen centres are tetrahedral, and consequently each *N*-2,6-diisopropylphenyl substituent of the ligands in **7** and **9** is prevented from remaining perpendicular to the phenylene ring. This results in two pairs of the lithiated ligand dimerising in the perpendicular way as described earlier.

2.3.5. Dilithiated O/N complexes – THF adducts

Each of the two ligands $ONPhH_2$ **4** and $ONDIPPH_2$ **5** were treated, respectively, with *n*-BuLi in 2:1 reactions in THF to yield the complexes $[\{Li_2(ONPh)\}_2(THF)_6]$ **11** and $[\{Li_2(ONDIPP)\}_2(THF)_4]$ **12** in 99 and 61 % yield, respectively, as shown in Scheme 2-4.

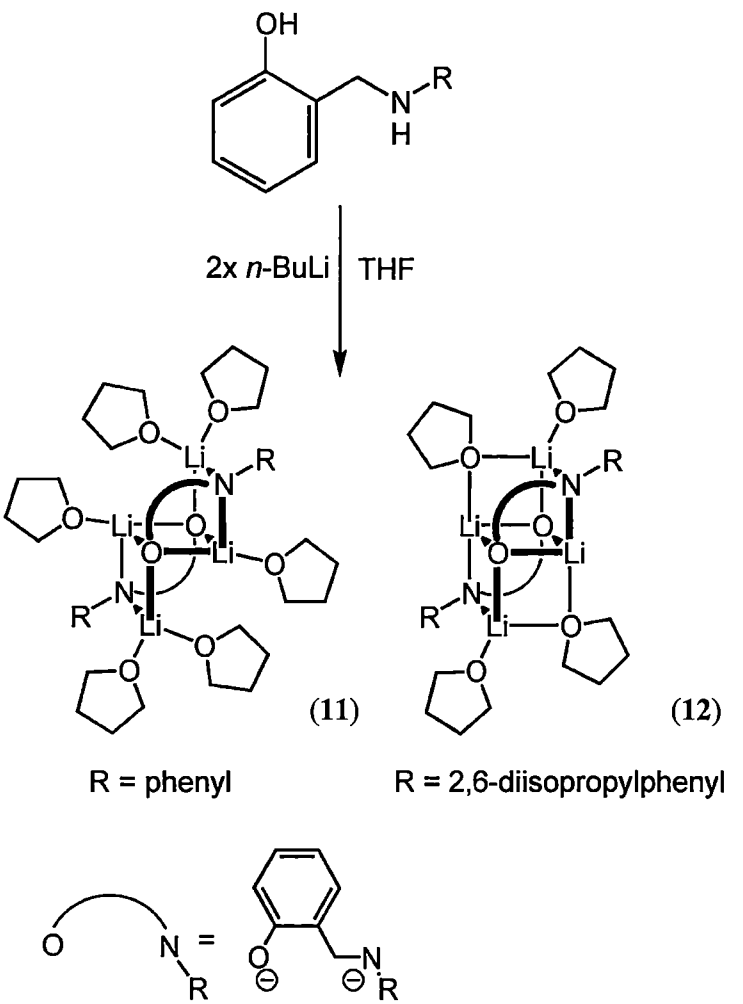

Scheme 2-4: Lithiation of the O/N ligands $ONPhH_2$ **4** and $ONDIPPH_2$ **5** to give the THF solvated complexes $[\{Li_2(ONPh)\}_2(THF)_6]$ **11** and $[\{Li_2(ONDIPP)\}_2(THF)_4]$ **12**.

The reaction mixtures of $ONPhH_2$ **4** and $ONDIPPH_2$ **5** were stirred with mild heating overnight and for three hours, respectively, to ensure complete reaction. The complex $[\{Li_2(ONPh)\}_2(THF)_6]$ **11** was observed to partially crystallise out of solution overnight and can be cropped multiple times. Alternatively the dilithiated

product can be easily purified from the crude evaporated reaction mixture by washing with chilled THF as the ligand $ONPhH_2$ **4** and monolithiated complex $[\{Li(ONPhH)\}_4(THF)_3]$ **8** are both readily soluble in cold THF whereas the dilithiated complex is relatively insoluble, yielding a clear and nicely crystalline product. The complex $[\{Li_2(ONDIPP)\}_2(THF)_4]$ **12** is more soluble in THF, but again can be isolated via reduction of the solution volume. It is not as convenient to separate the monolithiated complex from the dilithiated complex in this case, and careful fractional crystallisation is recommended. Complexes **11** and **12** were characterised by X-ray crystal structure determination, ^1H and ^{13}C NMR spectroscopy, and elemental analysis.

Both complexes form centrosymmetric dimers in the solid state with $Li_4O_2N_2$ cores having four-rung ladder configurations. The less bulky complex $[\{Li_2(ONPh)\}_2(THF)_6]$ **11** can accommodate a total of six THF molecules solvating the lithium centres, whereas the bulkier complex $[\{Li_2(ONDIPP)\}_2(THF)_4]$ **12** can only accommodate four, leading to half of the THF molecules adopting bridging positions each between two lithium centres. The less bulky complex $[\{Li_2(ONPh)\}_2(THF)_6]$ **11** has moderate solubility in toluene and is recoverable as the hexa-solvated THF complex without extensive heating. There was subsequently reason to test the thermal stability of each of these two complexes (see Chapter 3 for full discussion) and, though $[\{Li_2(ONDIPP)\}_2(THF)_4]$ **12** can be refluxed in benzene overnight without observable change or decomposition, the same treatment of $[\{Li_2(ONPh)\}_2(THF)_6]$ **11** led in one case to the formation of a new complex $[\{Li_2(ONPh)\}_4(THF)_4]$ **13** Scheme 2-5.

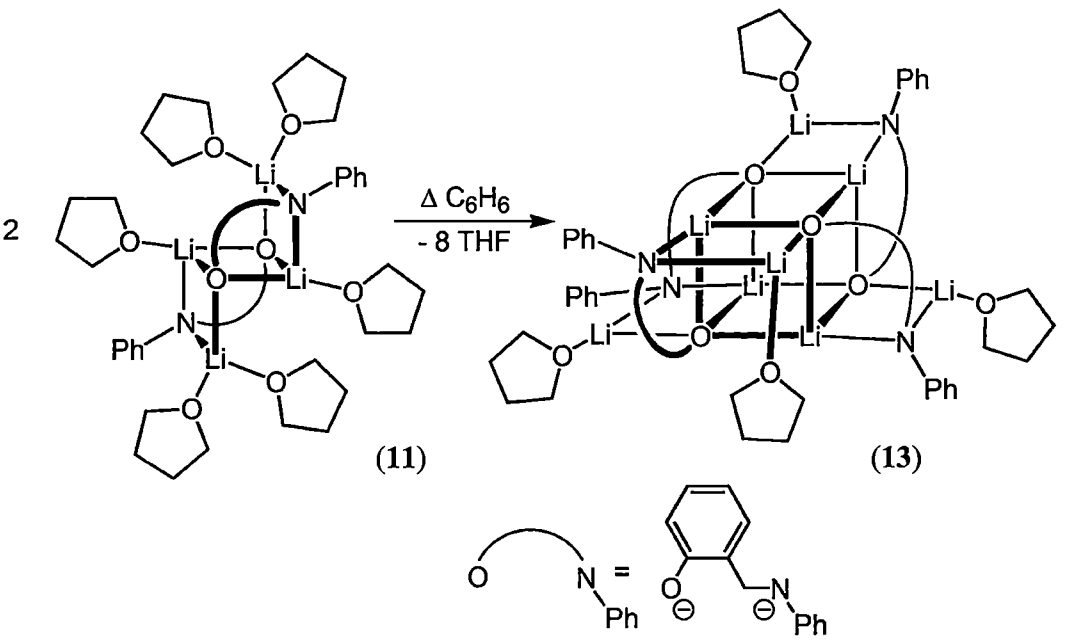

Scheme 2-5: Preparation of the dilithiated tetrameric complex [{Li_2(ONPh)}$_4$(THF)$_4$] **13**.

Complex [{Li_2(ONPh)}$_4$(THF)$_4$] **13** was characterised by X-ray crystal structure determination only as the reaction was not able to be repeated. The material was observed to be insoluble in benzene preventing characterisation by ^{1}H NMR spectroscopy. Complex **13** is a C_2 symmetric tetramer incorporating four unsolvated inner lithium atoms and four outer lithium atoms, each with a single coordinating molecule of THF. The mechanism by which complex **13** forms unclear. It is possible that the equilibrium concentration of THF available in solution was reduced due to the elevated solution temperature and this shifted the aggregation equilibrium of the lithiated material towards the less solvated tetrameric complex.

The complex [{Li_2(ONPh)}$_2$(THF)$_6$] **11** is quite soluble in benzene, yielding a ^{1}H NMR spectrum indicating some solution fluxionality. The six solvating THF molecules per dimer integrate correctly and show only a slight shift upfield compared to free THF. Despite there being three chemically different THF molecules in the observed solid state structure there is no evidence of different chemical environments observed in the ^{1}H NMR spectrum so it can be assumed that they are

fluxional in solution. The methylene proton resonance appears as a broad multiplet centred at approximately 4.4 ppm and shows evidence of splitting that is not fully resolved at room temperature. This suggests that the methylene protons might exist as an AB spin system within the dimeric complex, due to the limited flexibility of the O/N ligand backbone. The aromatic proton region appears as broadened multiplets and does not show any complete baseline resolution for the resonances.

Complex $[\{Li_2(ONDIPP)\}_2(THF)_4]$ **12** will dissolve in benzene with vigorous shaking of the mixture to give a ^1H NMR spectrum consistent with two species existing in solution as illustrated in Figure 2-22. Each of the species apparent in solution display symmetrical resonances in the aliphatic proton region. This results in the resonances for the methyl and methine protons appearing as complex multiplets between 1.21-1.36 ppm and 3.53-3.65 ppm, respectively. The methylene resonances appear as singlets at 4.54 and 4.58 ppm, respectively. The aromatic proton resonances appear as multiplets between 6.51 and 7.23 ppm. At room temperature it was observed that the ratio of the species in solution showed little variance towards changes in concentration. This suggests that the two species observed do not arise from a variation in aggregate size, such as a dimer and a tetramer. In the course of the investigation into the solution behaviour of complex **12** with concentration changes an effect on the ratio of species evident in solution was observed upon removal of toluene-d8 *in vacuo*. Removal of toluene-d8 also had the effect of removing some THF and this altered the relative proportion of the species in solution. This change is most evident in the less congested region corresponding to the methylene and methine proton resonances, with an increase in the relative intensity of the further upfield resonance in each case. This result indicated that the two species observed in solution correspond to two solution state species that have

varying solvation by THF in solution, with the less solvated complex being favoured upon removal of THF.

A similar variation in the relative amount of each species present in solution was also observed in a variable temperature ^{1}H NMR experiment (toluene-d8). At reduced temperatures (*ca.* <10 °C) the species corresponding to the downfield shifts for the methylene and methine protons was observed to be the only species present. While at elevated temperatures the converse was observed, with the species corresponding to the upfield shifts being by far the dominant species observed. The variation of the ^{1}H NMR spectrum with temperature is illustrated in Figure 2-22.

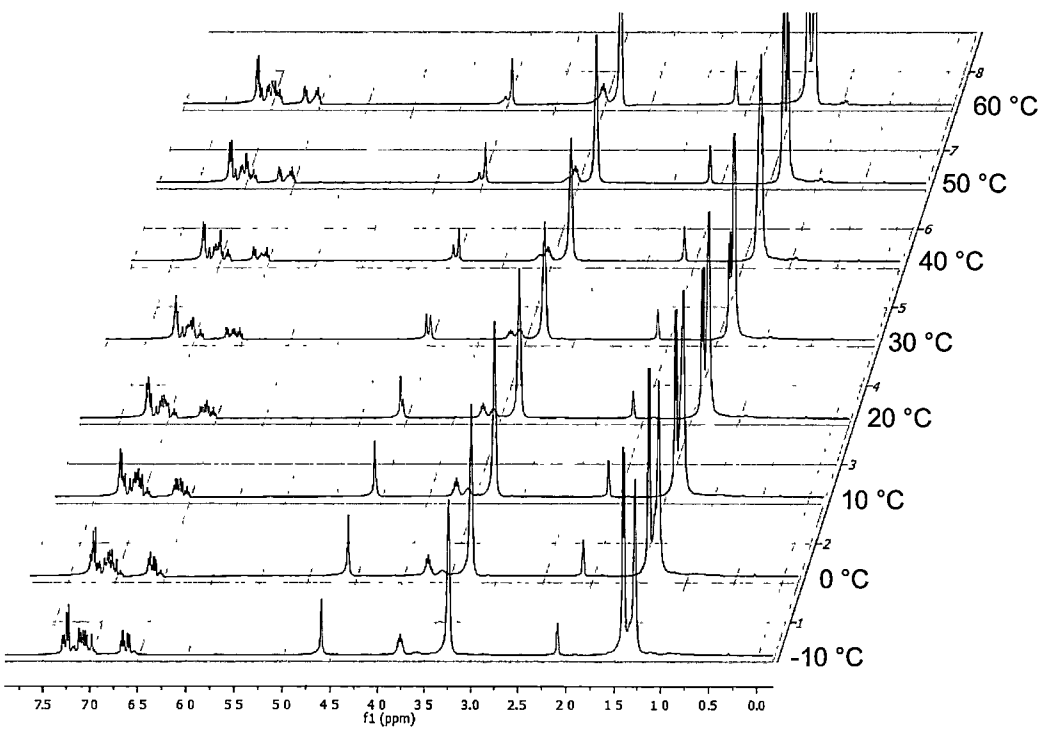

Figure 2-22: VT ^{1}H NMR of the complex $[\{Li_2(ONDIPP)\}_2(THF)_4]$ **12** in toluene-d8 between -10 °C and 60 °C.

The observed change in relative concentration of the two species with temperature is consistent with one of the species having a different degree of THF solvation, with the same species observed to be more prevalent at higher temperatures as the species observed to become more prevalent upon reduction of the amount of THF by partial

removal under vacuum. Although the structure of the two species evident in solution is not definitively known, the interconversion between them must be relatively slow in the NMR time scale, which is noted as unusual for alkoxido- and amidolithium complexes. The slow exchange between the two species may imply that a significant structural change occurs on partial desolvation, particularly since the THF resonances of all species demonstrate rapid inter- and intramolecular exchange at all temperatures. Further studies such as computational modelling are required to better understand this process. These studies were not undertaken within this project due to time constraints.

It was observed that the routine room temperature ^{1}H NMR experiments of complex $[\{Li_2(ONDIPP)\}_2(THF)_4]$ **12** showed some variability throughout the course of the study in regard to the ratio of species present. It is noted that this is not completely unexpected as the complex shows a very large variance in the relative concentration of the two species observed around room temperature; *ca.* 9:1 to 1:9 over a 30 °C temperature interval.

2.3.6. Molecular structures

Colourless crystals of the dilithiated THF solvated complex $[\{Li_2(ONPh)\}_2(THF)_6]$ **11** suitable for X-ray crystal structure determination were grown from a concentrated solution of **11** in THF left standing at room temperature for 30 mins. The crystals belong to the triclinic space group $P\bar{1}$ (No. 2), $a = 13.055(3)$, $b = 13.529(10)$, $c = 16.633(3)$ Å, $\alpha = 68.34(4)$, $\beta = 81.16(2)$, $\gamma = 62.76(3)$ °, with 2 $Li_4O_2N_2$ molecules in the unit cell, with the asymmetric unit consisting of two ½ centrosymmetric molecules of $[\{Li_2(ONPh)\}_2(THF)_6]$ **11** with

similar geometries. The molecular structure of **11** is shown in Figure 2-23 and Figure 2-24.

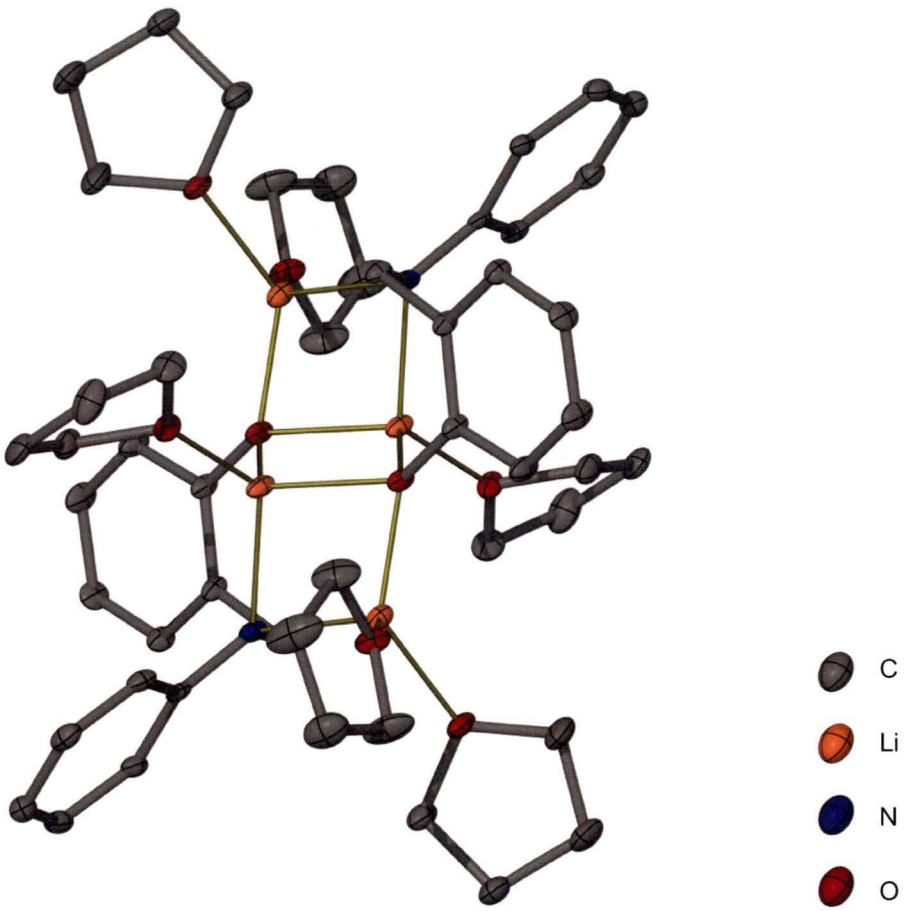

Figure 2-23: Front on view of the molecular structure of $[\{Li_2(ONPh)\}_2(THF)_6]$ **11** with thermal ellipsoids drawn at the level of 20 % probability. Hydrogen atoms removed for clarity.

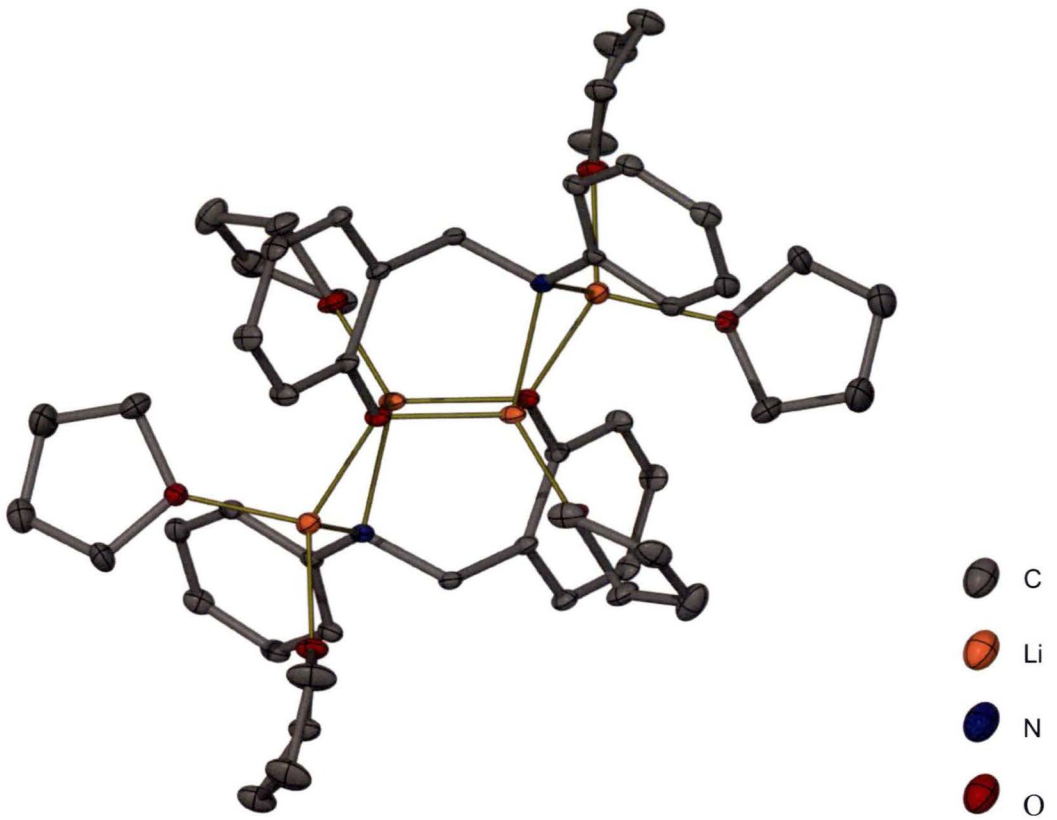

Figure 2-24: Side on view of the molecular structure of $[\{Li_2(ONPh)\}_2(THF)_6]$ **11** with thermal ellipsoids drawn at the level of 20 % probability. Hydrogen atoms removed for clarity.

Colourless crystals of the dilithiated THF solvated complex $[\{Li_2(ONDIPP)\}_2(THF)_4]$ **12** suitable for X-ray crystal structure determination were grown from a concentrated solution of **12** in THF left standing at room temperature for 1 hr. Two polymorphs were observed for this complex, both without any lattice solvent. The first reported crystals belong to the monoclinic space group $P2_1/c$ (No. 14), $a = 9.203(14)$, $b = 11.3491(18)$, $c = 24.539(6)$ Å, $\beta = 99.84(5)$ °, with 2 $Li_4O_2N_2$ molecules in the unit cell and the asymmetric unit consisting of ½ centrosymmetric molecule of $[\{Li_2(ONDIPP)\}_2(THF)_4]$ **12**. The second reported crystals belong to the monoclinic space group Pn (No. 7), $a = 9.429(2)$, $b = 26.82(3)$, $c = 20.659(4)$ Å, $\beta = 99.04(2)$ °, with 4 $Li_4O_2N_2$ molecules in the unit cell and the asymmetric unit consisting of two similar molecules of $[\{Li_2(ONDIPP)\}_2(THF)_4]$ **12**.

The structure of the first polymorph ($P2_1/c$) of **12** is shown in Figure 2-25 and Figure 2-26.

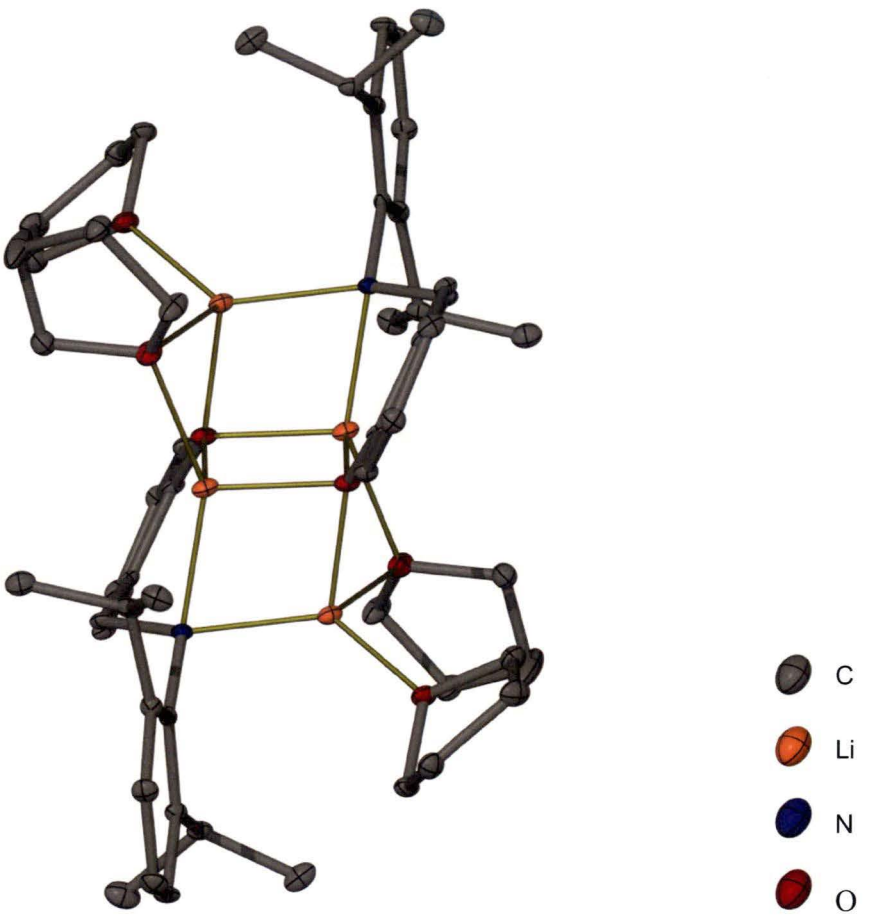

Figure 2-25: Front on view of the molecular structure of $[\{Li_2(ONDIPP)\}_2(THF)_4]$ **12** with thermal ellipsoids drawn at the level of 20 % probability. Hydrogen atoms removed for clarity.

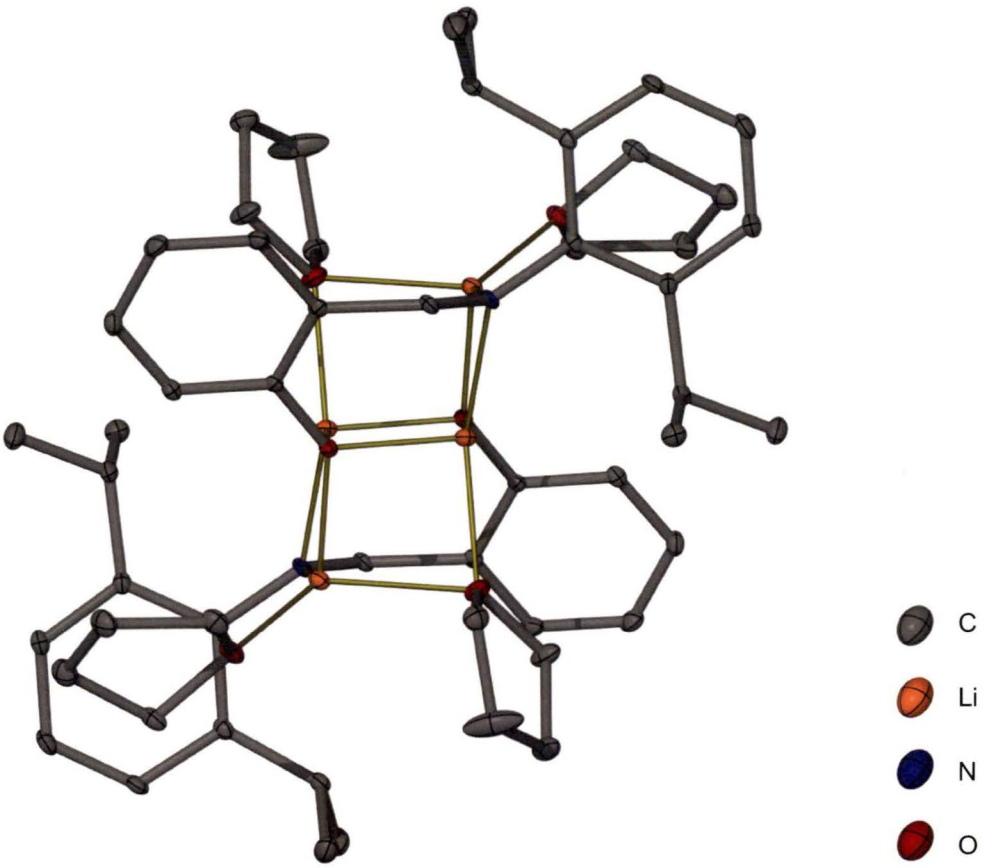

Figure 2-26: Side on view of the molecular structure of [{Li_2(ONDIPP)}$_2$(THF)$_4$] **12** with thermal ellipsoids drawn at the level of 20 % probability. Hydrogen atoms removed for clarity.

The two complexes [{Li_2(ONPh)}$_2$(THF)$_6$] **11** and [{Li_2(ONDIPP)}$_2$(THF)$_4$] **12** are centrosymmetric dimers and share the same $Li_4O_2N_2$ four-rung ladder core, arranged in an analogous way to that of **XIV**. The core consists of two distinct pairs of anions: two internal phenoxide anion pairs and two outer amide anion pairs. The internal two rungs of the ladder are formed by the two lithium phenoxide groups aggregating into a stacked pair creating a Li_2O_2 ring, which resembles a face of the cubic cores observed for the monolithiated complexes. The outer two rungs of the ladder are formed by the two lithium amide groups stacking in a laddering fashion, creating two Li_2ON rings that extend from opposite edges of the central Li_2O_2 ring in an *anti* arrangement. The arrangement of the $Li_4O_2N_2$ core is the same for both THF solvated complexes. The Li-O bond lengths are in the range of 1.87(2)-2.005(8) Å

and compare well with those observed in the unsolvated monolithiated complexes. In both of the complexes the dilithiated ligand adopts a three-rung edge strapping position, with the phenoxide anion contributing to the inner ladder rung and the amide anion contributing to the outer ladder rung.

In the less bulky dilithiated complex $[\{Li_2(ONPh)\}_2(THF)_6]$ **11** there is sufficient room surrounding the $Li_4O_2N_2$ core to accommodate six solvating THF molecules; there is one THF molecule coordinated to each of the lithium centres of the inner Li_2O_2 ring, thus forming two approximately tetrahedral four coordinate tri-anion (O3, N) lithium centres. The lithium atoms making up the outer two ladder rungs of the core are each solvated by two THF molecules, thus forming two approximately tetrahedral four coordinate di-anion (O3, N) centres. With the extra bulk of the substituted *N*-aryl rings in the complex $[\{Li_2(ONDIPP)\}_2(THF)_4]$ **12** there is no longer sufficient room to accommodate the same number of THF molecules and a total of four are incorporated into the complex. The outer lithium centres are still solvated by two of these THF molecules and again have approximately tetrahedral di-anion (O3,N) centre. Similarly, the inner two lithium centres are solvated by a single THF molecule and are approximately tetrahedral tri-anion (O3, N) centres. However, one of each of the THF molecules forming the di-anion (O3,N) lithium centres is also acting as the Lewis basic donor to a tri-anion lithium centre within the Li_2O_2 rings, thus it is in a bridging arrangement. This bridging arrangement results in the oxygen of the THF molecules positioned as a pseudo vertex of a double cubic stack. Complexes with double cubic stacks have been observed in mixed metal systems.[76, 121, 122] An example of a double cubic stack complex is illustrated in the following section in Figure 2-30.

As well as the reduced Lewis basic incorporation in the complex $[\{Li_2(ONDIPP)\}_2(THF)_4]$ **12** another significant effect of the increased bulk

surrounding the nitrogen anion is that there is a major conformational change in the orientation of the methylene group(s) within the complex. In the less bulky complex $[\{Li_2(ONPh)\}_2(THF)_6]$ **11** the methylene group is orientated towards the centre of the complex and is positioned over the face of the ladder core, as seen in the front on view of the complex in Figure 2-23. In the bulkier complex $[\{Li_2(ONDIPP)\}_2(THF)_4]$ **12** however, the orientation of the methylene has changed as a result of accommodating the larger substituent on the nitrogen atom and is orientated away from the centre of the complex and is no longer positioned over the core. This can be seen in the front view of the complex in Figure 2-25. This observation is assumed to be linked to the contrasting reactivity of the dimeric dilithiated complexes towards acyclic ether type Lewis basic donor molecules and is discussed in Chapter 3.

Small colourless crystals of the dilithiated THF solvated complex $[\{Li_2(ONPh)\}_4(THF)_4]$ **13** suitable for X-ray crystal structure determination using the PX1 beam line at the Australian Synchrotron were grown by heating the material in benzene to 100 °C overnight in a sealed NMR tube fitted with a Young's tap. The crystals belong to the tetragonal space group $P4_2/n$ (No. 86), $a = 17.315(2)$, $c = 11.728(2)$ Å, with 2 $Li_8O_4N_4$ molecules in the unit cell and the asymmetric unit consisting of ¼ molecule of $[\{Li_2(ONPh)\}_4(THF)_4]$ **13**, with molecules residing on S_4 symmetry sites. The molecular structure of **13** is shown in Figure 2-27 and Figure 2-28.

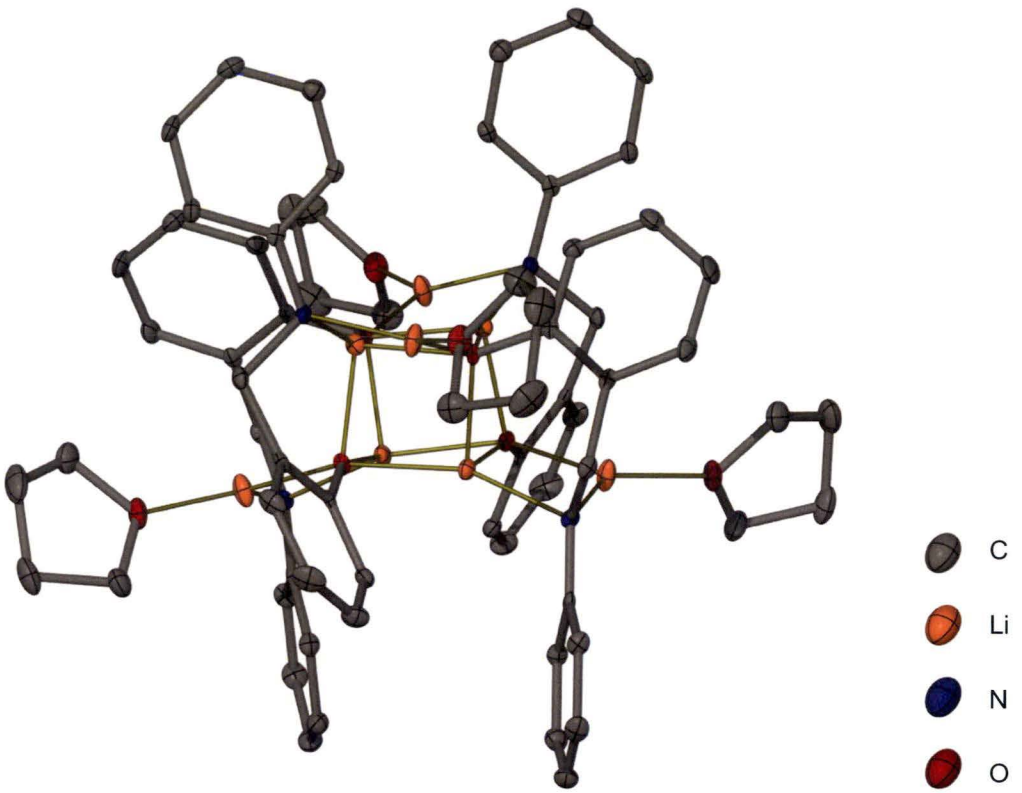

Figure 2-27: Molecular structure of [{Li_2(ONPh)}$_4$($THF)_4$] **13** with thermal ellipsoids drawn at the level of 50 % probability. Hydrogen atoms removed for clarity.

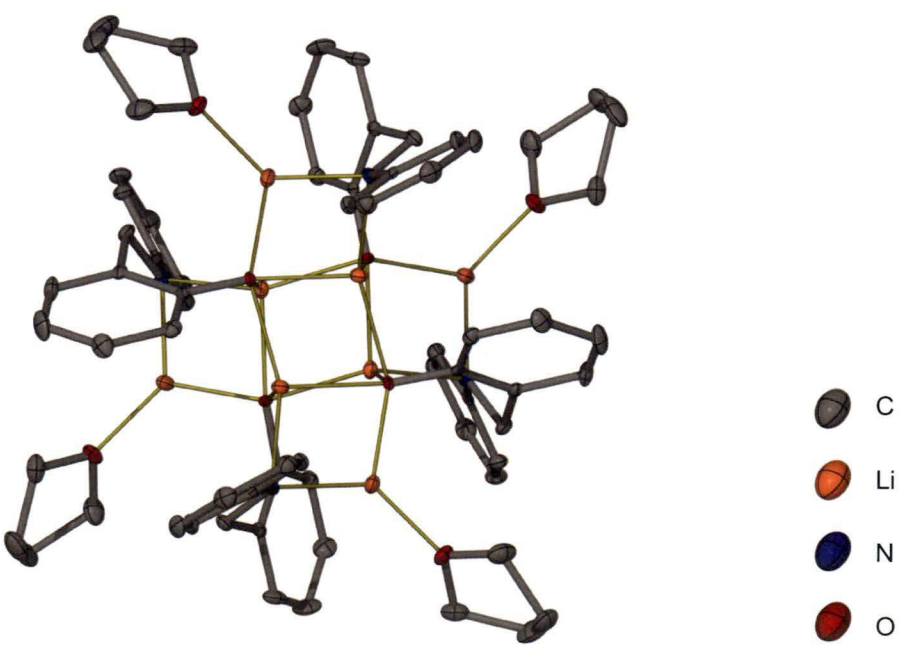

Figure 2-28: Top down view of the molecular structure of [{Li_2(ONPh)}$_4$($THF)_4$] **13** with thermal ellipsoids drawn at the level of 50 % probability. Hydrogen atoms removed for clarity.

The complex $[\{Li_2(ONPh)\}_4(THF)_4]$ **13**, is a tetramer. The four phenoxide anions form the inner part of the core and resemble the cubic cores of the monolithiated complexes in Section 2.3.3. The four nitrogen centres are now, however, amide anions and each form a single rung ladder extending away from the cube as Li_2ON rings. The amide ladder sections are arranged in two pairs; the first pair extend off opposite edges of the bottom face of the cube as shown in Figure 2-27, and the second pair extend off the alternate pair of opposite edges of the top face of the cube as shown in Figure 2-28. This creates the overall appearance of a 'double ladder' where two of dimers of $[\{Li_2(ONPh)\}_2(THF)_6]$ **11** have changed from an *anti* ladder arrangement to a *syn* ladder arrangement and fused their inner two central Li_2O_2 rings together in perpendicular fashion. The arrangement of the ligands within the tetramer is, however, not as such. The arrangement is more akin to a monolithiated complex having formed with all of the ligands orientated parallel to each other, and subsequently have been deprotonated at the amine site, with the ligands in the dilithiated tetramer $[\{Li_2(ONPh)\}_4(THF)_4]$ **13** adopting the same three-rung edge strapping positions as seen in the dilithiated dimers, but in alternating positions around the cube.

The complex $[\{Li_2(ONPh)\}_4(THF)_4]$ **13** contains two types of lithium centres; the inner lithiums form the familiar Li_4O_4 cube and are all four coordinate tetra-anion (O3, N) centres, however due to the laddering sections extending off the Li_4O_4 cube in approximately the same plane as the adjacent cube face, these lithium centres are no longer tetrahedral, are closer to a seesaw geometry. The oxygen atoms in the Li_4O_4 core of $[\{Li_2(ONPh)\}_4(THF)_4]$ **13** are also different to the oxygen atoms in the Li_4O_4 cores of the monolithiated complexes, as they are now five coordinate (C, Li4) and like the inner lithium centres of **13**, approximate a seesaw geometry. The geometry of these centres is shown in Figure 2-27.

The amide containing laddering portions of the dilithiated tetramer contain lithium centres that are only three coordinate (O2, N) and have a trigonal planar geometry. In the dilithiated dimers the amide containing rungs of the ladder have their lithium centre solvated by two THF molecules, as there is sufficient space to accommodate them. However, in the more sterically demanding tetramer there is sufficient room for only a single molecule of THF to solvate the amide lithiums. This reduction of electron density being donated onto the three coordinate (O2, N) lithium centres results in a significant reduction of the Li-N distances from 2.029(9)-2.06(1) Å in $[\{Li_2(ONPh)\}_2(THF)_6]$ **11** to 1.949(2) Å in $[\{Li_2(ONPh)\}_4(THF)_4]$ **13**.

2.3.7. Dilithiated O/N complexes – TMEDA adducts

Each of the two dilithiated THF solvated complexes $[\{Li_2(ONPh)\}_2(THF)_6]$ **11** and $[\{Li_2(ONDIPP)\}_2(THF)_4]$ **12** undergo ligand exchange reactions to form the two TMEDA solvated complexes $[\{Li_2(ONPh)\}_2(TMEDA)_3]$ **14** and $[\{Li_2(ONDIPP)\}_2(TMEDA)_2]$ **15** in >99 and 75 % yield, respectively, as shown in Scheme 2-6.

The dilithiated THF solvated dimer complex $[\{Li_2(ONPh)\}_2(THF)_6]$ **11** is soluble in TMEDA giving a pale yellow solution. Despite showing moderate solubility in TMEDA, a non-saturated solution of the TMEDA solvated complex $[\{Li_2(ONPh)\}_2(TMEDA)_3]$ **14** will precipitate out well formed crystals of the product if left standing for 1-2 hours. The solution can be taken to dryness yielding $[\{Li_2(ONPh)\}_2(TMEDA)_3]$ **14** free from THF and in approximately quantitative yield. Contrastingly, the bulkier dilithiated THF solvated complex $[\{Li_2(ONDIPP)\}_2(THF)_4]$ **12** is not observably soluble in TMEDA but will still undergo a ligand exchange reaction producing microcrystalline solid product,

[{Li_2(ONDIPP)}$_2$(TMEDA)$_2$] **15**. This TMEDA adduct shows very poor solubility in TMEDA and is very difficult to purify. Attempting to recrystallise [{Li_2(ONDIPP)}$_2$(TMEDA)$_2$] **15** from toluene results in a similar microcrystalline product.

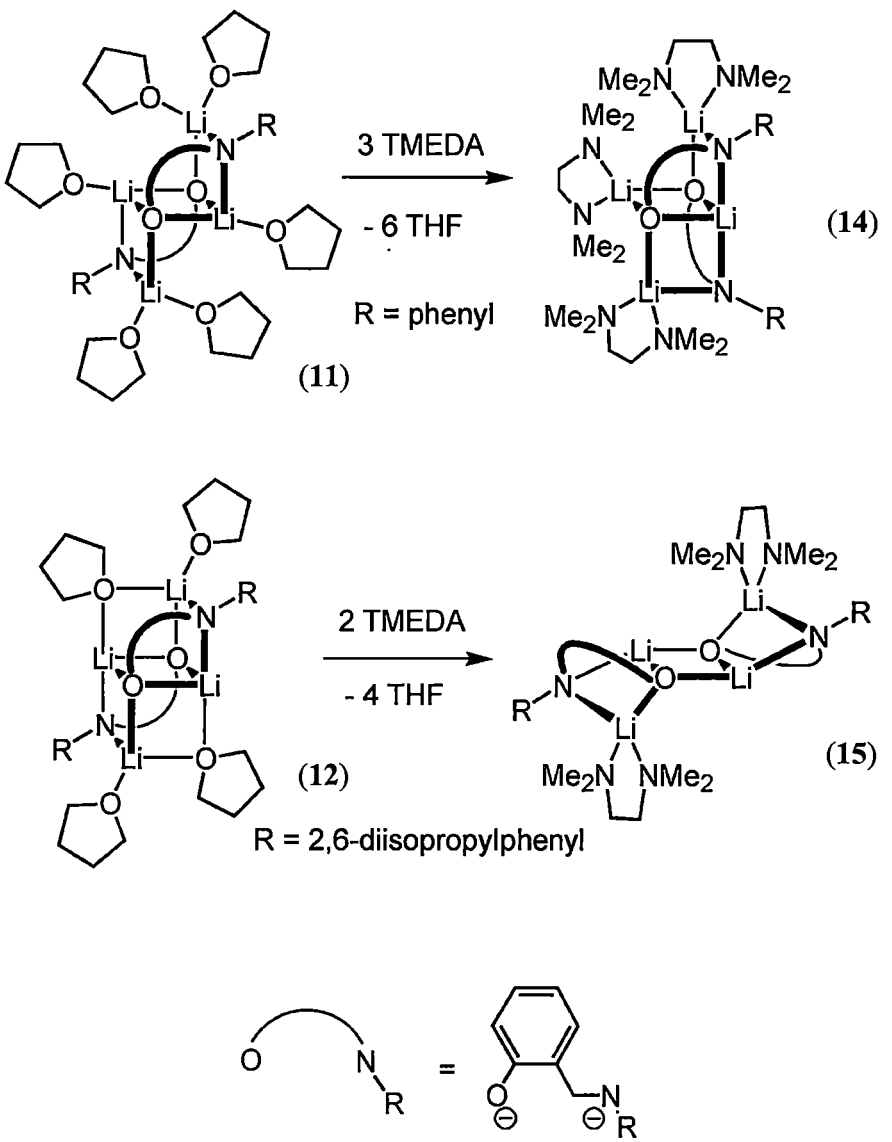

Scheme 2-6: Solvation of [{Li_2(ONPh)}$_2$(THF)$_6$] **11** and [{Li_2(ONDIPP)}$_2$(THF)$_4$] **12** with TMEDA to give complexes [{Li_2(ONPh)}$_2$(TMEDA)$_3$] **14** and [{Li_2(ONDIPP)}$_2$(TMEDA)$_2$] **15**.

The *N*-phenyl substituted complex [{Li_2(ONPh)}$_2$(TMEDA)$_3$] **14** and the bulkier *N*-2,6-diisopropylphenyl substituted complex [{Li_2(ONDIPP)}$_2$(TMEDA)$_2$] **15** were characterised by X-ray crystal structure determination, ^{1}H NMR spectroscopy and

elemental analysis. A ^{13}C NMR spectrum was only able to be obtained for complex **14**, as **15** is insufficiently soluble in benzene.

Both dilithiated TMEDA solvated complexes are dimers in the solid state. Although each dimer contains the same stoichiometry in its core as the THF solvated dimers of $Li_4O_2N_2$, the geometry of both TMEDA solvated dimers are different to the THF solvated dimers, and different to each other. This is unsurprising in the *N*-phenyl complex $[\{Li_2(ONPh)\}_2(TMEDA)_3]$ **14**, as the six sites of Lewis basic solvation around the ladder arrangement of the $Li_4O_2N_2$ core (observed in the THF solvated complex) are distributed as two pairs of sites, and two single sites; each lithium centre associated with the amide rungs of the ladder accommodating a pair of adjacent THF molecules, and each lithium centre associated with the phenoxide rungs of the ladder accommodating a single THF molecule. As the lithium centres accommodating the single Lewis basic interaction are on opposite sides of the molecule, it is impossible for a TMEDA to interact in a typical chelated bidentate way to both of these sites simultaneously. The solvation of this dilithiated dimer by six Lewis basic interactions arising from three molecules of TMEDA is achieved by the complex undergoing a structural rearrangement of its core to adopt an asymmetrical or 'grafted' ladder arrangement. This maintains the familiar three rings (Li_2O_2 and 2x Li_2ON) of the $Li_4O_2N_2$ ladder, however the two Li_2ON rings containing the laddering amide rungs extend of adjacent faces of the central phenoxide ring as shown in Figure 2-29.

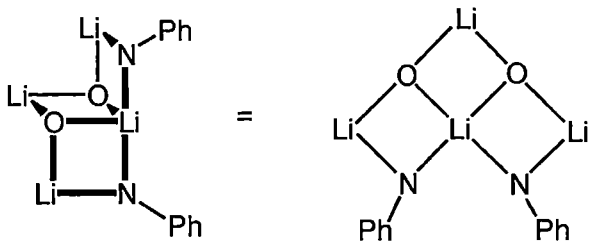

Figure 2-29: Two alternate views of the core of complex [{Li_2(ONPh)}$_2$(TMEDA)$_3$] **14**. The structure shown on the right represents the core of the complex when viewed from above, parallel with the central Li_2O_2 ring.

This grafted ladder arrangement of the eight atoms comprising the core of complex **14** is observed within of a handful of larger structures,[123, 124] as shown in Figure 2-30.[125] However, it is believed that as a discrete molecular core it is unique and only a single other report of a discrete molecular structure containing this grafted ladder arrangement of an organolithium complex was able to be found.[126]

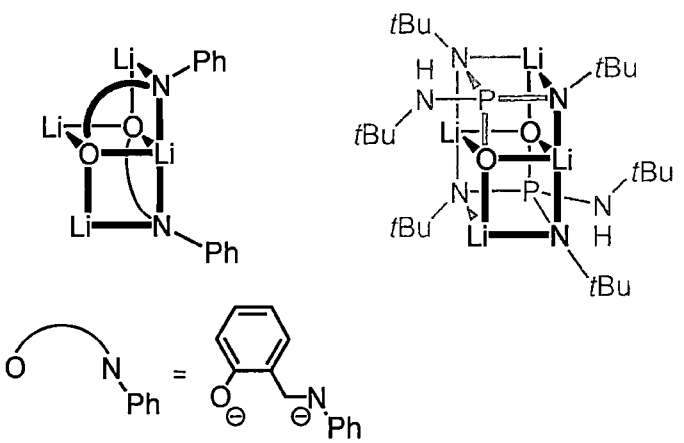

Figure 2-30: Illustration of the $Li_4O_2N_2$ grafted core of [{Li_2(ONPh)}$_2$(TMEDA)$_3$] **14** as part of a larger complex core.

The bulkier *N*-2,6-diisopropylphenyl substituted TMEDA complex does not have the same restriction regarding the accommodation of the Lewis basic solvation of TMEDA, as the four sites occupied by THF in the precursor complex are arranged around the $Li_4O_2N_2$ core in two pairs, each of which are sufficiently proximal to in theory allow two TMEDA molecules to solvate the complex, each coordinating in a bidentate fashion. The bulkier complex [{Li_2(ONDIPP)}$_2$(TMEDA)$_2$] **15** does not,

however, maintain the same ladder core of the THF precursor complex **12**, which may not be surprising as there are not any examples reported in the literature of tertiary amines bridging two lithium centres as would be required if the ladder core remained unaltered. Instead complex **15** forms a dimer of partially solvated double-butterfly bridging structures giving the $Li_4O_2N_2$ core a new, nearly planar four-rung ladder arrangement which has been labelled a 'face-bridged' ladder. The face-bridged core is still comprised of an inner Li_2O_2 ring comprising the two phenoxide rungs, and two outer Li_2ON rings comprising the amide rungs, however the dilithiated ligand straps between the inner and outer rungs of the ladder diagonally across the outer Li_2ON rings of the ladder in a face bridging arrangement, rather than an 'edge strapping' arrangement observed in the ladder core of the THF adduct **12** as well as the complexes with related structures $[\{Li_2(N(SiMe_3)CH_2CH_2NSiMe_3)\}_2(OEt)_2]$ reported by Gardiner,[127] and $[\{Li_2(N(DIPP)CH_2CH_2N(DIPP))\}_2]$ **XXV**.[101] This allows the terminal amide lithium centres to coordinate to TMEDA in the familiar bidentate fashion, with both Lewis basic interactions to a single centre as shown in Scheme 2-6.

The ^1H NMR spectrum of the dilithiated dianion complex $[\{Li_2(ONPh)\}_2(TMEDA)_3]$ **14** in benzene conveyed very little solution structural information. The aliphatic region only displays sharp resonances for the TMEDA protons, with the methylene protons of the O/N ligand being not clearly visible due to broadening. Similarly, the ^1H NMR spectrum of $[\{Li_2(ONDIPP)\}_2(TMEDA)_2]$ **15** conveyed minimal information. This was exacerbated by the complex being only sparingly soluble in C_6D_6. The resonances are similar to the parent complex $[\{Li_2(ONDIPP)\}_2(THF)_4]$ **12**, with the aromatic region appearing as overlapping multiplets but only extending as far upfield as approximately 6.6 ppm. The methylene proton resonance appears as a broad singlet centred at 4.66 ppm and the

methine proton resonance appears as a multiplet centred at 3.65 ppm. The remaining protons from the CH_3 groups and the TMEDA backbone all appear as multiplets between 1.44 and 1.76 ppm with little sharp structure visible.

2.3.8. Molecular structures

Colourless crystals of the TMEDA solvated complex $[\{Li_2(ONPh)\}_2(TMEDA)_3]$ **14** suitable for X-ray crystal structure determination grew from a 70-80 % saturated solution of $[\{Li_2(ONPh)\}_2(THF)_6]$ **11** in TMEDA left standing at room temperature for 30 mins. The crystals belong to the monoclinic space group *C*2/*c* (No. 15), $a = 12.188(5)$, $b = 20.725(4)$, $c = 18.85(4)$ Å, $\beta = 98.27(9)$ °, with 4 $Li_4O_2N_2$ molecules in the unit cell and the asymmetric unit consisting of ½ molecule of $[\{Li_2(ONPh)\}_2(TMEDA)_3]$ **14** having C_2 crystallographic symmetry. The molecular structure of **14** is shown in Figure 2-31 and Figure 2-32.

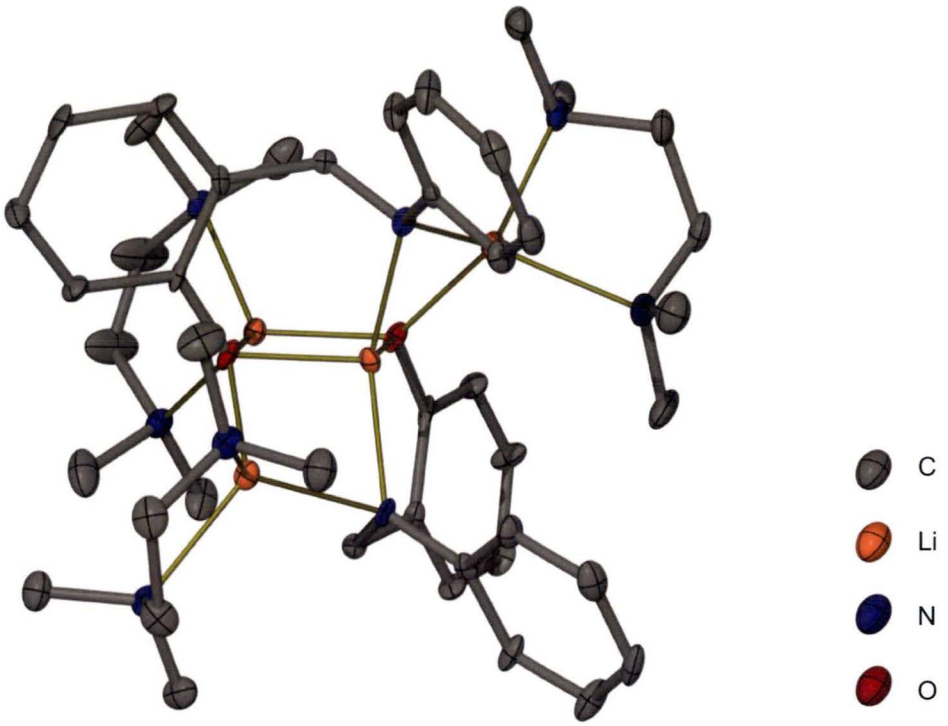

Figure 2-31: Front on view of the molecular structure of [{Li_2(ONPh)}$_2$(TMEDA)$_3$] **14** with thermal ellipsoids drawn at the level of 20 % probability. Hydrogen atoms removed for clarity.

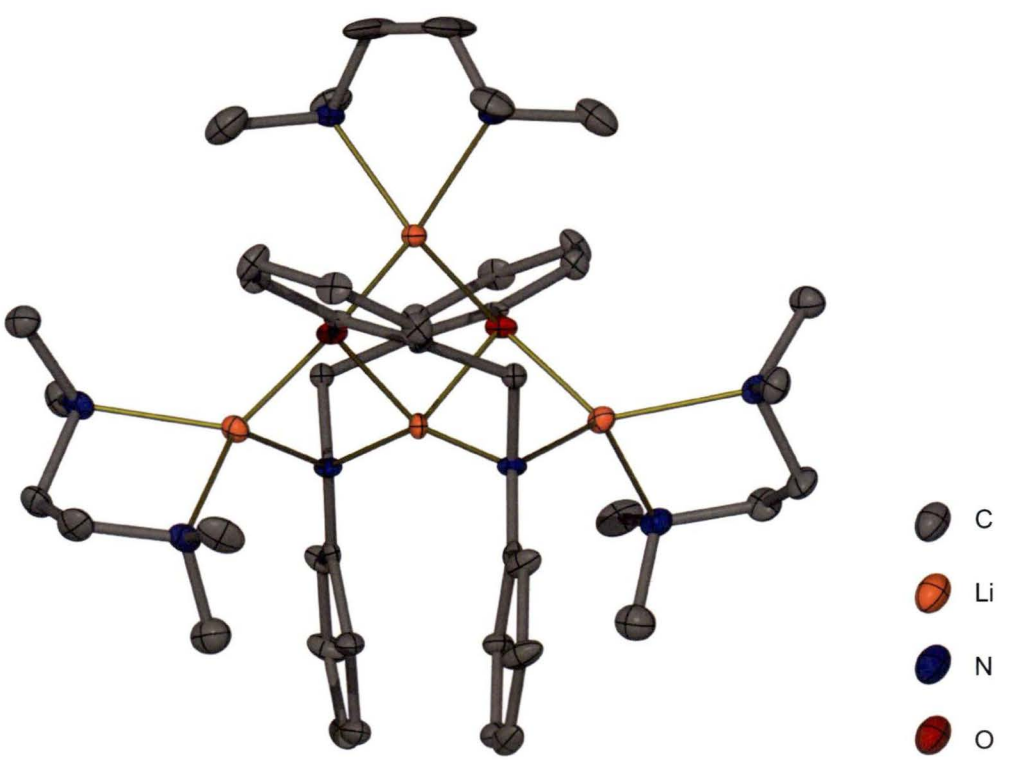

Figure 2-32: Molecular structure of [{Li_2(ONPh)}$_2$(TMEDA)$_3$] **14** viewed parallel with the central Li_2O_2 ring. Thermal ellipsoids drawn at the level of 20 % probability. Hydrogen atoms removed for clarity.

Colourless crystals of the TMEDA solvated complex $[\{Li_2(ONDIPP)\}_2(TMEDA)_2]$ **15** suitable for X-ray crystal structure determination using the PX1 beam line at the Australian Synchrotron grew above a solution of **15** in benzene and TMEDA heated to 90 °C overnight. The crystals belong to the orthorhombic space group $Pca2_1$ (No. 29), $a = 22.3320(13)$, $b = 11.7950(15)$, $c = 18.6970(13)$ Å, with 4 $Li_4O_2N_2$ molecules in the unit cell and the asymmetric unit consisting of one molecule of $[\{Li_2(ONDIPP)\}_2(TMEDA)_2]$ **15**. The dimer is non-crystallographically centrosymmetric. The molecular structure of **15** is shown in Figure 2-33 and Figure 2-34.

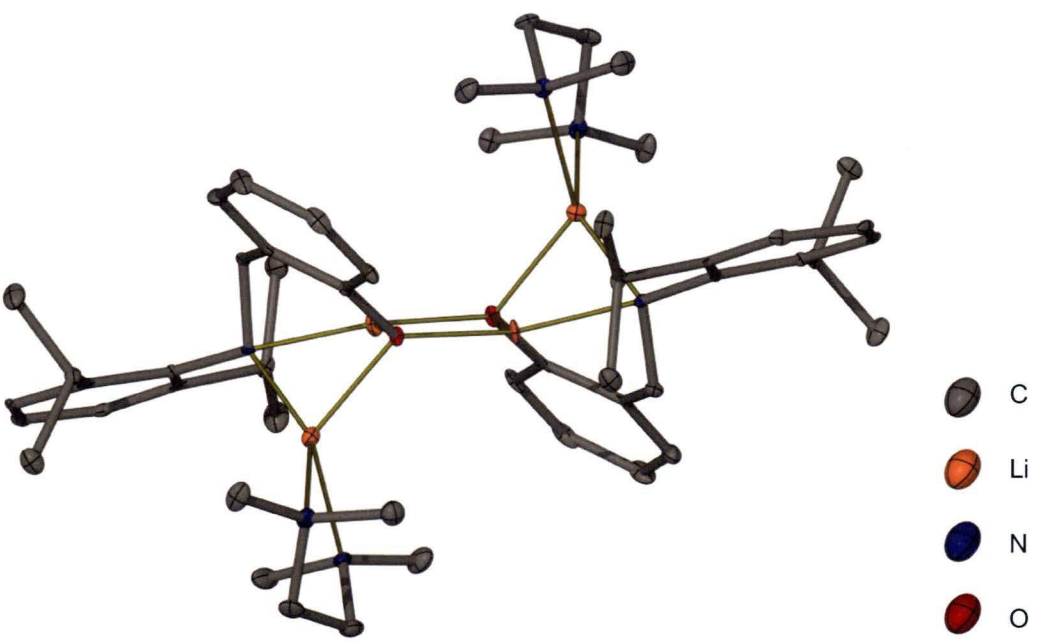

Figure 2-33: Side on view of the molecular structure of $[\{Li_2(ONDIPP)\}_2(TMEDA)_2]$ **15** with thermal ellipsoids drawn at the level of 50 %. Hydrogen atoms removed for clarity.

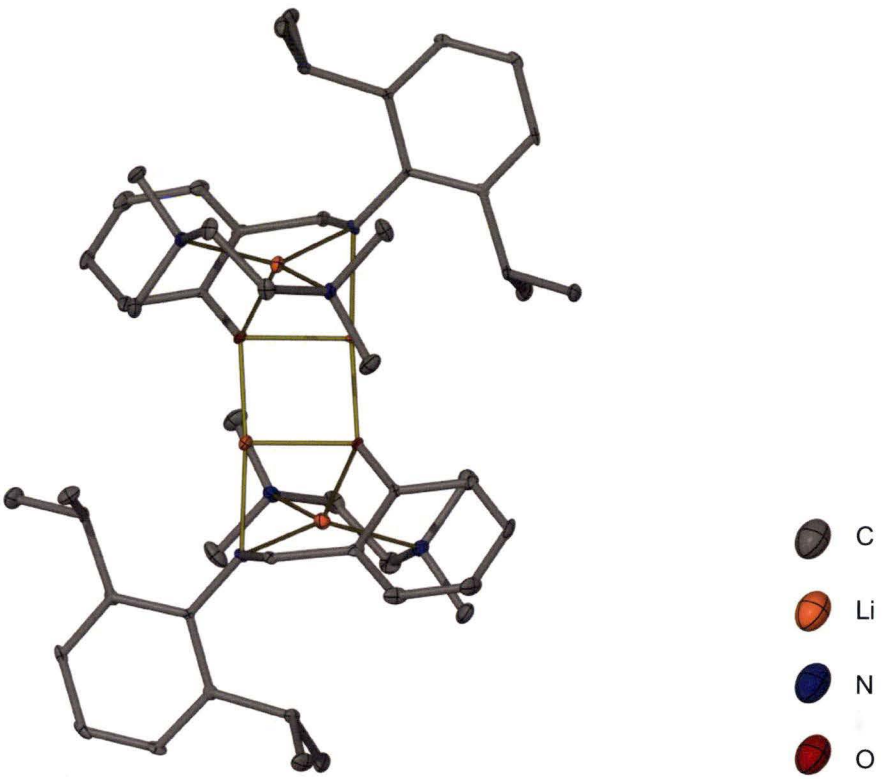

Figure 2-34: Side on view of the molecular structure of [{Li_2(ONDIPP)}$_2$(TMEDA)$_2$] **15** with thermal ellipsoids drawn at the level of 50 % probability. Hydrogen atoms removed for clarity.

The core of the *N*-phenyl substituted complex [{Li_2(ONPh)}$_2$(TMEDA)$_3$] **14** has a central Li_2O_2 ring formed by the phenoxide anions analogous to the dilithiated THF solvated dimer complex, as well as two outer Li_2ON rings formed by the amide anions. The outer two Li_2ON rings extend off adjacent faces of the Li_2O_2 rings, giving rise to the only tetra-anion four coordinate lithium centre observed within the dilithiated dimeric O/N complexes. This lithium centre participates in all three rings of the core is unique thus far in this report as being a four coordinate (O2, N2) centre attached to four monodentate anions. Noted by the authors who reported the other asymmetrical ladder, this type of coordination for a lithium centre to four monodentate anions within organolithium chemistry is rare.[126] By adopting this grafted arrangement, the two different anion types are able to maintain the observed aggregation tendencies as in the THF complex of stacking and laddering, whilst

opening up three of the lithium centres to be solvated by the bidentate TMEDA molecules and maintain the previously observed overall solvation number of six seen in the THF adduct **11**. There are three types of lithium centre within the complex; the tetra-anion four coordinate (O2, N2) centre, as well as two tetrahedral four coordinate (O, N3) centres in the outer Li_2ON rings, and one tetrahedral TMEDA chelated four coordinate (O2, N2) centre in the Li_2O_2 ring. The rearrangement of the core has done little to affect the distances between centres, the Li-O distances all still fall in the range 1.924(9)-1.98(1) Å and the two Li-N distances along the ladder edge are both 2.033(7) Å. The length of the outer amide ladder rungs are the only discernibly different interaction, appearing longer than in the THF solvated complexes at 2.16(1) Å compared to 2.029(9)-2.06(1) Å. This change is likely to be linked to the different Lewis basic donor atom rather than the change in the core of the complex.

The bulkier *N*-2,6-diisopropylphenyl substituted complex is prevented from accommodating three TMEDA molecules in the same way and forms a dimer with a linear $Li_4O_2N_2$ four-rung ladder core. Though adopting a different core, complex **15** contains many of the features of the analogous THF adduct **12**; there are three rings within the dimer, the central Li_2O_2 ring incorporating the phenoxide anions and the two Li_2ON rings containing the amide groups and forming the ladder like rungs extending from opposite edges of the inner Li_2O_2 ring. However, the dilithiated ligand adopts a face bridging arrangement diagonally across each of the outer Li_2ON rings of the core *anti* to each other. This alteration to the arrangement of the amide anion growth (relative to the grafted ladder of **12**) outwards from the central Li_2O_2 ring provides two free coordination sites on each of the two lithium atoms within the amide ladder rungs, allowing two molecules of TMEDA to coordinate to the terminal lithium centres in a bidentate fashion. The internal two lithium atoms contained

within the Li_2O_2 ring remain unsolvated and hence are three coordinate (O2, N) and have approximately T-shaped geometries. This modification of the $Li_4O_2N_2$ four-rung ladder core to a face-bridged ladder is likely due to the extra bulk surrounding the amine centres of the TMEDA, rather than the tendency of TMEDA to bind in a chelating manner as solvation of the dilithiated dimer complexes can be achieved with the $Li_4O_2N_2$ four-rung ladder remaining unchanged. This however, would require the TMEDA to coordinate to the complex in a bridging interaction, which would be a novel arrangement for TMEDA and is most likely prevented in complex **15** by steric interactions. It is possible to imagine alternative arrangements where TMEDA bridges not within a single complex but between two discrete dimeric $Li_4O_2N_2$ units, similar to the complex of MeLi with TMEDA, $[((MeLi)_4(TMEDA)_2)_\infty]$, **I** illustrated in Figure 1-3a. The formation of such a complex is presumably less favourable than the formation of **15** with exclusively chelating interactions as observed.

2.3.9. Dilithiated O/N complexes – DME adducts

Each of the two dilithiated THF solvated complexes $[\{Li_2(ONPh)\}_2(THF)_6]$ **11** and $[\{Li_2(ONDIPP)\}_2(THF)_4]$ **12** undergo ligand exchange reactions with DME to form $[\{[Li_2(ONPh)]_2(DME)_3\}_\infty]$ **16**, and $[\{Li_2(ONDIPP)\}_2(DME)_2]$ **17** in 72 and 91 % yield, respectively, as show in Scheme 2-7.

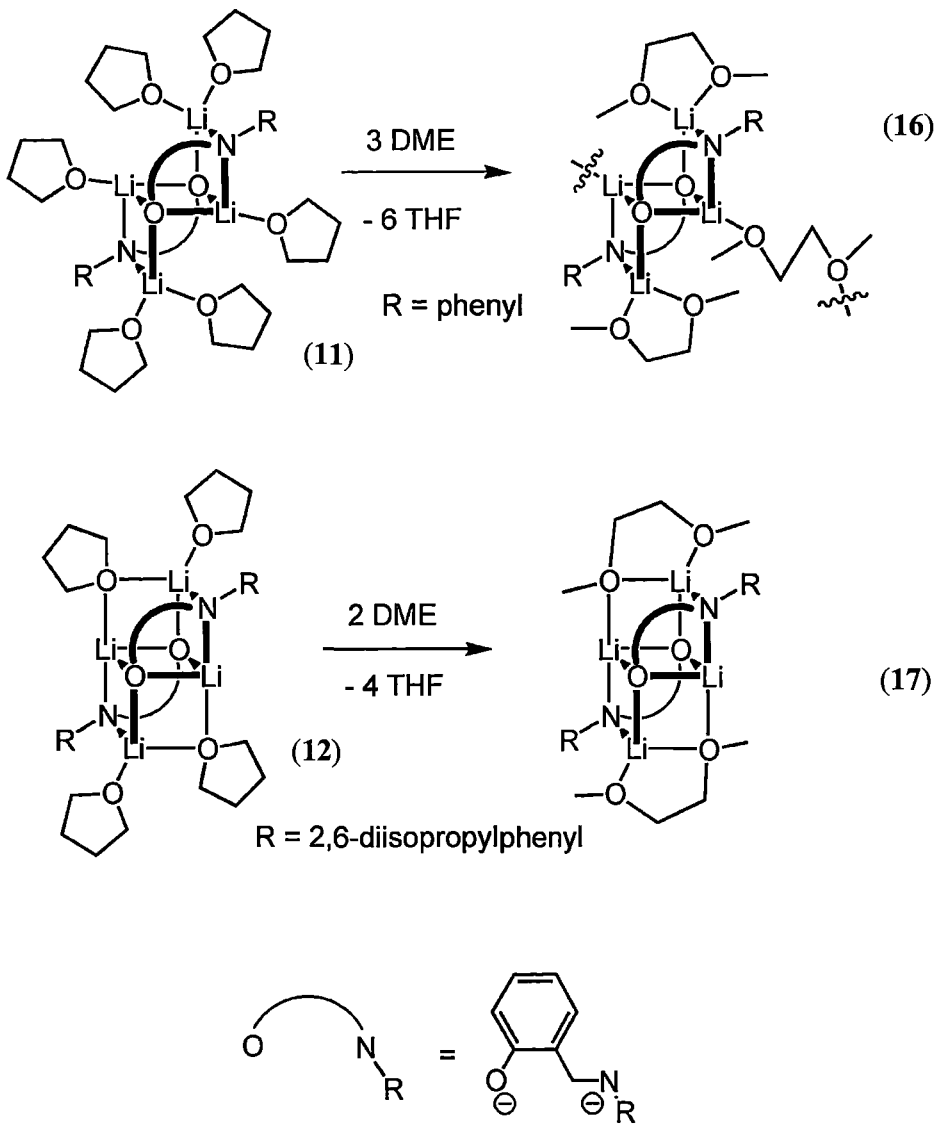

Scheme 2-7: Solvation of $[\{Li_2(ONPh)\}_2(THF)_6]$ **11** and $[\{Li_2(ONDIPP)\}_2(THF)_4]$ **12** with DME to give complexes $[\{[Li_2(ONPh)]_2(DME)_3\}_\infty]$ **16** and $[\{Li_2(ONDIPP)\}_2(DME)_2]$ **17**.

Solutions of each of the dimeric dilithiated THF dimer complexes $[\{Li_2(ONPh)\}_2(THF)_6]$ **11** and $[\{Li_2(ONDIPP)\}_2(THF)_4]$ **12** in benzene had added to them an excess of DME and were left standing overnight resulting in a good crystalline yield of the solvent exchange products $[\{[Li_2(ONPh)]_2(DME)_3\}_\infty]$ **16**, and $[\{Li_2(ONDIPP)\}_2(DME)_2]$ **17**, respectively.

The polymeric complex of the less bulky *N*-phenyl substituted dilithiated ligand $[\{[Li_2(ONPh)]_2(DME)_3\}_\infty]$ **16** was characterised by X-ray crystal structure determination, ^1H, ^{13}C, gCOSY and gHSQC NMR spectroscopy and elemental

analysis. The complex $[\{Li_2(ONDIPP)\}_2(DME)_2]$ **17** was characterised by X-ray crystal structure determination, ^1H NMR spectroscopy and elemental analysis. Complex **17** was insufficiently soluble in benzene to obtain a ^{13}C NMR spectrum.

Both complexes maintain the same $Li_4O_2N_2$ four-rung ladder cores as their precursor THF solvated complexes. Complex $[\{[Li_2(ONPh)]_2(DME)_3\}_\infty]$ **16** is a polymeric chain, each dimeric $Li_4O_2N_2$ unit linked by a bridging DME molecule. Complexes with DME bridging in this fashion exist, in both discrete dimeric complexes as well as polymers.[128-132] Both of the DME substituted complexes **16** and **17** also maintain the same degree of solvation by Lewis basic interactions as its precursor THF solvated complex with the oxygen donor atoms of the DME ligands positioned approximately in the same positions occupied by the oxygen centres from the THF.

Complex $[\{[Li_2(ONPh)]_2(DME)_3\}_\infty]$ **16** dissolves in benzene to give an ^1H NMR spectrum similar to its precursor complex $[\{Li_2(ONPh)\}_2(THF)_6]$ **11**. The methylene group appears as a broad multiplet, appearing to arise from two overlapping singlets, centred at approximately 4.36 ppm. The only other aliphatic resonance is from the DME, and somewhat surprisingly all of these protons appear as a singlet at 2.75 ppm. The aromatic region is almost without sharp feature, appearing between 6.55 and 7.69 ppm. It might be concluded from the broadness of the ^1H NMR features that the aggregation of complex **16** is fluxional in solution, and does not maintain the polymeric structure observed in the solid state.

Complex $[\{Li_2(ONDIPP)\}_2(DME)_2]$ **17** has a ^1H NMR spectrum more closely resembling that of the initial ligand $ONDIPPH_2$ **5** than the precursor complex $[\{Li_2(ONDIPP)\}_2(THF)_4]$ **12**. The aliphatic proton resonances do not show inequivalence as observed for complex **9** or multiple species in solution as observed for complex **12**. Consequently, the methyl, methine, and methylene resonances

appear as a doublet centred at 1.40 ppm, a heptet centred at 3.72 ppm and a singlet at 4.65 ppm, respectively. The DME proton resonances show some broadening, but are still resolved and integrate correctly. The complex has limited solubility, such that the ^{1}H NMR is likely to be representative of the sample, but minor impurities such as the decomposition product [{Li(ONDIPPH)}$_4$] **9** are disproportionately represented in higher than actual relative concentration. Note that it is not possible to increase the solubility of the complex by heating, as the process of warming begins the decomposition of the complex. It was found that the complex [{Li$_2$(ONDIPP)}$_2$(DME)$_2$] **17** will completely decompose upon heating in benzene yielding the monolithiated complex [{Li(ONDIPPH)}$_4$] **9** as a product. This reactivity is not limited to DME adducts but is however quite selective for a class of chelating Lewis bases and is discussed in detail in Chapter 3.

In addition to the DME substituted complex [{[Li$_2$(ONPh)]$_2$(DME)$_3$}$_\infty$] **16**, the reaction of the THF substituted precursor complex [{Li$_2$(ONPh)}$_2$(THF)$_6$] **11** with *ca.* 10 equivalents of DME on one occasion yielded an alternative, partially DME substituted complex, [{Li$_2$(ONPh)}$_2$(DME)$_2$(THF)$_2$] **18** as shown in Scheme 2-8. This reaction was not able to be repeated.

To a solution of the THF solvated starting complex [{Li$_2$(ONPh)}$_2$(THF)$_6$] **11**, approximately 2 drops of DME was added and the solution left standing overnight resulting in a good crystalline yield of the partially substituted DME complex **18** (65 % yield). The complex was only characterised by X-ray crystal structure determination. The preparation was unable to be repeated despite several attempts, to provide further material for ^{1}H and ^{13}C NMR spectroscopy and elemental analysis.

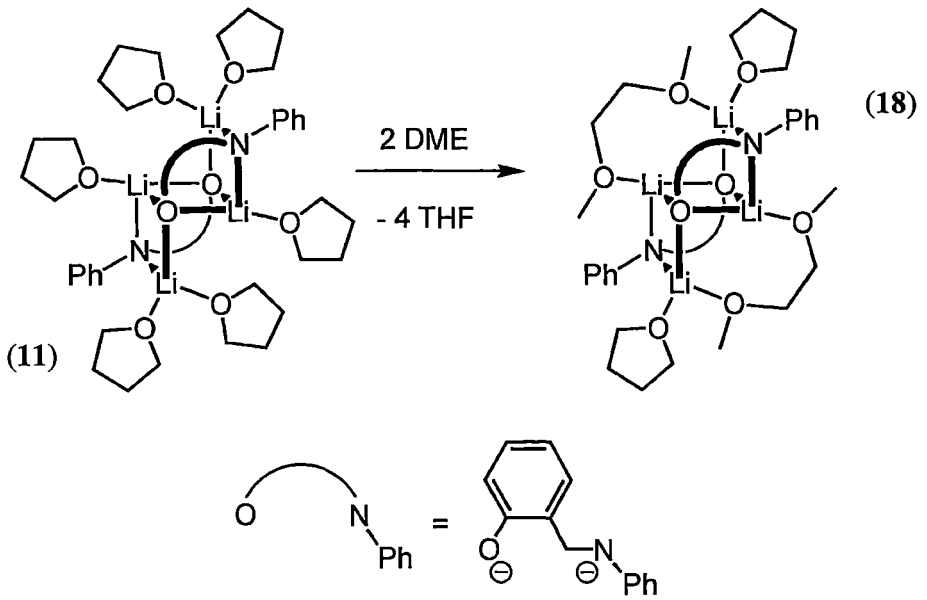

Scheme 2-8: Solvation of $[\{Li_2(ONPh)\}_2(THF)_6]$ **11** with limited DME to give $[\{Li_2(ONPh)\}_2(DME)_2(THF)_2]$ **18**.

The complex **18** is a centrosymmetric dimer with the $Li_4O_2N_2$ core maintained. The complex is a monomeric unit with each $Li_4O_2N_2$ dimer solvated by two THF molecules and two DME molecules, maintaining the total of six Lewis basic donor atoms. The DME adopts a bridging arrangement between the two lithium centres along each edge of the ladder core.

2.3.10. Molecular structures

Colourless crystals of the dilithiated DME solvated complex $[\{[Li_2(ONPh)]_2(DME)_3\}_\infty]$ **16** suitable for X-ray crystal structure determination were grown from a 60-70 % saturated solution of $[\{Li_2(ONPh)\}_2(THF)_6]$ **11** in benzene with DME added and left standing at room temperature overnight. The crystals belong to the monoclinic space group *C*2/*c* (No. 15), $a = 29.949(5)$, $b = 12.601(2)$, $c = 23.499(3)$ Å, $\beta = 112.541(8)$ °, with 8 dimeric $Li_4O_2N_2$ units in the unit cell. The asymmetric unit consisting of two similar ½ dimeric units of

$[\{[Li_2(ONPh)]_2(DME)_3\}_\infty]$ **16** having crystallographic centrosymmetry and a molecule of benzene disordered over a C_2 axis. Complex **16** is a polymer in the solid state; the polymer is built up of repeating dimeric $Li_4O_2N_2$ units, with DME molecules linking the inner lithium centres of each dimeric unit. The structure of $[\{[Li_2(ONPh)]_2(DME)_3\}_\infty]$ **16** is shown in Figure 2-35, Figure 2-36, and Figure 2-37.

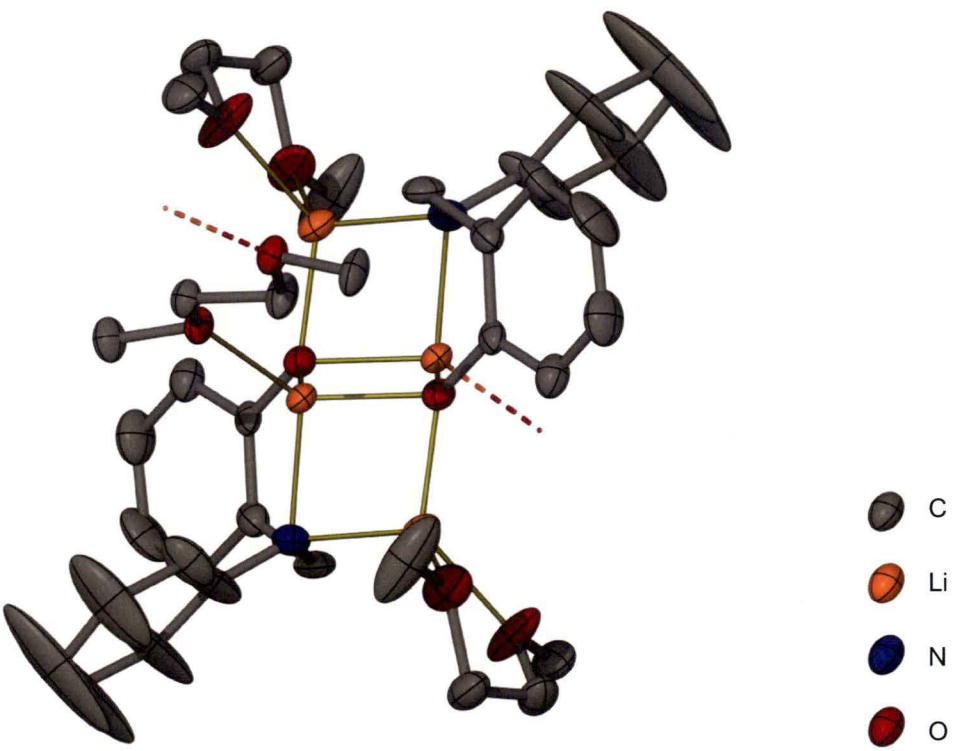

Figure 2-35: Front on view of a dimeric $Li_4O_2N_2$ unit of $[\{[Li_2(ONPh)]_2(DME)_3\}_\infty]$ **16** with thermal ellipsoids drawn at the level of 50 % probability. Hydrogen atoms removed for clarity.

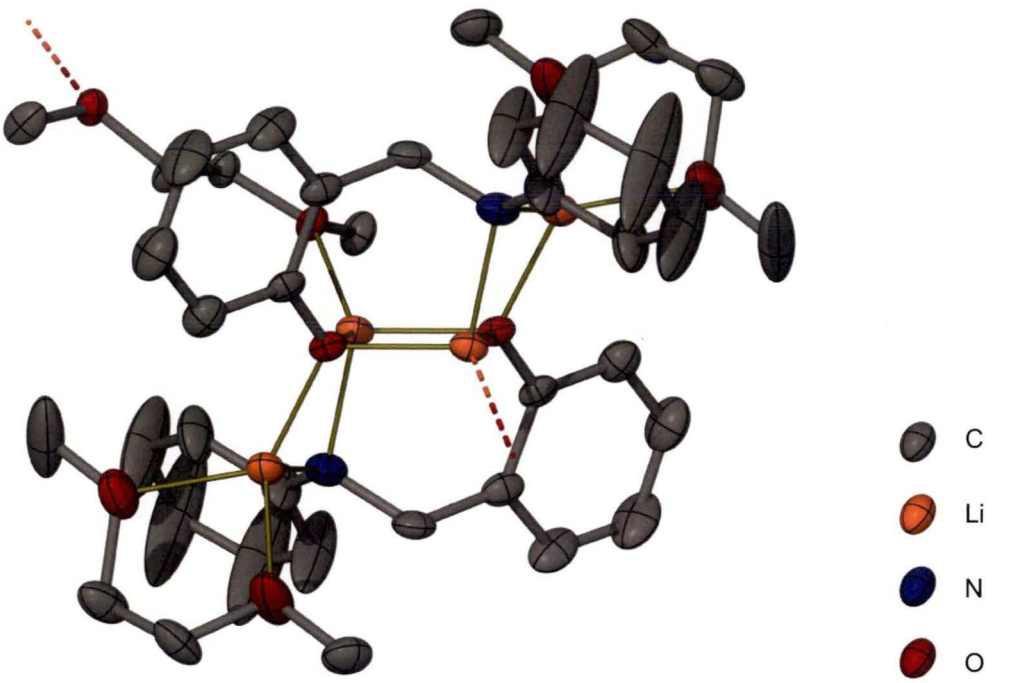

Figure 2-36: Side on view of a dimeric $Li_4O_2N_2$ unit of [{[Li_2(ONPh)]$_2$(DME)$_3$}$_\infty$] **16** with thermal ellipsoids drawn at the level of 50 % probability. Hydrogen atoms removed for clarity.

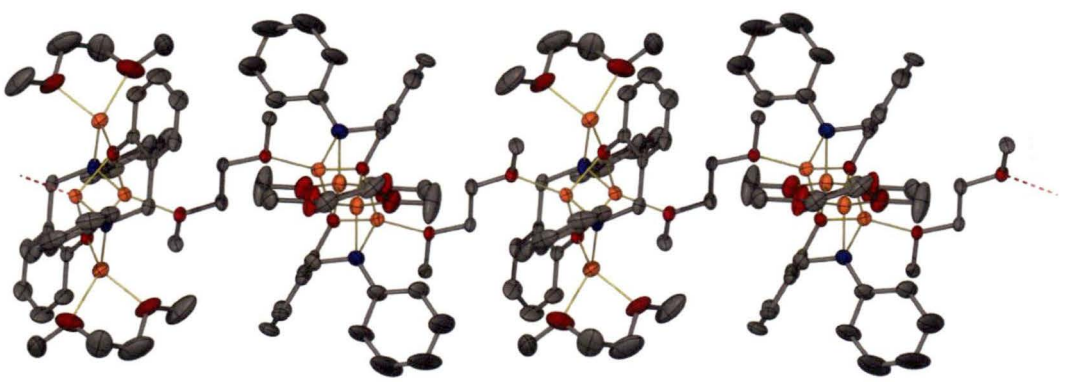

Figure 2-37: Polymeric structure of the complex [{[Li_2(ONPh)]$_2$(DME)$_3$}$_\infty$] **16** with thermal ellipsoids drawn at the level of 50 % probability. Hydrogen atoms removed for clarity.

Colourless crystals of the dilithiated DME solvated complex [{Li_2(ONDIPP)}$_2$(DME)$_2$] **17** suitable for X-ray crystal structure determination were grown from a 70-80 % saturated solution of [{Li_2(ONDIPP)}$_2$(THF)$_4$] **12** in benzene with DME added and left standing at room temperature overnight. The crystals belong to the triclinic space group $P\bar{1}$ (No. 2), $a = 9.0160(15)$, $b = 10.8700(7)$,

c = 11.8900(8) Å, α = 74.341(1), β = 89.522(1), γ = 87.463(3) °, with 1 $Li_4O_2N_2$ molecule in the unit cell and the asymmetric unit consisting of a ½ molecule of $[\{Li_2(ONDIPP)\}_2(DME)_2]$ **17** with crystallographic centrosymmetry.

Crystal structure determination of weakly diffracting crystals of $[\{Li_2(ONDIPP)\}_2(DME)_2]$ **17** as a benzene solvate were also achieved, with crystals belonging to the monoclinic space group *Pc* (No. 14), a = 12.477(15), b = 12.87(3), c = 17.40(3) Å, β = 102.91(12) °, with 2 molecules in the unit cell. The asymmetric unit consisting of one molecule of $[\{Li_2(ONDIPP)\}_2(DME)_2]$ **17** with non-crystallographic, approximate, centrosymmetry and two benzene solvent molecules. Further details of this structure are not presented. The molecular structure of $[\{Li_2(ONDIPP)\}_2(DME)_2]$ **17** is shown in Figure 2-38 and Figure 2-39.

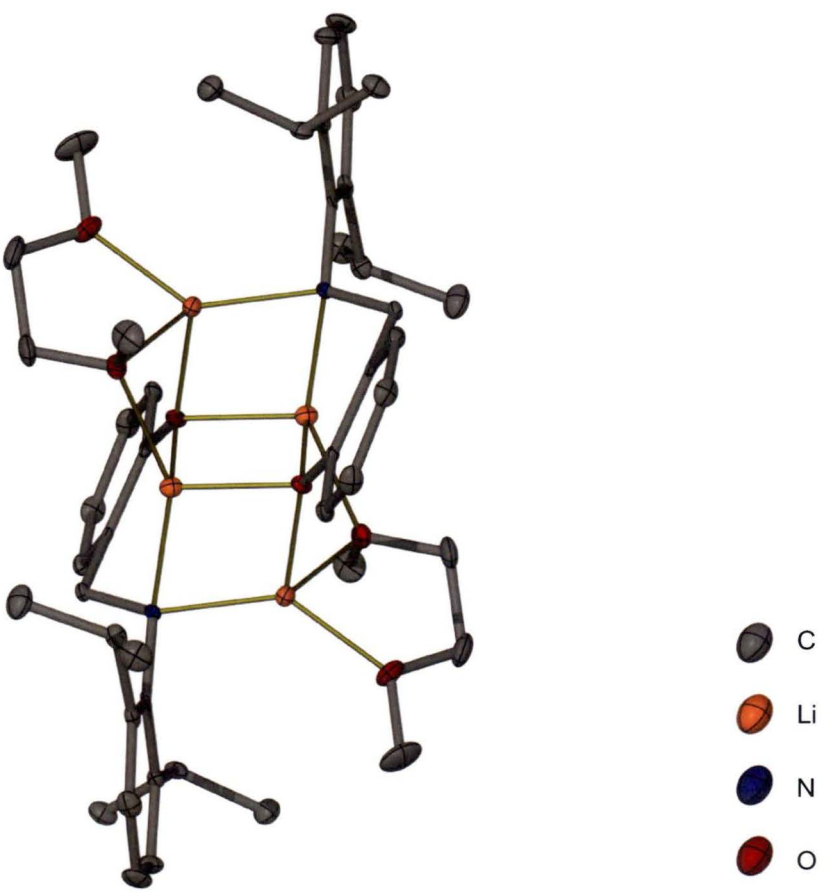

Figure 2-38: Front on view of the molecular structure of $[\{Li_2(ONDIPP)\}_2(DME)_2]$ **17** with thermal ellipsoids drawn at the level of 50 % probability. Hydrogen atoms removed for clarity.

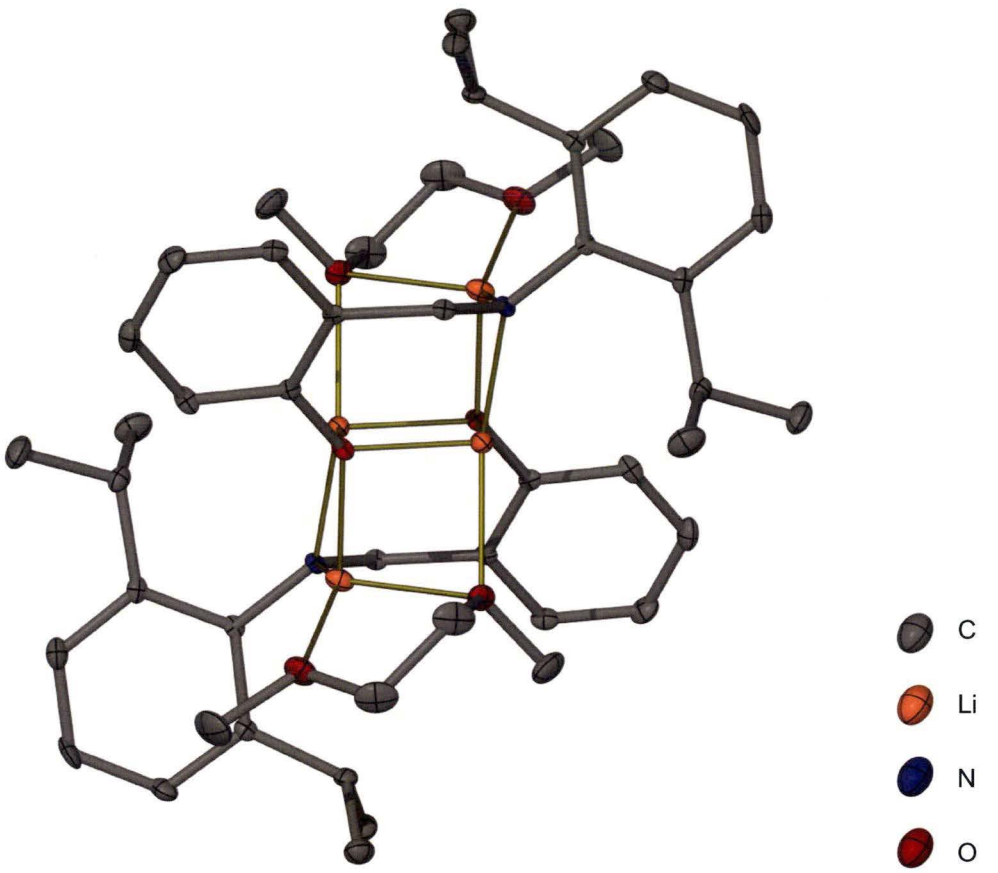

Figure 2-39: Side on view of the molecular structure of [{Li_2(ONDIPP)}$_2$(DME)$_2$] **17** with thermal ellipsoids drawn at the level of 50 % probability. Hydrogen atoms removed for clarity.

The two dilithiated DME solvated complexes [{[Li_2(ONPh)]$_2$(DME)$_3$}$_\infty$] **16**, and [{Li_2(ONDIPP)}$_2$(DME)$_2$] **17** maintain the same $Li_4O_2N_2$ four-rung ladder core as the THF solvated dimers described in Section 2.3.5. The relative positions of the donor atoms surrounding the $Li_4O_2N_2$ core is also maintained upon solvation with DME.

As in the less bulky THF solvated complex [{Li_2(ONPh)}$_2$(THF)$_6$] **11**, here in the DME solvated complex [{[Li_2(ONPh)]$_2$(DME)$_3$}$_\infty$] **16** there is sufficient room surrounding each $Li_4O_2N_2$ dimeric unit core to accommodate a total of six Lewis basic donor interactions. Two of the DME molecules coordinate to each $Li_4O_2N_2$ unit core in a chelating fashion at the terminal amide lithium centres, while the third

molecule coordinates singly to an inner lithium atom of each $Li_4O_2N_2$ dimeric unit with each of its oxygen donor atoms, forming the polymeric chain as shown in Figure 2-37. The DME coordination maintains the same geometries for the lithium centres; the terminal lithium centres being approximately tetrahedral, di-anion (O3, N), and the inner lithium centres being approximately tetrahedral, tri-anion (O3, N).

Similarly, in the bulkier *N*-2,6-diisopropylphenyl substituted complex the total number of Lewis basic donor atoms able to solvate the DME solvated complex $[\{Li_2(ONDIPP)\}_2(DME)_2]$ **17** is four as seen in the THF solvated complex $[\{Li_2(ONDIPP)\}_2(THF)_4]$ **12**. As for the less bulky DME solvated complex $[\{[Li_2(ONPh)]_2(DME)_3\}_\infty]$ **16**, the position of the donor atoms surrounding the $Li_4O_2N_2$ core is maintained upon solvation of the bulkier THF solvated complex **17** with DME. Hence, one end of each DME molecule is singly coordinated to the outer lithium centre within the amide rung, and the other end of each DME molecule is bridging two lithium centres, one from each of the Li_2O_2 and Li_2ON rings on the same side of the ladder as shown in Figure 2-38. This coordination of the DME molecules forms four approximately tetrahedral four coordinate lithium centres, two tri-anion (O3, N) and two di-anion (O3, N), as well as the pseudo double cube stack.

Colourless crystals of the dilithiated DME/THF solvated complex $[\{Li_2(ONPh)\}_2(DME)_2(THF)_2]$ **18** suitable for X-ray crystal structure determination were grown from a 60-70 % saturated solution of $[\{Li_2(ONPh)\}_2(THF)_6]$ **11** in benzene with small amount of DME added and left standing at room temperature overnight. The crystals belong to the monoclinic space group *P*2/*c* (No. 13), $a = 11.1920(11)$, $b = 11.127(4)$, $c = 16.971(2)$ Å, $\beta = 102.245(1)$ °, with 2 $Li_4O_2N_2$ molecules in the unit cell and the asymmetric unit consisting of ½ molecule of $[\{Li_2(ONPh)\}_2(DME)_2(THF)_2]$ **18** with crystallographic centrosymmetry. The

molecular structure of $[\{Li_2(ONPh)\}_2(DME)_2(THF)_2]$ **18** is shown in Figure 2-40 and Figure 2-41.

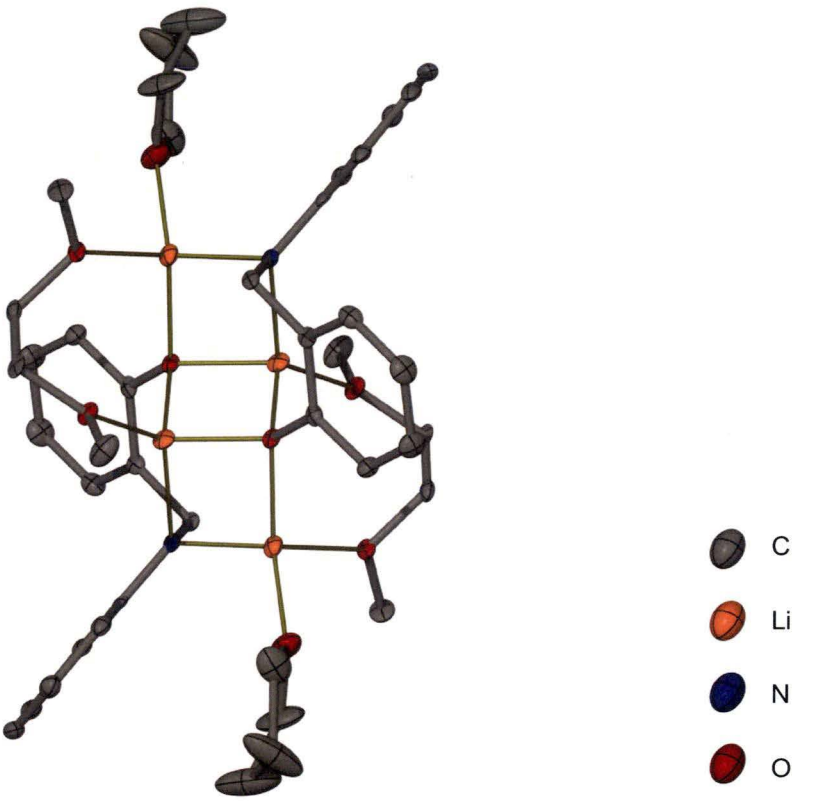

Figure 2-40: Front on view of the molecular structure of $[\{Li_2(ONPh)\}_2(DME)_2(THF)_2]$ **18** with thermal ellipsoids drawn at the level of 50 % probability. Hydrogen atoms removed for clarity.

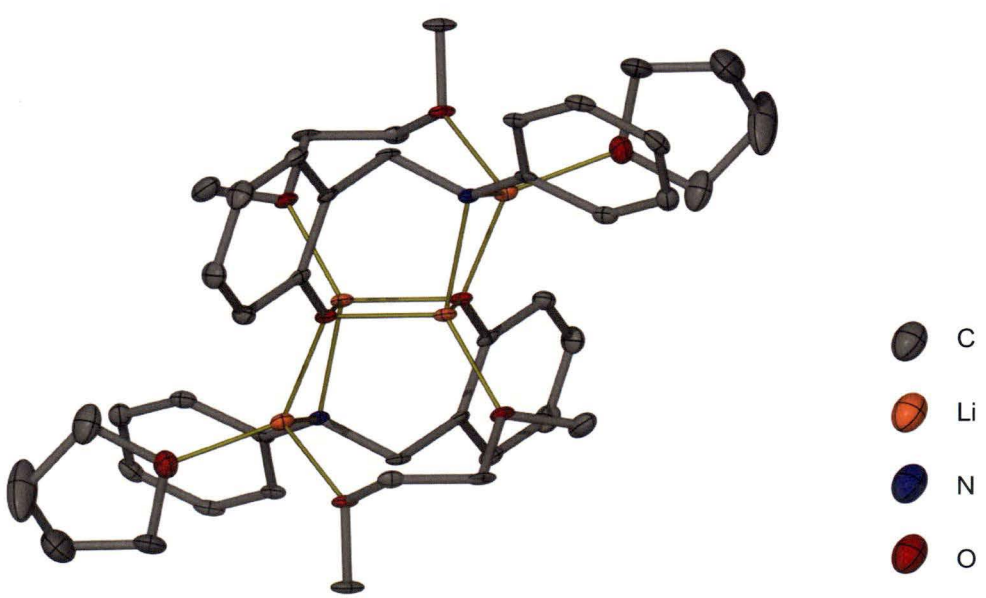

Figure 2-41: Side on view of the molecular structure of $[\{Li_2(ONPh)\}_2(DME)_2(THF)_2]$ **18**, with thermal ellipsoids drawn at the level of 50 % probability. Hydrogen atoms removed for clarity.

The complex $[\{Li_2(ONPh)\}_2(DME)_2(THF)_2]$ **18** maintains the same $Li_4O_2N_2$ four-rung ladder core as the DME solvated dimers described above, which is the same as the THF solvated dimers described in Section 2.3.5. As for $[\{[Li_2(ONPh)]_2(DME)_3\}_\infty]$ **16** the complex **18** has maintained its six Lewis basic interactions from THF in the starting material, four of which have been replaced with interactions with two molecules of DME. Each molecule of DME bridges the two lithium atoms along a single ladder edge, leaving the remaining Lewis basic interactions from THF to the terminal lithium centres. This results in the same coordination for the lithium centres in **18** as was observed in **16**; the terminal lithium centres being approximately tetrahedral, di-anion (O3, N), and the inner lithium centres being approximately tetrahedral, tri-anion (O3, N).

Throughout all of the dimeric dilithiated complexes, with the exception of the two TMEDA solvated complexes, the aggregated core and arrangement of Lewis basic solvation remains unchanged for complexes of each ligand. Illustrated in Figure 2-42 are the THF and DME solvated dimeric complexes showing the retention of structural features between each.

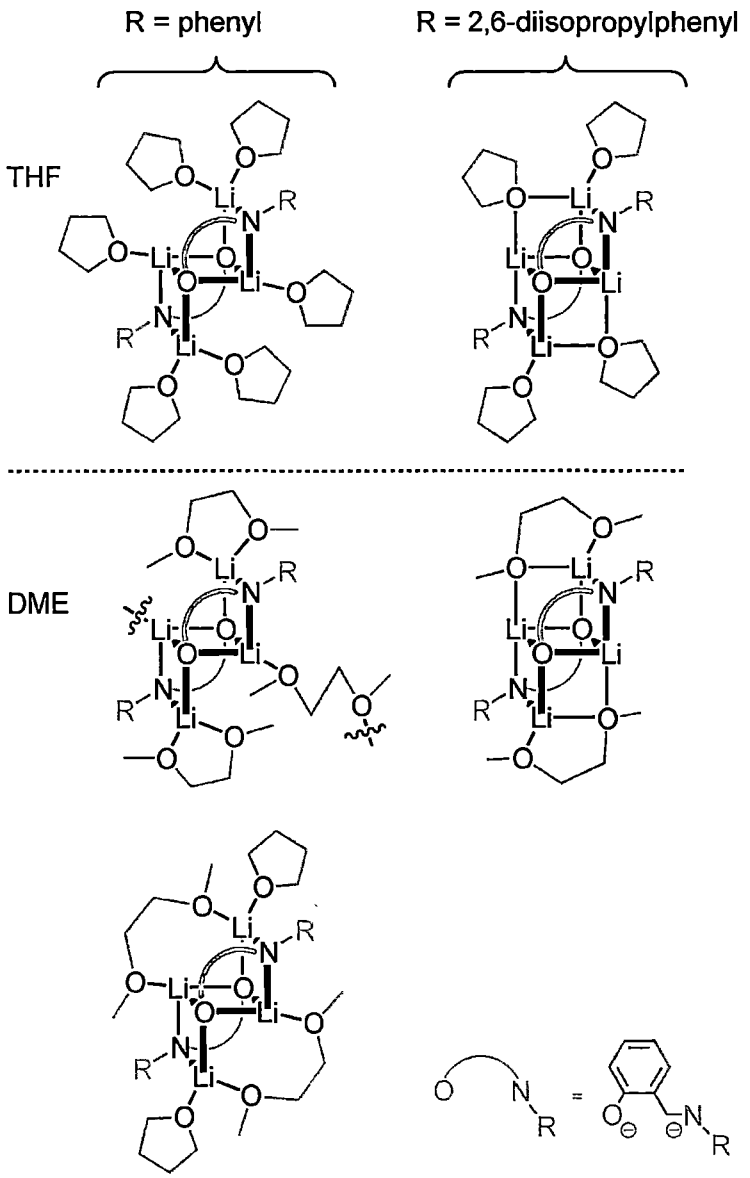

Figure 2-42: Illustration of the retention of structural features of the dimeric dilithiated O/N complexes with varying Lewis basic solvents.

It is significant to note that the details of the structural arrangement of the $Li_4O_2N_2$ ladder cores are retained in the DME solvated complexes from their THF solvated starting materials. This is particularly true for the bulkier *N*-2,6-diisopropylphenyl substituted complexes. This observation is significant particularly for the bulkier complexes as the arrangement of the dilithiated ligand is proposed to be directly linked to the specific proton abstraction reactivity discussed in Chapter 3 for this complex. To illustrate the retention of structural detail between the THF solvated

complex **12** and the DME solvated complex **17**, their overlayed structures are shown in Figure 2-43.

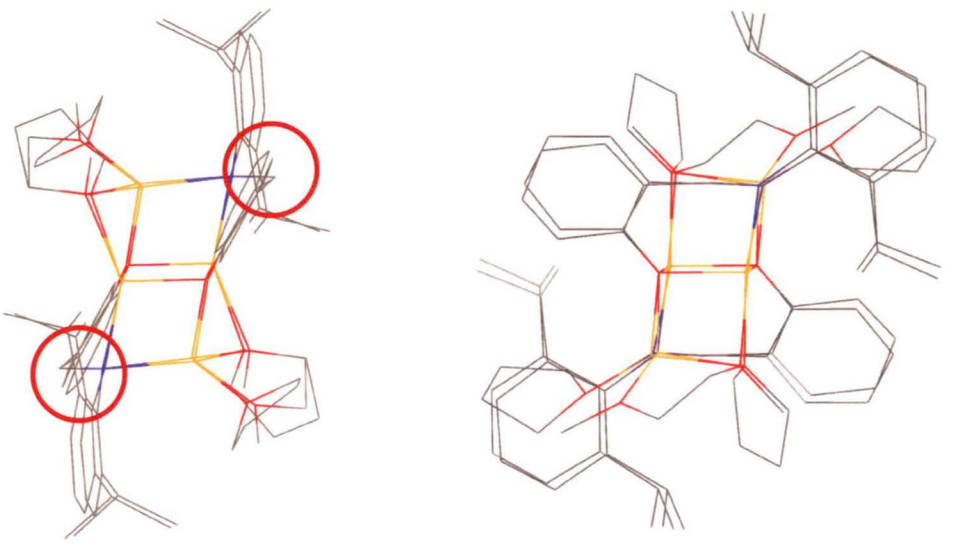

Figure 2-43: Front and side on overlayed view of the THF and DME solvated complexes [{Li_2(ONDIPP)}$_2$(THF)$_4$] **12** and [{Li_2(ONDIPP)}$_2$(DME)$_2$] **17**, respectively, showing the minimal difference in the molecular arrangement between the two. Hydrogen atoms removed for clarity.

Importantly, the orientation of the methylene link in the dilithiated ligands (circled above) is maintained in the DME solvated complexes from that of the THF solvated complexes. As mentioned, this is thought to be related to the observed reactivity of these dilithiated complexes towards particular solvents, which is the subject of the following chapter.

2.4. Theoretical considerations

The use of theoretical or computational chemistry as an additional investigational tool has become essentially standard practice in most areas of synthetic chemistry.[133] Computational chemistry allows researchers to model various aspects of synthetic chemistry at incredibly detailed levels from inspecting molecular orbitals

to gain an understanding into why a reaction produces certain products, through to screening catalysts for viability in particular reaction conditions saving the time and physical resources of preparing and testing them in the laboratory. In the 1990's researchers made advances into understanding the observed trends in aggregation and cluster size in organolithium complexes, particularly in the area of amidolithium species even though it remained difficult to prepare samples suitable for X-ray crystal structure determination. [57, 127, 134-136] For an excellent summary of the early work in this area see the reviews by Mulvey and Snaith.[2, 3] More recently, investigations have included mechanistic investigations into a variety of reactions involving organolithium reagents. Of particular interest to the work presented within this thesis are the investigations looking into metallation of TMEDA by particular organolithium species and the observed selectivities of some of them towards metallation at different positions.[137, 138] Recently significant investigations have been undertaken by Kondo and Uchiyama into some alkali metal mediated metallation reactions.[84, 139, 140]

In the work presented in this thesis, theoretical computational methods were utilised to investigate the fact that particular structural features and aggregation geometries were observed in the solid state in some lithium complexes, and not in others. This was investigated by modelling the theoretically possible alternatives and comparing their energies to the models of the observed compounds.

The lithium complexes presented in this thesis display a variety of aggregated cores, predominantly dimers for the dilithiated complexes, and predominantly tetramers for the monolithiated complexes. Of the dilithiated complexes the most commonly observed core is the centrosymmetric $Li_4O_2N_2$ four-rung ladder core. In Chapter 3 the stability of this core is further illustrated in additional solvent exchange reactions. This geometry is not unique for the dimeric dilithiated $Li_4O_2N_2$ complex cores

however. In complexes with TMEDA both the *N*-phenyl and the *N*-2,6-diisopropylphenyl substituted ligands adopt alternative core geometries which have been called 'grafted' and 'face-bridged' ladders, respectively, based on their relationship to their parent ladder complex geometry. These three $Li_4O_2N_2$ dimeric cores are illustrated in Figure 2-44.

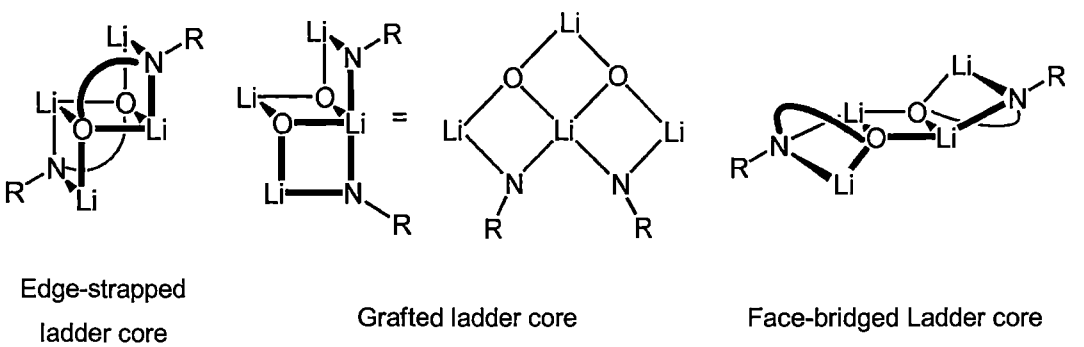

Figure 2-44: The three different dimeric $Li_4O_2N_2$ cores observed experimentally in the solid state for the O/N ligand complexes.

The grafted ladder core is observed for the TMEDA solvated dimeric complex $[\{Li_2(ONPh)\}_2(TMEDA)_3]$ **14**, and provides three chelation sites for bidentate Lewis base solvent rather than the two chelation sites and two isolated Lewis basic donation sites in the parent ladder core. In the grafted core the ligands still each span a distance of three ladder rungs, along the ladder edge. The face-bridged ladder core is observed for the TMEDA solvated dimeric complex $[\{Li_2(ONDIPP)\}_2(TMEDA)_2]$ **15** and provides two chelation sites, rather than the bridging chelated sites available in the parent ladder core. This is most likely favourable as the bulk surrounding the donor atoms in TMEDA would increase the steric crowding surrounding the lithium centre. In rearranging in this way complex **15** changes the arrangement of the dilithiated ligand from edge strapping to face strapping and they now span across the diagonal of each outer Li_2ON rings.

As discussed earlier in this chapter, the rationalisation of the observation of a different core in the TMEDA solvated complexes is relatively straight forward, as TMEDA is a bidentate Lewis basic solvent. What is less clear however, is why the grafted and face-bridged ladder cores are not observed in the presence of Lewis basic solvents other than TMEDA. To investigate this, theoretical models of the complexes of interest were calculated and their energies compared. Calculations were performed in Gaussian[141, 142] on the Vayu super computer cluster in Canberra, using the hybrid DFT method B3LYP[143, 144] with the basis set 6-31G(d)[145, 146] used for all atoms. The THF molecules were initially modelled using water as a cut-down Lewis base for computational feasibility, however, the acidic nature of the protons on the water made them unsuitable as the structure minimised to a hydroxide species. Consequently, dimethyl ether was used instead. It was shown that dimethyl ether gave a very good approximation of the geometry compared to using THF, while still reducing the computation time significantly. All optimised structures were found to have no imaginary frequencies and are assumed to represent local minima close to the global minimum for each respective structure. A comparison between the calculated and observed bonding parameters was made in a few specific cases and while the calculated bond lengths tended to be slightly shorter, the differences were typically less than 0.5 %.

It was found that in the presence of the monodentate Lewis basic solvent dimethyl ether, there is relatively little energy difference between the two core types observed in the solid state for each of the dilithiated ligand types. That is to say, that for complexes of the *N*-phenyl substituted ligand solvated with dimethyl ether, there is only a difference of 8.2 kJ/mol in favour of the ladder core versus the grafted ladder core, and for complexes of the *N*-2,6-diisopropylphenyl substituted ligand solvated with dimethyl ether, there is only a difference of 6.0 kJ/mol in favour of the ladder

core versus the face-bridged ladder core. There is a much greater energy difference predicted against the other alternative core in each case. That is, that for the *N*-phenyl substituted ligand the ladder core is 39.8 kJ/mol more stable than the face-bridged ladder core, and for the *N*-2,6-diisopropylphenyl substituted ligand the ladder core is 33.8 kJ/mol more stable than the grafted ladder core. These comparisons are shown in Figure 2-45.

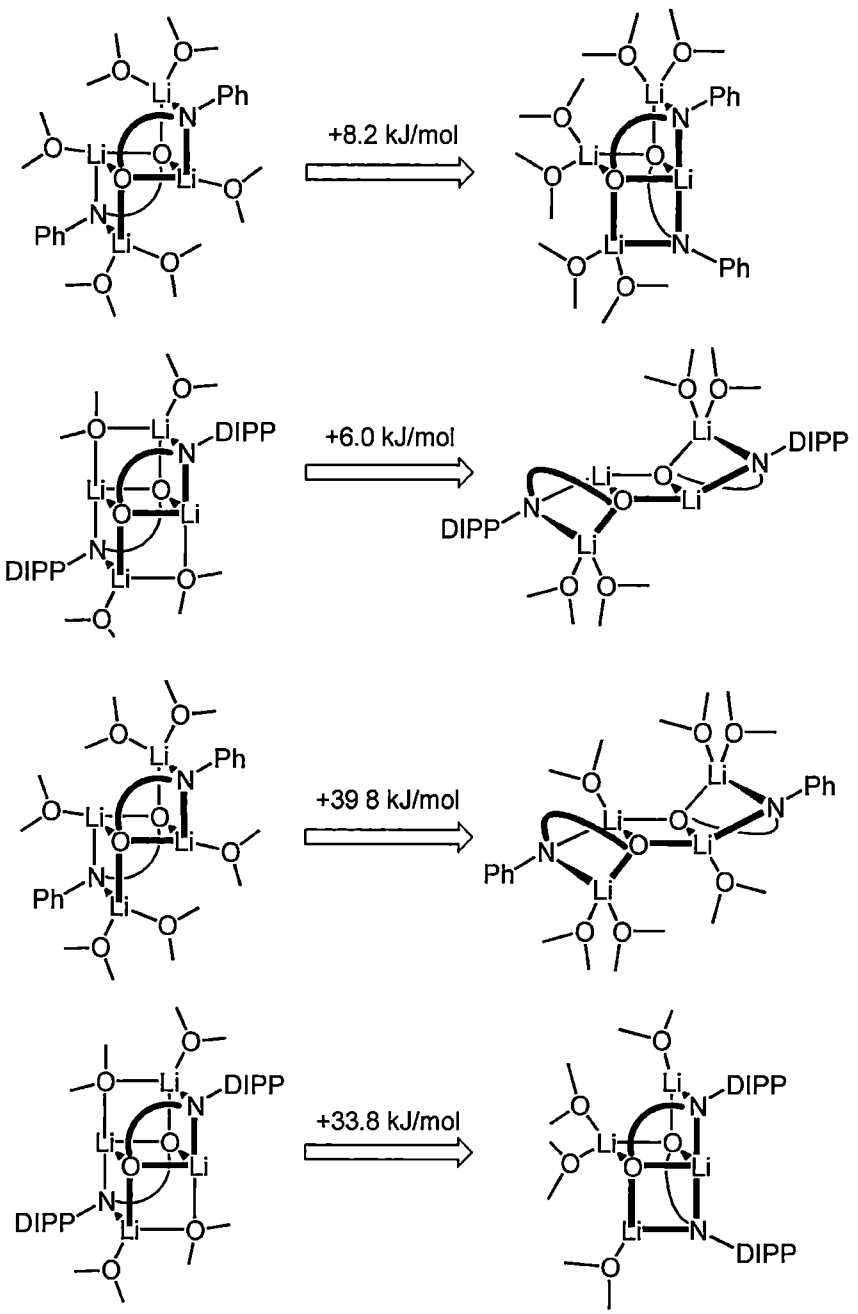

Figure 2-45: Calculated energy differences between observed core types and their alternate possibilities. THF modelled as Me_2O.

Although in the first two comparisons the energy difference is small, the model agrees with the experimentally observed case in both instances. The final two comparisons each show a strong preference for the experimentally observed cores. In the case of the bulkier complex adopting the grafted ladder arrangement this is unsurprising as there is considerable steric crowding between the two *N*-2,6-diisopropylphenyl substituents, which are positioned on the same side of the complex in this case. For the *N*-phenyl substituted complex adopting the face-bridged arrangement it is less obvious why it would be strongly unfavoured. There is a moderate amount of steric interaction between the *N*-phenyl ring and the lithium centres within the central Li_2O_2 ring, this is evident as an increase in the Li-O distance from 2.01 Å in the edge-strapped ladder core model to 2.10-2.20 Å in the face-bridged ladder core model.

A further possible variation that is not observed is the TMEDA solvated edge strapped ladder core of the *N*-2,6-diisopropylphenyl substituted ligand, analogous to the DME adduct $[\{Li_2(ONDIPP)\}_2(DME)_2]$ **17** with TMEDA in a bridging arrangement. This is not prevented in the same way that the TMEDA solvated edge strapped ladder core of the *N*-phenyl complex is, as only two TMEDA molecules are incorporated in total. The structure of this TMEDA bridging complex is shown in Figure 2-46. As noted earlier though, TMEDA adopting this bridging arrangement leads to a large amount of steric crowding, and consequently the complex is significantly less favoured than the observed face-bridged ladder core, by 61.1 kJ/mol.

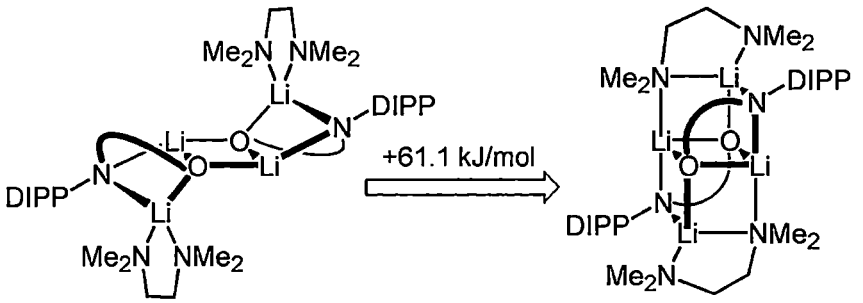

Figure 2-46: Calculated energy difference between the face-bridged core observed for complex [{Li_2(ONDIPP)}$_2$(TMEDA)$_2$] **15** and the alternate edge-strapped core arrangement.

Another possible geometry for the $Li_4O_2N_2$ core that must receive a further comment is the *syn* ladder core. As shown in Figure 2-47 this variation of the core contains the ligand in an edge strapping arrangement in the same way that the 'ladder core' does. However, in this case the two Li_2NO amide containing rings extend off opposite edges of the central Li_2O_2 phenoxide ring in a *syn* arrangement. This arrangement is not uncommon for organolithium complexes, and forms part of the theoretical investigations undertaken by Mulvey and Snaith referred to in the beginning of this section.

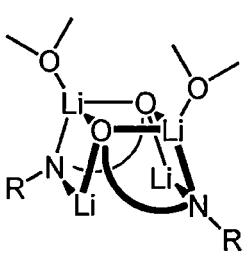

Syn ladder core

Figure 2-47: Arrangement of the $Li_4O_2N_2$ core for the O/N complexes as the *syn* ladder.

The *syn* arrangement of the $Li_4O_2N_2$ core was modelled as part of the work undertaken in this project, however it was observed that with only two dimethyl ether molecules the dimeric complex was already relatively sterically saturated. This was especially true in the complex of the bulkier *N*-2,6-diisopropylphenyl substituted ligand. Consequently, it is not possible to directly compare energies of the *syn* ladder core complex with the other cores discussed above. It is proposed however, that due

to the observed limited possibility of solvation by Lewis basic interactions, that for each of the dilithiated ligand molecules, aggregated dimers in a *syn* arrangement are unlikely to form in solution.

Another important structural feature of the dilithiated dimeric complexes is the orientation of the methylene group between the amide centre and the phenylene backbone of the dilithiated ligand of both the *N*-Ph and *N*-2,6-diisopropylphenyl systems. In the solid state structures of the THF adducts of the less bulky *N*-phenyl substituted ligand this group is observed to be exclusively positioned above the core of the complexes, whereas in complexes of the bulkier *N*-2,6-diisopropylphenyl substituted ligand it is exclusively observed to be positioned rotated outwards, no longer above the core. This difference is highlighted in Figure 2-48.

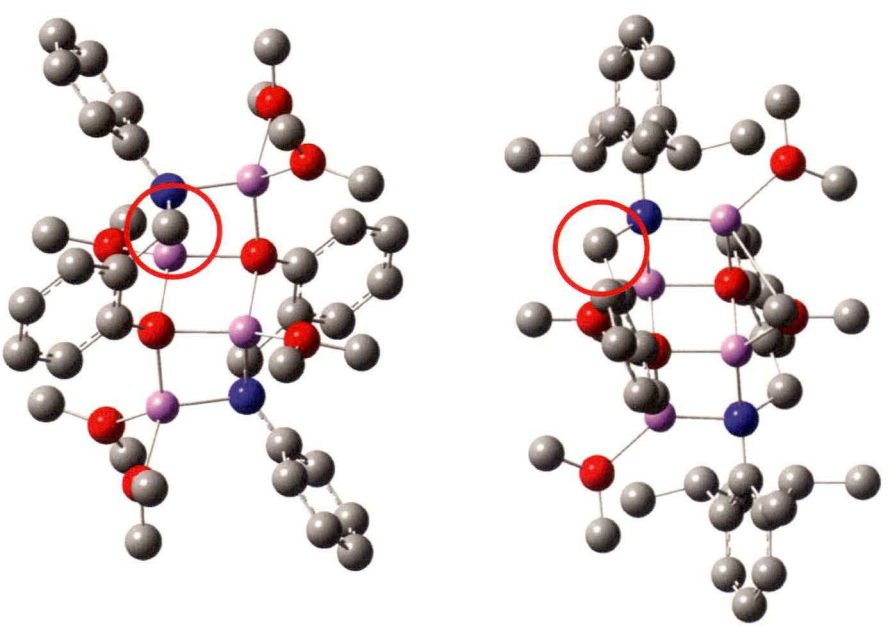

Figure 2-48: Calculated models of the two complexes $[\{Li_2(ONPh)\}_2(THF)_6]$ **11** and $[\{Li_2(ONDIPP)\}_2(THF)_4]$ **12**, showing the different methylene position. Hydrogen atoms removed for clarity.

The orientation of the methylene groups in these two systems is thought to be critically linked to the reactivity observed in the bulkier complexes, the details of which are reported in Chapter 3. By manually altering the starting geometry of each

of the dimethyl ether solvated ladder complexes, and subsequently allowing them to optimise freely, it was possible to determine the energy difference between the observed structure and the related structure with the methylene in the opposite position. The less bulky *N*-phenyl substituted complex is 39.0 kJ/mol less stable with the methylene rotated into the alternative position as observed in the bulkier *N*-2,6-diisopropylphenyl substituted complexes, and the *N*-2,6-diisopropylphenyl substituted complex is 18.9 kJ/mol less stable with the methylene rotated into the alternative position of above the core, as observed in the less bulky ligand complexes. This observation supports the idea that the rotation of the methylene is induced by the compromise between trends in aggregation, and strain induced by steric bulk, resulting in a high energy complex. These results are summarised in Figure 2-49 and Figure 2-50. Clearly, this infers the potential for higher reactivity on the more bulky system in reactions where this steric strain can be removed in the products.

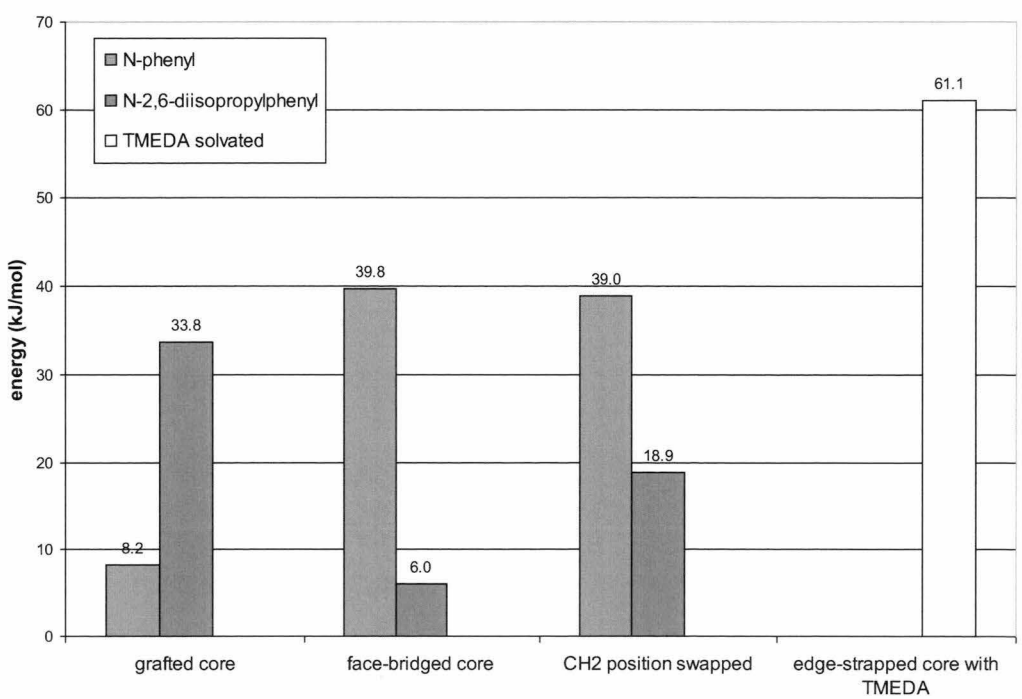

Figure 2-49: Calculated relative energies of the various dimeric $Li_4O_2N_2$ cores for each *N*-aryl O/N ligand. THF modelled as Me_2O.

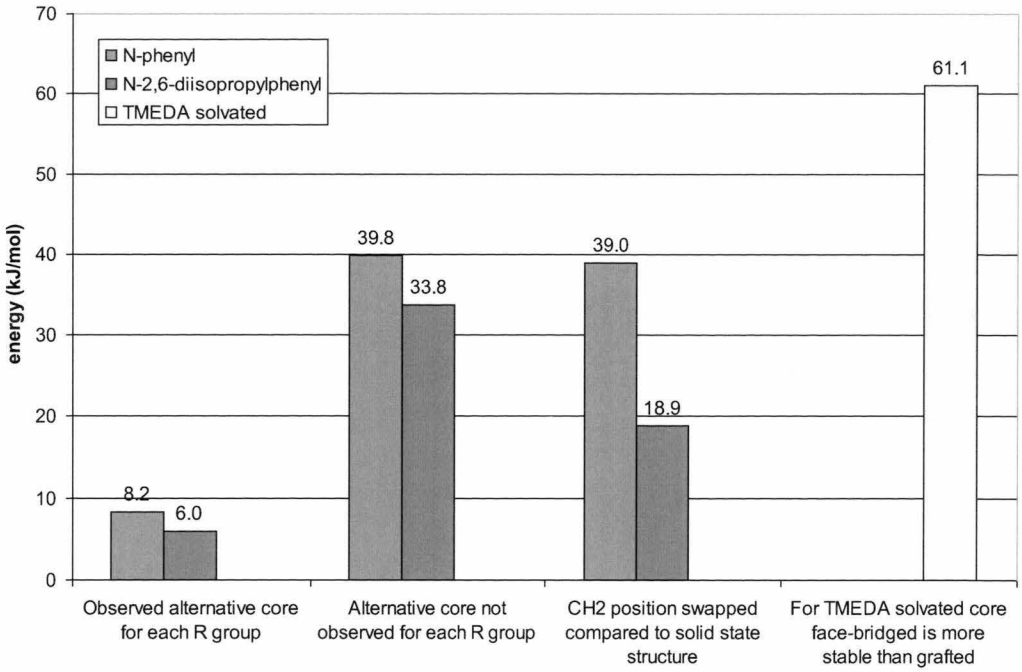

Figure 2-50: Calculated relative energies of the dimeric $Li_4O_2N_2$ complexes. Grouped by change relative to observed feature. THF modelled as Me_2O.

2.5. Conclusion

Chapter 2 reports the synthesis and structural characterisation of six mixed anion O/N ligands derived from *N*-substituted salicylaldamine and twelve mono- and dilithiated organolithium complexes containing them. Four unique monolithiated complexes were observed, [{Li(ONPhH)}$_4$] **7**, [{Li(ONPhH)}$_4$(THF)$_3$] **8**, [{Li(ONDIPPH)}$_4$] **9** and [{Li(ON=DIPPH)}$_4$] **10**, each aggregating as a tetramer with cubic Li_4O_4 cores. The O/N ligands surrounding these cubic cores adopted three alternate arrangements, each including the neutral amine group, at least partially, as internal Lewis basic donors. The monolithiated complex of the less bulky *N*-phenyl substituted ligand, **8** was the only complex observed to incorporate additional solvating Lewis base molecules.

The dilithiated complexes $[\{Li_2(ONPh)\}_2(THF)_6]$ **11** and $[\{Li_2(ONDIPP)\}_2(THF)_4]$ **12** were prepared by direct lithiation of the corresponding O/N ligand precursors in THF, while the TMEDA and DME adducts were prepared via a solvent exchange reaction from **11** and **12** to yield $[\{Li_2(ONPh)\}_2(TMEDA)_3]$ **14**, $[\{Li_2(ONDIPP)\}_2(TMEDA)_2]$ **15**, $[\{[Li_2(ONPh)]_2(DME)_3\}_\infty]$ **16**, $[\{Li_2(ONPh)\}_2(DME)_2(THF)_2]$ **18**, and $[\{Li_2(ONDIPP)\}_2(DME)_2]$ **17**, respectively. Each of these dilithiated complexes was isolated as a dimer in the solid state. With the exception of the TMEDA solvated complexes they all have a centrosymmetric four-rung $Li_4O_2N_2$ ladder core. The complexes incorporating the less bulky *N*-phenyl substituent exclusively accommodate six Lewis basic interactions while the complexes incorporating the bulkier *N*-2,6-diisopropylphenyl substituent exclusively accommodate four Lewis basic interactions. The two TMEDA solvated complexes **14** and **15** maintain the same degree of Lewis basic solvation as the THF adducts, however their cores are each unique; **14** adopting a 'grafted' ladder core and **15** adopting a 'face-bridged' ladder core.

One single dilithiated tetrameric complex was observed; upon heating of $[\{Li_2(ONPh)\}_2(THF)_6]$ **11** the complex $[\{Li_2(ONPh)\}_4(THF)_4]$ **13** was observed to form. The core of **13** consists of a central Li_4O_4 cubic portion, with four Li_2ON amide rungs extending from it.

In many cases a full assignment of the ^1H and ^{13}C NMR spectra for the lithium complexes **7-18** was not undertaken. The initial hope of determining detailed aggregation behaviour in solution using advanced NMR experiments was abandoned early on when it was observed that many of the complexes are insoluble in suitable NMR solvents. In addition, the complexes that were sufficiently soluble did not show significant evidence of different chemical environments for each of the ligands or the

solvent molecules within each complex indicating fluxional species. The identity of all of the reported compounds was confirmed by single crystal X-ray structure determination and in the majority of cases supported by elemental analysis data.

A theoretical investigation was undertaken to explore why, of the three $Li_4O_2N_2$ cores observed, edge-strapped ladder, grafted ladder and face-bridged ladder, the grafted ladder and face-bridged ladder were only observed in the presence of TMEDA. The results indicate that the edge-strapped ladder core is the most stable arrangement in all cases except when the complex is solvated with TMEDA, supporting the observed structures. Though not included in the theoretical investigation results, the *syn* $Li_4O_2N_2$ edge-strapped ladder core is suspected to be unfavourable for each of the *N*-aryl substituted dilithiated O/N ligands.

2.6. Experimental

Compounds ON=PhH **1**, ON=DIPPH **2**, and ON=*t*BuH **3** were all prepared using a modified literature method,[106] and are described partly below in the context of their *in situ* generation and reduction to give the secondary amine derivatives $ONPhH_2$ **4** $ONDIPPH_2$ **5** and $ONtBuH_2$ **6**.

2.6.1. Synthesis of $ONPhH_2$ 4

A solution of salicylaldehyde (0.19 mol, 20 mL) and aniline (0.19 mol, 17.4 mL) in methanol was stirred overnight to yield a dark green solution. The solution was reduced in volume to yield the intermediate imine ON=PhH **1** as a dark green crystalline product (30.58 g, 81 %). ON=PhH **1** (49 mmol, 9.63 g) was dissolved in

methanol and $NaBH_4$ (59 mmol, 2.22 g) was added portionwise and the solution stirred for 45 minutes yielding the secondary amine $ONPhH_2$ **4** as an off-white crystalline product dropping out of solution. The methanol was removed and $ONPhH_2$ **4** was taken up into diethyl ether (100 mL) and washed with $NaHCO_{3(sat)}$ (2x30 mL), water (2x20 mL), and washed finally against $NaCl_{(sat)}$ (20 mL) before being dried over Na_2SO_4 and taken to dryness affording off-white crystals. The product was purified by recrystallisation from hot toluene as off- white needles (8.43 g, 87 %). The ^1H NMR verified the purity and identity of the compound.[147]

2.6.2. Synthesis of $ONDIPPH_2$ 5

A solution of salicylaldehyde (0.11 mol, 11.3 mL) and 2,6-diisopropylaniline (0.11 mol, 20 mL) in methanol was refluxed overnight. The solution was reduced in volume to yield ON=DIPPH **2** as a yellow solid (22.8 g, 76 %). ON=DIPPH **2** (20 mmol, 5.62 g) was dissolved in methanol and $NaBH_4$ (24 mmol, 0.91 g) was added portionwise and the solution stirred for 4 hours. The reaction mixture was quenched and then extracted with diethyl ether (4x25 mL) and washed against $NaHCO_{3(sat)}$ (2x30 mL) and $NaCl_{(sat)}$ (20 mL) before being dried over Na_2SO_4 and taken to dryness affording $ONDIPPH_2$ **5** (5.39 g, 95 %) as an amorphous white solid (pure by NMR).

^1H NMR (300 MHz, $CDCl_3$), 25 °C): δ = 1.22 (12H, d $^3J_{HH}$ = 6.6 Hz, CH_3), 3.22 (2H, h $^3J_{HH}$ = 6.9 Hz, $CH(CH_3)_2$), 4.08 (2H, s, CH_2), 6.37 (1H, pt, $^3J_{HH}$ = 7.5 Hz, $^4J_{HH}$ = 1.2 Hz, Ar), 6.47 (1H, d, $^3J_{HH}$ = 8.1 Hz, $^4J_{HH}$ = 0.9 Hz, Ar), 6.61 (1H, pt, $^3J_{HH}$ = 7.2 Hz, $^4J_{HH}$ = 1.2 Hz, Ar), 6.84 (1H, d, $^3J_{HH}$ = 7.8 Hz, $^4J_{HH}$ = 1.5 Hz, Ar), 7.00 (3H, m, Ar).

^{13}C NMR (75 MHz, $CDCl_3$, 25 °C): δ = 24.6 (CH_3), 28.5 ($CH(CH_3)_2$), 56.2 (CH_2), 117.2 (Ar), 119.9 (Ar), 122.74 (Ar), 124.4 (Ar), 126.3 (Ar), 128.9 (Ar), 129.7 (Ar), 140.5 (Ar), 143.3 (Ar), 158.1 (Ar).

IR ν(cm^{-1}) N-H 3332 (w)

HRMS (M^+) Calculated: 283.19375 ($C_{19}H_{25}NO$)

Found: 283.19356

2.6.3. Synthesis of ON*t*BuH_2 6

A solution of salicylaldehyde (0.19 mol, 20 mL) and *t*-butylamine (0.19 mol, 20 mL) in methanol was stirred for 72 hours. The methanol was removed to leave ON=*t*BuH **3** as an impure yellow oil (23.81 g, 70 %). ON=*t*BuH **3** was purified by distillation under reduced pressure ($5.8x10^{-2}$ torr at 54 °C) (19.74 g, 58 %). ON=*t*BuH **3** (72 mmol, 12.88 g) was dissolved in methanol and $NaBH_4$ (89 mmol, 3.38 g) was added portionwise and the solution stirred for 2 hours. The reaction mixture was quenched and then extracted with diethyl ether (4x25 mL) and washed against $NaHCO_{3(sat)}$ (2x30 mL) and $NaCl_{(sat)}$ (20 mL) before being dried over Na_2SO_4 and taken to dryness affording an off-white crystalline solid. The product, ON*t*BuH_2 **6** was purified by recrystallisation from cold 40-60 °C petroleum spirits as thin off-white plates (7.2 g, 55 %). The ^{1}H NMR verified the purity and identity of the compound.[148]

2.6.4. Synthesis of [{Li(ONPhH)}$_4$] 7

To a suspension of ONPhH$_2$ **4** (1.0 g, 5.0 mmol) in 40-60 °C petroleum spirits *n*-BuLi (1.6 M in hexanes, 3.5 mL, 5.6 mmol) was added and the mixture stirred for 2 hours. The insoluble product was isolated as an amorphous white solid by removal of the petroleum 40-60 °C spirits (0.958 g, 93 %).

^{1}H NMR (300 MHz, C_6D_6, 25 °C): δ = N/A (insoluble).

^{13}C NMR (75 MHz, C_6D_6, 25 °C): δ = N/A (insoluble).

Anal. Calculated: C, 76.10; H, 5.89; N, 6.83; ($C_{13}H_{12}LiNO$)

Found: C, 75.29; H, 6.03; N, 6.61

2.6.5. Synthesis of [{Li(ONPhH)}$_4$(THF)$_3$] 8

A sample of [{Li(ONPhH)}$_4$] **7** (100 mg, 3.5x10^{-1} mmol) was dissolved in THF (*ca.* 3 mL) before having 40-60 °C petroleum spirits added to it (*ca.* 1 mL) to precipitate out the product. The solution was pipetted away after allowing the product to settle, and washed with fresh 40-60 °C petroleum spirits before being taken to dryness to yield the finely crystalline product (97 mg, 45 %).

^{1}H NMR (300 MHz, C_6D_6, 25 °C): δ = N/A (insoluble).

^{1}H NMR (300 MHz, C_6D_6 with d_8-THF, 25 °C): δ = 1.44 (12H, m, THF), 3.36 (4H, m, N-H), 3.55 (12H, m, THF), 3.88 (8H, d, $^3J_{HH}$ = 5.1 Hz, CH_2), 6.33 (8H, d, $^3J_{HH}$ = 7.8 Hz, Ar), 6.65 (8H, m, Ar), 6.75 (4H, d $^3J_{HH}$ = 7.8 Hz, Ar), 6.95 (12H, m, Ar), 7.21 (4H, t, $^3J_{HH}$ = 7.5 Hz, Ar).

^{13}C NMR (75 MHz, C_6D_6, 25 °C): δ = N/A (insoluble).

^{13}C NMR (75 MHz, C_6D_6 with d_8-THF, 25 °C): δ = 25.8 (THF), 49.4 (CH_2), 67.8 (THF), 114.8 (Ar), 116.3 (Ar), 119.7 (Ar), 119.8 (Ar), 127.2 (Ar), 129.2 (Ar), 129.6 (Ar), 131.1 (Ar), 149.5 (Ar), 166.0 (Ar).

IR ν(cm^{-1}) N-H 3336 (w), 3288 (w)

Anal. Calculated: C, 73.64; H, 7.27; N, 5.05; ($C_{17}H_{20}LiNO_2$)

Found: C, 73.74; H, 7.20; N, 5.22

2.6.6. Synthesis of [{Li(ONDIPPH)}$_4$] 9

To a suspension of $ONDIPPH_2$ **5** (1.0 g, 3.5 mmol) in 40-60 °C petroleum spirits (50 mL) *n*-BuLi (1.6 M in hexanes, 2.4 mL, 3.9 mmol) was added and the solution stirred for 1 hour. The solution was concentrated rapidly down to *ca.* 10 mL yielding the product as a white finely crystalline material. The remaining solution was filtered away and the product taken to dryness (0.773 g, 76 %).

^{1}H NMR (300 MHz, C_6D_6, 25 °C): δ = 0.77-1.10 (48H, m, CH_3), 2.31 (4H, br, N-H), 3.19-3.37 (12H, m, C*H*(CH_3) CH_2), 4.90 (4H, pt $^3J_{HH}$ = 10.4 Hz, CH_2) 6.37 (4H, pt, $^3J_{HH}$ = 7.0 Hz, Ar), 6.47 (4H, pd $^3J_{HH}$ = 7.8 Hz, Ar), 6.61 (4H, pt $^3J_{HH}$ = 7.4 Hz, Ar), 6.83 (4H, pd $^3J_{HH}$ = 6.6 Hz, Ar), 6.96-7.05 (12H, m, Ar).

^{13}C NMR (75 MHz, C_6D_6, 25 °C): δ = 22.3 (br, CH_3), 23.9 (br, CH_3), 24.3 (br, CH_3), 25.1 (br, CH_3), 28.4 (br, *C*H(CH_3)), 29.4 (br, *C*H(CH_3)), 57.0 (CH_2), 115.3 (Ar), 120.4 (Ar), 123.3 (br, Ar), 125.1 (Ar), 127.4 (Ar), 130.4 (Ar), 140.1 (br, Ar), 142. 1 (br, Ar), 143.8 (Ar), 165.4 (Ar).

IR ν(cm^{-1}) N-H 3338 (w)

Anal. Calculated: C, 78.87; H, 8.36; N, 4.84; ($C_{19}H_{24}LiNO$)

Found: C, 78.03; H, 8.26; N, 4.82

2.6.7. Synthesis of [{Li_2(ONPh)}$_2$(THF)$_6$] 11

To a solution of $ONPhH_2$ **4** (3.40 g, 17.1 mmol) in THF (*ca.* 100 mL) *n*-BuLi (1.6 M in hexanes, 22.4 mL, 35.8 mmol) was added and the solution stirred overnight at 50 °C. The resulting white precipitate was isolated via cannula filtration and washed with fresh THF with the solution chilled in an ice bath. The product was taken to dryness and isolated as a finely crystalline white powder (7.2 g, 99 %).

^{1}H NMR (300 MHz, C_6D_6, 25 °C): δ = 1.24 (24H, m, THF), 3.34 (24H, m, THF), 4.40 (4H, m, CH_2), 6.5-6.9 (10H, m, Ar), 7.18-7.54 (8H, m, Ar).

^{13}C NMR (75 MHz, C_6D_6, 25 °C): δ = 25.50 (THF), 53.1 (b, CH_2), 54.4 (CH_2), 68.3 (THF), 110.5 (Ar), 113.6 (b, Ar), 115.8 (Ar), 121.3 (Ar), 128.8 (Ar), 129.7 (Ar), 131.4 (Ar), 132.4 (Ar), 162.2 (Ar), 165.9 (Ar).

Anal. Calculated: C, 70.25; H, 8.25; N, 3.28; ($C_{25}H_{35}Li_2NO_4$)

Found: C, 68.73; H, 7.78; N, 3.35

2.6.8. Synthesis of [{Li_2(ONDIPP)}$_2$(THF)$_4$] 12

To a solution of $ONDIPPH_2$ **5** (4.0 g, 14.1 mmol) in THF cooled in ice, *n*-BuLi (1.6 M in hexanes, 19.4 mL, 31.0 mmol) was added slowly. The solution was then heated to 55 °C for 3 hours. Rapid reduction of the solvent volume by approximately

40 % yielded the first crop of product as a white amorphous solid (2.90 g, 47 %), and a second crop of crystalline material was obtained by further slower reduction of the solvent volume (0.90 g, 14 %).

^{1}H NMR (300 MHz, C_6D_6, 25 °C): δ = 1.21 (16H, s, THF), 1.34 (24H, d, $^3J_{HH}$ = 9.9 Hz, CH_3), 3.32 (16H, s, THF), 3.68 (4H, m, C*H*(CH_3)$_2$), 4.61 (4H, m, CH_2), 6.52-7.28 (14H, m, Ar).

^{13}C NMR (75 MHz, C_6D_6, 25 °C): δ = 25.2 (CH_3), 25.3 (CH_3), 28.6 (*C*H(CH_3)), 29.0 (THF), 60.7 (CH_2), 61.4 (CH_2), 68.0 (THF) 115.6 (Ar), 117.3 (Ar), 118.5 (Ar), 118.7 (Ar), 119.1 (Ar), 119.9 (Ar), 123.6 (Ar), 123.9 (Ar), 130.2 (Ar), 130.7 (Ar), 135.1 (Ar), 135.6 (Ar), 144.8 (Ar), 145.1 (Ar), 158.2 (Ar), 160.0 (Ar), 163.1 (Ar), 164.5 (Ar).

Anal. Calculated: C, 73.79; H, 8.94; N, 3.19; ($C_{27}H_{39}Li_2NO_3$)

Found: C, 73.40; H, 8.92; N, 3.37

2.6.9. Synthesis of [{Li$_2$(ONPh)}$_4$(THF)$_4$] 13

A sample of the complex [{Li$_2$(ONPh)}$_2$(THF)$_6$] **11** (14 mg, 1.6x10^{-2} mmol) had benzene added to it (*ca.* 1 mL) and the solution was heated overnight in a sealed Young's capped NMR tube at 95 °C resulting in precipitation of a moderate amount of extremely small crystalline material. X-ray crystal structure determination on this material yielded the reported complex. This reaction was not able to be repeated, and consequently only partial characterisation was possible.

2.6.10. Synthesis of [{Li_2(ONPh)}$_2$(TMEDA)$_3$] 14

A sample of the complex [{Li_2(ONPh)}$_2$(THF)$_6$] **11** (195 mg, 2.3x10^{-4} mol) had a small amount of TMEDA added to it (*ca.* 5 mL) yielding a yellowish solution. The solvent was removed *in vacuo* to yield **14** quantitatively as a colourless crystalline product.

^{1}H NMR (300 MHz, C_6D_6, 25 °C): δ = 2.01 (36H, s, TMEDA CH_3), 2.30 (12H, s, TMEDA CH_2), 3.54-4.09 (4H, m, CH_2), 5.80-6.96 (18H, m, Ar).

^{13}C NMR (75 MHz, C_6D_6, 25 °C): δ = 46.4 (TMEDA CH_3), 50.1 (CH_2, br), 58.7 (TMEDA CH_2), 116.5 (br, Ar), 120.8 (br, Ar), 126.6 (br, Ar), 148.8 (br, Ar), 166.3 (br, Ar).

Anal. Calculated: C, 68.56; H, 9.15; N, 14.54; ($C_{44}H_{70}Li_4N_8O_2$)

Found: C, 68.87; H, 8.41; N, 13.60

2.6.11. Synthesis of [{Li_2(ONDIPP)}$_2$(TMEDA)$_2$] 15

^{1}H NMR (300 MHz, C_6D_6, 25 °C): δ = 0.81-2.01 (48H, m, CH_3, TMEDA CH_3 CH_2), 3.65 (4H, m, C*H*(CH_3)), 4.66 (4H, br, CH_2), 6.69-7.38 (14H, m, Ar).

^{13}C NMR (75 MHz, C_6D_6, 25 °C): δ = N/A (insoluble).

Anal. Calculated: C, 72.97; H, 9.55; N, 10.21; ($C_{25}H_{39}Li_2N_3O$)

Found: C, 72.66; H, 9.43; N, 9.81

2.6.12. Synthesis of $[\{[Li(ONPh)]_2(DME)_3\}_\infty]$ 16

The solid material $[\{Li_2(ONPh)\}_2(THF)_6]$ **11** (35 mg, $4.1x10^{-5}$ mol) was dissolved benzene (*ca.* 1 mL), and had 5 drops of DME added to it. The clear, colourless solution was left standing overnight during which the product $[\{[Li_2(ONPh)]_2(DME)_3\}_\infty]$ **16** began to crystallise out. The full crop of material was collected after further standing for one week, washed with 40-60 °C petroleum spirits and dried *in vacuo* (22 mg, 72 %).

^{1}H NMR (300 MHz, C_6D_6, 25 °C): δ = 2.75 (30H, s, DME CH_3 CH_2), 4.24-4.44 (4H, m, CH_2), 6.55-7.69 (18H, m, Ar).

^{13}C NMR (75 MHz, C_6D_6, 25 °C): δ = 53.3 (CH_2), 54.1 (CH_2), 58.6 (DME CH_3), 70.4 (DME CH_2), 110.1 (br, Ar), 113.9 (br, Ar), 115.3 (Ar), 120.0 (Ar), 121.0 (Ar), 129.2 (Ar), 129.4 (Ar), 131.7 (Ar), 161.8 (Ar), 165.7 (Ar).

Anal. Calculated: C, 65.90; H, 7.57; N, 4.04; ($C_{38}H_{52}Li_4N_2O_8$)

Found: C, 65.84; H, 8.19; N, 3.81

2.6.13. Synthesis of $[\{Li_2(ONDIPP)\}_2(DME)_2]$ 17

A solution of $[\{Li_2(ONDIPP)\}_2(THF)_4]$ **12** (50 mg, $5.7x10^{-5}$ mol) in benzene (*ca.* 3 mL) had 4-5 drops of DME added to it and was allowed to stand overnight. The resulting crystalline material was washed with fresh benzene before being isolated as a clear crystalline product (40 mg, 91 %).

^{1}H NMR (300 MHz, C_6D_6, 25 °C): δ = 1.45 (24H, d $^3J_{HH}$ = 6.9 Hz, CH_3), 2.57 (12H, s, DME CH_3), 2.73 (8H, s, DME CH_2), 3.77 (4H, m,

C*H*(CH_3)$_2$), 4.70 (4H, s, CH_2), 6.64 (2H, d $^3J_{HH}$ = 7.8 Hz, Ar), 6.76 (2H, t $^3J_{HH}$ = 7.2 Hz, Ar), 7.22 (4H, m, Ar), 7.39 (2H, d $^3J_{HH}$ = 7.5 Hz, Ar).

^{13}C NMR (75 MHz, C_6D_6, 25 °C): δ = N/A (insoluble/decomposes at elevated temperature).

Anal. Calculated: C, 71.68; H, 8.63; N, 3.63; ($C_{23}H_{33}Li_2NO_3$)

Found: C, 71.76; H, 8.43; N, 3.56

2.6.14. Synthesis of [{Li_2(ONPh)}$_2$(DME)$_2$(THF)$_2$] 18

A solution of [{Li_2(ONPh)}$_2$(THF)$_6$] **11** (35 mg, 4.1x10^{-5} mol) in benzene (*ca.* 3 mL) had 1-2 drops of DME added to it and was allowed to stand overnight. The resulting crystalline material was washed with fresh benzene before being isolated as a clear crystalline product (22 mg, 72 %). As this reaction was not able to be repeated, X-ray crystal structure determination was the only characterisation achieved.

Chapter 3

Reactivity of the dilithiated O/N complexes towards solvents

3.1. Introduction

Much of the appeal of organometallic chemistry lies in the ability to use the unique chemical environments provided within its bountiful variability to achieve specific organic transformations. As indicated in the preceding chapter, reactivity was observed of the O/N dilithiated organolithium complexes towards ether type substrates. The latter half of this present chapter focuses on the extent of this observed reactivity.

Ether cleavage, or alternatively the *O*-dealkylation of ethers remains an organic reaction of great importance in the areas of functional group protection/deprotection, fine chemical production, as well as natural product chemistry. The topic has been recently reviewed by Weissman and Zewge,[149] and is the subject of several earlier reviews.[150-152] Classical ether dealkylation is achieved under drastic conditions, typically by using boiling concentrated hydroiodic acid.[153] This method has been modified to include the addition of a catalytic amount of a phase transfer agent such as hexadecyltributylphosphonium bromide, where the reaction proceeds as shown in Scheme 3-1.

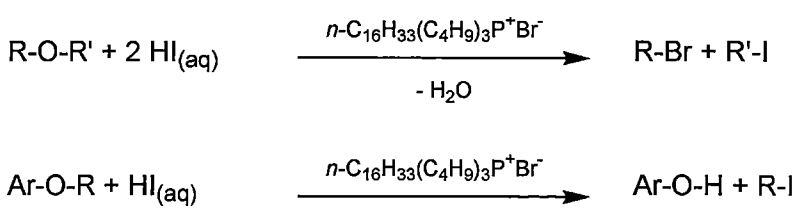

Scheme 3-1: Classical ether dealkylation methods.

These conditions are obviously restrictive in the types of substrate and functional groups that can be used successfully. Today there are a vast number of methods utilised for ether dealkylation reactions, most significantly, less aggressive. These include: i, Lewis acidic reagents, ii, basic reagents, iii, reductive cleavage, iv, oxidative cleavage, and v, photochemical cleavage. These methods are all discussed in the review by Bhatt.[152] Of particular interest to the work presented here are the basic methods of ether cleavage, specifically those involving organoalkali reagents.

In the mid 1930's researchers found that simple amidoalkali metal reagents such as sodium and potassium amide would cleave methoxy benzene type ethers.[154-157] Following this observation, they observed that aromatic amido alkali metal reagents were also able to perform ether cleavages. As a particular example, it was discovered by Loubinoux *et al.* that sodium *N*-methyl anilide can cleave alkyl aryl ethers in good yield.[158] These amido alkali metal reagents have advantages over the acidic cleavage agents, in that they could cleave diaryl ethers. The general reaction is shown in Scheme 3-2.

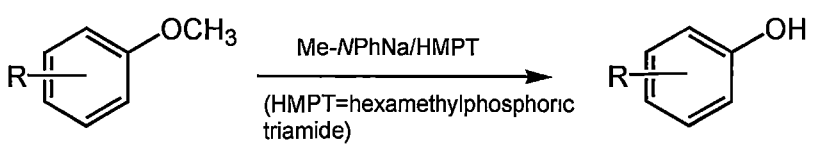

Scheme 3-2: Alkyl aryl ether cleavage using sodium *N*-methyl anilide.

It is often desirable to have selectivity in a reaction. It is important to the further development of such methods to have an understanding of the nature in which it occurs. This is the focus of the review by Maercker, who presents an excellent account of the findings of numerous deuterium labelled ether cleavage reactions performed by organoalkali metal compounds. In theory there are four mechanisms by which ether cleavage can occur; β-, α-, α,β'-elimination and Wittig rearrangement (the number of possibilities doubles when R≠R'), as shown in Scheme 3-3.

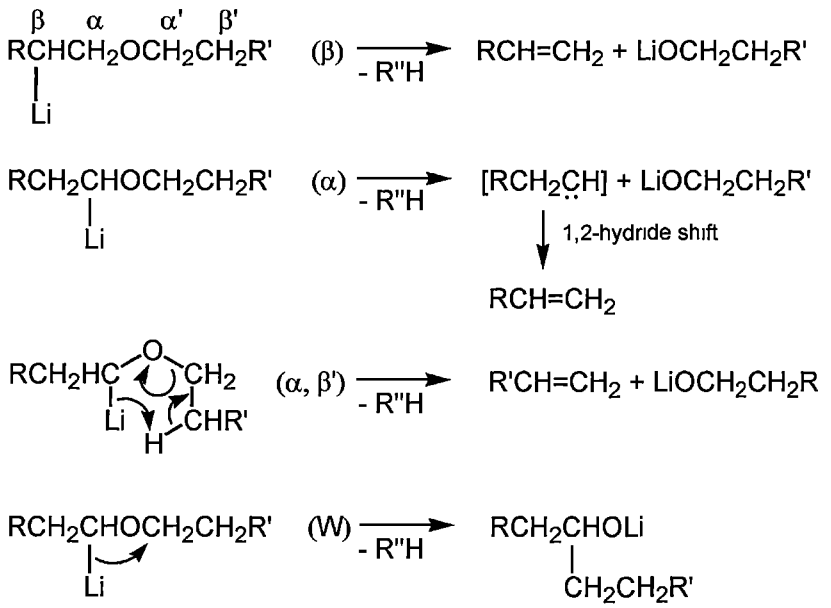

Scheme 3-3: Illustration of the four mechanisms by which ethers can theoretically undergo cleavage.

In the review Maercker noted that even in simple systems there is a variety of mechanisms occurring simultaneously leading to cleavage of the ether substrate. It should be noted, however, that it is not necessarily possible to distinguish the mechanism from examination of the reaction products.

Of particular interest to this thesis are ether dealkylation reactions of substrates that contain multiple ether functionalities. Poly-ether molecules occur in numerous situations, including a variety of isolated natural products, product syntheses, as well as simple chelating molecules. For example, as shown in Figure 3-1, aporphine alkaloids contain multiple methoxy functionalities. These molecules also contain an additional heteroatom methyl group with the tertiary *N*-methyl group.[159]

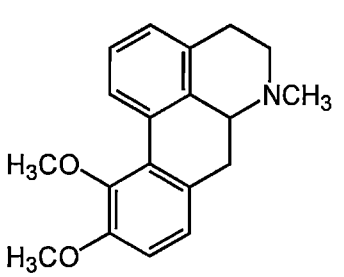

(XV)

Figure 3-1: Example of a poly-ether containing natural product – an aporphine alkaloid.

In such situations, researchers are often faced with the issue of achieving dealkylation at a specific ether site. To this end, there are several reports regarding the specificity that is achieved by particular reagents with various substrates.

It has been reported that $AlCl_3$ can cleave isopropyl aryl ethers while leaving methyl ethers intact. This work allowed the protection of phenol groups on lamellarin-type compounds, and their subsequent removal in the presence of multiple alkyl aryl ethers as shown in Scheme 3-4.[160]

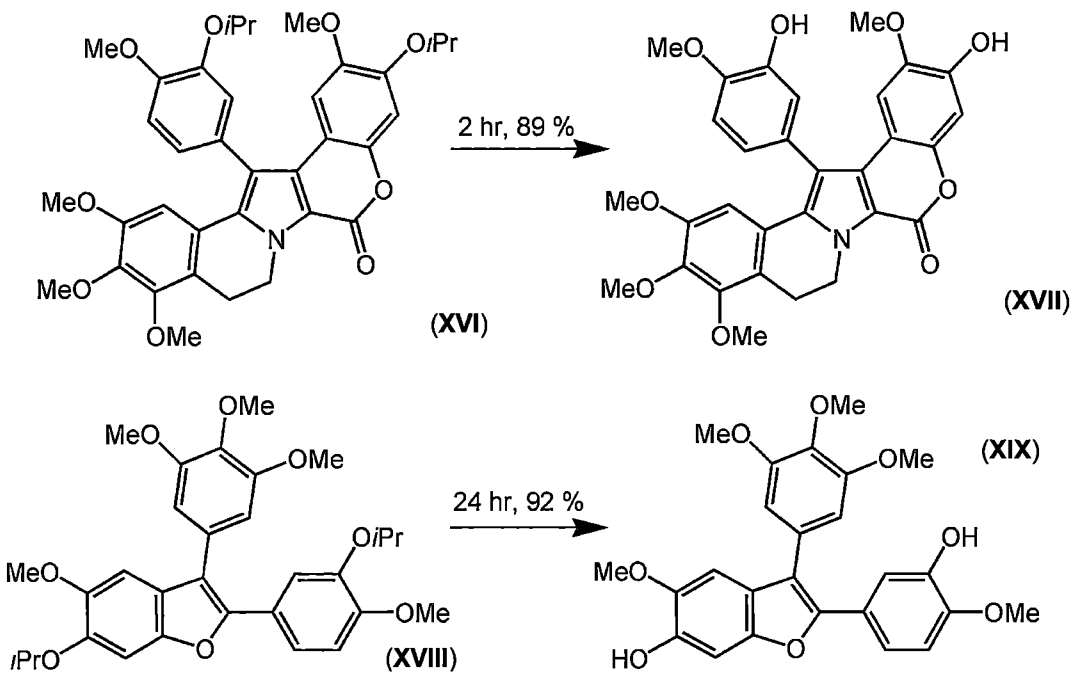

Scheme 3-4: Selective dealkylation of isopropyl ether groups from some lamellarin-type natural product substrates using $AlCl_3$.

Many other examples exist where selectivity has been achieved using reagents varying from Lewis acids, to main group metals, to alkali metal salts, and catalytic hydrogenation over palladium on charcoal. A good coverage of this work is found in the review by Ranu and Bhar,[150] and more recently by Weissman and Zewge.[149]

They observed significant selectivity with the reaction of sodium *N*-methyl anilide towards 1,2,4-trimethoxy benzene, with dealkylation occurring at the 2 position in 85 % yield as a result of the strong directing effect of the methoxy groups. This

effect was observed to be outweighed by the steric effect induced by replacing the methoxy group at position 2 with a *t*-Bu group, with dealkylation occurring at position 4 in 70 % yield in this case (although a higher temperature was required in the latter case). These results are illustrated in Scheme 3-5.

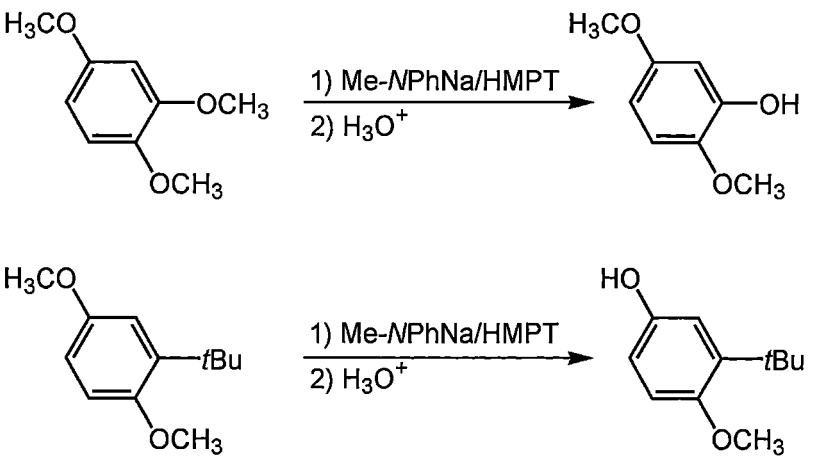

Scheme 3-5: Effect of steric bulk on the regioselectivity of dealkylation of poly methoxy benzenes using sodium *N*-methyl anilide.

Note, that although selectivity is observed for sodium *N*-methyl anilide towards dealkylation of polymethoxy benzenes, the apparent mechanism by which it is achieved is not clear. While the selectivity of dealkylation of 1,2,4-trimethoxy benzene occurs at the 2-position, and may potentially be related to a chelated arrangement of the organoalkali reagent, the reaction still proceeds at the 4 position if the possibility of chelation is removed.

Lithium amides are weaker bases than the heavier alkali metal amides and consequently are not known to cleave ethers. There are examples, however, where lithium reagents have been used to cleave ether substrates; suspended lithium metal will cleave certain ethers and the biphenyl/lithium adduct in THF is effective in cleaving several alkyl aryl and diaryl ethers. Selectivity of methyl cleavage over ethyl ethers can be achieved with triphenylsilyllithium, as well as diphenyl phosphidolithium, as shown in Scheme 3-6.[152]

Scheme 3-6: Dealkylation of the alkyl aryl ether methoxy benzene using diphenyl phosphidolithium.

Unlike the commonly reported ring cleavage reactions of THF, acyclic mono and diethers are not readily attacked during their routine use as Lewis basic additives in organometallic synthesis. A report of the serendipitous discovery of dealkylation of DME under mild conditions was published recently.[161] The researchers note that the cleavage of unrestrained C-O single bonds, such as those in DME, by Ln^{II} complexes is unusual, as there are several examples of redox transmetallation or redox transmetallation/ligand exchange reactions involving lanthanide metals in DME without cleavage.[162-164] In the attempted preparation of a ytterbium complex via a redox transmetallation ligand exchange reaction, in DME, they isolated a methoxy incorporated complex, as shown in Scheme 3-7.

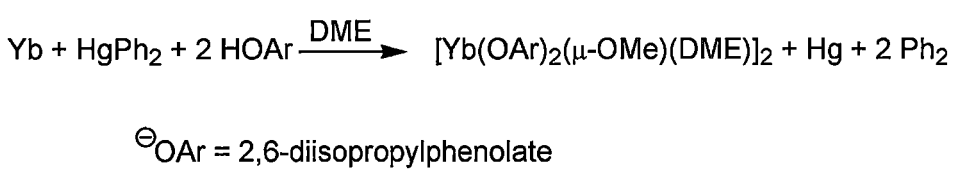

Scheme 3-7: Cleavage of DME during a lanthanide redox transmetallation ligand exchange reaction.

Though the inclusion of methoxy groups in Ln complexes is not uncommon, the source of the methoxy group is rarely DME derived. There are only a handful of structures reported containing methoxy groups resulting from cleavage of DME and these are usually under forcing conditions, such as strongly reducing environments.[161] One report of a DME derived methoxy group inclusion occurs via photolysis of a solution of YbI_2 in DME.[165] In this case they were able to identify ethylene as the by-product of the reaction by NMR spectroscopy. Often no mention is made of the fate of the remainder of the DME molecule. Other examples of DME

cleavage occurring in the presence of lanthanoid metals include alkali metal reagents and it is not as clear which reactive species is responsible for the resulting cleavage.[166, 167]

The metallation of TMEDA and other tertiary amine Lewis basic ligands by organolithium and organoalkali species is a closely related and centrally important area of organolithium chemistry to the reactivity of ethers towards organoalkali reagents. As the metallation of amine ligands such as TMEDA by organolithium reagents has been investigated[12, 168] and rationalised in terms of the structure property relationship it is prudent to provide a brief note of the topic here. For an excellent recent review on the topic see Strohmann *et al.*[1]

Investigations by Köhler in the 1980's found that TMEDA was susceptible to regioselective metallation, with the site of metallation being dependent on the choice of base used.[169] Solutions of *t*-BuLi and TMEDA yielded metallation of TMEDA at the methyl position, while solutions of the classical superbase mixture *n*-BuLi/*t*-BuOK and TMEDA yielded metallation of TMEDA at the methylene position, as shown in Scheme 3-8.

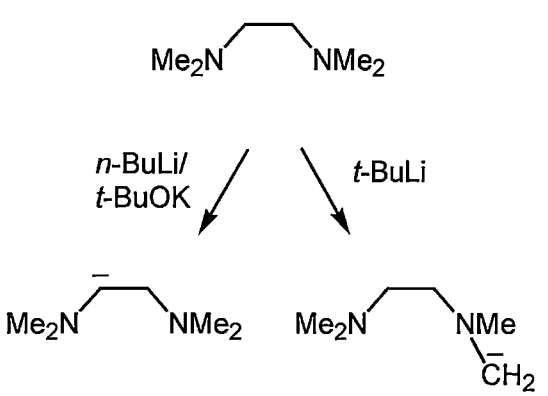

Scheme 3-8: Regioselectivity observed for metallation of TMEDA by different strong bases.

The metallated TMEDA complexes were not isolated, but rather identified through trapping with trimethylchlorostannane. Recently the solid state structure of methyl-lithiated TMEDA was reported.[13] In addition to this structure they were able

to prepare and characterise an intermediate complex prior to the unusual β-metallation observed of the related amine ligand TEEDA (*N,N,N',N'*-tetraethylethylenediamine).

TEEDA forms a monomeric complex with *t*-BuLi **XX**, as shown in Figure 3-2. The authors note that such monomeric complexes of saturated hydrocarbons are rare as they tend to form oligomers.

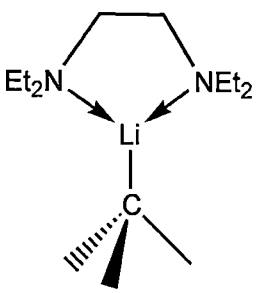

(**XX**)

Figure 3-2: Monomeric complex formed between TEEDA and *t*-BuLi.

As the authors point out, it is evident in the crystal structure that the β-hydrogens are proximally better suited to interaction with the carbanionic centre as the closest C···H distance to a β-hydrogen centre is 3.15 Å while the closest C···H distance to a α-hydrogen centre is 3.95 Å. In addition to this, the β-hydrogen is already directed towards the carbanion, whereas the α-hydrogen requires a conformational change to interact with the carbanion. The arrangement of the complex for different deprotonations are shown in Figure 3-3a and Figure 3-3b.

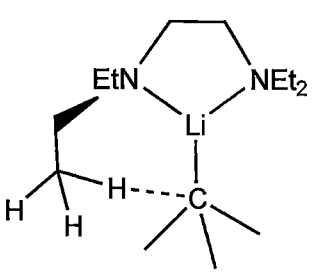

Figure 3-3a: β-deprotonation

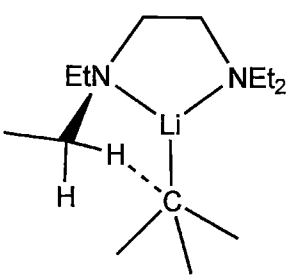

Figure 3-3b: α-deprotonation

The observation of a preferential structural arrangement for β-deprotonation rather than α-deprotonation correlates with the theoretical investigations undertaken. It was found that the barrier for deprotonation at the α-carbon of the TEEDA was 27 kJ/mol higher than for deprotonation at the β-carbon. They also modelled the analogous monomeric TMEDA complex and found that deprotonation at the α-position was energetically favourable. Thus, the regioselectivity of the metallation of TEEDA can be understood in terms of the Complex Induced Proximity Effect (CIPE). Although there is less structurally authenticated mechanistic understanding of the reactivity of organoalkali reagents towards ethers, it has been shown by Maercker that the decomposition of diethyl ether by alkyllithiums may share aspects of their reactivity with tertiary amine Lewis bases as he has shown that ethers also react via a β-elimination reaction.[170]

Fundamental studies into the mechanism by which lithiation reactions occur are of the upmost importance in rationalising reaction outcomes and directing reactions towards alternative outcomes. In particular the investigation into the interaction of amine Lewis basic ligands with organolithium reagents to facilitate novel reactions is an ongoing area of research.[137, 138, 171, 172]

3.2. Research aim

Further investigation the observed reactivity of the dimeric dilithiated complex $[\{Li_2(ONDIPP)\}_2(DME)_2]$ **17** towards DME via an unexpected intramolecular deprotonation was to be undertaken. It was observed that in the presence of excess DME the complex $[\{Li_2(ONDIPP)\}_2(THF)_4]$ **12** spontaneously deprotonates DME giving the monolithiated complex $[\{Li(ONDIPPH)\}_4]$ **9** and producing the DME

derived fragments of vinyl methyl ether and methanol after workup. This result was highly unexpected given the formal Brønsted basicity of the two constituent anions within the dilithiated complex and prompted further investigation into the structure property relationship giving rise to this observed reactivity.

It was also intended to test the hypothesis that the fragmentation products arising from the reaction of the dilithiated complex with related chelating ether Lewis bases were predictable. This hypothesis was based on the presumption that the Lewis bases required interaction with a specific part of the dilithiated complex, and hence would be highly dependent on the detailed conformational arrangement of the complex. Finally, it was also intended to further investigate the nature of complexes resulting from interactions with related ether type Lewis bases, predicting that the $Li_4O_2N_2$ four-rung ladder core would be maintained in these cases.

3.3. Results and discussion

3.3.1. Dilithiated O/N complexes – $MeOCH_2CH_2O$*t*-Bu adducts

After observing reactivity of the dilithiated complex $[\{Li_2(ONDIPP)\}_2(THF)_4]$ **12** towards DME, and subsequently managing to prepare the DME adduct via a modified synthetic method to that used to prepare the TMEDA adducts. It was attempted to prepare the asymmetrically substituted dialkyl diether, $MeOCH_2CH_2O$*t*-Bu, adduct for both the *N*-phenyl substituted and *N*-2,6-diisopropylphenyl substituted dilithiated ligands, as well as investigate the reactivity of $MeOCH_2CH_2O$*t*-Bu towards a cleavage reaction. Each of the dilithiated complexes $[\{Li_2(ONPh)\}_2(THF)_6]$ **11** and $[\{Li_2(ONDIPP)\}_2(THF)_4]$ **12** were shown to undergo ligand exchange reactions to form

$[\{Li_2(ONPh)\}_2(MeOCH_2CH_2Ot\text{-}Bu)_2(THF)_2]$ **19** and $[\{Li_2(ONDIPP)\}_2(MeOCH_2CH_2Ot\text{-}Bu)_2]$ **20** in 85 and 99 % yield, respectively, as shown in Scheme 3-9.

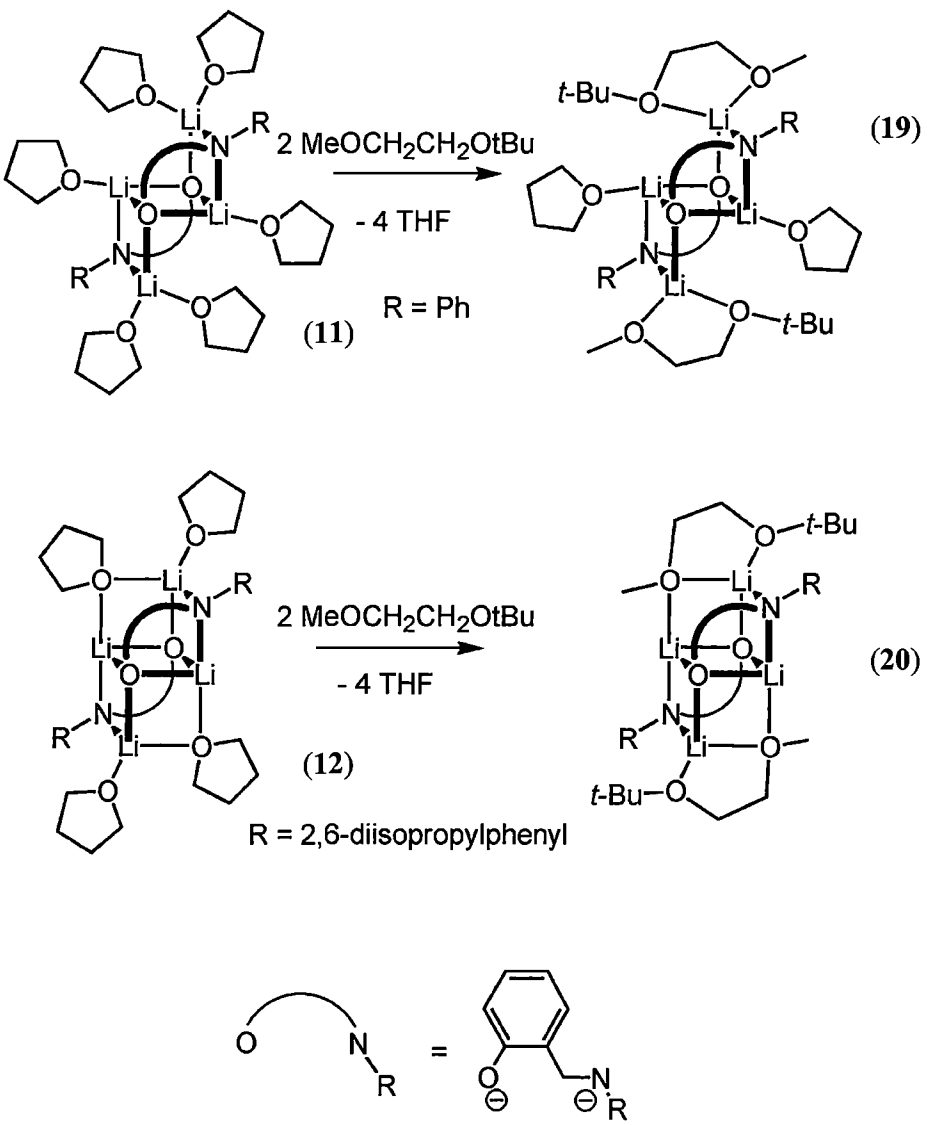

Scheme 3-9: Solvation of $[\{Li_2(ONPh)\}_2(THF)_6]$ **11** and $[\{Li_2(ONDIPP)\}_2(THF)_4]$ **12** with $MeOCH_2CH_2Ot$-Bu to give complexes $[\{Li_2(ONPh)\}_2(MeOCH_2CH_2Ot\text{-}Bu)_2(THF)_2]$ **19** and $[\{Li_2(ONDIPP)\}_2(MeOCH_2CH_2Ot\text{-}Bu)_2]$ **20**.

As for the related DME ligated complexes discussed in Chapter 2, benzene solutions of each of the two starting dilithiated THF complexes were prepared and had a small amount of $MeOCH_2CH_2Ot$-Bu added to them. In both cases this resulted in the product precipitating out of solution as colourless crystalline material. The bulkier complex $[\{Li_2(ONDIPP)\}_2(MeOCH_2CH_2Ot\text{-}Bu)_2]$ **20** was observed to be so

insoluble that upon $MeOCH_2CH_2Ot$-Bu coming into contact with the solution of the initial dilithiated THF complex $[\{Li_2(ONDIPP)\}_2(THF)_4]$ **12** in an NMR tube, solid product immediately began to precipitate out as very fine crystals. Consequently, subsequent preparations of both $MeOCH_2CH_2Ot$-Bu substituted complexes $[\{Li_2(ONPh)\}_2(MeOCH_2CH_2Ot\text{-}Bu)_2(THF)_2]$ **19** and $[\{Li_2(ONDIPP)\}_2(MeOCH_2CH_2Ot\text{-}Bu)_2]$ **20** were carried out using vapour diffusion of $MeOCH_2CH_2Ot$-Bu into the solutions of the initial dilithiated THF complexes, resulting in high yield crops of each of the products as large crystalline samples.

The two $MeOCH_2CH_2Ot$-Bu substituted complexes were characterised by X-ray crystal structure determination and elemental analysis. $[\{Li_2(ONPh)\}_2(MeOCH_2CH_2Ot\text{-}Bu)_2(THF)_2]$ **19** was also characterised by ^1H, ^{13}C, gCOSY and gHMBC NMR spectroscopy, while $[\{Li_2(ONDIPP)\}_2(MeOCH_2CH_2Ot\text{-}Bu)_2]$ **20** was unable to be characterised by NMR as it is insoluble in benzene. It is worth noting that when the sample was analysed no free THF or remaining complex **12** was evident in the NMR spectrum.

As predicted, both complexes **19** and **20** maintain the centrosymmetric $Li_4O_2N_2$ four-rung ladder core of their precursor complexes. Additionally, it was possible to correctly predict that in the bulkier complex $[\{Li_2(ONDIPP)\}_2(MeOCH_2CH_2Ot\text{-}Bu)_2]$ **20** the $MeOCH_2CH_2Ot$-Bu would coordinate to the complex with the oxygen atom bearing the bulkier *t*-Bu group taking the position of the non-bridging THF molecule, resulting in the bulkier end of $MeOCH_2CH_2Ot$-Bu extending away nearer the extremity of the laddering section of the core, as shown in Scheme 3-9. It was less evident as to what the orientation of the $MeOCH_2CH_2Ot$-Bu would be in the less bulky complex $[\{Li_2(ONPh)\}_2(MeOCH_2CH_2Ot\text{-}Bu)_2(THF)_2]$ **19**, as there are less steric constraints in the molecule. It was possible, however, to correctly predict that the complex

would retain two of the initial six THF molecules and maintain the $Li_4O_2N_2$ four-rung ladder core of the starting complex. The orientations of the $MeOCH_2CH_2Ot$-Bu ligand in $[\{Li_2(ONPh)\}_2(MeOCH_2CH_2Ot\text{-}Bu)_2(THF)_2]$ **19** is the reverse of that in the bulkier complex $[\{Li_2(ONDIPP)\}_2(MeOCH_2CH_2Ot\text{-}Bu)_2]$ **20**, however, the non-bridging (chelating only) binding mode enables the bulky *t*-Bu group to be accommodated by pivoting at the chelated lithium centre. The orientation of $MeOCH_2CH_2Ot$-Bu within complexes **19** and **20** is shown in Scheme 3-9.

Complex $[\{Li_2(ONPh)\}_2(MeOCH_2CH_2Ot\text{-}Bu)_2(THF)_2]$ **19** displays ^1H NMR resonances consistent with a single species in solution. The features of the aromatic region are similar to the precursor dilithiated complex $[\{Li_2(ONPh)\}_2(THF)_6]$ **11**. The *t*-Bu protons appear as a single resonance at 0.91 ppm. The methylene resonance for the ligand is a broad singlet appearing at 4.53 ppm, while both methylene proton resonances and the *O*-methyl resonance of the $MeOCH_2CH_2Ot$-Bu overlap to give multiplets between 3.07-3.18 ppm.

3.3.2. Dilithiated O/N complex – 1,4-dioxane adduct

The bulkier dilithiated complex $[\{Li_2(ONDIPP)\}_2(THF)_4]$ **12** was shown to undergo a ligand exchange reaction with 1,4-dioxane to form $[\{[Li_2(ONDIPP)]_2(1,4\text{-dioxane})(THF)\}_\infty]$ **21** in 99 % yield, as shown in Scheme 3-10.

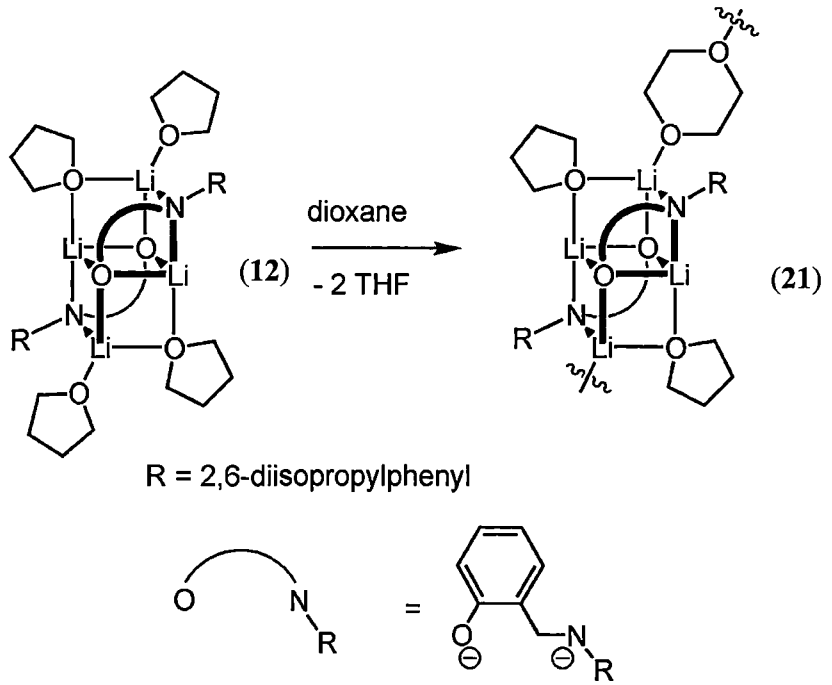

Scheme 3-10: Solvation of $[\{Li_2(ONDIPP)\}_2(THF)_4]$ **12** with 1,4-dioxane to give complex $[\{[Li_2(ONDIPP)]_2(1,4\text{-dioxane})(THF)\}_\infty]$ **21**.

As for the previous ligand substitution reactions, a solution of the dilithiated THF complex $[\{Li_2(ONDIPP)\}_2(THF)_4]$ **12** in benzene had added to it a small amount of 1,4-dioxane, and the solution was left standing overnight yielding a good crop of colourless crystalline product, $[\{[Li_2(ONDIPP)]_2(1,4\text{-dioxane})(THF)\}_\infty]$ **21**.

The complex was characterised by X-ray crystal structure determination and elemental analysis. The compound was not characterised by NMR as it is insoluble in benzene. Here it is noted again, that when the sample was analysed no free THF or remaining complex **12** was evident in the NMR spectrum.

The 1,4-dioxane adduct of the bulkier *N*-2,6-diisopropylphenyl substituted dilithiated ligand was prepared with the specific intention of determining how a 1,4-diether Lewis basic ligand would impact the $Li_4O_2N_2$ four-rung ladder core, if the diether was not able to participate in a bridging binding mode as observed for the previous dimeric complexes of the bulkier ligand. Consequently the *N*-phenyl substituted complex was not prepared as part of this work.

The structure of the 1,4-dioxane adduct, **21** maintains the same $Li_4O_2N_2$ four-rung ladder core for each dimerised pair of dilithiated ligands. However, each Li_4 unit is linked to an adjacent Li_4 unit via 1,4-dioxane molecules in a bridging arrangement forming a 1,4-dioxane polymeric adduct. The dimeric complex has undergone a single ligand substitution per dilithiated ligand, replacing the terminally bound THF molecules for an oxygen donor atom of 1,4-dioxane. Rather than this substitution resulting in a stoichiometry of 2:1 for 1,4-dioxane:dimer, by bridging between adjacent Li_4 units, the 1,4-dioxane remains in a stoichiometry of 1:1:2 for 1,4-dioxane:dimer:THF, as shown in Scheme 3-10.

3.3.3. Dilithiated Molecular structures

Colourless crystals of $[\{Li_2(ONPh)\}_2(MeOCH_2CH_2O\textit{t}\text{-}Bu)_2(THF)_2]$ **19** suitable for X-ray crystal structure determination were grown from a 70-80 % saturated solution of $[\{Li_2(ONPh)\}_2(THF)_6]$ **11** in benzene with small amount of $MeOCH_2CH_2O\textit{t}$-Bu added and left standing at room temperature overnight. The crystals belong to the triclinic space group $P\bar{1}$ (No. 2), $a = 10.059(2)$, $b = 11.013(2)$, $c = 12.752(3)$ Å, $\alpha = 65.14(3)$, $\beta = 70.33(3)$, $\gamma = 85.24(3)$ °, with 1 $Li_4O_2N_2$ molecule in the unit cell and the asymmetric unit consisting of ½ molecule of $[\{Li_2(ONPh)\}_2(MeOCH_2CH_2O\textit{t}\text{-}Bu)_2(THF)_2]$ **19**. The complex is crystallographically centrosymmetric. The molecular structure of $[\{Li_2(ONPh)\}_2(MeOCH_2CH_2O\textit{t}\text{-}Bu)_2(THF)_2]$ **19** is shown in Figure 3-4 and Figure 3-5.

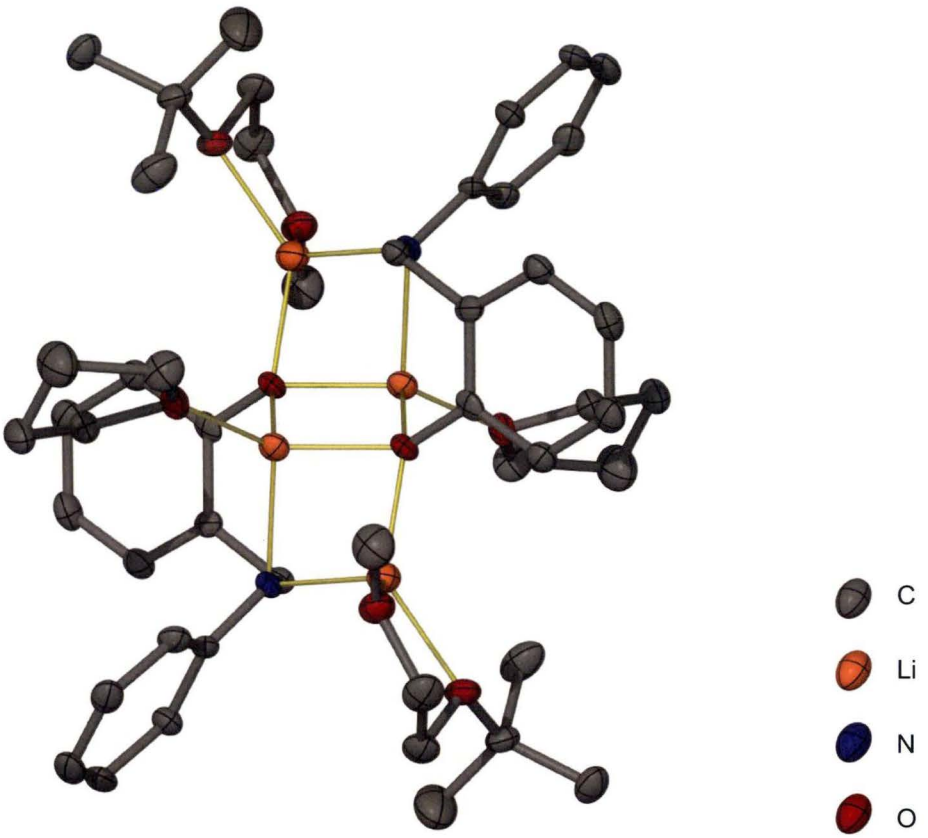

Figure 3-4: Front on view of the molecular structure of $[\{Li_2(ONPh)\}_2(MeOCH_2CH_2O\textit{t}\text{-}Bu)_2(THF)_2]$ **19** with thermal ellipsoids drawn at the level of 50 % probability. Hydrogen atoms removed for clarity.

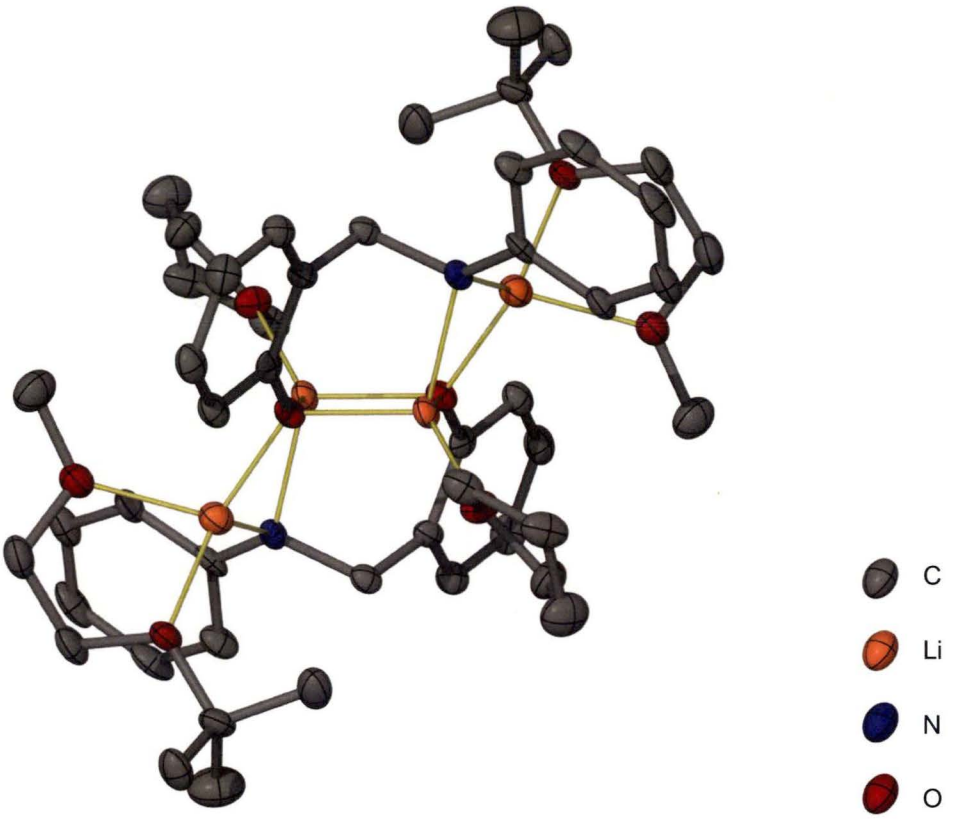

Figure 3-5: Side on view of the molecular structure of $[\{Li_2(ONPh)\}_2(MeOCH_2CH_2O\textit{t}\text{-}Bu)_2(THF)_2]$ **19**, with thermal ellipsoids drawn at the level of 50 % probability. Hydrogen atoms removed for clarity.

Complex **19** is a dimer containing the familiar $Li_4O_2N_2$ four-rung ladder core. As observed in the precursor THF solvate complex $[\{Li_2(ONDIPP)\}_2(THF)_4]$ **12**, the methylene group in the dilithiated O/N ligand is orientated such that it lies over the core of the complex. Furthermore the arrangement of the solvating Lewis basic ligand interactions is very similar to that of the precursor THF solvate complex **12**, with a single monodentate interaction to each of the lithium atoms in the central two Li-O rungs of the ladder to a THF molecule (remaining from the starting material), and a bidentate chelating interaction of the $MeOCH_2CH_2O\textit{t}$-Bu to the lithium atoms comprising the outer Li-N ladder rungs. The $MeOCH_2CH_2O\textit{t}$-Bu ligand orientates itself so that the *t*-Bu group is closest to the THF molecule on that same side of the ladder. Looking at Figure 3-4 and Figure 3-5 the intramolecular bias for the

arrangement of the $MeOCH_2CH_2Ot$-Bu is not obvious as the end of the $MeOCH_2CH_2Ot$-Bu containing the methyl group is positioned between the salicylaldehyde ring of one ligand molecule, and the *N*-phenyl substituent of the other ligand but is not tightly constrained there.

Colourless crystals of $[\{Li_2(ONDIPP)\}_2(MeOCH_2CH_2Ot\text{-}Bu)_2]$ **20** suitable for X-ray crystal structure determination were grown from a 70-80 % saturated solution of $[\{Li_2(ONDIPP)\}_2(THF)_4]$ **12** in benzene with small amount of $MeOCH_2CH_2Ot$-Bu added and left standing at room temperature overnight. The crystals belong to the triclinic space group $P\bar{1}$ (No. 2), $a = 9.4730(16)$, $b = 10.956(6)$, $c = 13.0420(8)$ Å, $\alpha = 75.566(4)$, $\beta = 69.470(2)$, $\gamma = 83.831(11)$ °, with 1 $Li_4O_2N_2$ molecule in the unit cell and the asymmetric unit consisting of ½ molecule of $[\{Li_2(ONDIPP)\}_2(MeOCH_2CH_2Ot\text{-}Bu)_2]$ **20**. The complex is crystallographically centrosymmetric. The molecular structure of $[\{Li_2(ONDIPP)\}_2(MeOCH_2CH_2Ot\text{-}Bu)_2]$ **20** is shown in Figure 3-6 and Figure 3-7.

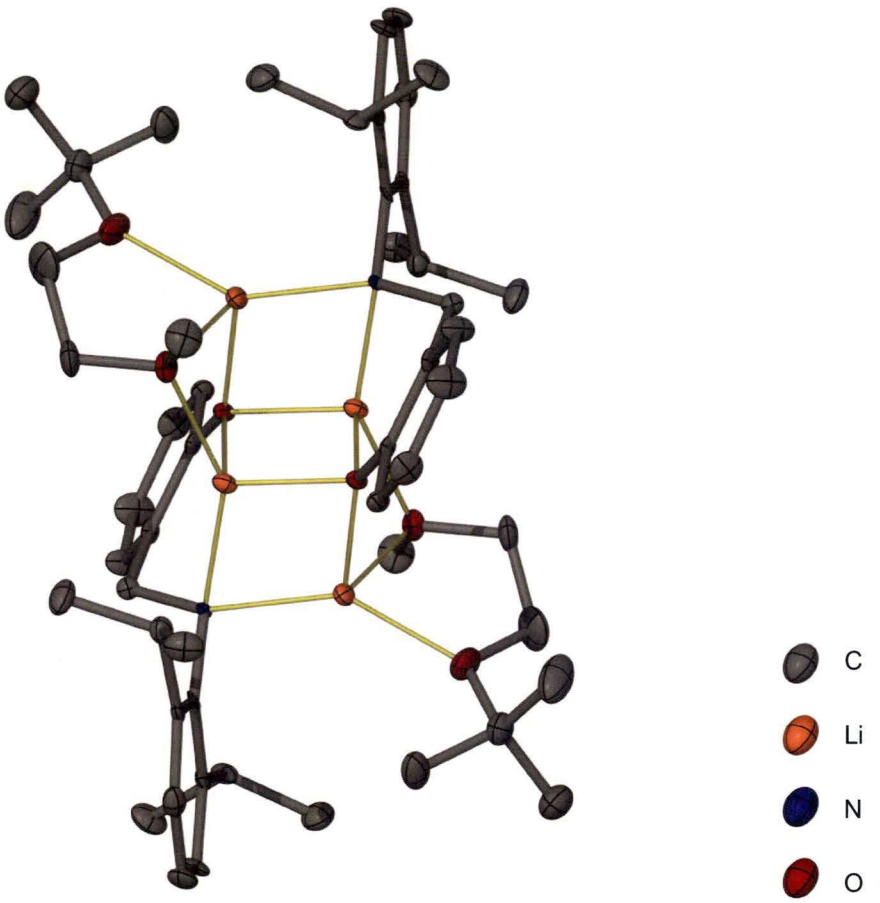

Figure 3-6: Front on view of the molecular structure of $[\{Li_2(ONDIPP)\}_2(MeOCH_2CH_2O\textit{t}\text{-}Bu)_2]$ **20** with thermal ellipsoids drawn at the level of 50 % probability. Hydrogen atoms removed for clarity.

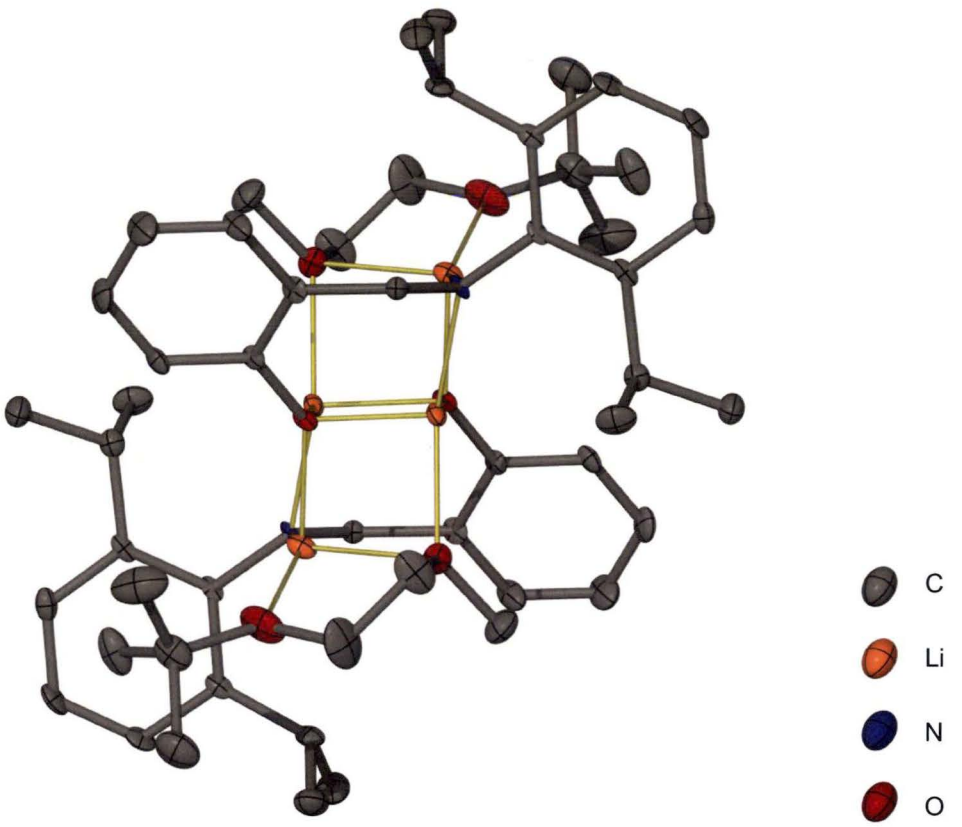

Figure 3-7: Side on view of the molecular structure of $[\{Li_2(ONDIPP)\}_2(MeOCH_2CH_2O\textit{t}\text{-}Bu)_2]$ **20** with thermal ellipsoids drawn at the level of 50 % probability. Hydrogen atoms removed for clarity.

Complex **20** contains many of the characteristics of the related dimeric dilithiated complexes $[\{Li_2(ONDIPP)\}_2(THF)_4]$ **12** and $[\{Li_2(ONDIPP)\}_2(DME)_2]$ **17**. It has maintained the $Li_4O_2N_2$ four-rung ladder core, as well as the restricted number of Lewis basic donor atoms compared to the less bulky complexes, this dimer again achieving six Lewis basic interactions through only four Lewis basic donor atoms. Similarly, the orientation of the methylene linker in the O/N ligand is maintained from the precursor complex, pointing 'away' from the core of the complex. Again, as observed in the precursor complex and the related DME complex, two of the Lewis basic interactions remain as bridging interactions. This again has the effect of inducing a reduction of the interplanar angles between the adjacent Li_2O_2 and Li_2ON rings along each ladder edge. The orientation of the asymmetrically substituted

Lewis base ligand in this complex is, however, reversed compared to the less bulky analogue **19** with the *N*-phenyl substituent. The O-*t*-Bu group is not involved in the bridging interaction. It is not unexpected that the Lewis basic ligand is orientated this way because, as observed in the THF solvated complex $[\{Li_2(ONDIPP)\}_2(THF)_4]$ **12**, the methylene group from the O/N ligand is twisted away to create sufficient space for the isopropyl groups of the aniline derived component, resulting in a binding groove as indicated in the following section in Figure 3-13. The *t*-Bu group is too bulky to fit in this region and so is orientated so that the bulk is outside the binding groove. This restriction on the orientation of the Lewis basic ligand is consistent with the observed specificity of O-C cleavage for the complex as discussed in the following section. The influence of steric bulk on the cleavage of ether substrates has been observed for sodium *N*-methyl anilide as discussed in the introduction of this chapter.[158] The ability to predict structural features and ensuing observed reactivity is a significant step forward for establishing a structure-base reactivity pattern for this area of homometallic superbasic reagents. The pattern of successful anticipated aggregation behaviour is extended further with the observation of the structural features being maintained in the complex with 1,4-dioxane below.

Colourless crystals of $[\{[Li_2(ONDIPP)]_2(1,4\text{-dioxane})(THF)\}_\infty]$ **21** suitable for X-ray crystal structure determination were grown from a 70-80 % saturated solution of $[\{Li_2(ONDIPP)\}_2(THF)_4]$ **12** in benzene with small amount of 1,4-dioxane added and left standing at room temperature overnight. The crystals belong to the orthorhombic space group $P2_12_12_1$ (No. 19), $a = 16.018(7)$, $b = 17.098(3)$, $c = 20.764(3)$ Å, with 4 dimeric $Li_4O_2N_2$ units in the unit cell and the asymmetric unit consisting of 1 dimeric $Li_4O_2N_2$ unit, one benzene and DME solvent molecules. Each dimeric $Li_4O_2N_2$ unit is non-crystallographically centrosymmetric. Complex **21**

is a polymer in the solid state, being built up of repeating dimeric $Li_4O_2N_2$ units with 1,4-dioxane molecules linking the terminal lithium centres of each dimeric unit. The structure of [{[Li_2(ONDIPP)]$_2$(1,4-dioxane)(THF)}$_\infty$] **21** is shown in Figure 3-8 and Figure 3-9.

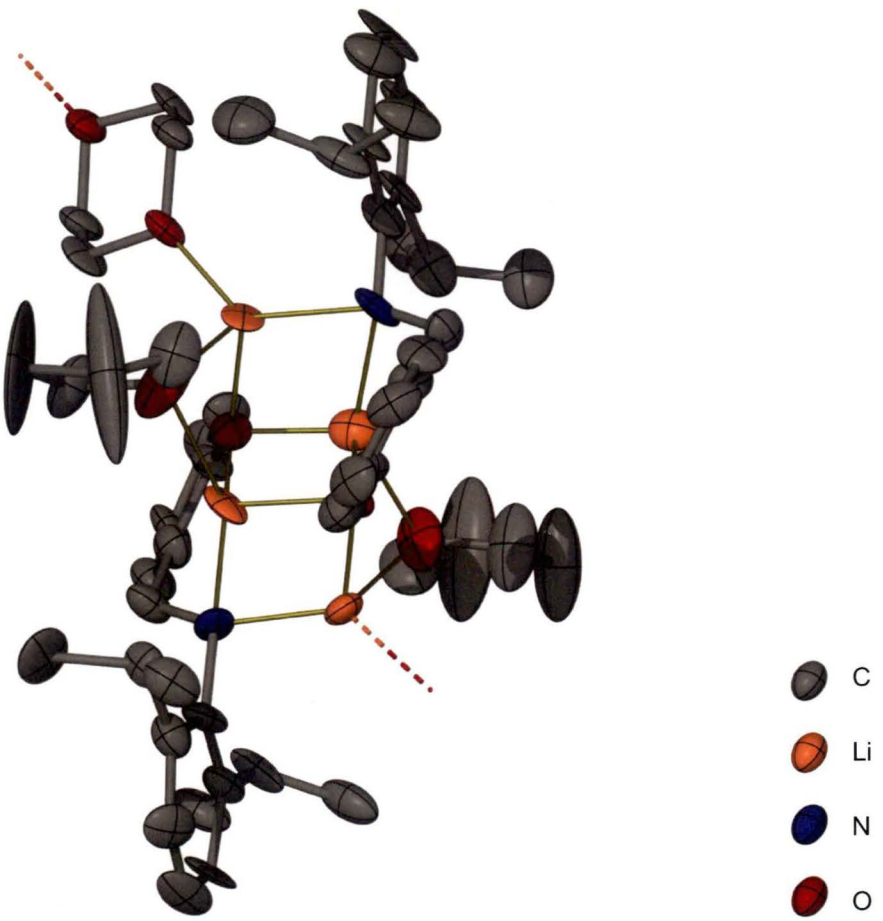

Figure 3-8: Front on view of a dimeric $Li_4O_2N_2$ unit of [{[Li_2(ONDIPP)]$_2$(1,4-dioxane)(THF)}$_\infty$] **21** with thermal ellipsoids drawn at the level of 50 % probability. Hydrogen atoms removed for clarity.

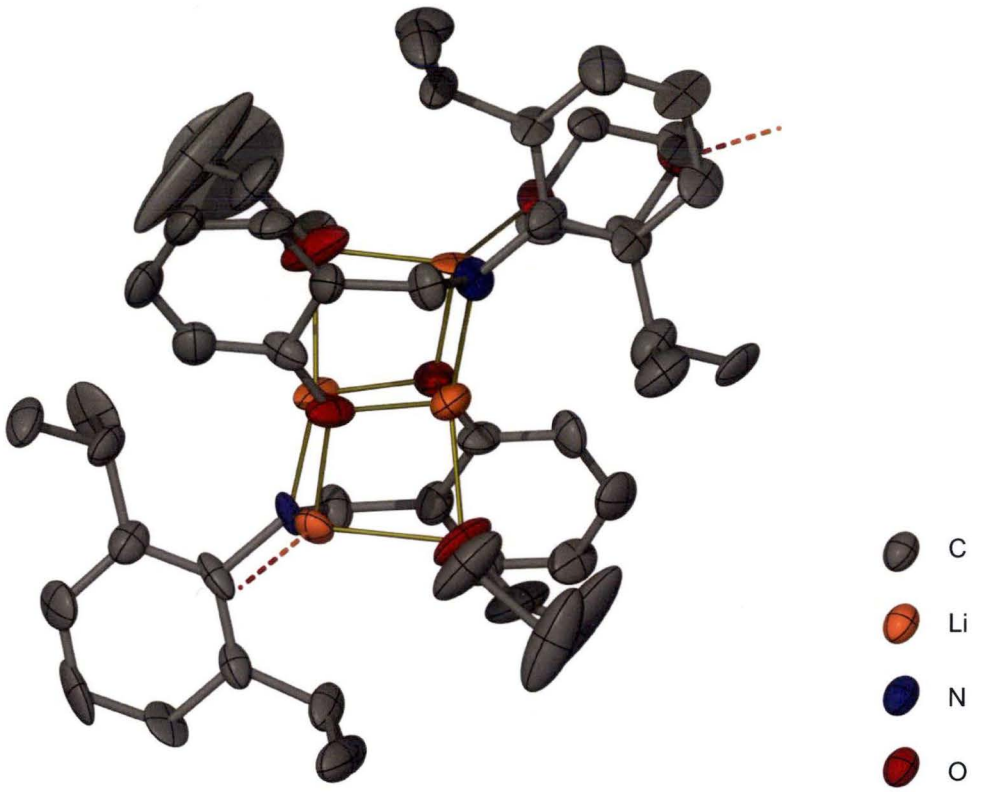

Figure 3-9: Side on view of a dimeric $Li_4O_2N_2$ unit of $[\{[Li_2(ONDIPP)]_2(1,4\text{-dioxane})(THF)\}_\infty]$ **21** with thermal ellipsoids drawn at the level of 50 % probability. Hydrogen atoms removed for clarity.

The individual dimeric units of the 1-D polymer chain of **21** maintain the previously noted features of the related bulky dimeric $Li_4O_2N_2$ units. The dimers maintain a total of four Lewis basic interactions, and have the methylene group of the dilithiated ligand pointing 'away'. The dimers have undergone a single ligand substitution, substituting their monodentate THF ligand for a molecule of 1,4-dioxane, which also coordinates to the analogous position in the neighbouring dimeric complex, thus forming the polymeric chain shown in Figure 3-10.

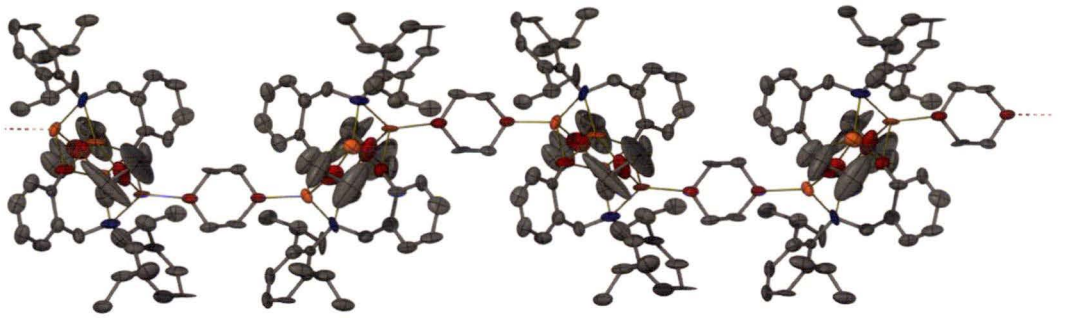

Figure 3-10: Polymeric structure of the complex [{[Li_2(ONDIPP)]$_2$(1,4-dioxane)(THF)}$_\infty$] **21** with thermal ellipsoids drawn at the level of 50 % probability. Hydrogen atoms removed for clarity.

3.3.4. Dilithiated O/N complexes – reactions with solvents

It was observed that treatment of the dilithiated complex [{Li_2(ONDIPP)}$_2$(THF)$_4$] **12** with neat DME resulted in the formation of vinyl methyl ether, MeOLi and the monolithiated complex [{Li(ONDIPPH)}$_4$] **9**, as shown in Scheme 3-11. The monolithiated complex [{Li(ONDIPPH)}$_4$] **9** had been isolated as a product a number of times previously from reactions using the dilithiated complex [{Li_2(ONDIPP)}$_2$(THF)$_4$] **12** as a starting material. On these occasions, the isolation of this reprotonated product was attributed to either a small amount of by-product, which had a strong tendency to crystallise out of solution, and/or poor experimental technique. The observation of methanol and vinyl methyl ether by GC-MS sampling of the reaction headspace after quenching the reaction mixture, however, prompted further investigation into the possibility that the reprotonation of the starting complex was occurring via deprotonation of one of the substrates within the reaction mixture, as the by-products of vinyl methyl ether and MeOLi can only conceivably have originated as fragmentation products from DME.

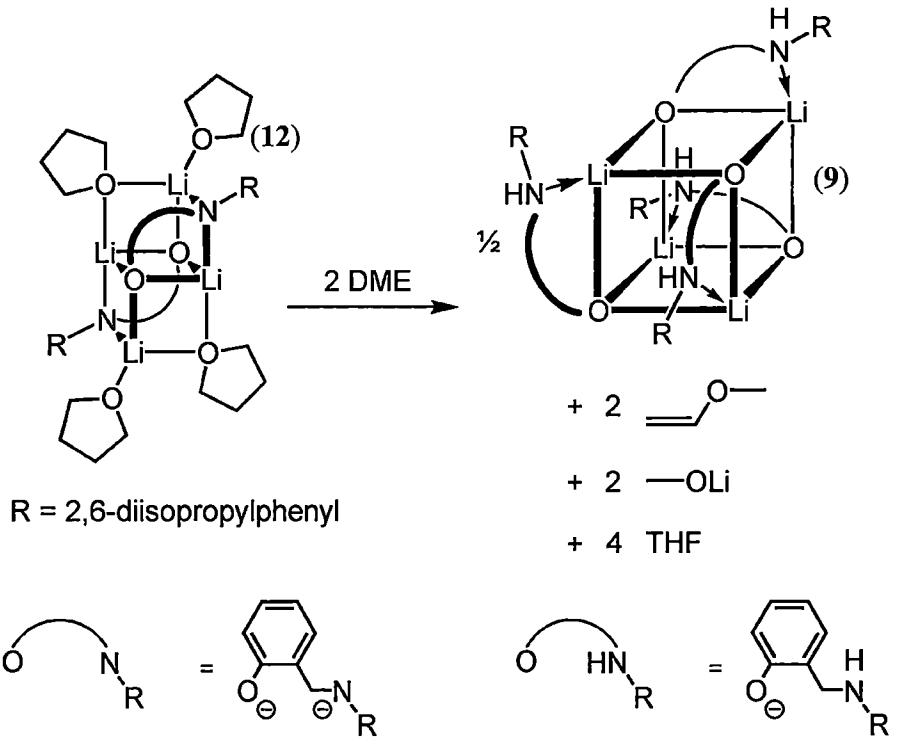

Scheme 3-11: Observed reaction of the dilithiated complex [{Li_2(ONDIPP)}$_2$(THF)$_4$] **12** with DME.

The observation of fragmentation products from DME lead to the idea of using dilute solutions of the starting dilithiated THF complexes in benzene and adding a small amount of the new Lewis basic ligand to obtain the ligand exchanged complexes for the ether type ligands described in Section 3.3.1 and Section 3.3.2. Whereas, previously, the procedure had been to use similar methodology to the exchange that occurs successfully with neat TMEDA to obtain the complexes [{Li_2(ONPh)}$_2$(TMEDA)$_3$] **14** and [{Li_2(ONDIPP)}$_2$(TMEDA)$_2$] **15**, as described in Section 2.3.7. When the dilithiated complex [{Li_2(ONDIPP)}$_2$(THF)$_4$] **12** is exposed to dilute DME the ligand substituted complex [{Li_2(ONDIPP)}$_2$(DME)$_2$] **17** is obtainable as a pure crystalline solid. Once formed however, even in the absence of excess DME if the complex is heated it will undergo an intermolecular deprotonation reaction to yield vinyl methyl ether and MeOLi, as observed when the complex synthesis is attempted in neat DME. This same reactivity was not observed for

[{[Li_2(ONPh)]$_2$(DME)$_3$}$_\infty$] **16**, however. These observed reactivities of the DME substituted dilithiated complexes are detailed in Scheme 3-12.

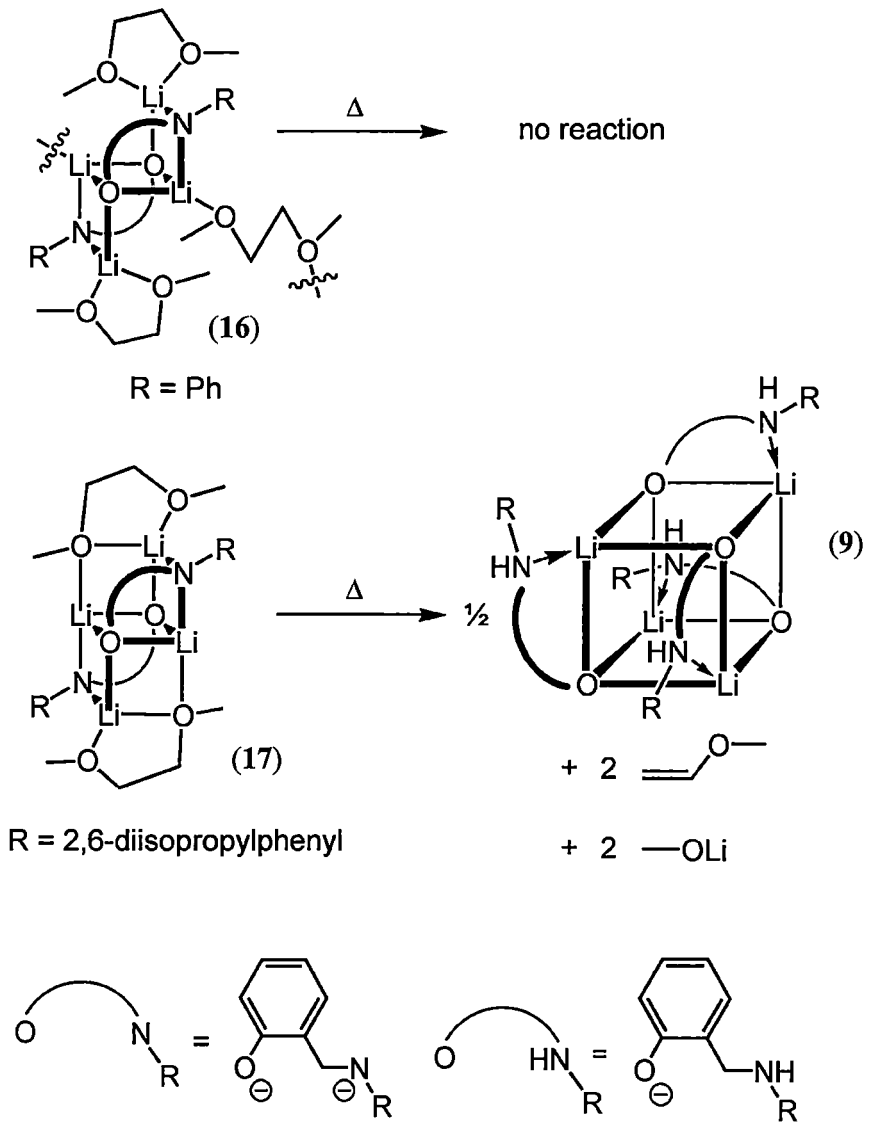

Scheme 3-12: Thermal stability of the complexes [{[Li_2(ONPh)]$_2$(DME)$_3$}$_\infty$] **16** and [{Li_2(ONDIPP)}$_2$(DME)$_2$] **17**.

In order to identify the reason for this contrasting behaviour between the very similar complexes **11** and **12**, the molecular structures of these dilithiated complexes and the DME adducts **16** and **17** were closely examined. Throughout the series of dimeric dilithiated complexes, with the exception of the two TMEDA solvated complexes, the same core geometry is observed, a centrosymmetric $Li_4O_2N_2$ four-rung ladder. The two internal Li-O rungs are formed by the phenoxido-lithium pairs, and the outer

two Li-N rungs are formed by the amido-lithium pairs. Another consistent feature of the dimeric dilithiated complexes is that the number of Lewis basic interactions is preserved for each of the two groups of analogous complexes containing the same substituent on the nitrogen atom; *N*-phenyl substituent giving rise to six Lewis basic interactions, and the larger *N*-2,6-diisopropylphenyl substituent giving rise to only four Lewis basic interactions. This is one potential source of the observed variation in reactivities between the DME substituted complexes. In the complexes incorporating the larger *N*-2,6-diisopropylphenyl substituent two of the four Lewis basic interactions are bridging interactions, whereas this binding mode is not seen for the complexes incorporating the less bulky *N*-phenyl substituent. The bridging interaction results in a contraction of the Li-O-Li angle along the ladder edge in $[\{Li_2(ONDIPP)\}_2(DME)_2]$ **17** by an average of approximately 20 ° compared to $[\{[Li_2(ONPh)]_2(DME)_3\}_\infty]$ **16** and approximately 25 ° in comparison to $[\{Li_2(ONPh)\}_2(DME)_2(THF)_2]$ **18**, as the terminal lithium atoms of the ladder are pulled together by the bridging oxygen centre in the bulkier case, as illustrated in Figure 3-11.

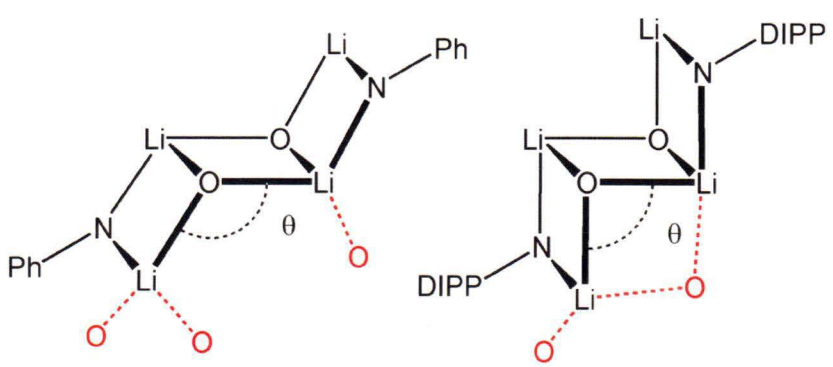

Figure 3-11: Diagram illustrating the difference between the inter planar angles of the $Li_4O_2N_2$ four-rung ladder core for the different *N*-substituents of the O/N dilithiated ligands.

This contraction of the 'step angle' in the $Li_4O_2N_2$ four-rung ladder core allows the same coordination number for each of the lithium atoms in the core, however leaves the dilithiated ligand, which is still strapping a distance of two rungs along the ladder

edge, less room to accommodate the four N-C, C-C, C-C, C-O bonds that make up the length of the strap between the two anions that have relatively little conformational flexibility.

In addition to this tightening of the ladder step angles, the incorporation of the larger substituent on the nitrogen alters how the dilithiated ligand positions its methylene group within the complex. As mentioned in Chapter 2, in the dimeric complexes of the dilithiated less bulky ligand $ONPhH_2$ **4**, the methylene within the dilithiated ligand is positioned pointing towards the centre of the dimer, lying over the face of the ladder core as viewed perpendicular to them. Whereas in the dimeric complexes of the dilithiated bulkier ligand $ONDIPPH_2$ **5** the methylene group has been flipped so that it is positioned pointing 'away' from the centre of the dimer and no longer lies over the face of the ladder core as viewed perpendicular to them. This is illustrated in Figure 3-12.

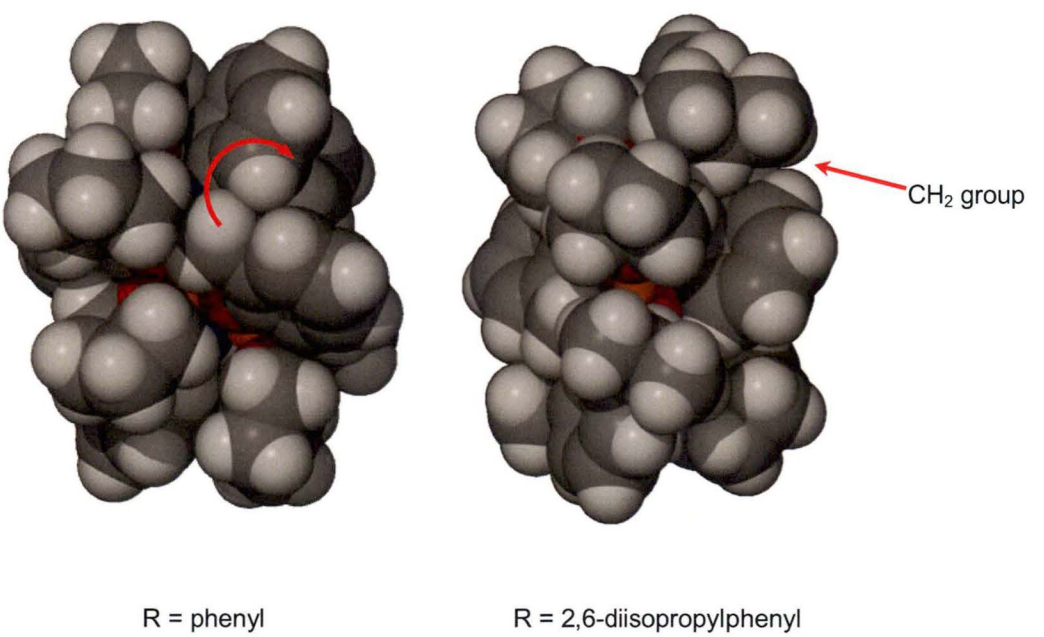

Figure 3-12: Space filling diagrams of the dimeric dilithiated THF complexes illustrating the different positions of the methylene group in the ligand. Viewing orientations of the $Li_4O_2N_2$ core are the same in each diagram.

The two above noted effects in the bulkier dilithiated complexes of the tightening of the ladder 'step angle' and the flip outwards in the position of the methylene group results in a more tightly constrained 'groove' in the complexes where solvent molecules can interact with the core of the dimer. This is shown in the space filling representations of $[\{Li_2(ONDIPP)\}_2(THF)_4]$ **12** with and without coordinated solvent in Figure 3-13.

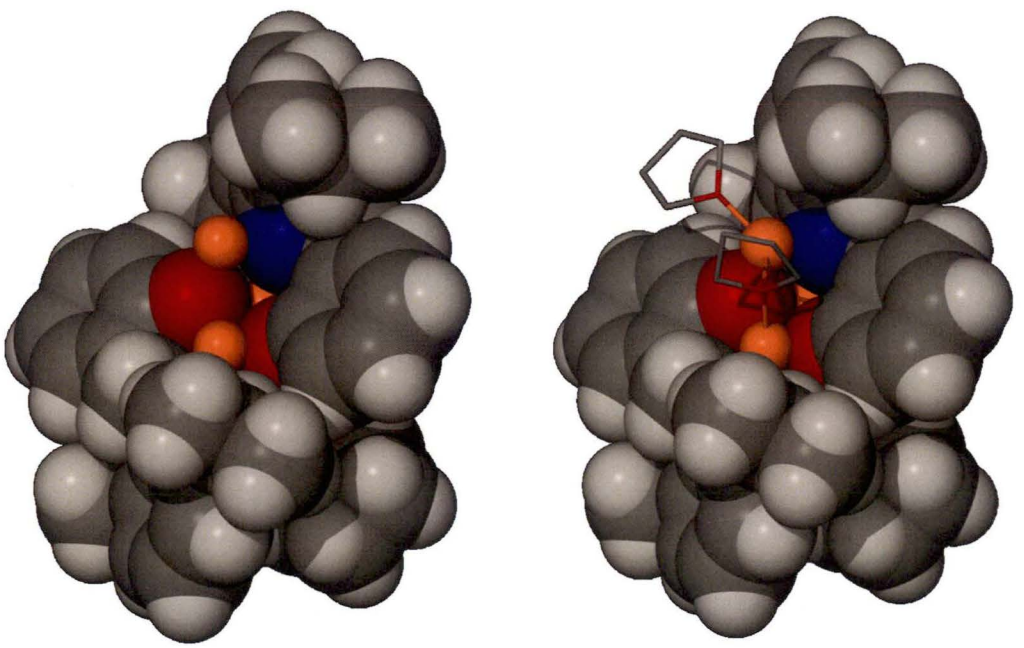

(a) (b)

Figure 3-13: Space filling representations of the groove into which solvent molecules can bind in the dimeric dilithiated complexes incorporating the *N*-2,6-diisopropylphenyl substituent; a) with no solvent, b) with THF.

In addition to the observed reaction with DME, a similar solvent attack reaction with diethyl ether was observed. It was of particularly interest to try and obtain the diethyl ether solvated complex of dilithiated $ONDIPPH_2$ **5** because if the $Li_4O_2N_2$ four-rung ladder core geometry was maintained with the bridging Lewis basic oxygen donor atom, and a crystal structure was able to be obtained, it would have been the first reported case of diethyl ether bridging two lithium centres. The complex was not able to be isolated, instead a complex containing a modified O/N ligand

incorporating a silicon grease fragment was obtained, as well as the monolithiated complex [{Li(ONDIPPH)}$_4$] **9**. This reactivity towards silicon grease is discussed further in Chapter 5. In a more controlled experiment, a solution of the dilithiated complex [{Li_2(ONDIPP)}$_2$(THF)$_4$] **12** in benzene was heated at 100 °C overnight in the presence of a small amount of diethyl ether. This reaction yielded similar products as observed for the reaction of DME with the dilithiated complex as described above in Scheme 3-11 and Scheme 3-12. The products in this case are ethylene and EtOLi.

Similar C-O reactivity was observed for the asymmetric diether ligand $MeOCH_2CH_2O$*t*-Bu. When heated, a solution of the dilithiated complex [{Li_2(ONDIPP)}$_2$(THF)$_4$] **12** in benzene with a small excess of $MeOCH_2CH_2O$*t*-Bu undergoes decomposition to yield the monolithiated complex [{Li(ONDIPPH)}$_4$] **9**, vinyl methyl ether and *t*-BuOLi. Interestingly, the reaction specifically produced these products and no detectable amounts of the reverse case products *t*-butyl vinyl ether and MeOLi. This observed specificity was key to investigating the mechanism of the fragmentation reaction pathway. The computational investigation is discussed in Section 3.3.6.

The evidence thus far supports the hypothesis that if a ligand molecule interacts with the bulkier dilithiated complex containing the $Li_4O_2N_2$ four-rung ladder core in a chelating way, it is likely to be susceptible to intramolecular deprotonation. Chelating is obviously not possible in the case of diethyl ether, and presumably an alternate interaction leading to fragmentation is occurring in that case. It is noted, also, that the complex [{Li_2(ONDIPP)}$_2$(THF)$_4$] **12** when heated in benzene in the absence of additional solvent results in no THF solvent fragments being observed, remaining as the dilithiated complex by NMR. Similarly, when the less bulky complex [{Li_2(ONPh)}$_2$(THF)$_6$] **11** is heated in benzene, no THF solvent fragments

or reprotonation are observed to occur. The observation of an increased reactivity towards DME compared to THF by complex **12** is significant, as there are many known mechanisms by which THF can undergo ring opening decomposition.[149, 151, 173-178] In particular the biphenyl/lithium adduct mentioned in the introduction of this chapter will ring-open THF, however is not known to react with acyclic alkyl ethers.[152] The observed reactivity of complex **12** towards particular alkyl ethers focuses attention on the geometry of the reactive complex, where a chelating Lewis base binds in the binding groove before reacting.

The observed decomposition products of the ether type ligands presented thus far are consistent with a deprotonation reaction occurring at the internal hydrogen α- to the bridging oxygen centre within the ether type ligands followed by C-O bond cleavage. This would suggest they proceed via the α- elimination pathway described in the introduction of this chapter. The general mechanism by which this might occur is shown for DME and $MeOCH_2CH_2Ot$-Bu in Scheme 3-13.

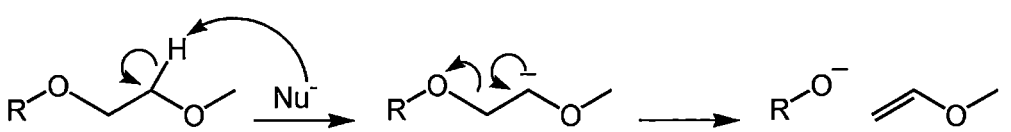

R = Me, *t*Bu

Scheme 3-13: Generalised mechanism for the α- elimination reaction pathway in a diether.

In the cases of reactivity towards DME and $MeOCH_2CH_2Ot$-Bu, the deprotonation reaction appears to be regioselectively controlled via the orientation in which the ligand molecule chelates to the complex. Thus, to investigate what the resulting reaction product would be, if any, if an ether substrate did not contain any internal α- hydrogen atoms veratrole (1,2-dimethoxybenzene) was trialled, as it retained the chelating functionality, but lacked any internal α- hydrogen atoms.

Initially the reaction of the dilithiated complex [{Li_2(ONDIPP)}$_2$(THF)$_4$] **12** with veratrole was trialled. It is reasonable to assume that the veratrole can still achieve bidentate binding with the bulky dimeric dilithiated complex, and indeed reaction between the dilithium complex and veratrole was still observed, with *O*-demethylated veratrole (guaiacol, 2-methoxyphenol) being detected by GC-MS. In this case, however, rather than a deprotonation reaction occurring, the GC-MS results indicated that the reaction results in a methyl transfer from the veratrole to the nitrogen centre of the O/N ligand. The observed solvent attack results discussed so far are summarised in Scheme 3-14.

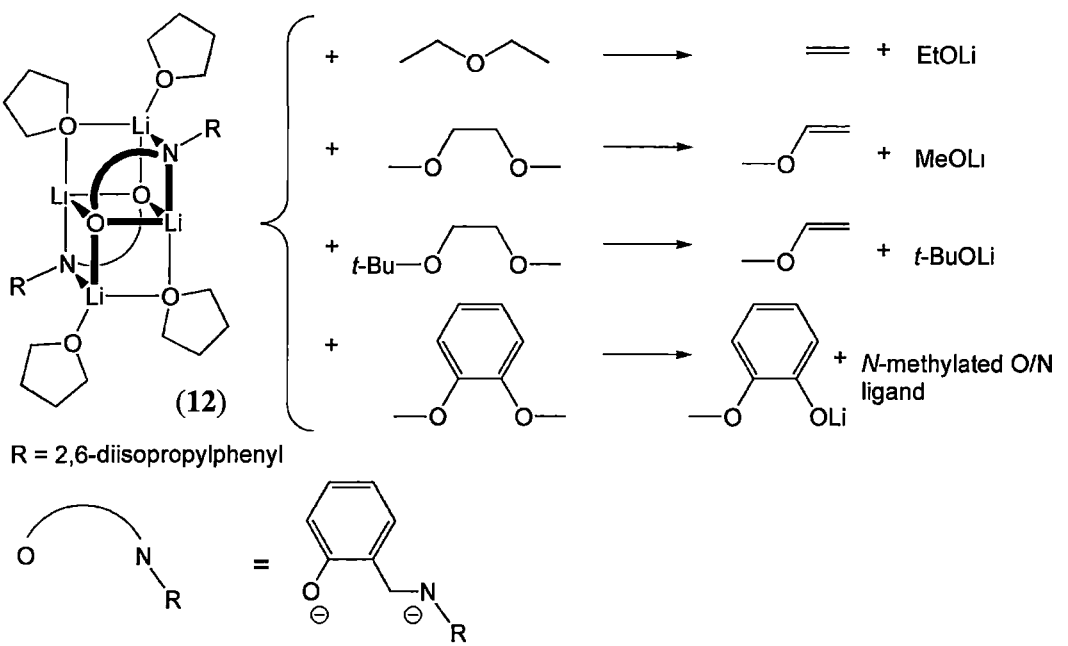

Scheme 3-14: Summary of the observed reaction products from the reaction of [{Li_2(ONDIPP)}$_2$(THF)$_4$] **12** with various ether type substrates.

It was not possible to obtain any characterisation of the veratrole adduct with the dilithiated *N*-2,6-diisopropylphenyl substituted ligand, as the reaction only occurred in neat veratrole rather than in benzene solution and no solid was able to be isolated from the reaction mixture. However, supporting evidence that the reaction still proceeds from a molecular adduct was obtained, as it was possible to predict and

verify that coordination via an *ortho* diether arrangement capable of chelating was necessary for reaction to occur. Whereas 1,2-dimethoxybenzene undergoes *O*-demethylation, 1,3-dimethoxybenzene was not observed to produce any demethylated product when reacted under the same conditions. There was a very small amount of solid material produced from this reaction, which yielded the crystal structure of the monolithiated imine tetramer [{Li(ON=DIPPH)}$_4$] **10**, discussed in Section 2.3.4. This by-product was shown to be present in only a very small amount, and is not thought to be directly linked to the demethylation reactivity.

Further to the observed lack of reactivity towards *meta* substituted ether substrates, when the reaction is carried out in 1,2,4-trimethoxybenzene only two products are produced, consistent with a single reaction occurring to a ligand interacting in a bidentate coordination arrangement. These results are summarised in Scheme 3-15.

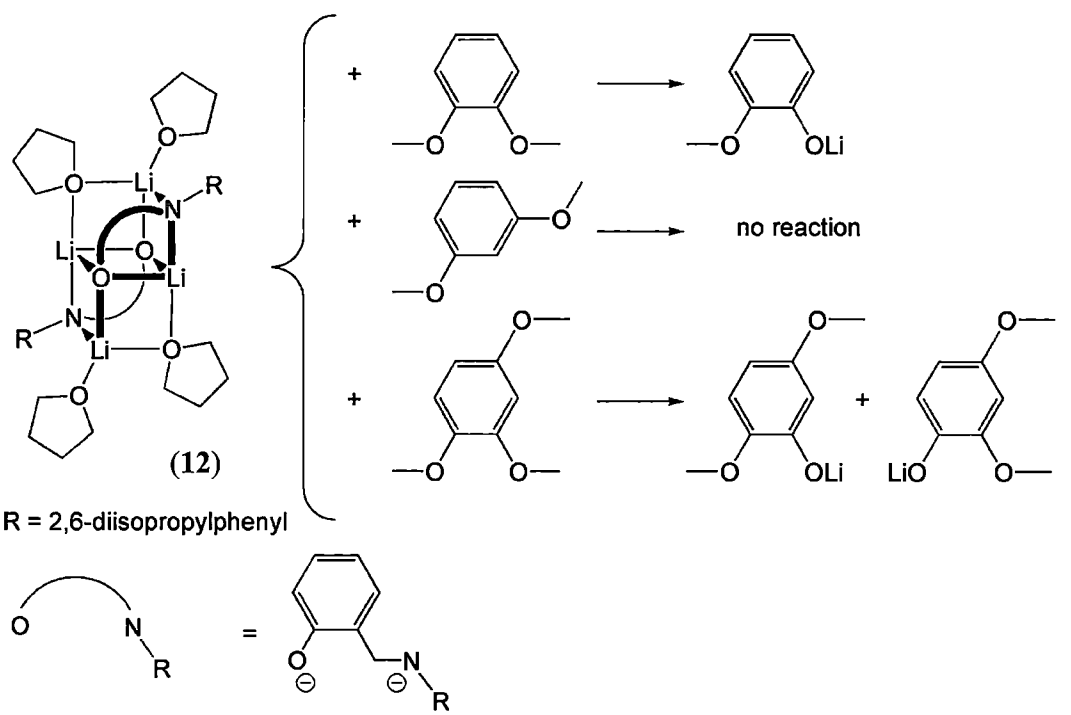

Scheme 3-15: A summary of the observed reaction products from the reaction of [{Li_2(ONDIPP)}$_2$(THF)$_4$] **12** with various aromatic ether type substrates. O/N ligand by-products not shown.

This result is in contrast to the behaviour of sodium *N*-methyl anilide, as discussed in the introduction of this chapter, where typically it is observed that multiple methoxy groups will undergo cleavage, as there was no detectable trace of multi-demethylation occurring from the reaction of these methoxy benzenes with complex **12**. Further measures were taken to demonstrate that the guaiacol produced was far from a minor by-product, but is produced stoichiometrically (1 per Li_2ON unit) in the reaction with dimeric dilithiated complex. The amount of guaiacol produced in the reaction was quantified by preparing a three-point standard curve for guaiacol ($R^2 = 0.99$) , spiked with 10 μg/mL cresol. GC-MS analysis of a reaction mixture (of known concentration) spiked with 10μg/ml cresol showed 91% yield of guaiacol.

It was expected that the *N*-phenyl substituted dilithiated complex $[\{Li_2(ONPh)\}_2(THF)_6]$ **11** would show no reactivity towards veratrole, as it was unreactive towards both DME and $MeOCH_2CH_2O$*t*-Bu. This is consistent with the differences in binding arrangement of the Lewis base ligands between **11** and **12** discussed earlier in this section. Surprisingly, reactivity between complex **11** and veratrole was observed. While attempting to isolate the veratrole adduct of the *N*-phenyl substituted dilithiated complex (this was the anticipated outcome, with the hope of confirming some structural features of the veratrole adduct), crystals suitable for X-ray crystal structure determination of an alternate product were obtained. They turned out to be of a decomposition product that was quite remarkable as it represented the only solvent attack arising from complex **11**. The structure was of the complex $[\{Li(ON(Me)Ph)\}_4]$ **22** which contains a modified monolithiated O/N ligand, now with a tertiary amine, incorporating an *N*-methyl presumably originating from the veratrole. The reaction is detailed in Scheme 3-16.

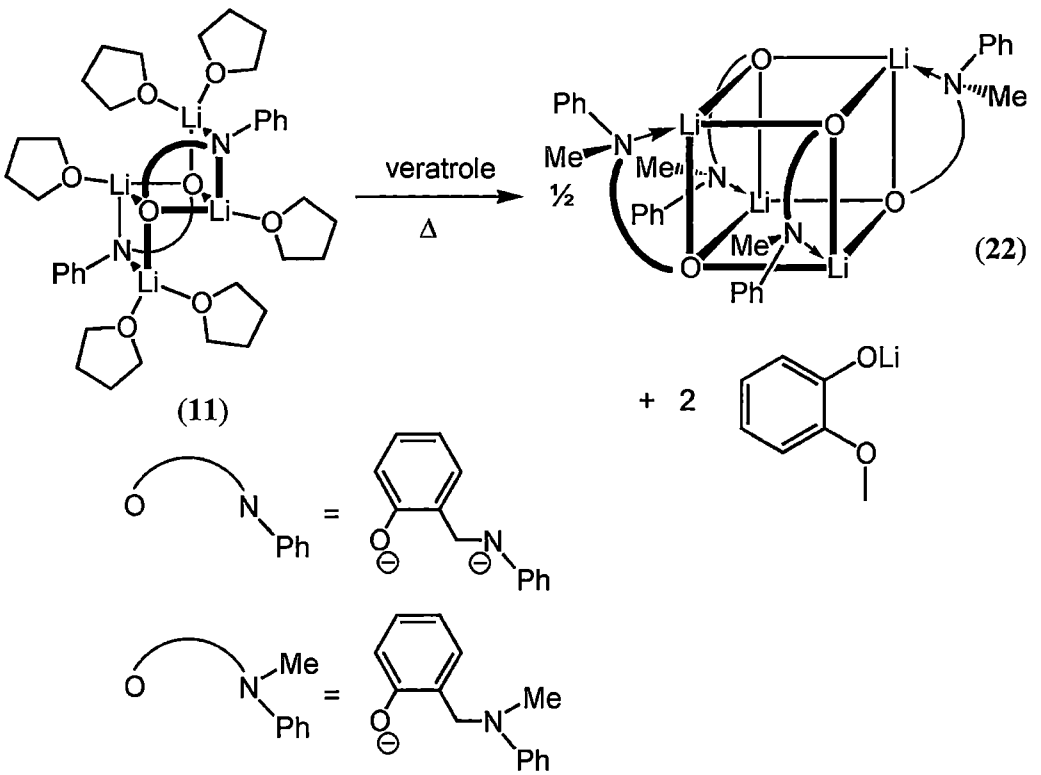

Scheme 3-16: Reaction of complex [{Li_2(ONPh)}$_2$(THF)$_6$] **11** with veratrole to produce complex [{Li(ON(Me)Ph)}$_4$] **22**.

Complex [{Li(ON(Me)Ph)}$_4$] **22** is a symmetric tetrameric monolithiated complex. All of the tertiary amines act as internal Lewis bases in a similar way to that observed for the monolithiated complexes reported in Section 2.3.3. The complex was characterised by X-ray crystal structure determination and elemental analysis. Although the analogous complex was not able to be isolated from the reaction of [{Li_2(ONDIPP)}$_2$(THF)$_4$] **12** with veratrole, as indicated earlier, there was evidence that a similar methyl transfer reaction was occurring from the GC-MS results of the reaction mixture with a O/N ligand derived mass fragment of 191 matching *N*-methyl 2,6-diisopropylaniline, which was shown to most likely be a thermal decomposition product of the *N*-methylated O/N ligand. Note, that the molecular ion was not always observed in the GC-MS analysis of the O/N ligand ONDIPPH_2 **5** and its derivatives, as the C-N bond between the aniline fragment and the remainder of the ligand seems

particularly prone to thermally induced cleavage. Consequently, the aniline fragment was typically identified as the characteristic mass fragment.

The *N*-phenyl substituted complex **11** was observed to be less reactive towards veratrole attack than the *N*-2,6-diisopropylphenyl substituted complex **12**, with clear evidence by GC-MS of the demethylation reaction occurring after 2 hours at 80 °C in the latter case, while the *N*-phenyl substituted complex was observed to require overnight at 100 °C to produce detectable reaction products.

Based on observing the *N*-methylated complex [{Li(ON(Me)Ph)}$_4$] **22**, it is assumed that lithium 2-methoxy phenoxide is formed in the reaction between veratrole and the dilithiated complex **11** (and most likely in the reaction with **12** also). Verification of this was attempted by trying to derivatise out the lithiated species by adding 1-bromobutane to the reaction of **11** and veratrole. However, analysis of the reaction mixture by GC-MS revealed new products arising from nucleophilic substitution at both the nitrogen and oxygen centres of the O/N ligand, but no butylated phenoxide, hinting at a lack of a persistent anionic oxygen centre formed upon demethylation of the veratrole. In the reaction of the dilithiated complex [{Li$_2$(ONDIPP)}$_2$(THF)$_4$] **12** with DME, part of the reaction products (vinyl methyl ether) are observed as a molecular species from the headspace above the reaction prior to quenching. However, due to the lower volatility of both the veratrole and guaiacol samples of the reaction mixture are run as a liquid. Consequently, at this stage it has not been possible to know if the demethylated veratrole is present as a neutral species or as an anionic component that gets reprotonated during GC-MS analysis.

3.3.5. Molecular structure of [{Li(ON(Me)Ph)}$_4$], 22

Colourless crystals of [{Li(ON(Me)Ph)}$_4$] **22** suitable for X-ray crystal structure determination were grown by heating a solution of [{Li_2(ONPh)}$_2$(THF)$_6$] **11** in veratrole at 100 °C overnight and concentrating the resulting solution. The crystals belong to the tetragonal space group *P*4/*n* (No. 85), $a = 14.8000(19)$, $c = 12.093(2)$ Å, with 2 Li_4O_4 molecules in the unit cell and the asymmetric unit consisting of ¼ molecule of [{Li(ON(Me)Ph)}$_4$] **22**. The complex has crystallographic S_4 symmetry and a ½ a disordered benzene solvent molecule. The molecular structure of [{Li(ON(Me)Ph)}$_4$] **22** is shown in Figure 3-14 and Figure 3-15.

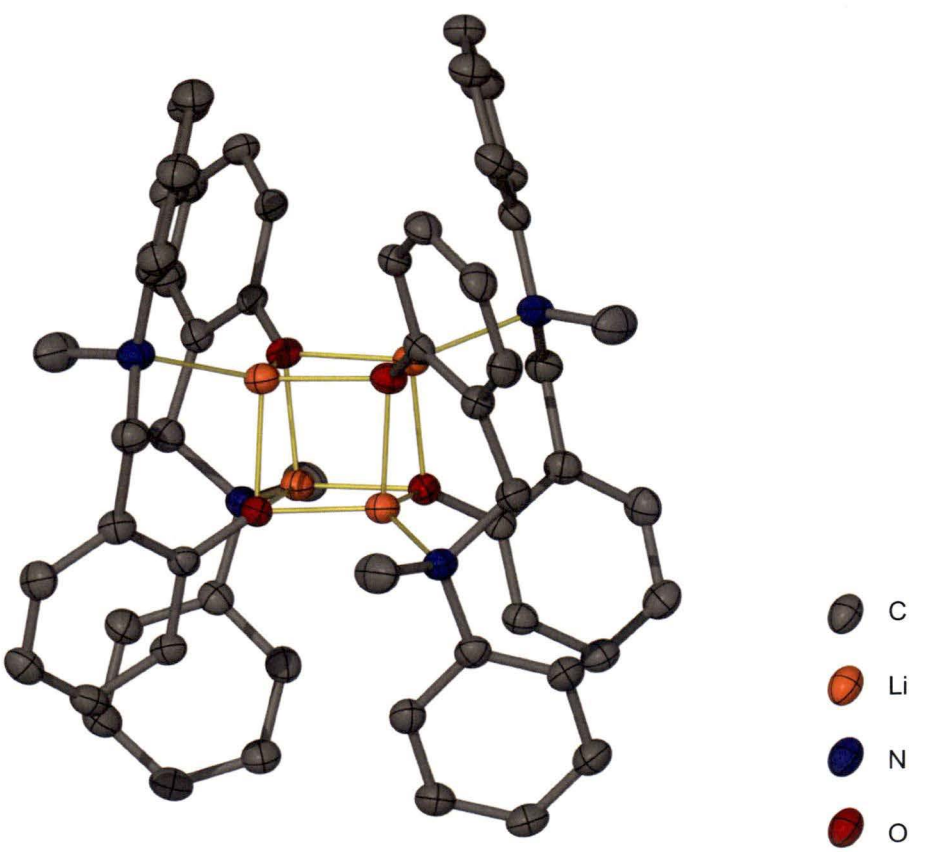

Figure 3-14: Molecular structure of [{Li(ON(Me)Ph)}$_4$] **22** with thermal ellipsoids drawn at the level of 50 % probability. Hydrogen atoms removed for clarity.

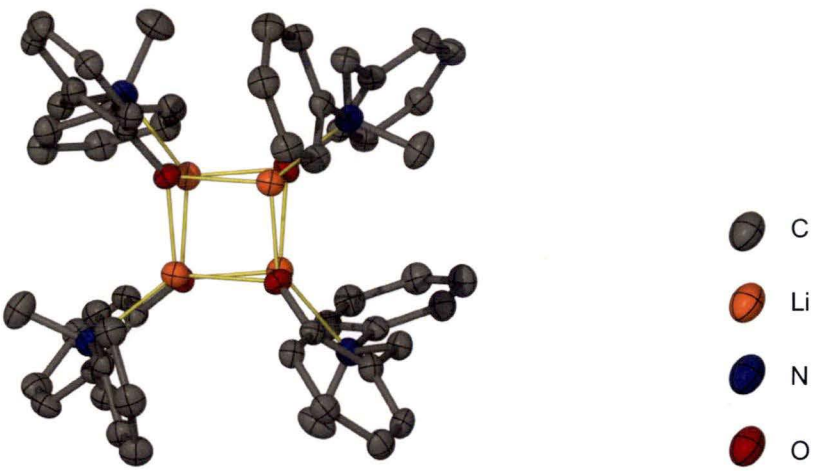

Figure 3-15: Top down view of the molecular structure of [{Li(ON(Me)Ph)}$_4$] **22** with thermal ellipsoids drawn at the level of 50 % probability. Hydrogen atoms removed for clarity.

Complex **22** forms a tetramer based on the phenoxide Li_4O_4 core seen for the other monolithiated complexes discussed in Section 2.3.3. In this case the tetramer has a different arrangement of ligands to that observed previously. All four of the ligands are arranged along four parallel edges of the cube, giving the complex a pseudo central axis of rotational symmetry. The ligands are a mixture of R and S configurations around the new tertiary amine centre, and alternate configurations around the rotation axis of the core.

3.3.6. Theoretical considerations

In the absence of a crystallographically confirmed veratrole adduct it was appropriate to model the complex presumed to form prior to it reacting and losing a methyl group as well as investigating this reactivity. In the complex with the bulkier *N*-2,6-diisopropylphenyl substituent it was assumed that veratrole would coordinate in a similar way to that observed for DME; that is one veratrole molecule per dilithiated ligand, with one oxygen atom bridging two lithium centres and the other singly donating to the amide lithium centre in the outer rung of the ladder core. The

optimised geometry for the veratrole adduct coordinating to [{Li_2(ONDIPP)}$_2$($THF)_4$] **12** in this way is shown in Figure 3-16, as an overlapping structure with the optimised geometry for the DME adduct.

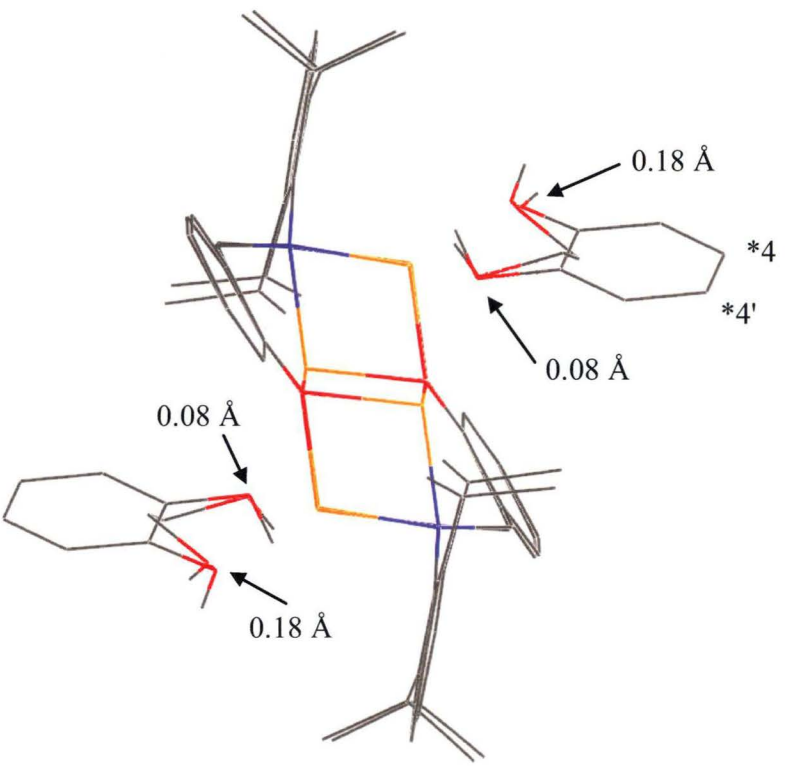

Figure 3-16: Optimised structures of the DME and veratrole adducts of the *N*-2,6-diisopropylphenyl substituted dilithiated ligand, overlayed together. Distances between the oxygen donor atoms between the two structures pointed out.

The two structures show nearly identical atom positioning in the core and ligand backbone. Only minimal differences in the location of the oxygen centres of the solvating molecule are apparent. This indicated that a complex would be able to form between the dimeric complex and the veratrole prior to reaction occurring at the methyl site of the veratrole. From examining this model of the veratrole adduct it is unsurprising that the reaction of 1,2,4-trimethoxy benzene with [{Li_2(ONDIPP)}$_2$($THF)_4$] **12** shows no specificity for demethylation of the 1- or

2-position as there are no steric interactions preferencing the location of the additional methoxy group in either the 4 or 4' position, as indicated in Scheme 3-15.

In the case of a veratrole adduct of the *N*-phenyl substituted ligand it wasn't immediately clear which orientation would be preferred; whether it would displace the two THF molecules from the amide lithium as in the complex with $MeOCH_2CH_2O$*t*-Bu, $[\{Li_2(ONPh)\}_2(MeOCH_2CH_2O$*t*$-Bu)_2(THF)_2]$ **19**, or if it would displace one THF molecule from each lithium as in the complex with DME, $[\{Li_2(ONPh)\}_2(DME)_2(THF)_2]$ **18**. Optimised structures were calculated for both possibilities, and their structures are shown in Figure 3-17a and Figure 3-17b with hydrogen atoms removed for clarity. The calculated energies for these two complexes differ in energy by 35.5 kJ/mol in favour of the veratrole displacing the two THF molecules from the amide lithium (Figure 3-17b), as observed in the complex $[\{Li_2(ONPh)\}_2(MeOCH_2CH_2O$*t*$-Bu)_2(THF)_2]$ **19**.

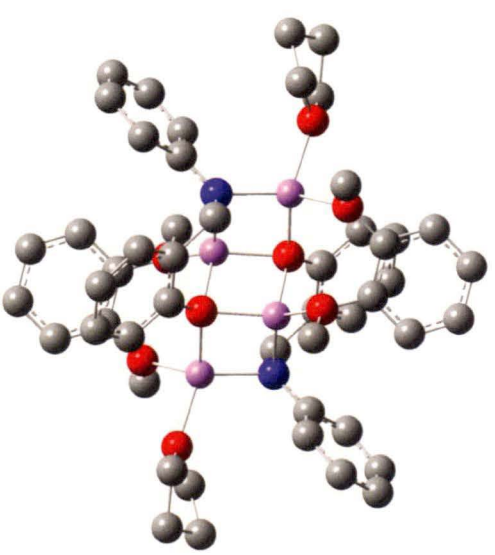

Figure 3-17a: *N*-phenyl dimer calculated with veratrole in a bridging arrangement.

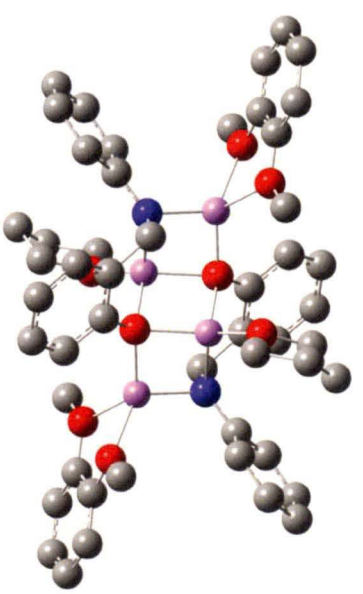

Figure 3-17b: *N*-phenyl dimer calculated with veratrole in a chelating arrangement.

From this observation, it is still unclear how the cleavage reaction might proceed, and further investigations would be required to ascertain the mechanism by which

demethylation occurs. Note also, that the mechanism by which the reaction of the *N*-phenyl substituted dilithiated complex with veratrole does proceed may not relate to the mechanism for the reaction of the bulkier *N*-2,6-diisopropylphenyl substituted dilithiated complex with veratrole. A possible mechanism by which the veratrole is demethylated in the latter case is shown in Scheme 3-17. Clearly this mechanism must be different from the α- elimination mechanism illustrated in Scheme 3-13, as there are no α protons available. Instead in this case, a lithium assisted S_N2 mechanism is proposed as the most feasible alternative pathway, leading to demethylation of the veratrole. The mechanism of veratrole attack was not investigated computationally as part of this work as it was anticipated that a significant amount of time would need to be spent determining the most likely possible pathway, out of several possible for both of the different nitrogen substituted ligand systems.

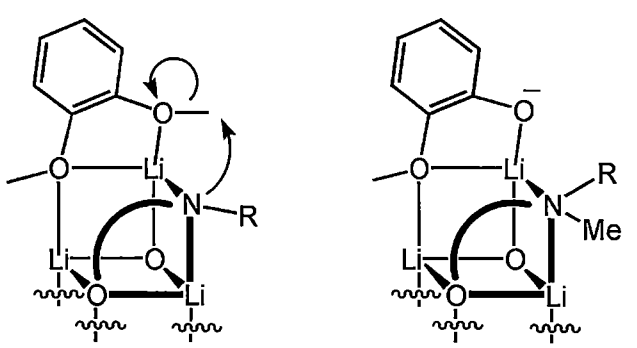

Scheme 3-17: Proposed mechanism of demethylation of veratrole by complex [{Li_2(ONDIPP)}$_2$(THF)$_4$] **12**.

Because the cleavage reaction of the aliphatic ether substrate $MeOCH_2CH_2Ot$-Bu in the presence of the complex [{Li_2(ONDIPP)}$_2$(THF)$_4$] **12** was observed to occur

regioselectivity, cleaving to yield exclusively vinyl methyl ether and *t*-BuOLi, a reaction pathway by which the fragmentation reaction occurs was able to be proposed. It was proposed that the fragmentation occurred via the α- elimination process, as noted earlier. Based on this, a theoretical reaction pathway was modelled for the DME fragmentation reaction. The steps of this mechanism for the fragmentation of DME are detailed in Scheme 3-18.

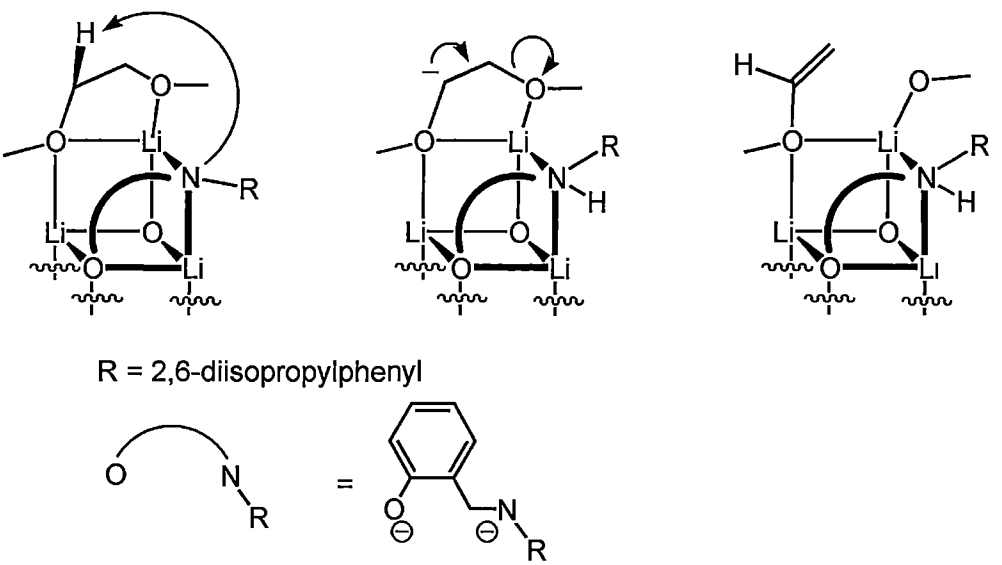

Scheme 3-18: Proposed mechanism of DME fragmentation by the *N*-2,6-diisopropylphenyl substituted dimeric complex.

The first step of the proposed reaction pathway is abstraction of an internal α- proton of the DME type ligand. For this to be a feasible first step, the ligand must first undergo a slight conformational rearrangement so that the methyl group attached to the bridging oxygen atom is not as well aligned with the bent binding groove, as observed in the solid state. A minimum energy structure was located corresponding to this modified conformation and the change in the conformation is shown in Figure 3-18a and Figure 3-18b . It is noted here that this computational study did not include an exhaustive conformational search for alternate local minima that would also lead to α-deprotonation. Similarly, deprotonation of the alternate internal α-proton in DME was not investigated. Inspection of both the optimised structure

matching the DME conformation in the crystal structure, Figure 3-18a, as well as the optimised alternate conformation noted above, Figure 3-18b, indicated that deprotonation at the alternate position was not feasible.

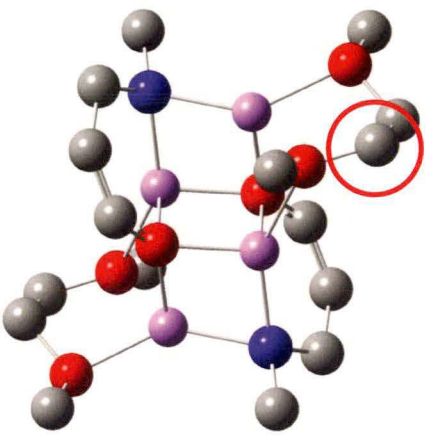

Figure 3-18a: Cut down model of complex [{Li_2(ONDIPP)}$_2$(DME)$_2$] **17** with methylene position highlighted. H's removed for clarity.

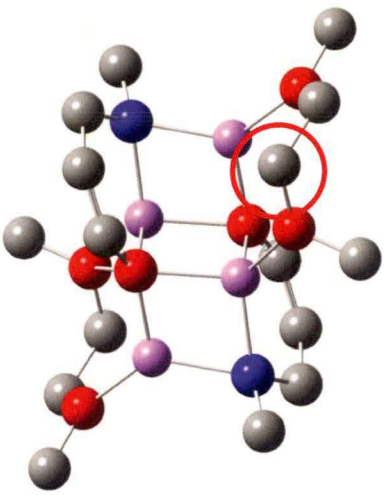

Figure 3-18b: Cut down model of complex [{Li_2(ONDIPP)}$_2$(DME)$_2$] **17** with altered methylene position highlighted. H's removed for clarity.

The model compounds used for this investigation are cut down more extensively than those used in the work for Chapter 2, and have only a methyl group as a nitrogen substituent, and a double bond in place of the phenylene ring in the O/N ligand backbone. The calculated energy difference between the complex with both of the methyl groups on the DME molecules in the modified configuration compared to the complex with the methyl groups positioned as observed in the solid state structure is 16.5 kJ/mol, which is a feasible energy to consider for this simplified model pathway relative to reactions at elevated temperatures. From this starting point, the transition states and reaction intermediates detailed in Scheme 3-18 were located and the optimised geometries calculated. The geometries were calculated at the moderate basis set that was used in Section 2.4 of 6-31G(d),[145, 146] again using DFT and the B3LYP[143, 144] functional. Following this, single point energies were

calculated using the larger basis set 6-311+G(2d,p).[179-181] The energy profile for the reaction is shown in Figure 3-19.

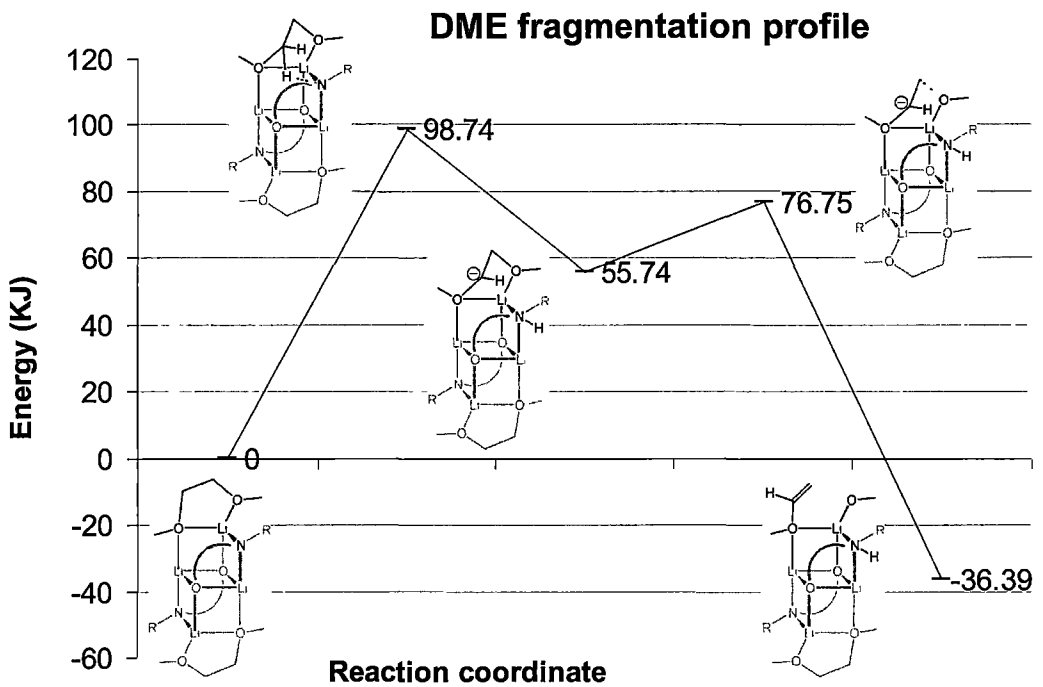

Figure 3-19: Energy diagram for the fragmentation of DME (Values are in kJ/mol).

The reaction pathway modelled is exothermic overall. As vinyl methyl ether is observed in the headspace of the reaction prior to quenching the reaction mixture, there are obviously further parts to this reaction whereby the newly formed bridging monodentate ether is lost from the complex. This could include a rearrangement of the dimer, or a displacement solvation interaction, or interaction with a separate dimer, or possibly the dimer could undergo a further fragmentation reaction. Certainly, it is known that the monolithiated tetramer is produced in this reaction. The reaction pathway was not investigated computationally any further past this point, but it is evident such a process would yield lower energy species due to this. The activation energy for the initial transition state of α-deprotonation by the amide group is quite large. This is consistent with the reaction observed to require heating

to proceed, however the barrier is likely to be over estimated as stabilising solvation effects were not included in this model.

The computational results obtained provide further supporting evidence that the fragmentation occurs as an intramolecular process, with predictable regioselectivity and importantly supports the overarching premise of this research that unusual chemical properties may be linked with combining anion types to induce unusual geometries and binding modes.

3.4. Conclusion

Chapter 3 reports the synthesis of a further three dilithiated dimeric lithium complexes based on the O/N ligand systems, $[\{Li_2(ONPh)\}_2(MeOCH_2CH_2O\textit{t}\text{-}Bu)_2(THF)_2]$ **19**, $[\{Li_2(ONDIPP)\}_2(MeOCH_2CH_2O\textit{t}\text{-}Bu)_2]$ **20**, and $[\{[Li_2(ONDIPP)]_2(1,4\text{-dioxane})(THF)\}_\infty]$ **21**. These dimeric complexes maintain the features discussed in the preceding chapter; in particular, they all contain a $Li_4O_2N_2$ ladder core, maintained from the starting complex. The dimeric complexes also maintain the degree of Lewis base solvation; four solvation interactions for the bulkier *N*-2,6-diisopropylphenyl substituted ligand complex, and six interactions for the less bulky *N*-phenyl substituted ligand complex. Complex **21** is similar to $[\{[Li_2(ONPh)]_2(DME)_3\}_\infty]$ **16** reported in Chapter 2 in that the dimeric $Li_4O_2N_2$ units are linked together by the bi-functional Lewis basic solvent, forming a polymeric chain. The complexes **19** and **20** are adducts of the asymmetrically substituted dialkyl diether molecule $MeOCH_2CH_2O\textit{t}$-Bu. The orientation of the $MeOCH_2CH_2O\textit{t}$-Bu molecules within **20** was correctly predicted to be such that the bulkier end is positioned away from the centre of the dimer. This result correlates

with the corresponding observed selectivity in the fragmentation of the $MeOCH_2CH_2Ot$-Bu molecule.

The remainder of Chapter 3 discusses the observed reactivity of the two THF solvated dilithiated dimeric complexes $[\{Li_2(ONPh)\}_2(THF)_6]$ **11** and $[\{Li_2(ONDIPP)\}_2(THF)_4]$ **12** towards various ether solvents. It was observed, initially serendipitously, that complex **12** would react with some ether type solvent molecules, resulting in reprotonation of the complex to form $[\{Li(ONDIPPH)\}_4]$ **9**, as well as solvent molecule fragments. Reactivity was observed with diethyl ether, DME, $MeOCH_2CH_2Ot$-Bu, as well as the alkyl aryl ethers 1,2-dimethoxy benzene and 1,2,4-trimethoxy benzene. In the case of the dialkyl ethers, reaction was observed to occur at the internal α- position. This resulted in diethyl ether fragmenting to give ethylene and (after work-up) ethanol. In a similar fashion DME reacted to give vinyl methyl ether as well as (after work-up) methanol. The asymmetrically substituted dialkyl diether, $MeOCH_2CH_2Ot$-Bu reacted to give exclusively vinyl methyl ether and (after work-up) *t*-butanol. The alkyl aryl ethers reacted in a different way, to give the demethylated solvent fragment, with a corresponding modified *N*-methylated ligand. In the case of reaction of $[\{Li_2(ONPh)\}_2(THF)_6]$ **11** with 1,2-dimethoxy benzene, the product was isolated as the monolithiated tetrameric complex $[\{Li(ON(Me)Ph)\}_4]$ **22**. Although no solid material was able to be isolated from the analogous reaction with $[\{Li_2(ONDIPP)\}_2(THF)_4]$ **12**, there was GC-MS evidence that a similar *N*-methylation occurred. Significantly, no reaction between **12** and 1,3-dimethoxy benzene was observed, and reaction of **12** with 1,2,4-trimethoxy benzene was observed to produce two mono-demethylated isomers only.

The proposed reaction mechanism for the fragmentation of DME was investigated theoretically. Transition states were found for all of the intermediate steps in the fragmentation pathway, and the results support the observations as the process was found to be thermodynamically favourable with relatively high activation barriers.

The observation that the fragmentation reaction of $MeOCH_2CH_2Ot$-Bu is specific for the products vinyl methyl ether and *t*-butanol is significant as it provides strong supporting evidence for the proposed reaction mechanism, which is linked with the altered position of the methylene carbon in the dilithiated O/N ligand backbone, as discussed in Chapter 2. This reaction outcome supports and emphasises the value of studies such as this work into fundamental processes. It has been possible to build up a detailed structure-property relationship that provides understanding and rationale for the highly unexpected reaction of these 'model' superbase compounds towards ethers. Further to the observed regioselectivity in the fragmentation of $MeOCH_2CH_2Ot$-Bu, the reactivity of the complexes **19** and **20** towards the methoxy benzene type ethers supports the hypothesis that the reaction occurs via coordination of the ether molecules to the complex as no reaction was observed with 1,3-dimethoxy benzene.

3.5. Experimental

3.5.1. Synthesis of $MeOCH_2CH_2Ot$-Bu

$MeOCH_2CH_2Ot$-Bu was prepared from $HOCH_2CH_2Ot$-Bu using a modified literature method.[182] To a stirred solution of NaH (4.60 g, 192 mmol) in THF a solution of $HOCH_2CH_2Ot$-Bu (10 mL, 76 mmol) in anhydrous THF (40 mL) was added via a dropping funnel over 20 minutes under an argon atmosphere and the mixture stirred

for 1 hour. MeI (9.47 mL, 152 mmol) was added dropwise via syringe and the resulting slurry stirred for a further 2 hours. The mixture contained a large amount of white solid that was dissolved with the addition of water prior to extraction with diethyl ether (4x20 mL). The diethyl ether was back extracted with water (30 mL) and then $NaCl_{(sat)}$ before being dried over Na_2SO_4. The diethyl ether was removed to afford the desired product as an impure yellow oil, with the main contaminant being $HOCH_2CH_2O$*t*-Bu (8.72 g, 87 %). A portion was obtained pure (by ^{1}H NMR spectroscopy [183]) via cold distillation from NaH (static vacuum of approximately $1x10^{-1}$ mbar) and used thereafter.

3.5.2. Synthesis of [{Li$_2$(ONPh)}$_2$(MeOCH$_2$CH$_2$O*t*-Bu)$_2$(THF)$_2$] 19

A solution of [{Li_2(ONPh)}$_2$(THF)$_6$] **11** (42 mg, $4.9x10^{-5}$ mol) in benzene (*ca.* 2 mL) was prepared and $MeOCH_2CH_2O$*t*-Bu (0.5 mL) was allowed to vapour diffuse into the solution overnight. The crystalline product deposited out overnight and was washed with 40-60 °C petroleum spirits before being collected as a colourless crystalline material (35 mg, 85 %).

^{1}H NMR (300 MHz, C_6D_6, 25 °C): δ = 1.01 (18H, s, C(C*H*$_3$)$_3$), 1.31 (8H, m, THF), 3.07-3.18 (14H, m, DME OCH_3 CH_2), 3.44 (8H, m, THF), 4.53 (4H, s, CH_2), 6.53-6.88 (10H, m, Ar), 7.24-7.74 (8H, m, Ar).

^{13}C NMR (75 MHz, C_6D_6, 25 °C): δ = 26.1 (THF), 27.8 (C(*C*H$_3$)$_3$), 53.0 54.5 (CH_2), 59.2 (DME O*C*H$_3$), 60.9 (DME CH_2), 68.6 (THF), 72.7 (DME CH_2), 74.6 (DME *C*(CH$_3$)$_3$), 109.6 (Ar), 110.8 (Ar), 114.2

(Ar), 115.8 (Ar), 120.3 (Ar), 121.8 (Ar), 129.8 (Ar), 131.5 (Ar), 132.3 (Ar), 162.6 (Ar).

Anal. Calculated: C, 69.39; H, 8.49; N, 3.37; ($C_{48}H_{70}Li_4N_2O_8$)

Found: C, 68.41; H, 8.94; N, 3.31

3.5.3. Synthesis of [{Li_2(ONDIPP)}$_2$(MeOCH$_2$CH$_2$O*t*-Bu)$_2$] 20

A solution of [{Li_2(ONDIPP)}$_2$(THF)$_4$] **12** (42 mg, 5.6x10^{-2} mmol) in benzene (*ca.* 2 mL) was prepared and MeOCH$_2$CH$_2$O*t*-Bu (0.5 mL) was allowed to vapour diffuse into the solution overnight. The crystalline product deposited out overnight and was washed with 40-60 °C petroleum spirits before being collected as a colourless crystalline material (53 mg, 99 %).

^{1}H NMR (300 MHz, C_6D_6, 25 °C): δ = N/A (insoluble).

^{13}C NMR (75 MHz, C_6D_6, 25 °C): δ = N/A (insoluble).

Anal. Calculated: C, 73.05; H, 9.20; N, 3.28; ($C_{52}H_{78}Li_4N_2O_6$)

Found: C, 72.77; H, 8.98; N, 3.13

3.5.4. Synthesis of [{[Li_2(ONDIPP)]$_2$(1,4-dioxane)(THF)}$_\infty$] 21

A solution of [{Li_2(ONDIPP)}$_2$(THF)$_4$] **12** (48 mg, 5.5x10^{-2} mmol) in benzene (*ca.* 2 mL) was prepared and 1,4-dioxane (0.5 mL) was allowed to vapour diffuse into the solution overnight. The crystalline product deposited out overnight and was washed with petroleum 40-60 °C petroleum spirits before being collected as a clear crystalline material (54 mg, 99 %).

^{1}H NMR (300 MHz, C_6D_6, 25 °C): δ = N/A (insoluble).

^{13}C NMR (75 MHz, C_6D_6, 25 °C): δ = N/A (insoluble).

Anal. Calculated: C, 72.42; H, 9.12; N, 2.82; ($C_{27}H_{42}Li_2NO_4$. ½ C_6H_6)

Found: C, 72.59; H, 8.66; N, 2.91

3.5.5. Alternate solvates and polymorphs of [{Li(ONDIPPH)}$_4$] 9

Crystal structure determination of the monolithiated complex [{Li(ONDIPPH)}$_4$] **9** was performed a number of times, yielding a variety of different pseudopolymorphs containing a variety of lattice solvation. Many of these complexes were isolated from reactions where solvent underwent attack. The structure reported in Chapter 2 contains three lattice THF molecules per tetramer. Another crystal structure was determined with a single lattice THF molecule per tetramer. The crystal belongs to the monoclinic space group $P2_1/c$ (No. 14), $a = 20.11(2)$, $b = 14.013(12)$, $c = 27.519(6)$ Å, $\beta = 103.48(4)$ °, with 4 $Li_4O_2N_2$ molecules in the unit cell and the asymmetric unit consisting of 1 molecule of [{Li(ONDIPPH)}$_4$] **9** and 1 THF molecule.

When the monolithiated complex is isolated without lattice solvent present, in this case from 40-60 °C petroleum spirits and diethyl ether, the crystals belong to the monoclinic space group $C2/c$ (No. 15), $a = 21.96(2)$, $b = 15.856(9)$, $c = 20.893(8)$ Å, $\beta = 102.13(5)$ °, with 4 Li_4O_4 molecules in the unit cell and the asymmetric unit consisting of 1/2 molecule of [{Li(ONDIPPH)}$_4$] **9** processing C_2 crystallographic symmetry.

Another time the monolithiated complex was crystallised from benzene and incorporated a molecule of benzene in the lattice. In this case the crystals belong to

the monoclinic space group $C2/c$ (No. 15), $a = 21.57(2)$, $b = 16.510(13)$, $c = 22.510(9)$ Å, $\beta = 94.10(6)$ °, with 4 Li_4O_4 molecules in the unit cell and the asymmetric unit consisting of 1/2 molecule of [{Li(ONDIPPH)}$_4$] **9** processing C_2 crystallographic symmetry and one benzene molecule.

Finally, the monolithiated complex was isolated from a reaction in veratrole, with a molecule of veratrole incorporated in the lattice. In this case the crystal belongs to the triclinic space group $P\bar{1}$ (No. 2), $a = 13.216(2)$, $b = 14.386(2)$, $c = 22.470(3)$ Å, $\alpha = 73.399(6)$, $\beta = 79.125(8)$, $\gamma = 71.396(4)$ °, with 2 $Li_4O_2N_2$ molecules in the unit cell and the asymmetric unit consisting of 1 of a molecule of [{Li(ONDIPPH)}$_4$] **9** and veratrole molecule.

3.5.6. GC-MS quantification of guaiacol

Three solutions of guaiacol (1, 5, and 10 μg/mL) were prepared in toluene (100 mL) and spiked with *m*-cresol (10 μg/mL). Each of these solutions were analysed by GC-MS and a standard curve of the peak areas calculated ($R^2 = 0.99$). The reaction mixture of [{Li_2(ONDIPP)}$_2$(THF)$_4$] **12** in 0.50 mL veratrole was spiked to 10 μg/mL *m*-cresol and analysed by GC-MS. The amount of guaiacol present was back calculated from the concentration determined in solution from the standard curve.

3.5.7. Synthesis of [{Li(ON(Me)PhH)}$_4$] 22

The complex [{Li_2(ONPh)}$_2$(THF)$_6$] **11** (19 mg, 2.2 mmol) was dissolved in benzene (*ca.* 1 mL) and had 5 drops of veratrole added to it. The solution was heated at

100 °C overnight. Concentration of the resulting solution yielded a small crop of colourless crystalline material (4 mg, 19 %). A portion of the crystalline sample was dissolved in THF and filtered yielding a non-crystalline material that gave satisfactory elemental analysis.

^{1}H NMR (300 MHz, C_6D_6, 25 °C): δ = N/A (insoluble).

^{13}C NMR (75 MHz, C_6D_6, 25 °C): δ = N/A (insoluble).

Anal. Calculated: C, 74.21; H, 7.61; N, 4,81; ($C_{72}H_{88}Li_4N_4O_8$)

Found: C, 74.49; H, 7.88; N, 4.94

Chapter 4

Mixed anion N/C ligands and their lithiated complexes

4.1. Introduction

Though phenoxide anions bear similarities in their lithium complex aggregation to alkyllithium compounds, lithium phenoxides are considerably weaker bases than alkyllithiums as the parent organic fragment of a phenol is considerably more acidic than the protons on an alkyl fragment. It is largely for this reason that the label of 'model' superbases was used in this study, as the superbasic systems shown by Lochmann to be of most significant synergistic enhancement towards proton abstraction ability were mixtures incorporating at least one strong alkali metal base component, such as *n*-BuLi[68, 70] or *n*-amylsodium.[67] As discussed earlier, the heavier alkali metal reagents were not chosen for investigation in this study as there are frequently issues with their solubility, which drastically limit the ability to characterise any mixed anion complexes that might form within the reaction mixture.

As outlined in Chapter 2 it was the intention within this project to extend the investigation of the effect of mixing anion types on the aggregation of organolithium complexes from O/N mixed systems to N/C mixed systems. The appeal of extending to the mixed N/C system includes being more directly applicable to the previously reported 'superbase' systems, where selective proton abstraction of extremely weakly acidic protons becomes more relevant. In addition, a further variable to explore into the system is introduced, with the bulk at both anionic centres now being potentially variable.

There are many processes that can lead to stabilisation of a carbon centred anion in solution. A popular choice for synthetic chemists is to include a silyl group α- to the site of the anion.[184-186] The stabilising effect of silyl groups on carbanions was first quantified in the mid 1970's by Petrov *et al.* and found to induce a stabilisation effect of approximately 1 pH unit.[187, 188] Though, as pointed out by Streitwieser, the effect of the silyl group can be quite variable.[189] The effect of a heteroatom α- to a carbanion is of course a generalised phenomena. A good coverage of the various effects that different heteroatoms can have is presented by Krief.[190]

A common choice of silyl group is trimethylsilyl, as it offers not only good stabilisation but frequently aids in increasing solubility. This is particularly useful in the highly polar alkyl- and amidolithium reagents, such as bis(trimethylsilyl)amido lithium. Further to this, the trimethylsilyl group provides a useful 'NMR handle' without inducing significant extra complexity. It was for these reasons that the molecular scaffold chosen here for investigation of mixed N/C aggregation utilised a trimethylsilyl stabilising group α- to the carbanion site. The other principles of the ligand scaffold were maintained; that is the ligand scaffold is based on an *o*-phenylene backbone with the two anions included one on each arm, as shown here again in Figure 4-1a. The length of the rigid backbone of the ligand, as was seen in the preceding two chapters, helps to ensure that the common binding mode for lithium of the 'double-butterfly' is prevented from dominating the aggregation of the complexes. The 'double-butterfly' aggregation is shown in Figure 4-1b.

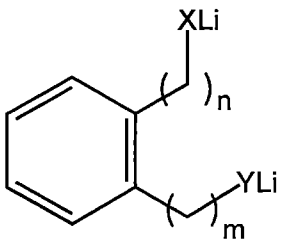

n, m = 0, 1, 2...,

X, Y = anion (alkyl, amide, alkoxide)

Figure 4-1a: Generalised multi-anion ligand scaffold.

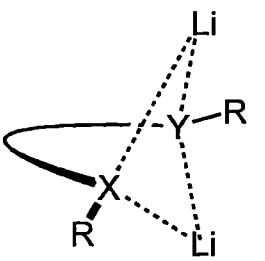

Figure 4-1b: 'Double-butterfly' binding mode of lithium.

Again, by considering how each portion of the functionality of the ligand would be included, and keeping in mind the desire for ease of synthetic variability, a synthetic scheme for the preparation of a mixed amide/alkyl anion system was devised, shown in Scheme 4-1. As for previous chapters, the ligands that include this combination of anion types will be referred to in terms of the anionic centres present in the metallated complexes, i.e., the N/C ligands.

4.2. Research aim

The synthetic variability of a nucleophilic substitution of an alkyl bromide with a primary amine was to be exploited, in conjunction with the stabilising influence of a trimethylsilyl group to allow the production of a variety of ligands based on the alkyl/amide pairing of potential anion centres with different substituents at the nitrogen atom. Subsequently, the aggregation modes of the lithiated mixed N/C anion ligand scaffolds were to be explored. In a similar manner to the material presented in Chapter 2, the intention was to investigate how systematic variations to the system affected the aggregation of the anions and the corresponding structure of the

aggregates. The variations that were intended to be explored were initially the difference between the aggregation of the monoanionic ligand scaffold and the dianionic ligand scaffold; it was predicted that the monoanionic amide compounds, as more acidic than alkyl functionality, would have a tendency to aggregate as ladders, contrasting to the stacking aggregates observed for the monoanions in Chapter 2. As noted in Chapter 2, it was unknown what influence solvation would have on altering this aggregation. Consequently, the effect that different Lewis basic solvents had on the aggregation was to be investigated. Further to this, the effect that altering the bulk of the substituent attached to the nitrogen anion had on the structure and aggregation was to be explored. Unfortunately, only very limited success was had in preparing these mixed alkyl/amide ligands, with difficulties in the ligand synthesis and purification as well as unforseen fragmentation of the ligand under metallation conditions preventing the successful synthesis of most of the target complexes.

4.3. Results and discussion

4.3.1. Ligand synthesis

Starting from commercially available 2-methylbenzyl alcohol, a modified literature procedure was used to prepare a brominated, *ortho*-trimethylsilyl substituted xylene precursor.[191] This alkyl bromide was then reacted with various primary amines in a similar fashion to Chapter 2 producing, after workup with base, the target mixed N/C anion ligand scaffold, as shown in Scheme 4-1.

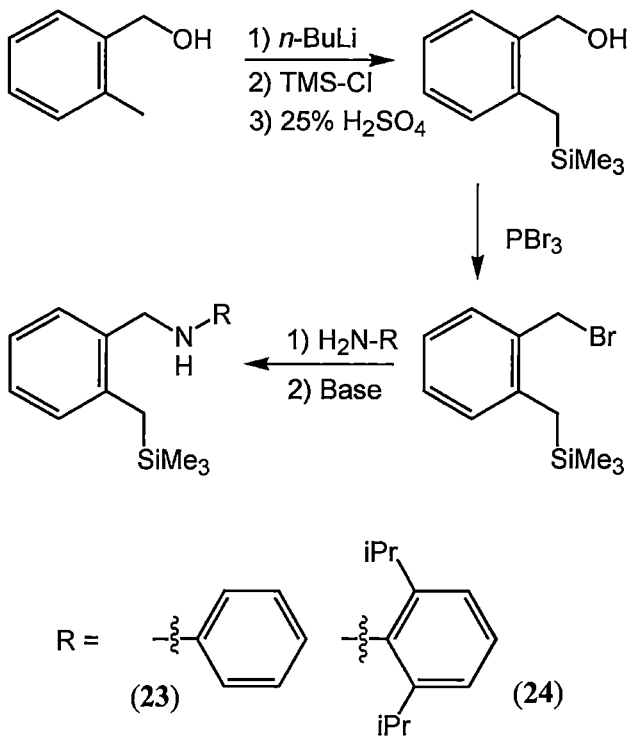

Scheme 4-1: Synthesis for the mixed N/C ligands.

Initially the 2-methylbenzyl alcohol was reacted with two equivalents of *n*-BuLi in diethyl ether. The first lithiation occurs at the phenolic position, which directs the second lithiation to the adjacent methyl group, resulting in an insoluble mixed O/C anion intermediate. The potential relevance of this material to this project was noted, however suitable crystals were not observed of the yellow dilithiated solid and a specific attempt to isolate them was not made. The dilithiated intermediate was then cooled to -78 °C and further reacted with two equivalents of trimethylsilyl chloride, resulting in a pink solution containing visible precipitated $LiCl_{(s)}$. The solution colour bleached overnight to give a colourless solution as the bis(trimethylsilyl) substituted material formed. At this stage the ether bound trimethylsilyl group was cleaved by hydrolysis by stirring overnight with 100 mL 1:4 H_2SO_4:H_2O, restoring the phenol group (>99 % crude yield).

The trimethylsilyl substituted 2-methylbenzyl alcohol was then reacted with PBr_3 in diethyl ether at 0 °C for two hours resulting, after work up, in the alkyl bromide intermediate (88 % crude yield).

After preparing the alkyl bromide precursor a method of preparing the aminated ligands was developed. Initially a nucleophilic substitution of the alkyl bromide with aniline was attempted by refluxing overnight with aniline (1:1.5 molar excess aniline) in DMF with potassium carbonate as the base. Analysis of the reaction mixture by TLC and ^{1}H NMR spectroscopy indicated that this method did not yield a complete or clean reaction to the desired product. The reaction was repeated using triethylamine as the solvent and the base. This method also did not show adequate conversion to the desired product by TLC or ^{1}H NMR spectroscopy. After repeating the reaction using Hünig's Base (*N,N*-diisopropylethylamine) as a non-nucleophilic base, conversion to the desired product was observed, however, it was discovered by GC-MS analysis of some of the crude reaction mixture that the reaction was prone to proceeding through to a second addition of the alkyl bromide. After significant trial and error it was found that by adding the alkyl bromide slowly to a stirred solution of the amine (1:1.5 molar excess) in THF, with three equivalents of Hünig's Base and refluxing overnight a good conversion to the desired amine substituted ligand was able to be obtained. Using this method two mixed N/C anion ligands were prepared; the *N*-phenyl substituted ligand, $NCPhH_2$ **23**, from aniline (53 % distilled yield) and the *N*-2,6-diisopropylphenyl substituted ligand, $NCDIPPH_2$ **24** from 2,6-diisopropylaniline (74 % distilled yield). It was discovered later, through serendipitous inclusion in a crystal structure, that the *N*-phenyl substituted ligand $NCPhH_2$ **23** remains contaminated after distillation with some of the corresponding imine, NC=PhH. It is unclear exactly how this occurred, because unlike the O/N ligands described in Chapter 2, the imine is not directly prepared as an intermediate

in the synthesis of the N/C ligands. After discovering the imine impurity, it was found that it was possible to remove it by treatment of the mixture with sodium borohydride in an analogous way to the reduction of the O/N imine ligand precursors to the O/N amine ligands described in Chapter 2.

4.3.2. NMR characterisation of the N/C ligands

The ^{1}H NMR spectrum of the N/C ligands do not show any unexpected features. The *N*-phenyl substituted ligand $NCPhH_2$ **23** shows a single environment for the trimethylsilyl protons, appearing as a singlet at 0.03 ppm. There is a single resonance for each of the two methylene groups, the one adjacent to the trimethylsilyl group appearing the furthest upfield at 2.19 ppm and the one adjacent to the amine appearing in a similar region to that observed in the O/N ligands at 4.20 ppm. The aromatic region appears as two groups of resonances, the upfield group is made up of two pseudo first order coupled resonances, a triplet and a doublet integrating for one and two protons of the *N*-phenyl substituent, respectively. The remainder of the aromatic resonances are not resolved fully, but integrate correctly for the remaining six protons of the *N*-phenyl substituent and *ortho*-xylene backbone of the ligand. The amine proton was not clearly distinguishable.

The *N*-2,6-diisopropylphenyl substituted ligand, $NCDIPPH_2$ **24** has a very similar ^{1}H NMR spectrum to **23**, with the inclusion of the expected isopropyl resonances. The trimethylsilyl protons appear as a single resonance appearing at 0.06 ppm. The resonances for both of the methylene groups have moved slightly, with the resonances for the groups adjacent to the trimethylsilyl and amine substituents appearing at 2.31 ppm and 4.01 ppm, respectively. The methyl groups of the isopropyl substituents appear as a doublet centred at 1.31 ppm and the associated

methine proton appears as a heptet centred at 3.39 ppm. The aromatic region again appears as two separated regions, this time the furthest upfield grouping accounting for six of the total proton resonances, with a doublet at 7.53 ppm accounting for the seventh aromatic proton. Again the amine proton was not clearly distinguishable, however, there is a broad resonance centred at 3.03 ppm, which was tentatively assigned as the N-H proton.

It was anticipated that in the dilithiated species much more information would be available from the ^{1}H NMR spectrum as the carbon centred anion would drastically alter the shift of the upfield methylene group and vary depending on the local anion environment within the aggregated lithium complexes.

4.3.3. Lithiation of $NCPhH_2$, 23

As for the mixed O/N anion ligands, the intention was to prepare and isolate various Lewis basic solvated complexes of both the mono- and dilithiated mixed N/C ligand. The *N*-phenyl substituted ligand $NCPhH_2$ **23** was initially treated with two equivalents of *n*-BuLi in 40-60 °C petroleum spirits as shown in Scheme 4-2.

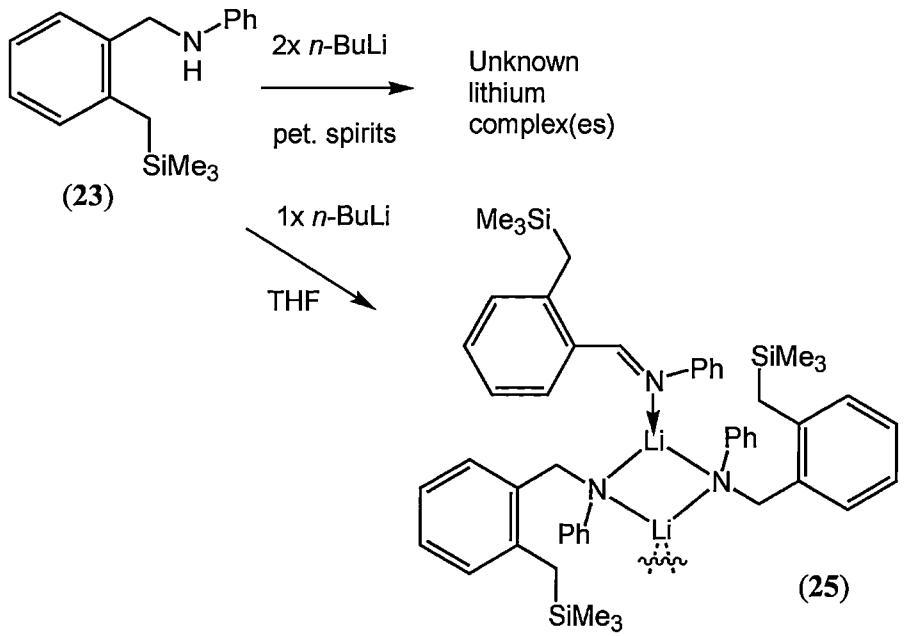

Scheme 4-2: Lithiation of the N/C ligand $NCPhH_2$ **23**. The monolithiated product **25** crystallises as a weak dimer. The dimerisation occurs between the xylene rings of a monolithiated ligand and the lithium atoms. Shown here is a single dimeric unit for clarity.

The addition of the first equivalent of *n*-BuLi was observed to rapidly produce a red/brown solution from the initial pale yellow starting solution. Allowing the solution to stir momentarily after addition of the first equivalent produced no further change and no visible solid. The addition of the second equivalent of *n*-BuLi caused the solution to fade in colour, back to yellow. Allowing the solution to stir for one hour produced an amorphous yellow precipitate. The mixture was warmed to 45 °C and stirred for a further two and a half hours resulting in a slight darkening of the yellow colour of the solution. The yellow solid was isolated but exhibited an uninformative ^{1}H NMR spectrum due to the apparent fluxionality of the complex.

A portion of the yellow solid isolated was dissolved in THF in an attempt to isolate the THF solvated material. However, once solubilised it proved very difficult to re-precipitate and no suitable crystals for X-ray crystal structure determination were obtained.

The lithiation reaction was repeated using a single equivalent of *n*-BuLi to try to isolate the red/brown material observed to form transiently in the dilithiation reaction, as shown in Scheme 4-2. The *N*-phenyl substituted ligand $NCPhH_2$ **23** was treated with one equivalent of *n*-BuLi in 40-60 °C petroleum spirits and allowed to stir for half an hour. During this time white solid material was observed to precipitate. The solid was not suitable for X-ray crystal structure determination. After standing for 72 hours no change to the solid was observed, however the solution had started to turn orange. The supernatant solution was removed by cannula filtration leaving a small amount of white solid. The supernatant solution was cooled resulting in precipitation of an orange solid. However, again it was unsuitable for X-ray crystal structure determination. The white solid was taken to dryness and isolated, however it continued to turn orange and became a sticky solid. A portion of the white/orange solid was dissolved in deuterated benzene for ^{1}H NMR spectral analysis; multiple signals were observed for each of the anticipated aliphatic resonances of the ligand suggesting more than one environment present in solution, however reduction of the solution volume did not yield any crystalline material so X-ray crystal structure determination could not be performed. The orange solid was also soluble in deuterated benzene and the ^{1}H NMR spectrum showed evidence of two ligand types being present in solution, the lithiated ligand, as well as another species. The resonances furthest downfield indicated the presence of an imine species with a singlet at 8.54 ppm, and this was confirmed by X-ray crystal structure determination as reduction of the solution volume of this NMR solution yielded some solid from which a suitable crystal of the complex $[\{[Li(NCPhH)]_2(NC{=}PhH)\}_2]$ **25** was obtained. After observing the imine NC=PhH as a Lewis basic donor in the crystal structure it became evident that the ligand $NCPhH_2$ **23** was contaminated with the

imine from the final purification step of the work up. The crystal structure of this monolithiated $NCPhH_2$ complex containing the imine is discussed in Section 4.3.5.

4.3.4. Lithiation of $NCDIPPH_2$, 24

The *N*-2,6-diisopropylphenyl substituted ligand was treated with two equivalents of *n*-BuLi in THF at 0 °C giving an orange/red solution, from which $[(2,6\text{-}i\text{Pr}_2C_6H_3)N(SiMe_3)Li(THF)_3]$ **26** was eventually isolated, as shown in Scheme 4-3.

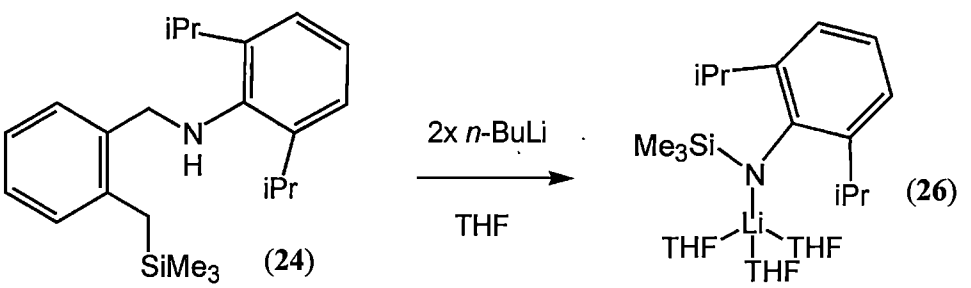

Scheme 4-3: Lithiation of $NCDIPPH_2$ **24** to produce $[(2,6\text{-}i\text{Pr}_2C_6H_3)N(SiMe_3)Li(THF)_3]$ **26**.

The lithiation was not carried out in 40-60 °C petroleum spirits due to the very low likelihood of obtaining the unsolvated dilithiated complex (based on the observed poor dilithiation reactivity of the O/N ligand systems towards *n*-BuLi in 40-60 °C petroleum spirits, described in Section 2.3.3). Upon addition of the *n*-BuLi to the ligand solution the pale yellow colour intensified to a bright yellow, which continued to deepen through to orange/red as the full two equivalents were added. The reaction mixture was stirred for a further hour at room temperature. The volume was reduced by 50 %, however no solid was observed to precipitate. After 48 hours standing at -20 °C the red colour of the solution had disappeared and the solution had become deep purple in colour. The lithiated material was observed to be very soluble; the

addition of an equal volume of 40-60 °C petroleum spirits did not yield any solid precipitation. The total volume was reduced to approximately 10 mL and the flask left standing at -20 °C for an extended period, resulting in a small crop of apparently dark purple crystals suitable for X-ray crystal structure determination. Upon isolation of the crystals it was discovered that they were, in fact, colourless with a purple coating of the solution. Further to this, it was discovered that the solid material isolated was a lithium amide arising from a fragmentation and rearrangement of $NCDIPPPH_2$ **24** as shown in Scheme 4-3. The structure of this complex is discussed in the following section.

The ^1H NMR spectrum of the purple material is consistent with it being a mixture of the structurally characterised complex $[(2,6\text{-}i\text{Pr}_2C_6H_3)N(SiMe_3)Li(THF)_3]$ **26** and the ligand $NCDIPPPH_2$ **24**: it revealed that THF was present in a greater than 1:1 ratio to the ligand, and the spectrum contains several functional group resonances showing multiple environments. The spectrum displays multiple environments for the trimethylsilyl groups as well as the isopropyl groups, but shows a single environment for each of the methylene groups. The resonances assigned to the methylene groups appear at 1.81 and 4.05 ppm for the groups adjacent to the trimethylsilyl and amide groups, respectively. The resonance assigned as the methylene group adjacent to the trimethylsilyl group appears 0.5 ppm further upfield compared to neutral ligand, while the downfield resonance shows little change. This suggests that the purple material may in fact contain a carbon centred anion as desired. The ^{13}C NMR spectrum of the purple material shows a highly complex mixture with approximately seventy resonances observed. Unlike the imine ligand contamination in the previous section, no evidence of the modified ligand fragment *N*-trimethylsilyl-2,6-diisopropylamine was found by ^1H NMR spectroscopy or

GC-MS of the ligand $NCDIPPH_2$ **24** prior to lithiation. A full assignment of the NMR spectra for this mixture was not made.

4.3.5. Molecular structures

Orange crystals from the monolithiation reaction of $NCPhH_2$ **23** suitable for X-ray crystal structure determination were isolated from a concentrated benzene solution. The crystals belong to the triclinic space group $P\bar{1}$ (No. 2), $a = 11.7589(8)$, $b = 15.4711(10)$, $c = 15.5446(11)$ Å, $\alpha = 62.937(3)$, $\beta = 72.041(3)$, $\gamma = 81.933(3)$ °, with 1 Li_4N_4 molecule in the unit cell. The asymmetric unit consists of ½ of the centrosymmetric Li_4N_4 complex. The structure of the complex is shown in Figure 4-2.

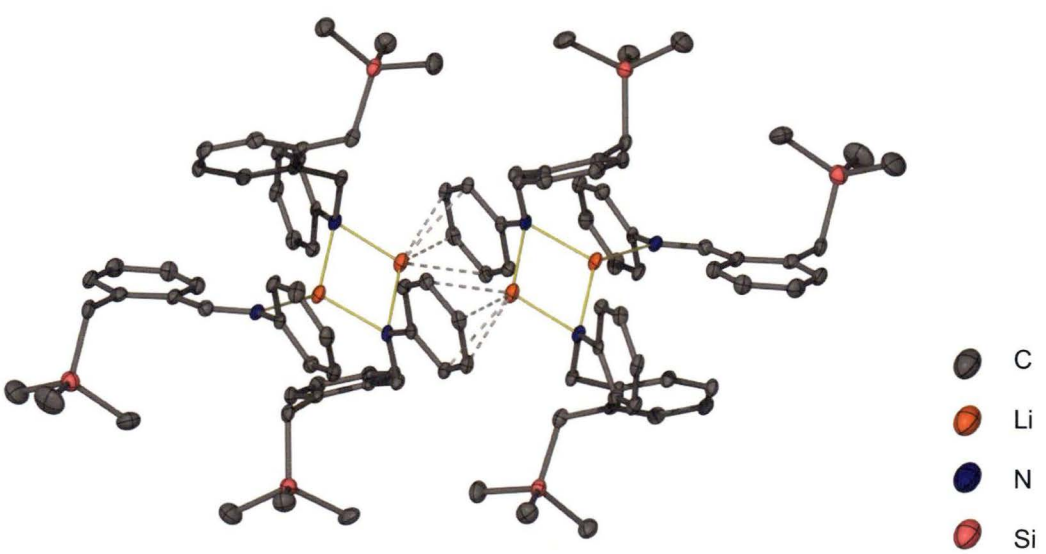

Figure 4-2: Molecular structure of $[\{[Li(NCPhH)]_2(NC{=}PhH)\}_2]$ **25** with thermal ellipsoids drawn at the level of 50 % probability. Hydrogen atoms removed for clarity.

This complex is a weak dimer of dimers. The first dimerisation occurs between two of the monoanionic LiNCPhH units forming a typical lithium amide Li_2N_2 ring. One of the lithium centres in this dimeric pair is solvated by the nitrogen atom of the related imine molecule NC=PhH and the second lithium centre is solvated in η^4

fashion by a *N*-phenyl substituent of a neighbouring monolithiated ligand dimer forming the complex [{[Li(NCPhH)]$_2$(NC=PhH)}$_2$] **25**. One would expect that in the presence of THF these secondary dimerisation interactions might be replaced by the more familiar Lewis basic solvation.

The imine is distinguishable from the amide N/C ligands as the N-C distance to the carbon atom is 1.469(3) Å in each of the monolithiated ligands and only 1.283(4) Å in the imine. Furthermore, the N-C-C angle between nitrogen atom, linking carbon and *ortho*-xylene backbone of each of the molecules is also markedly different between the imine and the monolithiated complex; with the amide nitrogen forming an N-C-C bond of between 111.9(2) °-115.6(2) ° and the imine nitrogen forming a N-C-C bond angle of 125.2(3) °.

Colourless crystals from the dilithiation reaction of NCDIPPH$_2$ **24** suitable for X-ray crystal structure determination were isolated from a THF/40-60 °C petroleum spirits solution. The crystals belong to the monoclinic space group $P2_1/n$ (No. 14), a = 10.930(5), b = 16.323(2), c = 16.366(4) Å, β = 90.577(17) °, with 4 molecules in the unit cell and the asymmetric unit consisting of 1 molecule of [(2,6-*i*Pr$_2$C$_6$H$_3$)N(SiMe$_3$)Li(THF)$_3$] **26**. The molecular structure of the monolithiated complex is shown in Figure 4-3.

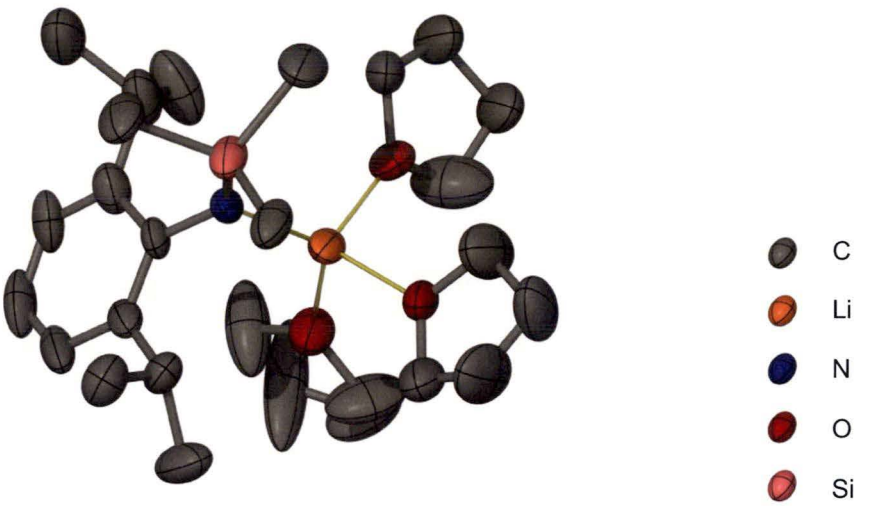

Figure 4-3: Molecular structure of [(2,6-*i*Pr$_2$C$_6$H$_3$)N(SiMe$_3$)Li(THF)$_3$] **26** with thermal ellipsoids drawn at the level of 50 % probability. Hydrogen atoms removed for clarity.

Complex **26** is a monomeric complex of an unexpected fragmentation and rearrangement of the original N/C ligand. The *ortho*-xylene ring has been displaced from the ligand and the nitrogen atom of the substituted aniline has picked up the trimethylsilyl as a second substituent. Lithiated complexes of this *N*-trimethylsilyl-2,6-diisopropylaniline have been reported in the literature as both the mono pyridine mono diethyl ether bis solvated monomeric complex,[192] and the unsolvated dimeric complex, which was prepared directly from the secondary amine and is the first reported unsolvated Li_2N_2 dimer.[193] The lithium complex here is a simple tris(THF) solvate and does not contribute further to the discussion of the aggregation of mixed anion lithium complexes.

4.4. Conclusion

Investigation into the mixed N/C anion lithium complexes via the *ortho*-xylene trimethylsilyl substituted ligands discussed in this chapter did not yield the desired range of varying Lewis base solvated analogues as observed in the mixed O/N anion

ligand system. The observation of ligand fragmentation in the case of the bulkier N/C ligand $NCDIPPH_2$ suggests that a different approach to stabilising the carbon centred anion would be required to allow a systematic investigation into the aggregation of the mixed N/C lithium complexes.

4.5. Experimental

4.5.1. Synthesis of $NCPhH_2$ 23

To a stirred solution of aniline (2.94 g, 31.6 mmol) and Hünig's Base (3.27 g, 25.3 mmol) in THF (20 mL) was added a 50 % THF solution of the alkyl bromide (5.42 g, 21.1 mmol) via dropping funnel over a period of 20 minutes, and was then refluxed overnight. The reaction mixture was extracted with diethyl ether (4x25 mL) and washed against $NaHCO_{3(sat)}$ (2x30 mL) and $NaCl_{(sat)}$ (20 mL) before being dried over Na_2SO_4 and taken to dryness affording the ligand as an impure yellow oil. The product was distilled under reduced pressure (110 °C, $4.8x10^{-2}$ torr) yielding $NCPhH_2$ **23** (2.79 g, 53 %) with some of the imine impurity remaining. The NMR characterisation was performed on the mixture.

^{1}H NMR (300 MHz, C_6D_6, 25 °C): δ = 0.03 (9H, m, Me_3Si), 2.19 (2H, s, Me_3Si-CH_2), 4.20 (2H, s, N-CH_2), 6.64 (2H, d, $^3J_{HH}$ = 7.8 Hz Ar), 6.73 (1H, pt, $^3J_{HH}$ = 7.5 Hz Ar), 7.02-7.32 (6H, m, Ar). Partial assignment of the imine impurity; 0.01 (s, Me_3Si), 2.52 (s, Me_3Si-CH_2), 8.04 (d, $^3J_{HH}$ = 7.8 Hz), 8.66 (s, N=CH).

^{13}C NMR (75 MHz, C_6D_6, 25 °C): δ = -1.10 (Me_3Si), 23.3 (Me_3Si-CH_2), 24.5 (Me_3Si-CH_2), 46.8 (N-CH_2), 113.0 (Ar), 117.8 (Ar), 121.0 (Ar), 124.7 (Ar), 127.5 (Ar), 129.2 (Ar), 129.5 (Ar), 129.6 (Ar), 130.4

(Ar), 131.0 (Ar), 139.3 (Ar), 148.3 (Ar), 160.1 (Ar). The resonances arising from the imine were not assigned.

HRMS ($M^{+\cdot}$) Calculated: 269.15998 ($C_{17}H_{23}NSi$)

Found: 269.15997

4.5.2. Synthesis of NCDIPPH$_2$ 24

To a stirred solution of 2,6-diisopropylaniline (4.30 g, 24.3 mmol) and Hünig's Base (2.51 g, 19.4 mmol) in THF (20 mL) was added a 50 % THF solution of the alkyl bromide (4.16 g, 16.2 mmol) via dropping funnel over a period of 20 minutes, and was then refluxed overnight. The following day a further equivalent of Hünig's Base was added to the reaction and the mixture refluxed a second night. The reaction mixture was extracted with diethyl ether (4x25 mL) and washed against $NaHCO_{3(sat)}$ (2x30 mL) and $NaCl_{(sat)}$ (20 mL) before being dried over Na_2SO_4 and taken to dryness affording the ligand as an impure yellow oil. The product was distilled under reduced pressure (112 °C, 5.1x10^{-2} torr) yielding NCDIPPH$_2$ **24** (4.22 g, 74 %).

^{1}H NMR (300 MHz, C_6D_6, 25 °C): δ = 0.06 (9H, s, Me_3Si), 1.31 (12H, d, $^3J_{HH}$ = 6.9 Hz, $CH(CH_3)_2$), 2.31 (2H, s, Me_3Si-CH_2), 3.06 (1H, br, N-H), 3.39 (2H, h, $^3J_{HH}$ = 6.9 Hz, $CH(CH_3)_2$), 4.01 (2H, s, N-CH_2), 7.09-7.27 (6H, m, Ar), 7.53 (1H, d, $^3J_{HH}$ = 7.2 Hz, Ar).

^{13}C NMR (75 MHz, C_6D_6, 25 °C): δ = -1.2 (Me_3Si), 23.50 (Me_3Si-CH_2), 24.6 ($CH(CH_3)_2$), 28.0 ($CH(CH_3)_2$), 54.3 (N-CH_2), 123.9 (Ar), 124.4 (Ar), 124.8 (Ar), 127.4 (Ar), 128.9 (Ar), 129.6 (Ar), 136.8 (Ar), 139.1 (Ar), 143.2 (Ar), 143.6 (Ar).

HRMS ($M^{+\cdot}$) Calculated: 353.25388 ($C_{23}H_{35}NSi$)

Found: 353.25390

4.5.3. Synthesis of [{[Li(NCPhH)]$_2$(NC=PhH)}$_2$] 25

To a solution of $NCPhH_2$ (365 mg, 1.4 mmol) in 40-60 °C petroleum spirits *n*-BuLi (1.6 M in hexanes, 0.85 mL, 1.4 mmol) was added and the mixture stirred for half an hour before standing overnight. The resulting white solid was isolated via cannula filtration and the orange supernatant solution was taken to dryness under reduced pressure. The resulting orange solid was recrystallised from benzene yielding a small crop of the reported material. The NMR and elemental analysis characterisations were performed on the orange solid. The NMR data was only able to be partially assigned.

^{1}H NMR (300 MHz, C_6D_6, 25 °C): δ = -0.13-0.03 (54, m, Me_3Si), 2.01 (8H, s, Me_3Si-C*H*$_2$), 2.36 (s), 3.26 (4H, br, N-H), 3.94-3.96 (8H, m, N-C*H*$_2$), 6.44 (8H, d, $^3J_{HH}$ = 8.1 Hz, Ar), 6.69-7.16 (m, Ar), 8.10 (4H, d, $^3J_{HH}$ = 7.8 Hz, Ar), 8.50 (2H, s, N=C*H*).

^{13}C NMR (75 MHz, C_6D_6, 25 °C): δ = -1.7, -1.5, -1.3, 22.4, 22.9, 23.9, 46.7, 50.7, 111.2, 113.0, 113.3, 117.8, 121.1, 124.8, 124.8, 125.4, 125.8, 126.7, 127.4, 129.0, 129.3, 129.4, 129.5, 129.9, 130.1, 130.2, 130.4, 130.8, 132.9, 135.5, 138.9, 142.3, 148.6, 153.3, 160.4.

Anal. Calculated: C, 74.86; H, 8.01; N, 5.14; ($C_{51}H_{65}Li_2N_3Si_3$)

Found: C, 73.14; H, 8.15; N, 4.95

4.5.4. Synthesis of [(2,6-*i*Pr$_2$C$_6$H$_3$)N(SiMe$_3$)Li(THF)$_3$] 26

To a solution of NCDIPPH$_2$ (573 mg, 1.6 mmol) in THF *n*-BuLi (1.6 M in hexanes, 2.13 mL, 3.4 mmol) was added and the mixture stirred for an hour resulting initially in a bright yellow solution which deepened in colour to orange/red. The solution volume was reduced by half and cooled to -20 °C for 48 hours. This resulted in the solution turning deep purple. The solution had an equal volume of 40-60 °C petroleum spirits added to it, after which the total volume was reduced to approximately 10 mL before standing at -20 °C for an extended period of time, eventually allowing colourless crystals of the reported product to grow. The NMR characterisation was performed on the purple mixture, consequently only a partial assignment has been made.

^{1}H NMR (300 MHz, C_6D_6, 25 °C): δ = 0.15-0.40 (m), 0.77-1.38 (m), 1.81 (s, Me_3Si-C*H*$_2$), 2.21 (s, Me_3Si-C*H*$_2$), 2.31 (s, Me_3Si-C*H*$_2$), 3.23 (m, C*H*(CH$_3$)$_2$), 3.58 (m, THF), 4.05 (s, N-CH$_2$), 6.82-7.14 (m, Ar).

^{13}C NMR (75 MHz, C_6D_6, 25 °C): δ = -1.3, -1.2, -1.1, -0.3, 0.9, 1.5, 1.8, 3.2, 3.9, 12.0, 14.4, 14.7, 14.9, 18.8, 19.2, 20.0, 20.1, 20.2, 21.2, 21.8, 23.1, 23.4, 23.6, 23.7, 23.9, 24.2, 24.7, 24.9, 25.0, 25.2, 25.9, 26.3, 27.2, 27.8, 28.5, 28.7, 29.2, 29.8, 32.6, 34.3, 36.8, 42.0, 52.2, 52.8, 54.4, 55.1, 68.7, 123.8, 124.4, 124.6, 124.7, 125.0, 125.1, 125.4, 126.5, 126.8, 127.0, 127.3, 127.5, 127.7, 127.9, 129.5, 129.6, 130.0, 130.1, 130.5, 130.8, 131.1, 131.3, 132.3, 132.7, 137.6, 138.3, 139.4, 140.1, 143.1, 143.5, 149.1, 139.4, 161.6.

Anal. Calculated: C, 65.08; H, 9.88; N, 3.61; ($C_{21}H_{38}LiNO_3Si$)

Found: A satisfactory elemental analysis was not able to be obtained for this compound.

Chapter 5

Lithiated complexes incorporating serendipitous molecular fragments

5.1. Introduction

Silicon grease is routinely used in organometallic chemistry laboratories to seal ground glass joints of Schlenk flasks and other glassware used for air and moisture sensitive chemistry. Silicon grease is a dimethylsiloxane polymer, $(Me_2SiO)_n$, and like the glassware itself, it is regarded as essentially inert towards most common reagents and solvents. Consequently little consideration is usually given to the possible consequence of it coming into contact with a reaction solution, beyond possible difficulties in recrystallisation and the implication regarding poor technical skill if the 'grease peak' in a compound's ^{1}H NMR spectrum is excessively large.

Although not mentioned in laboratory handbooks, silicon grease is partially soluble in many organic solvents and the polar silicon-oxygen bond is known to be reactive toward both alkaline and acidic reagents. It is perhaps not surprising, then, that several reports exist of compounds isolated that incorporate portions of silicon grease polymer. A recent review compiles a selection of these compounds.[194] It is worth noting that in the majority of cases where silicon grease 'activation' is observed it is not a reflection on experimental technique, but rather a reflection of the reactivity of the compounds present in the reaction, as it is quite typical for there to be a small amount of grease present without incorporation observed. It is possible to use grease-free glassware to avoid contact with silicon grease if activation of the grease is known to be a problem.

A rare example of silicon grease activation by a transition metal arising from the attempted preparation of an *N*-heterocyclic carbene (NHC) complex yielded the complex shown in Scheme 5-1.[195]

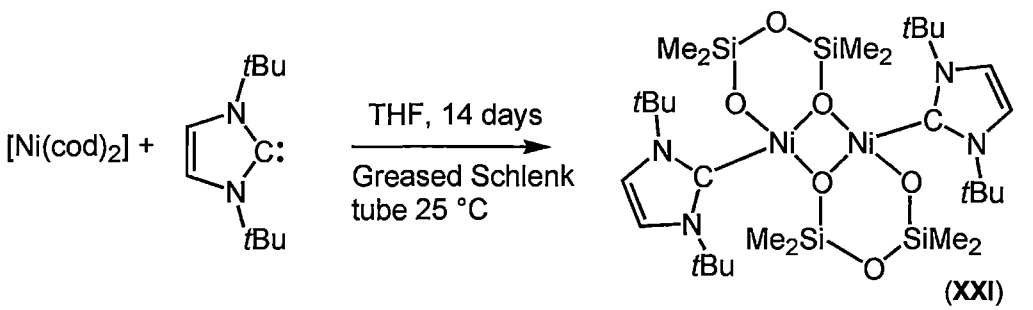

Scheme 5-1: Formation of a Ni complex with NHC ligands incorporating a silicon grease fragment.

Also from work involving NHC chemistry of transition metals, the complex shown in Scheme 5-2 was reported.[196]

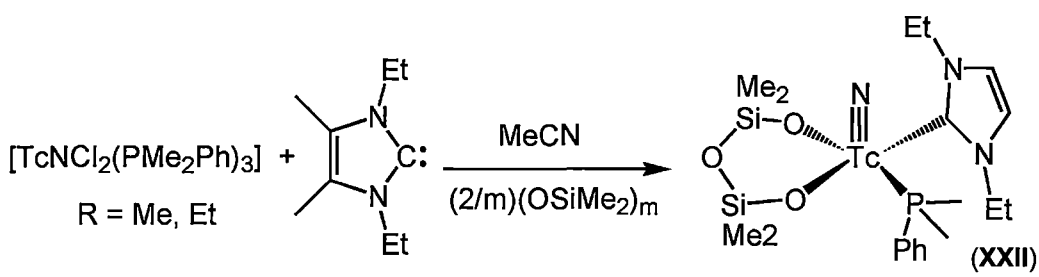

Scheme 5-2: Formation of a Tc complex with NHC ligands incorporating a silicon grease fragment.

The nickel complex **XXI** reported was isolated instead of the bis (NHC) complex that was successfully prepared when the reaction was repeated in the absence of silicon grease. The technetium complex **XXII**, similarly, was isolated in place of an intended NHC substituted complex. In this case, the isolation of the grease fragment incorporated complex is favoured by carrying out the reaction in acetonitrile. If the reaction is done in THF, the less soluble tetra-substituted NHC nitrido complex is isolated in good yield. Both of the complexes **XXI** and **XXII** incorporate the dianionic grease fragment $(O\text{-}Si(Me)_2\text{-}O\text{-}Si(Me)_2\text{-}O)^{2-}$, with both terminal oxygen anions coordinating to the metal centre(s). In the nickel complex, one end of each of

the two grease fragments is bridging the two metal centres, forming a central Ni_2O_2 ring, while the fragment is chelating a metal centre through each terminal oxygen centre. The technetium complex is monomeric, including a single grease fragment in a chelating fashion giving a square pyramidal geometry around the metal.

Two further examples of grease incorporation, occurring with lanthanide and heavy p-block elements rather than NCH ligands are shown in Scheme 5-3 and Scheme 5-4 respectively.[197, 198]

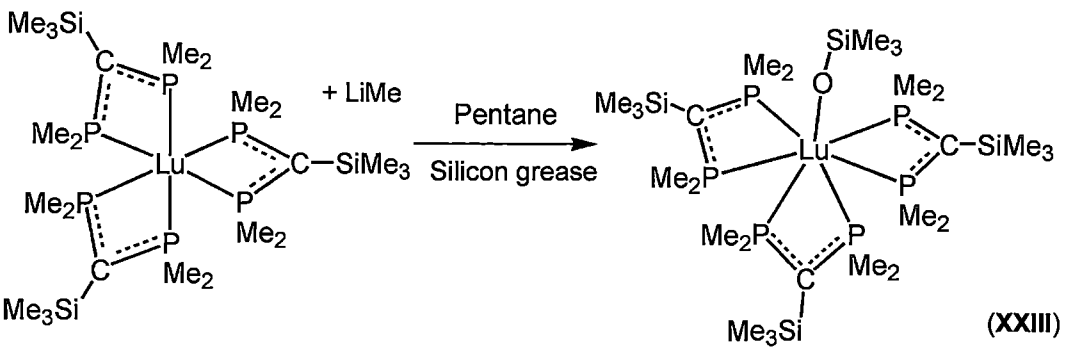

Scheme 5-3: Formation of a Lu complex incorporating a silicon grease fragment.

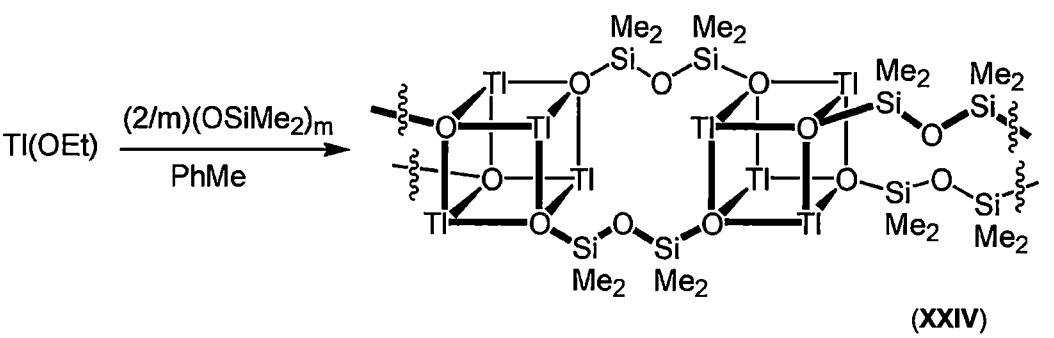

Scheme 5-4: Formation of a Tl polymeric complex incorporating silicon grease fragments.

The lutetium complex **XXIII** incorporates one of the more unusual grease fragments, the $(Me_3Si\text{-}O)^-$ group. In the review article, the author notes that with such group incorporation it is often unclear whether the grease fragment arose from the end of the dimethylsiloxane polymer, or from attack with a suitable reagent such as MeLi. The complex **XXIII** was isolated in place of the methylated complex they were

attempting to prepare, and has a nearly linear Lu-O-Si bond. The thallium complex **XXIV** incorporates the same grease fragment observed in the two NHC incorporated complexes, $(O\text{-}Si(Me)_2\text{-}O\text{-}Si(Me)_2\text{-}O)^{2-}$. The thallium ions are arranged into a Tl_4O_4 cubic stack, linked by two vertices to an adjacent Tl_4O_4 cubic stack by two bridging grease fragments, forming a polymeric structure.

In organolithium chemistry there are several examples of structures isolated with silicon grease incorporated. The following three complexes provide a useful correlation to the examples of structural types presented in this thesis.

Over a period of months, a solution of $LiPEt_2$ was observed to precipitate crystals of the complex shown in Scheme 5-5.[199] The complex **XXV** is a Li_6O_6 distorted hexagonal prism, familiar to alkoxidolithium chemistry. Despite being published a year after the ground-breaking reviews by Mulvey and Snaith[2, 3] regarding ring stacking and ring laddering in organolithium chemistry, the authors suggest an alternative description of the complex as a cyclic ladder structure.

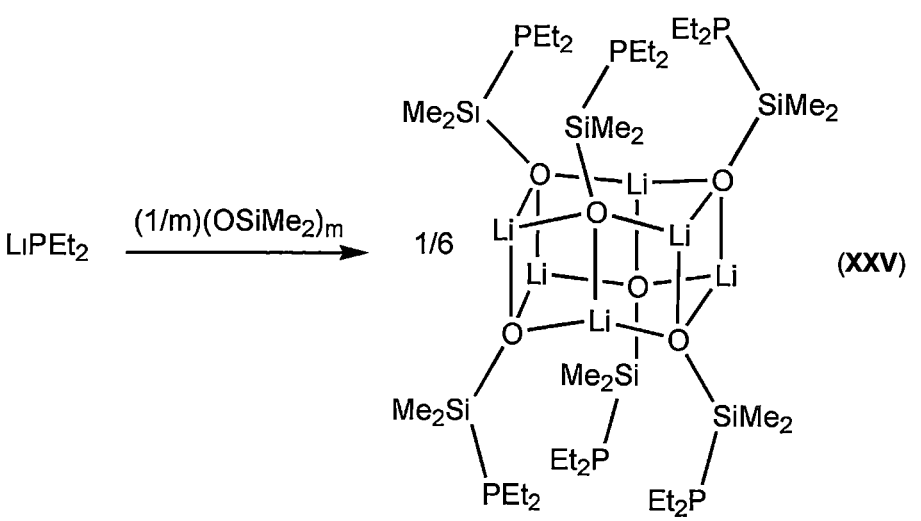

(**XXV**)

Scheme 5-5: Formation of a hexameric lithium complex including organic fragments modified with a silicon grease fragment inserted into the Li-R bond.

Unlike the previously discussed complexes, this complex contains a grease fragment –O-$SiMe_2$- that has undergone insertion into a bond within the complex. The process of silicon grease undergoing bond insertion can be viewed as shown in Equation 5-1.

$$-[Si(Me)_2\text{-}O]_x\text{-} + Li^{\delta+}\ R^{\delta-} \rightarrow R\text{-}Si(Me)_2\text{-}O\text{-}Li$$

Equation 5-1

The fragment undergoing insertion may also be more than one monomer in length. Because the insertion of the grease fragment is into a Li-X bond, the resulting anionic centre will at be the siloxo oxygen atom. In organolithium complexes these anions have a tendency to aggregate into stacked rings. It is not surprising then, that many of the complexes arising from insertions of grease fragments in this way contain familiar aggregated geometries. A second example of grease insertion into an organolithium complex is shown in Scheme 5-6,[199] in which the product adopts a conventional Li_4O_4 stacked cage.

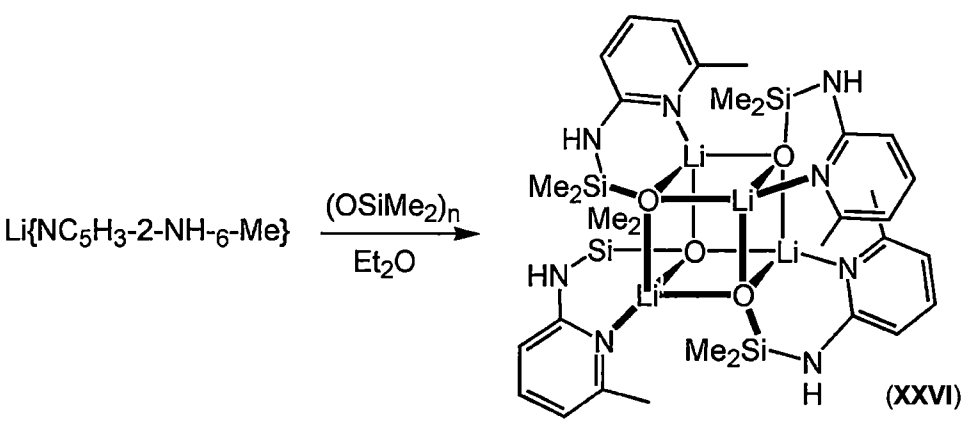

(XXVI)

Scheme 5-6: Formation of a tetrameric lithium complex including organic fragments modified with a silicon grease fragment inserted into the Li-R bond.

The insertion observed in **XXVI** is again of a monomer of silicon grease, this time into a N-Li bond. The resulting anionic ligand aggregates as a tetramer forming a Li_4O_4 cubic core, with the pyridine groups acting as intramolecular Lewis basic donors in a similar way to that observed in the monolithiated O/N complex [{Li(ON=DIPPH)}$_4$] **10**.

The following example of a grease incorporated organolithium complex contains multiple types of dianionic silicon grease fragments, which aggregate together to produce the remarkable Li_{16} cluster shown in Figure 5-1.[200]

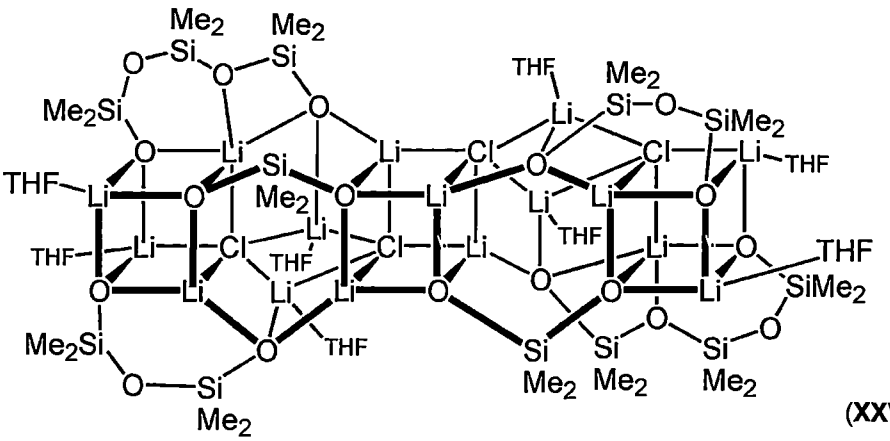

(XXVII)

Figure 5-1: A Li_{16} complex incorporating multiple types of silicon grease fragments.

The complex **XXVII** demonstrates that the fragmentation of silicon grease is not always a selective process, as can be seen here there are three different fragments incorporated into this structure $(O\text{-}Si(Me)_2\text{-}O)^{2-}$, $(O\text{-}Si(Me)_2\text{-}O\text{-}Si(Me)_2\text{-}O)^{2-}$ and $(O\text{-}Si(Me)_2\text{-}O\text{-}Si(Me)_2\text{-}O\text{-}Si(Me)_2\text{-}O)^{2-}$. Despite this, there are a few reports, particularly within lanthanide work, of researchers deliberately introducing silicon grease into their reactions, as a source of various silyl fragments.[201-203]

5.2. Research outcome

Presented in this chapter are some of the synthetically serendipitous results arising from incorporation of unexpected molecular fragments arising from both solvent molecules, as well as silicon grease. Incorporation of these fragments occurs both as inclusion into the aggregated lithium complex, as well as via insertion of the fragment into the lithiated ligands themselves. These results are related to the observed reactivities of the dilithiated dimeric O/N complexes discussed in Chapter 3

and further supports the proposal noted in this thesis that superbasic behaviour may be linked to a mixing of different alkali metal anion types inducing molecular arrangements that can lead to unusual and sometimes selective reactivity.

5.3. Results and discussion

5.3.1. Ethoxide fragment incorporation

In Chapter 3 the recurrence of the monolithiated complex [{Li(ONDIPPH)}$_4$] **9** being isolated from reaction mixtures that were prepared from a dilithiated complex was noted. In some of the early attempts to isolate various Lewis basic solvated complexes of the dilithiated O/N compounds, diethyl ether displacement reactions were attempted several times without success. As discussed in Section 3.3.4 further investigation of this led to the discovery that the molecular fragments of ethylene and EtOLi were produced, most likely resulting from an intramolecular deprotonation of diethyl ether by the dilithiated complex. As well as the GC-MS detection of these molecular fragments, evidence of unexpected reactivity of the dilithiated O/N ligand complexes was observed with the determination of two serendipitous crystal structures. The crystals were obtained from reactions carried out in diethyl ether, and showed inclusion of an ethoxide fragment into the aggregated complex. The simplest ethoxide incorporated structure was obtained from the reaction of the *N*-*t*-Bu substituted ligand ON*t*BuH$_2$ **6** with two equivalents of *n*-BuLi in diethyl ether as shown in Scheme 5-7.

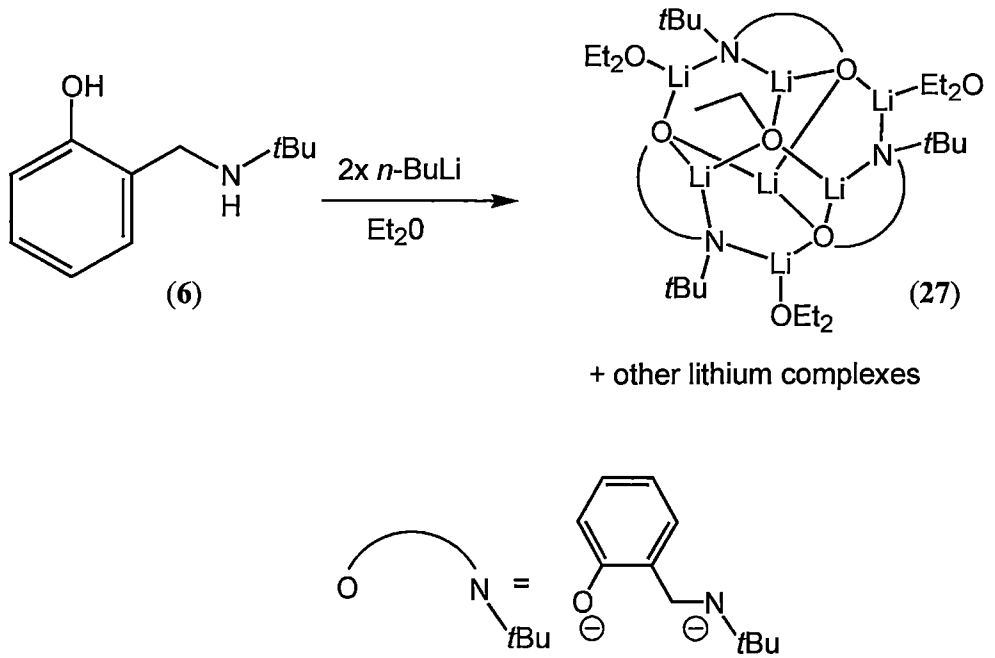

Scheme 5-7: Formation of complex [{Li_2(ON*t*Bu)}$_3$Li(OEt)(Et_2O)$_3$] **27** from the O/N ligand ON*t*BuH_2 **6**.

The reaction was carried out in grease free glassware allowing the solution to be sealed and heated to 50 °C for two minutes. The reaction mixture was reduced in volume and had 40-60 °C petroleum spirits added to it to help crystallise out the product. Clear well-formed crystals formed, however they proved exceedingly difficult to mount, desolvating very rapidly and appearing to dissolve in the immersion oil used for the cold stage mounting. After attempting to recrystallise the sample from THF, and subsequently taking the sample to dryness some of the solid crystalline material was able to be separated from the chalky desolvated solid and the single crystal that was characterised by X-ray crystal structure determination was shown to be [{Li_2(ON*t*Bu)}$_3$Li(OEt)(Et_2O)$_3$] **27**.

The bulk material was soluble in benzene and was characterised by IR, ^{1}H, ^{13}C NMR spectroscopy, and elemental analysis. The IR spectrum showed no evidence of an N-H stretch, however it also did not show the appearance of one after exposure of the mixture to air. The ^{1}H NMR spectrum shows a small amount of THF in the sample,

however, there is no evidence of diethyl ether, indicating that the bulk material is not the same complex as characterised by X-ray crystal structure determination. The elemental analysis ratios are close to that of a monolithiated, unsolvated complex. It can be concluded then that the single crystal isolated for X-ray analysis was a rogue crystal and that the bulk material is an unknown, unsolvated monolithiated species.

The *t*-Bu resonance appears at 0.80 ppm and integrates correctly compared to the other ligand resonances. The methylene resonance also integrates correctly once the residual THF peak (7 %) is subtracted from it, despite being very broad. The aromatic region of the ^{1}H NMR spectrum is relatively simple, with a pseudo triplet centred at 6.69 ppm and a doublet centred at 7.03 ppm. The other two aromatic signals appear as a broad resonance centred at 6.90 ppm and a broad multiplet centred at 7.25 ppm. It is noted that the aromatic resonances for this complex extend slightly further downfield than for the dilithiated complexes discussed in Chapters 2 and 3. The ^{13}C NMR spectrum was able to be assigned, but does not show any unexpected features. The THF signals in the ^{13}C NMR spectrum are exceedingly weak, and there is not evidence of other solvents or an ethoxide group, further suggesting that the major species present in the bulk solid is an unsolvated complex.

A second serendipitous incorporation of ethoxide into a crystal structure was obtained from the reaction of the *N*-2,6-diisopropylphenyl substituted ligand ONDIPPH$_2$ **5** with two equivalents of *n*-BuLi in diethyl ether, as shown in Scheme 5-8.

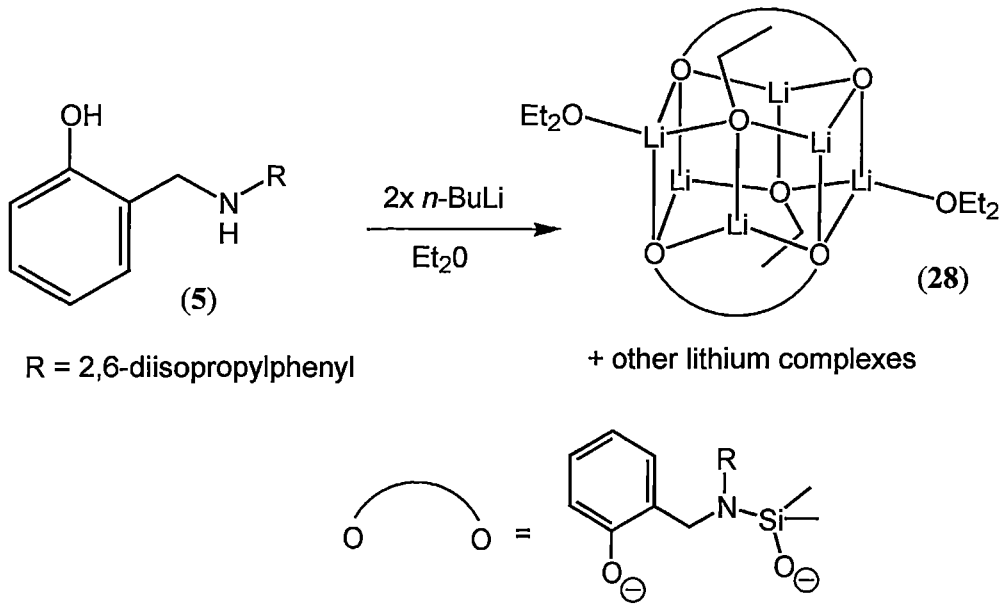

Scheme 5-8: Formation of complex $[\{Li_2(OODIPPSi)\}_2\{Li(OEt)\}_2(Et_2O)_2]$ **28** from the O/N ligand $ONDIPPH_2$ **5**.

This complex is remarkable as it incorporates both ethoxide anions into the core, as well as being based on a modified dilithiated ligand. A monomeric unit of polydimethylsiloxane (silicon grease) has become incorporated into the ligand backbone, forming a tertiary nitrogen centre and resulting in a mixed phenoxide/siloxide dianionic ligand. Though no further crystals of this material were isolated, presumably after aqueous workup the neutral ligand would be the doubly re-protonated species $OODIPPSiMe_2H_2$.

Complex $[\{Li_2(OODIPPSi)\}_2\{Li(OEt)\}_2(Et_2O)_2]$ **28** exhibits a hexameric prism Li_6O_6 cage core, formed from a dimer of six-membered Li_3O_3 rings, each ring containing two oxygen based anionic centres from a modified dilithiated ligand and a third oxygen anionic centre from an ethoxide fragment. Subsequent crystals from the reaction mixture were examined and shown to be of the previously isolated monolithiated cube complex $[\{Li(ONDIPPH)\}_4]$ **9**, consequently no further characterisation was performed on the products of this reaction. The observation of **9** is consistent with the solvent fragmentation occurring through interaction of the

diethyl ether with the dilithiated complex, as proposed in Scheme 3-14 and discussed in Section 3.3.4. It is not clear however, if the attack on the diethyl ether occurs through interaction with the dilithiated complex of the original ligand $ONDIPPH_2$ **5** or with the dilithiated complex of the modified ligand $OODIPPSiMe_2H_2$.

The complex **28** was the first piece of evidence that came to light in the course of this study about the increased reactivity of the dilithiated complex of the *N*-2,6-diisopropylphenyl substituted ligand. As a result of observing the incorporation of a silicon grease fragment into the ligand backbone, some reactions, such as the one leading to the previous structure $[\{Li_2(ONtBu)\}_3Li(OEt)(Et_2O)_3]$ **27** were specifically carried out in grease free apparatus. The observation of grease attack arising from the reaction yielding complex **28** is particularly remarkable because the reaction was carried out in relatively mild conditions, heated at 50 °C for approximately two hours, and occurs in the presence of relatively mild bases. An interesting aspect of this result is that the incorporation of silicon grease appears to facilitate attack of the complex on diethyl ether. As mentioned in Chapter 3, the attack on diethyl ether can occur in the absence of silicon grease, however, the reaction was observed to be slower and required more significant heating. Due to the sparse and sporadic nature of the results regarding grease incorporation in conjunction with solvent attack, it is not possible to draw any specific conclusions regarding their interactions.

5.3.2. Molecular structures

A colourless crystal of $[\{Li_2(ONtBu)\}_3Li(OEt)(Et_2O)_3]$ **27** suitable for X-ray crystal structure determination was sampled from the bulk solid remaining from the lithiation of $ONtBuH_2$ **6** in diethyl ether. The crystals belong to the monoclinic space

group $C2/c$ (No. 15), $a = 19.824(2)$, $b = 22.156(2)$, $c = 24.8640(11)$ Å, $\beta = 101.675(4)$ °, with 8 Li_7O_7 molecules in the unit cell and the asymmetric unit consisting of 1 molecule of $[\{Li_2(ONtBu)\}_3Li(OEt)(Et_2O)_3]$ **27**. The complex has non-crystallographic C_3 symmetry. The molecular structure of the complex is shown in Figure 5-2 and Figure 5-3.

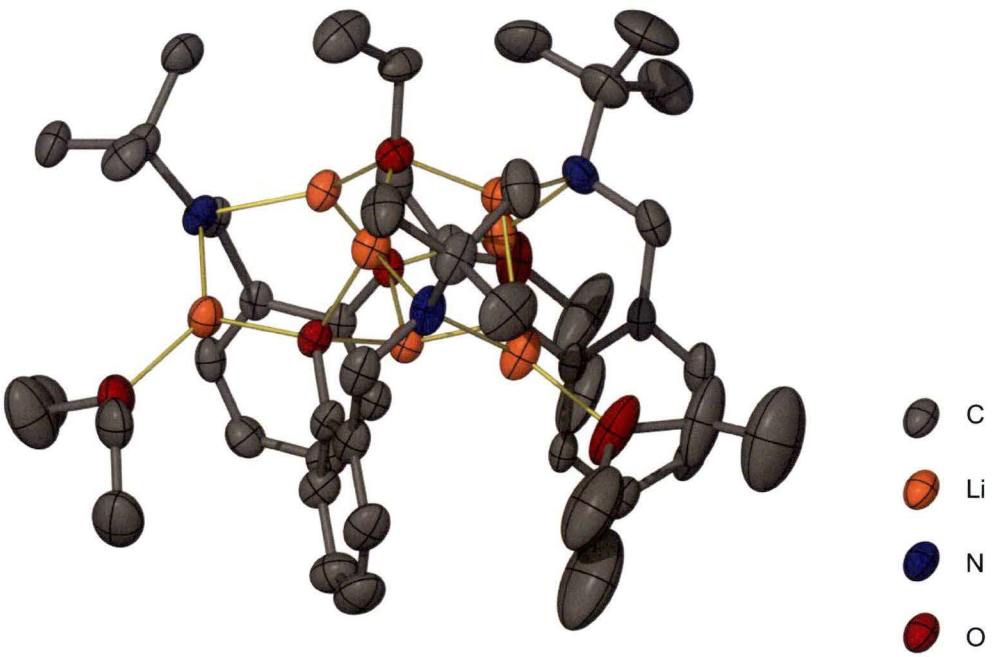

Figure 5-2: Side on view of the molecular structure of $[\{Li_2(ONtBu)\}_3Li(OEt)(Et_2O)_3]$ **27** with the ethoxide group positioned at the top of the complex. Thermal ellipsoids drawn at the level of 50 % probability. Hydrogen atoms removed for clarity.

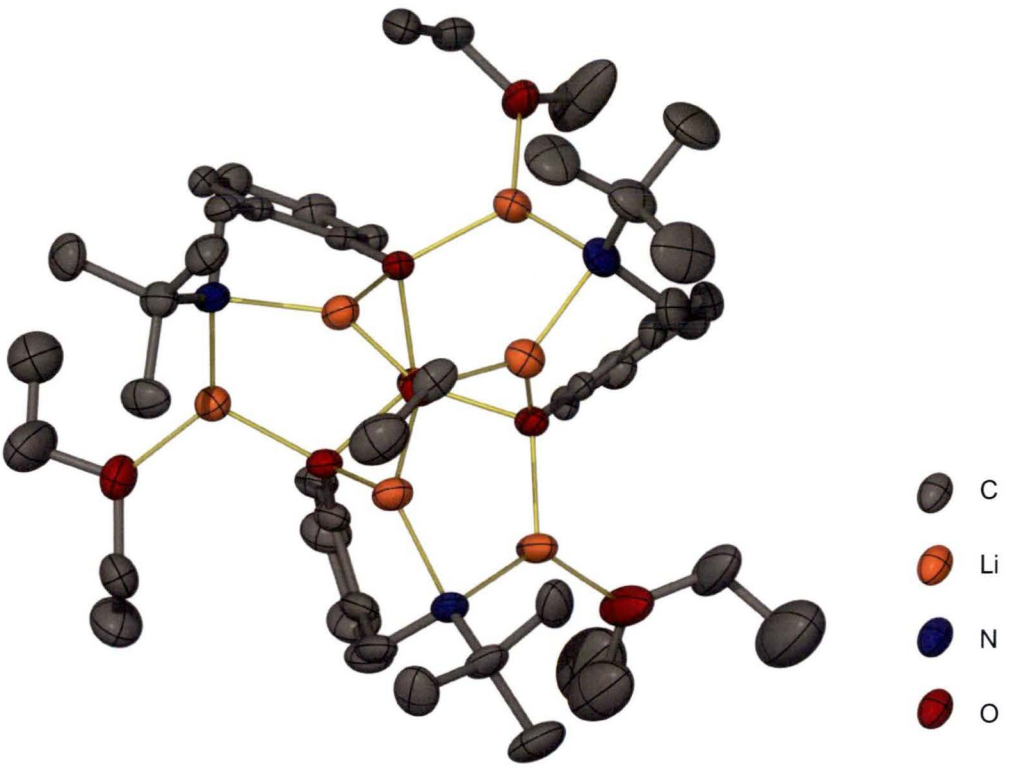

Figure 5-3: Top down view of the molecular structure of [{$Li_2(ONtBu)$}$_3$Li(OEt)(Et_2O)$_3$] **27** with thermal ellipsoids drawn at the level of 50 % probability. Hydrogen atoms removed for clarity.

The structure of [{$Li_2(ONtBu)$}$_3$Li(OEt)(Et_2O)$_3$] **27** has three units of the ligand $ONtBuH_2$ **6** as the dianion, with a single unit of ethoxide and an additional balancing lithium atom incorporated. The structure of the core of this complex is based on a non-crystallographic C_3 rotational axis on which lies on the O-C bond of the ethoxide anion and an additional lithium centre on the other vertex of the $Li_7O_4N_3$ cage. Complexes with this structural arrangement have been reported before,[204, 205] and there are multiple reports of structures containing this arrangement as part of a larger complex in both lithium incorporated clusters,[206, 207] as well as in metal clusters involving copper and silver with either sulphur or selenium.[208-213] It is believed, however, this is the first report of this molecular arrangement for a lithium alkoxide/amide complex.

Each dilithiated ligand within the complex chelates one lithium centre between its two O and N based anionic centres, as well as interacting with a further two lithium centres. The core of the complex is a fused cage consisting of six, six membered rings as observed in the $C_{14}H_{20}$ hydrocarbon congressane (decahydro-3,5,1,7-[1,2,3,4]butanetetraylnapthalene). The complex is shown adjacent to the $C_{14}H_{20}$ hydrocarbon in Figure 5-4.

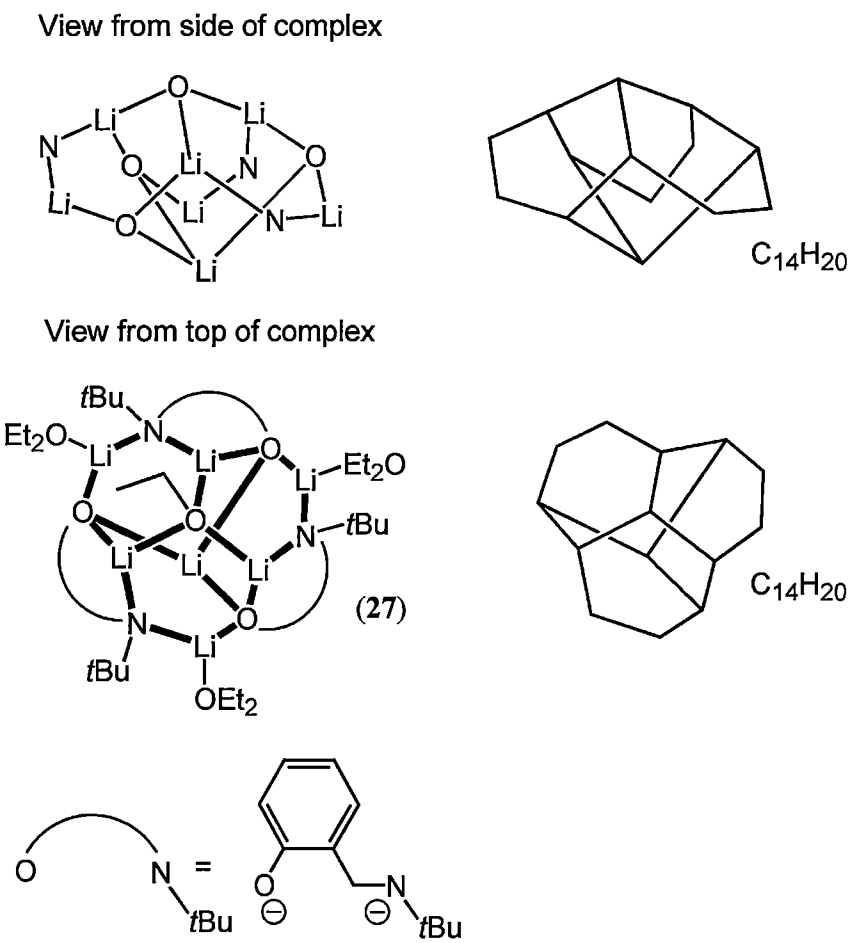

Figure 5-4: Illustration of the core of complex $[\{Li_2(ONtBu)\}_3Li(OEt)(Et_2O)_3]$ **27** adjacent to congressane, $C_{14}H_{20}$.

Each ring in the complex is a Li_3O_2N ring. Three of the Li_3O_2N rings are fused at the top vertex sharing the oxygen centre of the ethoxide. These three rings form the top surface of the core, while the remaining three Li_3O_2N rings are fused at the bottom vertex, sharing a lithium centre, and form the bottom surface of the core. There are

three unique types of lithium centre, although they are all three coordinate. Three of the lithium centres are "internal" bridgehead sites of the Li_3O_2N rings with O_2N coordination and are not solvated and have an approximately trigonal planar geometry. Another three of the lithium centres are "external" non-bridgehead sites of the Li_3O_2N rings with O_2N coordination and have approximate trigonal planar geometry. The "external" lithium centres are each solvated by a molecule of diethyl ether. The third type of lithium is that forming the bottom vertex of the core, is also three coordinate with O3 coordination, and has approximate trigonal pyramidal geometry. Solvation of this exposed lithium centre is prevented by the three phenylene rings of the dilithiated ligands occupying the space on the underside of the complex. The Li-O distances are all within the expected range at 1.882(5)-1.946(5) Å. The shortest three distances are those to the ethoxide anion. Similarly, the N-Li distances are also within the expected range at 1.947(6)-1.997(6) Å.

A colourless crystal of $[\{Li_2(OODIPPSi)\}_2\{Li(OEt)\}_2(Et_2O)_2]$ **28** suitable for X-ray crystal structure determination was isolated from the reaction of $ONDIPPH_2$ **5** with *n*-BuLi in diethyl ether. The crystals belong to the monoclinic space group $P2_1/n$ (No. 14), $a = 11.617(13)$, $b = 13.905(9)$, $c = 19.50(2)$ Å, $\beta = 105.98(8)$ °, with 2 Li_6O_6 molecules in the unit cell and the asymmetric unit consisting of ½ of a centrosymmetric molecule of $[\{Li_2(OODIPPSi)\}_2\{Li(OEt)\}_2(Et_2O)_2]$ **28**. The molecular structure of the complex is shown in Figure 5-5 and Figure 5-6.

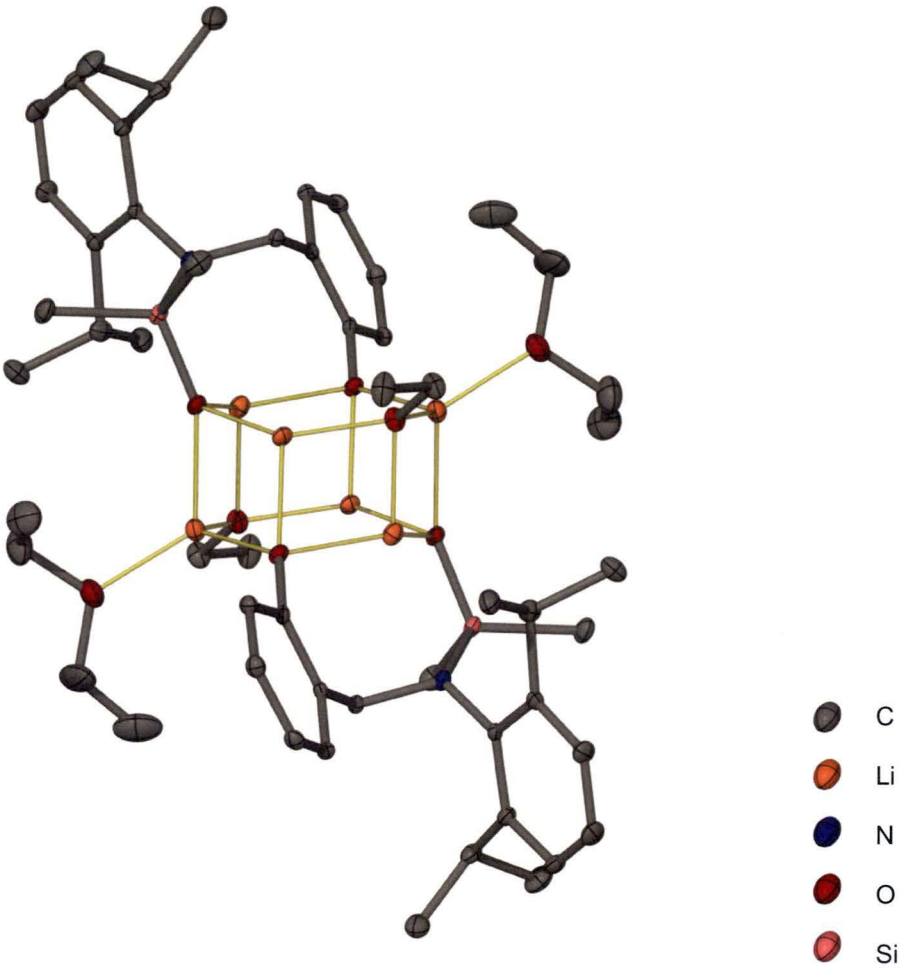

Figure 5-5: Front on view of the molecular structure of $[\{Li_2(OODIPPSi)\}_2\{Li(OEt)\}_2(Et_2O)_2]$ **28** with thermal ellipsoids drawn at the level of 50 % probability. Hydrogen atoms removed for clarity.

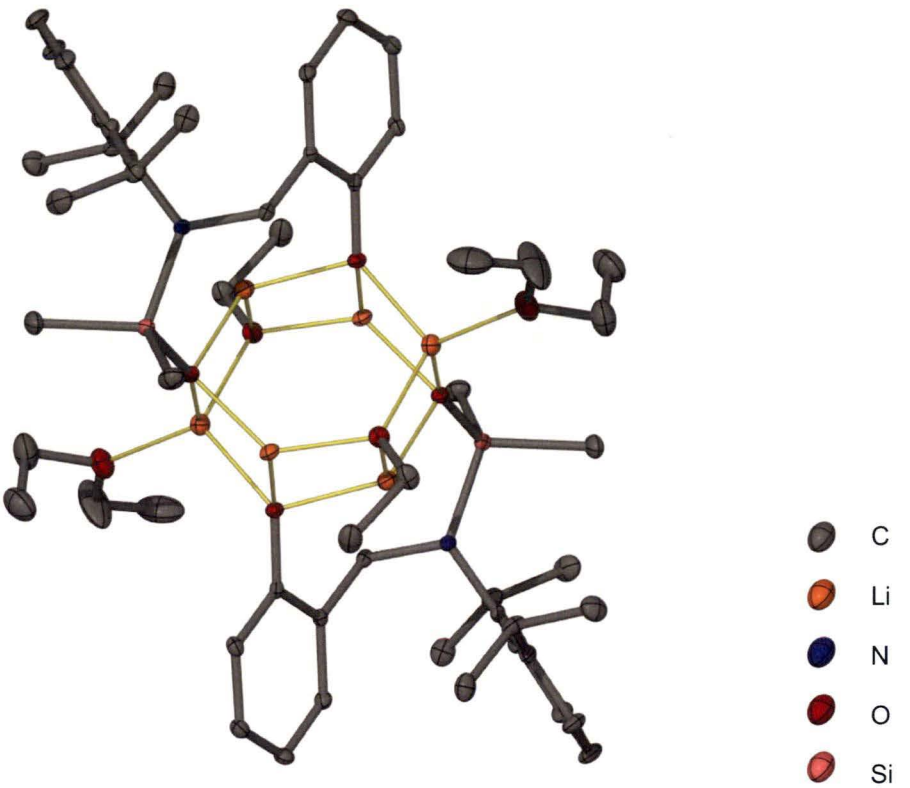

Figure 5-6: Top down view of the molecular structure of $[\{Li_2(OODIPPSi)\}_2\{Li(OEt)\}_2(Et_2O)_2]$ **28** with thermal ellipsoids drawn at the level of 50 % probability. Hydrogen atoms removed for clarity.

The structure of $[\{Li_2(OODIPPSi)\}_2\{Li(OEt)\}_2(Et_2O)_2]$ **28** consists of a hexameric prism formed by the stacking of two six-membered Li_3O_3 rings. Each ring is slightly nonplanar, having a shallow chair conformation. The dimer is crystallographically centrosymmetric, with the modified O/O ligand spanning a familiar distance of two faces of the edge of the prism (akin to three rungs of a ladder), each ligand contributing to a single hexagonal face of the prism. Several reports of complexes featuring a Li_6O_6 hexameric prism core exist. Predominantly these complexes do not incorporate external solvation.[214-218] A handful of the complexes incorporate internal Lewis basic solvation,[219] while only a single reported structure was able to be found that had partial external Lewis basic solvation.[220] Only two of the complexes containing this hexameric prism core contained a dianionic ligand similar to that observed in complex **28**.[217, 221] These two complexes also featured

incorporation of two different anion types within the core and have the same arrangement of the anions as complex **28**. However, reports of complexes featuring this core comprising two different anion types with any external solvation were not able to be found making **28** unique.

Complex **28** contains two types of lithium centre; four unsolvated 4 coordinate O_3 coordination lithium centres, with approximately T-shaped geometries, and two diethyl ether solvated 4 coordinate O_4 coordination lithium centres with approximately tetrahedral geometry. There is a significant difference in the internal O-Li-O angles within the hexameric ring between these two types of lithium centres, with the 3 coordinate centres having internal angles in the range of 125.3(4)-129.2(4) °, at least 12 ° larger than the 4 coordinate centres with an internal angle of only 113.3(4) °. A similar variation within the previously reported Li_6O_6 hexameric prism core complexes is observed. However, even in the fully THF solvated lithium phenolate complex $[\{LiOPh\}_6(THF)_6]$ reported by Jackman,[222] the internal O-Li-O angles are larger than the internal angle of the 4 coordinate lithium centres in complex **28**, falling within the range 117(1)-119(1) °. The Li-O distances to the 3 coordinate centres in **28** are also shorter, in the range 1.872(7)-1.964(8) Å, than those to the 4 coordinate centres, which are in the range 1.920(8)-2.058(9) Å.

It is important to note that in the case of the observed complex $[\{Li_2(OODIPPSi)\}_2\{Li(OEt)\}_2(Et_2O)_2]$ **28** the only source of silicon grease was that used to seal the tap and stopper of the Schlenk flask used in the reaction – as no evidence of silicon grease was detected in the parent solvent diethyl ether, or as a contaminant of the starting ligand $ONDIPPH_2$ **5**. It is reasonable to assert then, that the source of the grease fragments must be related to an interaction with the dilithiated O/N complex. This result highlights the importance of the work undertaken in this thesis into expanding the understanding of how organolithium

compounds interact throughout the process of a reaction, or indeed in any situation where multiple anion types are present.

5.3.3. Silicon grease fragment incorporation

As already discussed in the complex $[\{Li_2(OODIPPSi)\}_2\{Li(OEt)\}_2(Et_2O)_2]$ **28**, in addition to solvent molecule attack, the lithiation reactions of the mixed O/N ligands presented in this thesis have shown reactivity towards silicon grease. Crystal structures of four unique complexes were obtained with O/N ligands that had been modified with either monomer or dimer units of silicon grease covalently incorporated into the framework of the mixed anion ligand within the complex. Structurally the incorporation of the grease fragment results in "insertion" into the N-Li bond.

It is unclear what the exact chemical process is that led to the fragmentation of the silicon grease in each case that it was observed crystallographically. In the complex $[\{Li_2(OODIPPSi)\}_2\{Li(OEt)\}_2(Et_2O)_2]$ **28** it is likely a result of an unexpected interaction of the grease polymer with the dilithiated complex that led to the fragmentation. However, in the cases presented in this Section, grease fragments were most likely introduced into the reaction mixtures with the solvent, though again the method of fragmentation remains unclear.

The first compound reported here was obtained from within a solvent ampoule. DME was dried over sodium, distilled, collected, and stored over a potassium mirror. After a period of weeks the potassium mirror had largely disappeared, and a small amount of colourless crystals had formed. Though very weak diffracting, a structure was eventually obtained of the dipotassium salt of the silicon grease fragment

$(O\text{-}Si(Me)_2\text{-}O\text{-}Si(Me)_2\text{-}O)^{-2-}$. The structure of the complex is shown in Figure 5-7 and Figure 5-8.

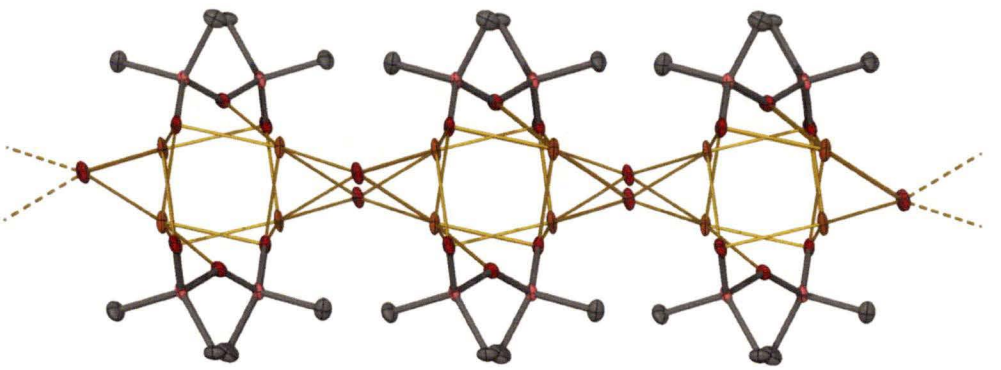

Figure 5-7: Side on view of the polymeric structure of $[\{[K_2(OSi(Me)_2O)_2]_2(H_2O)\}_\infty]$ with thermal ellipsoids drawn at the level of 50 % probability.

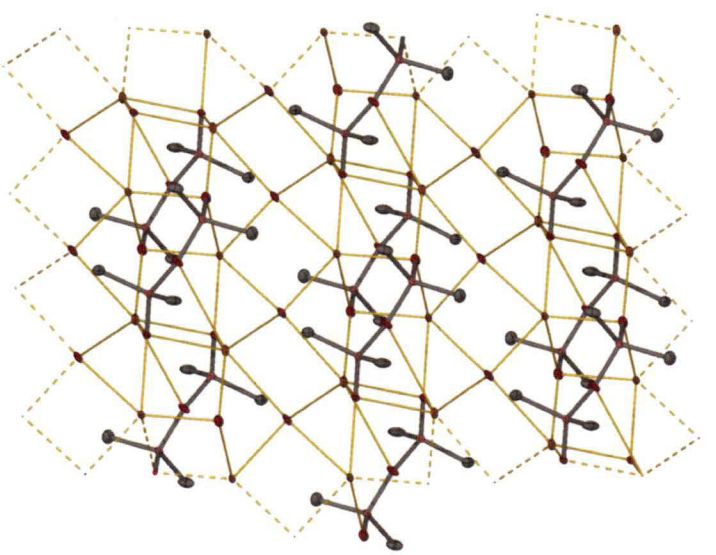

Figure 5-8: Top down view of the polymeric structure of $[\{[K_2(OSi(Me)_2O)_2]_2(H_2O)\}_\infty]$ with thermal ellipsoids drawn at the level of 50 % probability.

The DME from this ampoule was originally used to try to prepare a DME adduct of the dilithiated O/N complex, resulting in the two unexpected structures as shown in Scheme 5-9. Subsequent to this observation, the structures presented in Chapters 2 and 3 were prepared in the absence of grease.

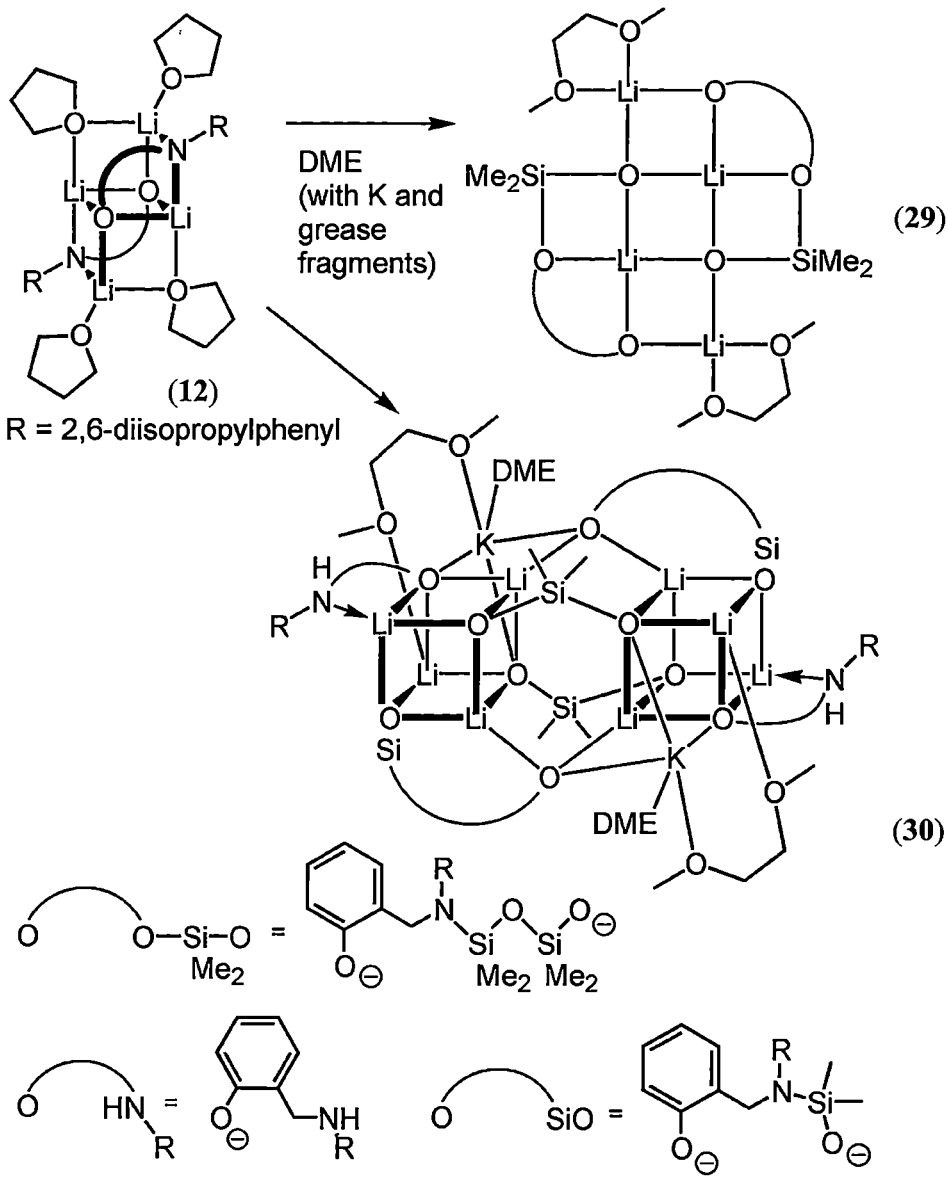

Scheme 5-9: Synthesis of complexes $[\{Li_2(OODIPPSi_2)\}_2(DME)_2]$ **29** and $[K_2\{Li_2(OODIPPSi)\}_2\{Li(ONDIPPH)\}_2\{LiOSi(Me)_2O\}_2(DME)_4]$ **30** from complex $[\{Li_2(ONDIPP)\}_2(THF)_4]$ **12**.

The complexes $[\{Li_2(OODIPPSi_2)\}_2(DME)_2]$ **29** and $[K_2\{Li_2(OODIPPSi)\}_2\{Li(ONDIPPH)\}_2\{LiOSi(Me)_2O\}_2(DME)_4]$ **30** both contain modified dilithiated ligands based on $ONDIPPH_2$ **5**; complex **29** contains a dilithiated ligand that has had a dimer of silicon grease incorporated into the N-Li bond, ($OODIPPSi_2$), and complex **30** contains a dilithiated ligand that has had a monomer of silicon grease incorporated into the N-Li bond, (OODIPPSi). In both

cases the silicon grease unit is covalently bound through the silicon to the nitrogen atom, forming a tertiary amine, and resulting in O/O dilithiated ligands. The core of the smaller complex $[\{Li_2(OODIPPSi_2)\}_2(DME)_2]$ **29** appears similar to some of the cores observed for the dilithiated complexes reported in Chapter 2 and Chapter 3, however in this case the central part of the core is no longer formed by the phenoxide anions, but rather the terminal siloxyl anions. As the dilithiated ligand no longer contains an amide anion, it would be reasonable to predict that the aggregated complex of the new dilithiated O/O ligand might be akin to $[\{Li_2(OODIPPSi)\}_2\{Li(OEt)\}_2(Et_2O)_2]$ **28**, that is forming a hexameric stacked aggregate. This is prevented however, by the inclusion of a dimer of silicon grease, which places the additional Lewis basic donating oxygen atom between the two anions for each dilithiated ligand. This effectively blocks one face of the initial Li_2O_2 ring formed, and restricts the aggregation number to two, producing the structure shown in Scheme 5-9.

The larger complex $[K_2\{Li_2(OODIPPSi)\}_2\{Li(ONDIPPH)\}_2\{LiOSi(Me)_2O\}_2(DME)_4]$ **30** incorporates the largest number of varying components observed in this work. Within it there are two types of lithiated ligand; both the dilithiated grease monomer inserted ligand, as well as a monolithiated unaltered ligand. Additionally there are two discrete dianionic grease fragments with the structure $(O\text{-}Si(Me)_2\text{-}O)^{2-}$ as well as two potassium atoms incorporated into the complex. The lithium containing part of the core is comprised from familiar aggregation modes for alkoxide anions with cubic stacking and Li_2SiO_3 rings. Each end of the core contains a Li_4O_4 cubic structure, with the middle section formed from four Li_2O_3Si hexameric rings, each linking to adjacent internal vertices of the cubic sections. The monolithiated ligands are incorporated in the same way as observed in the simple homoanionic complexes, in

an edge strapping way and act as intramolecular Lewis basic donors. Similarly the monomeric grease incorporated ligand spans two anion-anion bonds, equivalent to the distance of three rungs, as observed in $[\{Li_2(OODIPPSi)\}_2\{Li(OEt)\}_2(Et_2O)_2]$ **28**.

The fourth complex obtained incorporating a silicon grease fragment arose from an attempted preparation of the TMEDA solvated dilithiated complexes. In this case the solvent was again the source of the grease fragments, although how this arose and in what form the grease is within the solvent remains unclear. The complex was prepared via ligand substitution, in the same way as the DME solvated grease incorporated structures, as shown in Scheme 5-10.

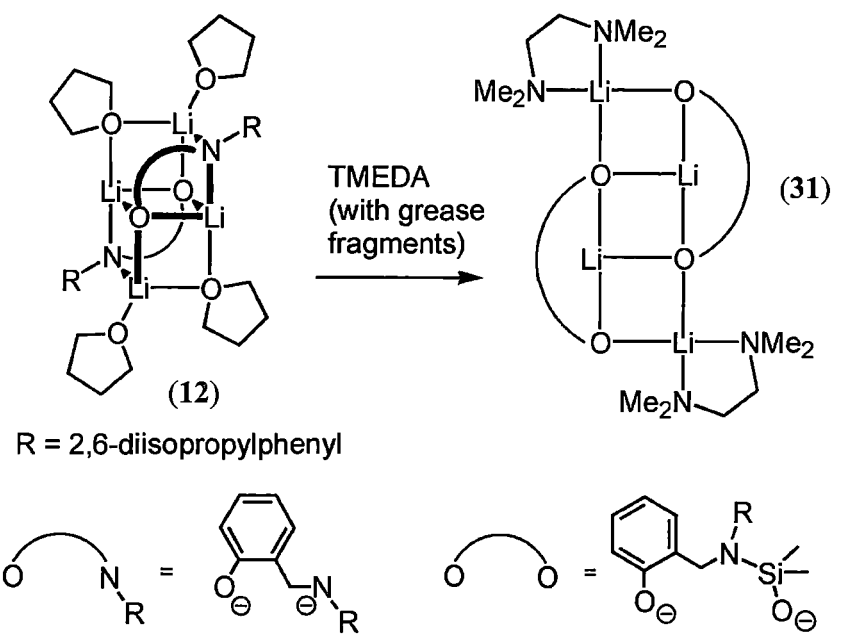

Scheme 5-10: Synthesis of complex $[\{Li_2(OODIPPSi)\}_2(TMEDA)_2]$ **31** from complex $[\{Li_2(ONDIPP)\}_2(THF)_4]$ **12**.

The TMEDA solvated complex is a C_2 symmetric dimer, incorporating a modified ligand containing a silicon grease monomer in the same way as $[\{Li_2(OODIPPSi)\}_2\{Li(OEt)\}_2(Et_2O)_2]$ **28** and $[K_2\{Li_2(OODIPPSi)\}_2\{Li(ONDIPPH)\}_2\{LiOSi(Me)_2O\}_2(DME)_4]$ **30**. Remarkably, the TMEDA solvated complex $[\{Li_2(OODIPPSi)\}_2(TMEDA)_2]$ **31** was isolated in good yield and was the only observed product from the reaction. The complex was

characterised by ^{1}H, ^{13}C, gCOSY, gHMQC and gHMBC NMR spectroscopy, X-ray crystal structure determination, and elemental analysis.

The Li_4O_4 core of the complex is arranged in a four-rung *syn*-ladder geometry. The bulk of the dilithiated molecules lie on the convex side of the complex with the TMEDA molecules surrounding each end of the ladder and leaving a relatively open concave side to the molecule, as seen in Figure 5-14.

The ^{1}H NMR spectrum of **31** shows multiple chemical environments for all of the aliphatic resonances within the dilithiated ligand, consistent with the observed *syn*-ladder structure, indicating that this complex is less fluxional on the NMR time scale than many of the other dilithiated complexes. There are two resonances of equal intensity visible for the methylsilyl protons, appearing at 0.01 ppm and 0.61 ppm, respectively. Each of the methyl groups from the isopropyl substituents appears as separate doublets centred on 0.57 ppm, 1.41 ppm, 1.47 ppm, and 1.58 ppm, respectively. The two methine protons appear as two separate heptets at 3.45 ppm and 3.85 ppm, respectively, with the methylene protons appearing as an AB spin system at 4.05 ppm and 5.28 ppm, respectively. All of the protons within the TMEDA molecules appear as a single broad resonance around 1.97 ppm. The aromatic region is not baseline resolved and appears as multiplets from 6.27 ppm to 7.22 ppm. The ^{13}C NMR shows a matching pattern of unique resonances; the two methylsilyl carbons are at 2.3 ppm and 2.5 ppm, respectively. The methyl carbons from the isopropyl groups only resolve to three resonances, appearing at 25.3 ppm and 25.6 ppm and 28.2 ppm, respectively, with the resonance at 25.6 ppm appearing at twice the height of the other two. The methylene carbon resonance appears at 48.8 ppm, with the TMEDA carbons showing minimal changes to their shifts compared to free TMEDA appearing at 45.8 ppm and 57.9 ppm, although the downfield resonance is broadened significantly. It is perhaps ironic that the lithium

complex best suited to undertake detailed NMR studies on for solution structure studies was prepared by accident, from a serendipitous silicon grease contaminated sample of dried TMEDA.

5.3.4. Molecular structures

Colourless crystals of $[\{Li_2(OODIPPSi_2)\}_2(DME)_2]$ **29** suitable for X-ray crystal structure determination were isolated from the reaction of $[\{Li_2(ONDIPP)\}_2(THF)_4]$ **12** with DME contaminated with silicon grease derived fragments. The crystals belong to the monoclinic space group *C*2/*c* (No. 15), $a = 23.425(16)$, $b = 9.92(3)$, $c = 29.191(15)$ Å, $\beta = 92.50(6)$ °, with 4 $Li_4O_2N_2$ molecules in the unit cell and the asymmetric unit consisting of ½ a molecule of $[\{Li_2(OODIPPSi_2)\}_2(DME)_2]$ **29** having C_2 crystallographic symmetry. The molecular structure of **29** is shown in Figure 5-9 and Figure 5-10.

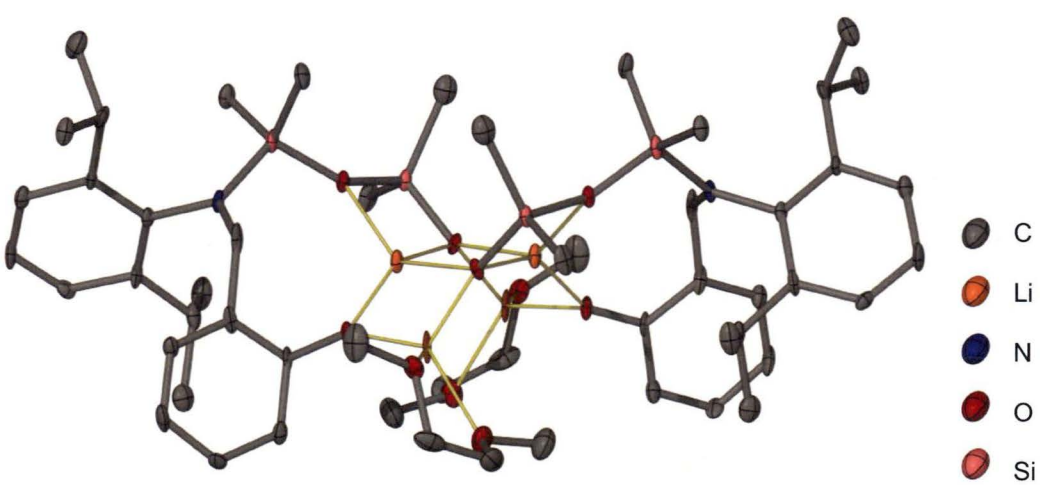

Figure 5-9: Molecular structure of $[\{Li_2(OODIPPSi_2)\}_2(DME)_2]$ **29** with thermal ellipsoids drawn at the level of 20 % probability. Hydrogen atoms removed for clarity.

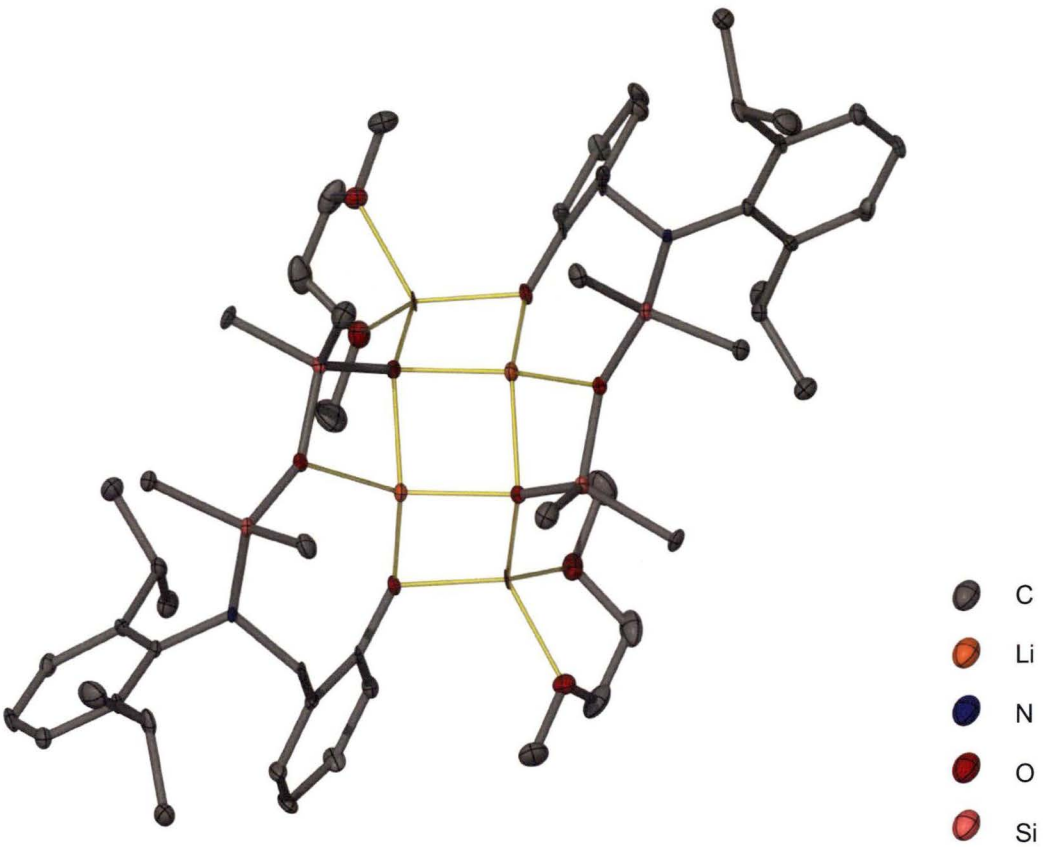

Figure 5-10: Front on view of the molecular structure of [{Li_2(OODIPPSi_2)}$_2$(DME)$_2$] **29** with thermal ellipsoids drawn at the level of 20 % probability. Hydrogen atoms removed for clarity.

The structure of [{Li_2(OODIPPSi_2)}$_2$(DME)$_2$] **29** is a *syn* four-rung ladder dimer formed from two modified dilithiated ligands. A silicon grease dimer (Si(Me)$_2$O)$_2$ has been covalently incorporated into the original ligand ONDIPPH$_2$ **5** at the nitrogen atom, forming a tertiary amine centre and extending the distance between the two anionic centres. The arrangement of the ladder is different to the dimeric complexes reported in Chapter 2 and Chapter 3, as the phenoxide anions form the outer most Li-O rungs, while the siloxane anions comprise the central two. In addition to the main Li_4O_4 four-rung ladder core, the second oxygen within each dimeric silicon grease fragment acts as an internal Lewis basic donor, forming two additional *syn* dispositioned LiO_2Si rings, which extend from the central Li_2O_2 ring, *anti* and orthogonally to the outer Li_2O_2 rings of the four-rung ladder core, as shown in Figure 5-9.

The *anti* arrangement of each adjacent rings surrounding the central Li_2O_2 ring allows the lithium centres within it to attain an approximately tetrahedral four coordinate geometry. The remaining two lithium centres are solvated by a chelating molecule of DME each, hence are also four coordinate with approximately tetrahedral geometry. The Li-O distances are all typical, falling within the range 1.83(2)-2.02(1) Å. The distances in the outer Li_2O_2 rings of 1.83(2)-1.86(1) Å (excluding the Li-O distance contained within the central Li_2O_2 ring) are shorter than those in the central Li_2O_2 ring, 1.94(1)-2.02(1) Å, due to di- and tri- bridging oxygen centres in each case, respectively.

Colourless crystals of $[K_2\{Li_2(OODIPPSi)\}_2\{Li(ONDIPPH)\}_2\{LiOSi(Me)_2O\}_2(DME)_4]$ **30** suitable for X-ray crystal structure determination were isolated from the reaction of $[\{Li_2(ONDIPP)\}_2(THF)_4]$ **12** with DME contaminated with silicon grease as well as potassium cation and anionic $(O\text{-}Si(Me)_2\text{-}O\text{-}Si(Me)_2\text{-}O)^{2-}$ fragments. The crystals belong to the triclinic space group $P\bar{1}$ (No. 2), $a = 15.167(10)$, $b = 15.799(5)$, $c = 15.84(2)$ Å, $\alpha = 109.72(5)$, $\beta = 92.95(8)$, $\gamma = 117.21(6)$ °, with 1 $Li_8K_2O_{10}$ core-containing molecule in the unit cell and the asymmetric unit consisting of ½ of a centrosymmetric molecule of **30** and a molecule of DME. The molecular structure of **30** is shown in Figure 5-11 and Figure 5-12.

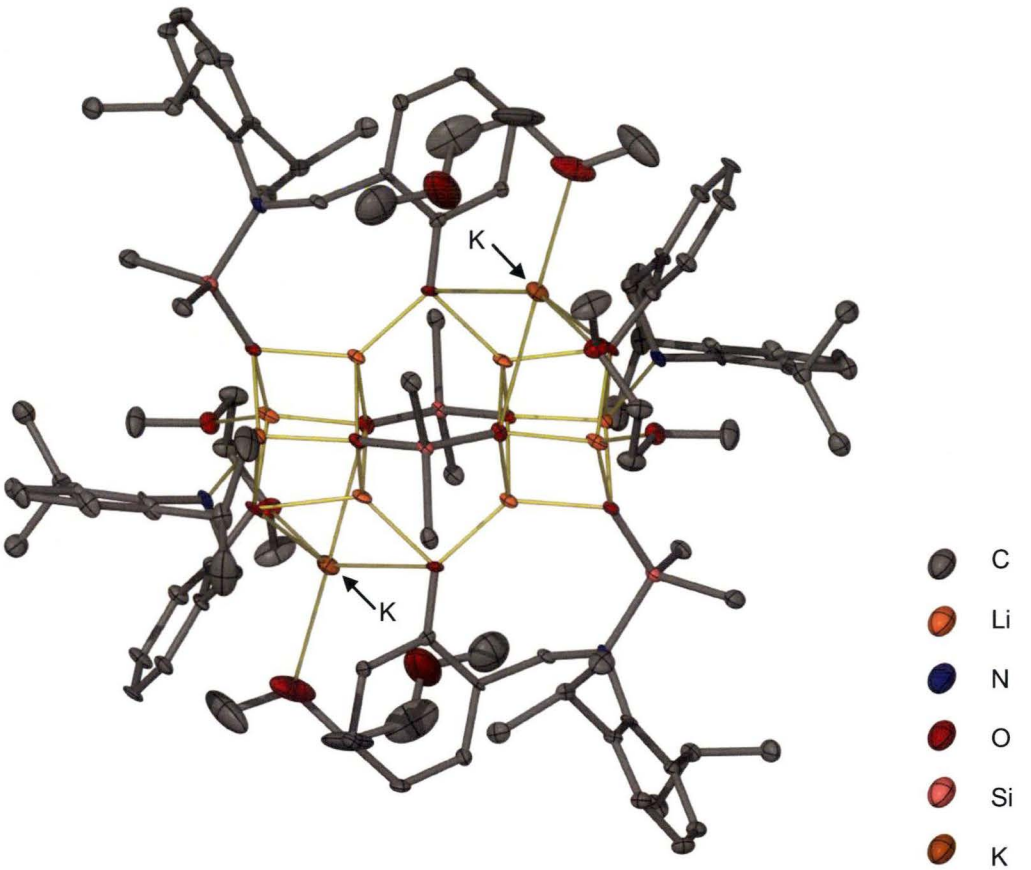

Figure 5-11: Side on view of the molecular structure of $[K_2\{Li_2(OODIPPSi)\}_2\{Li(ONDIPPH)\}_2\{LiOSi(Me)_2O\}_2(DME)_4]$ **30** with thermal ellipsoids drawn at the level of 20 % probability. Hydrogen atoms removed for clarity.

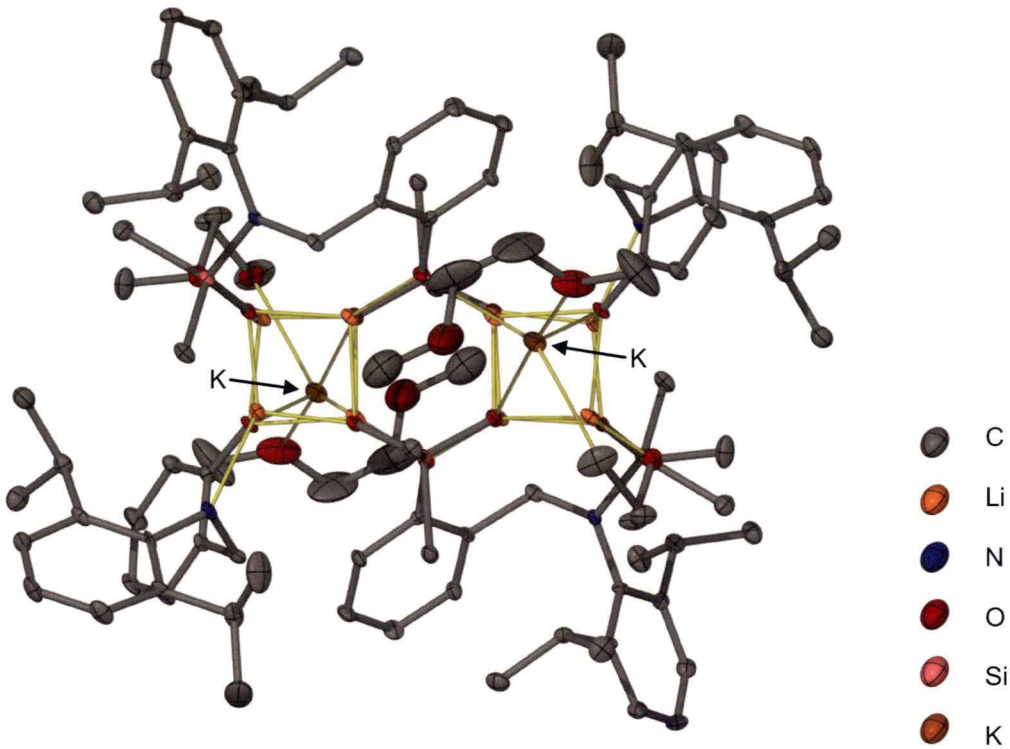

Figure 5-12: Top down view of the molecular structure of $[K_2\{Li_2(OODIPPSi)\}_2\{Li(ONDIPPH)\}_2\{LiOSi(Me)_2O\}_2(DME)_4]$ **30** with thermal ellipsoids drawn at the level of 20 % probability. Hydrogen atoms removed for clarity.

The complex $[K_2\{Li_2(OODIPPSi)\}_2\{Li(ONDIPPH)\}_2\{LiOSi(Me)_2O\}_2(DME)_4]$ **30** is a crystallographically centrosymmetric dimer. Each half of the dimer contains one $ONDIPPH_2$ **5** ligand that has been singly deprotonated, as well as a modified ligand, $OODIPPSiMe_2H_2$ which has contains the same covalently incorporated silicon grease monomer as observed in the complex $[\{Li_2(OODIPPSi)\}_2\{Li(OEt)\}_2(Et_2O)_2]$ **28**, and has been doubly deprotonated. Also incorporated into each portion of the dimer is a dianionic silicon grease fragment $(O\text{-}Si(Me)_2\text{-}O)^{2-}$ and a potassium cation. Each dimer is solvated by two DME molecules; one DME molecule that bridges to both a potassium cation and a lithium centre, the other DME molecule being bound through only one oxygen centre to the potassium cation, as shown in Figure 5-11. The complex has a 22 atom $Li_8K_2O_{10}Si_2$ core. The silicon atoms do not carry any charge,

but as they link the two oxygen anionic centres they form part of the core's aggregated geometry.

The core consists of two Li_4O_4 cubes spanned by four single atom links, which join the two cubes at adjacent vertices of their inner Li_2O_2 faces. Two of the links are the phenoxide anions from the dilithiated modified ligand $OODIPPSiMe_2H_2$ while the other two links are the silicon atoms in the isolated silicon grease fragments mentioned above. These links form four hexameric Li_3O_2Si rings, giving the structure a look somewhat akin to $[(n\text{-BuLi})(t\text{-BuOLi})]_4$, **III** described in Chapter 1 as a partially opened tri-cube stack. The potassium cations are located outside the aggregated lithium complex portion of the core, adjacent to each of the Li_4O_4 cubic sections. Their inclusion does not significantly alter the aggregated geometry of the lithium centres other than to lengthen the adjacent Li-O distances. The Li-O distances show large variation throughout the core falling in the range 1.880(8)-2.167(7) Å, the longest distance corresponding to the two five coordinate oxygen anionic centres, contained in the isolated silicon grease fragment adjacent to the potassium centre.

The monolithiated ligands $ONDIPPH_2$ **5** in complex **30** show the familiar cube edge spanning intramolecular Lewis basic solvation observed for all the monolithiated complexes discussed in Chapter 2. The N-Li distance is typical at 2.142(8) Å.

Colourless crystals of $[\{Li_2(OODIPPSi)\}_2(TMEDA)_2]$ **31** suitable for X-ray crystal structure determination were isolated from the reaction of $[\{Li_2(ONDIPP)\}_2(THF)_4]$ **12** with TMEDA contaminated with silicon grease. Two polymorphs of this compound were observed; the first belongs to the monoclinic space group $C2/c$ (No. 15), $a = 23.052(13)$, $b = 10.477(13)$, $c = 27.724(19)$ Å, $\beta = 113.53(6)$ °, with 4 $Li_4O_2N_2$ molecules in the unit cell and the asymmetric unit consisting of ½ of a centrosymmetric molecule of **31**. The second belongs to the

monoclinic space group $C2/c$ (No. 15), $a = 23.365(19)$, $b = 10.398(17)$, $c = 25.701(16)$ Å, $\beta = 102.02(9)$ °, with 4 molecules in the unit cell and the asymmetric unit consisting of ½ of a centrosymmetric molecule of **31**. The molecular structure of the first polymorph of **31** is shown in Figure 5-13 and Figure 5-14.

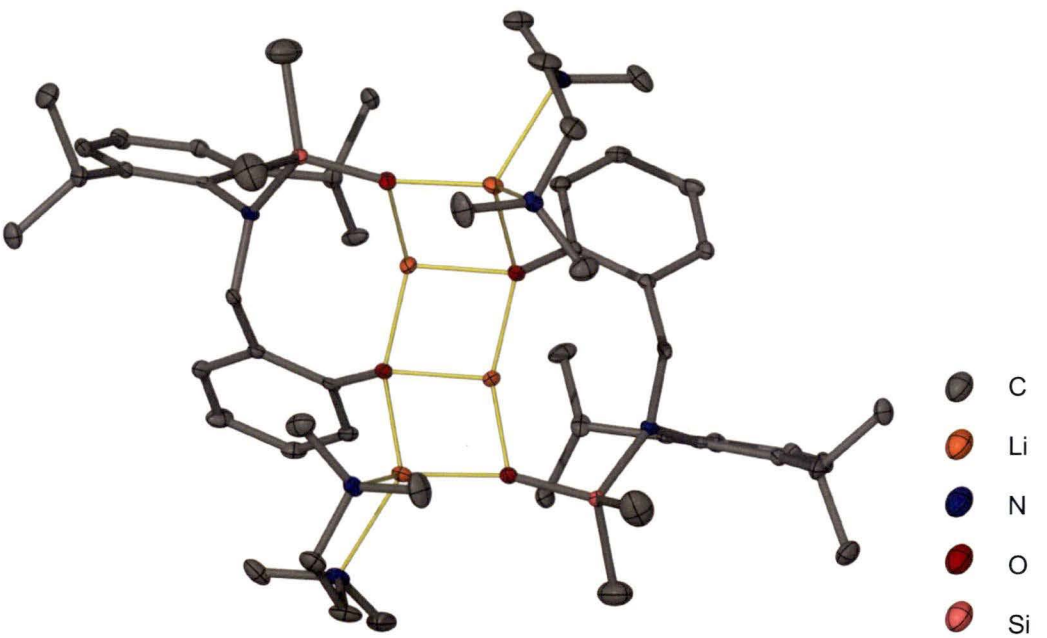

Figure 5-13: Front on view of the molecular structure of [{Li_2(OODIPPSi)}$_2$(TMEDA)$_2$] **31** with thermal ellipsoids drawn at the level of 20 % probability. Hydrogen atoms removed for clarity.

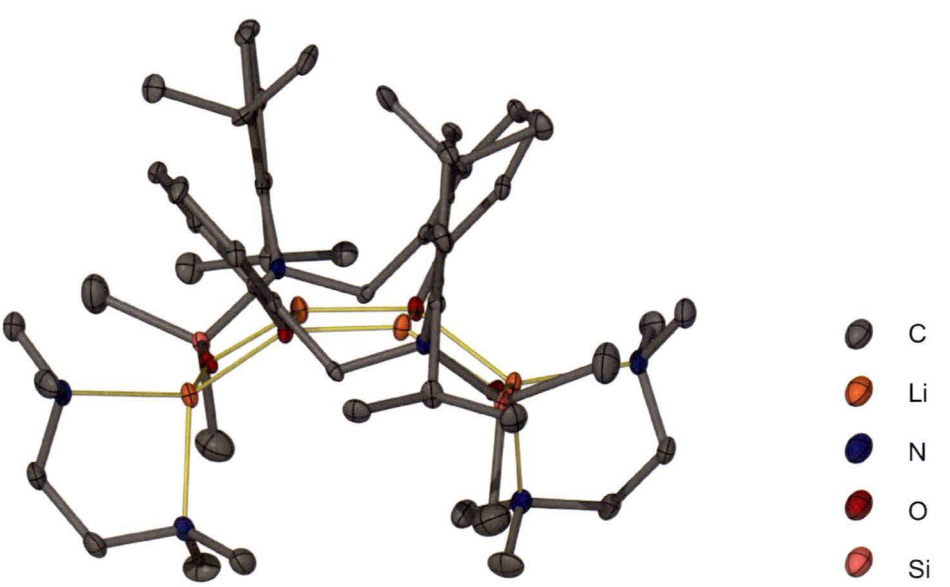

Figure 5-14: Side on view of the molecular structure of [{Li_2(OODIPPSi)}$_2$(TMEDA)$_2$] **31** with thermal ellipsoids drawn at the level of 20 % probability. Hydrogen atoms removed for clarity.

The structure of **31** is a C_2 symmetric four-rung ladder dimer. The familiar three-ring core consists of three Li_2O_2 rings in a *syn* arrangement as shown in Figure 5-14. The complex consists of the modified ligand $ONDIPPH_2$ **5** with a monomer of silicon grease covalently incorporated, as seen in the previous structure. The three rings within the ladder core of this complex are much closer to being planar than in other dimeric dilithiated complexes. This is likely due to the combination of the longer ligand backbone, as well as the chelating Lewis basic solvent and absence of a Lewis base bound to the internal lithium centres.

The two internal lithiums are not solvated and are consequently only three coordinate and have approximately T-shaped geometry. The lithium centres within the outer two rungs each have a chelating molecule of TMEDA, affording them four coordinate, (O2, N2) with a distorted tetrahedral coordination geometry. The Li-O distances mostly show minimal variation falling in the range 1.835(7)-1.906(6) Å, except for two that are 1.998(7) and 2.01(1) Å. These longer two interactions are on the ladder edge, adjacent to the TMEDA, which is known to weaken lithium aggregation interactions. In addition to this though, the oxygen centre in the two longer Li-O distances is three coordinate, while the other oxygen centre associated with the second Li-O interaction of the terminal lithium centre is only two coordinate, and remains a shorter distance.

5.4. Conclusion

With the inclusion of different molecular fragments into the lithium complexes, new core geometries are to be expected. The trimeric complex $[\{Li_2(ONtBu)\}_3Li(OEt)(Et_2O)_3]$ **27** is a remarkable serendipitous observation and an example of an unprecedented molecular architecture. The remainder of the

complexes presented in this chapter include lithiated O/N ligands which have undergone insertion of either the monomeric silicon grease fragment -$Si(Me)_2O$- or the dimeric silicon grease fragment -$Si(Me)_2OSi(Me)_2O$-, resulting in modified O/O dilithiated ligands. In the cases of the complexes $[\{Li_2(OODIPPSi)\}_2\{Li(OEt)\}_2(Et_2O)_2]$ **28** and $[K_2\{Li_2(OODIPPSi)\}_2\{Li(ONDIPPH)\}_2\{LiOSi(Me)_2O\}_2(DME)_4]$ **30** familiar stacked aggregation geometries are observed for the cores of the complexes, through inclusion of additional ethoxide fragments in the former case, and additional $(O\text{-}Si(Me)_2\text{-}O)^{2-}$ fragments in the latter case. In the cases of the complexes $[\{Li_2(OODIPPSi_2)\}_2(DME)_2]$ **29** and $[\{Li_2(OODIPPSi)\}_2(TMEDA)_2]$ **31** stacking to give cages has been prevented. This supports the importance of the design of this project in incorporating the anions being investigated within a single molecular ligand framework.

Furthermore, the observation of four unique complexes incorporating fragments of silicon grease, with evidence that in at least one case the grease was not present as fragments prior to exposure to the mixed anion lithium complex, adds further weight to the assertion that the observed synergistic properties of homometallic superbasic reagents is linked to the effect of generating hybrid anion aggregation modes through mixing of different anion aggregations.

5.5. Experimental

5.5.1. Synthesis of $[\{Li_2(ONtBu)\}_3Li(OEt)(Et_2O)_3]$ 27

To a solution of $ONtBuH_2$ **6** (350 mg, 2.0 mmol) in Et_2O (*ca.* 20 mL) *n*-BuLi (1.6 M in hexanes, 3.0 mL, 4.8 mmol) was added at 0 °C and allowed to warm to room

temperature with stirring in a grease free Schlenk flask. The solution was warmed to *ca.* 50 °C for approximately 2 minutes resulting in the formation of small crystals after standing for 1 hour. The solution was reduced in volume by half, and had approximately equal volume of 40-60 °C petroleum spirits added, resulting in a crop of large well-formed crystals. After several unsuccessful attempts to mount crystals for X-ray crystal structure determination the crystals were isolated, and recrystallised from THF resulting again in a crop of large well-formed crystals. It also proved to be unsuccessful to mount these crystals for X-ray crystal structure determination so the sample was taken to dryness yielding a chalky mix of partially desolvated colourless crystalline material. It was from this material that the crystal of the reported complex was isolated and elemental analysis performed. The yield of the material was not determined as a significant portion was lost in attempted X-ray crystal structure determination, and the residue was dissolved in benzene directly from the flask after isolation of the crystal of the reported complex.

^{1}H NMR (300 MHz, C_6D_6, 25 °C): δ = 0.80 (9H, s, CH_3), 3.53 (2H, br, CH_2), 6.69 (1H, pt, $^3J_{HH}$ = 7.2 Hz, Ar), 6.90 (1H, br, Ar), 7.03 (1H, d, $^3J_{HH}$ = 6.3 Hz, Ar), 7.25 (1H, bm, Ar).

^{13}C NMR (75 MHz, C_6D_6, 25 °C): δ = 28.7 (CH_3), 47.2 (CH_2), 51.3 ($C(CH_3)$), 114.6 (Ar), 121.0 (Ar), 129.5 (Ar), 131.2 (Ar), 166.5 (Ar).

Anal. Calculated: C, 71.34; H, 8.71; N, 7.56; ($C_{11}H_{16}LiNO$)

Found: C, 72.05; H, 8.78; N, 7.53

5.5.2. Synthesis of $[\{Li_2(OODIPPSi)\}_2\{Li(OEt)\}_2(Et_2O)_2]$ 28

To a solution of $ONDIPPH_2$ **5** (320 mg, 1.1 mmol) in Et_2O (*ca.* 10 mL) *n*-BuLi (1.6 M in hexanes, 1.5 mL, 2.4 mmol) was added and the solution heated to 50 °C and stirred for approximately half an hour resulting in a clear yellow solution. A portion was taken to dryness and showed no *N*-H stretch in the IR spectrum. The volume was reduced heavily to approximately 1 mL, resulting in rapid formation of a colourless crystalline material. X-ray crystal structure determination of one of these crystals yielded the reported ethoxide containing complex. The remainder of the crystals were redissolved in Et_2O before accidently being exposed to air. Consequently, no further characterisation was able to be performed on the bulk material.

5.5.3. Synthesis of $[\{Li_2(OODIPPSi_2)\}_2(DME)_2]$ 29 and $[K_2\{Li_2(OODIPPSi)\}_2\{Li(ONDIPPH)\}_2\{LiOSi(Me)_2O\}_2(DME)_4]$ 30

DME (*ca.* 40 mL containing a mixture of potassium-grease fragment complexes) was added to the complex $[\{Li_2(ONDIPP)\}_2(THF)_4]$ **12** (0.6 g, $6.8x10^{-1}$ mmol) resulting in a pale yellow solution. The solution was warmed to elicit dissolution of the complex resulting in a pale yellow solution with a small amount of fine solid material remaining. The solution was filtered and the volume reduced by approximately half, resulting after standing over several nights in a small crop of colourless crystals. X-ray crystal structure determination of two of these crystals yielded the reported complexes. ^1H NMR of the material indicated that the bulk of the crystalline product was the unsolvated monolithiated complex

[{Li(ONDIPPH)}$_4$] **9**, consequently no further characterisation was obtained for the grease incorporated complex.

5.5.4. Synthesis of [{Li$_2$(OODIPPSi)}$_2$(TMEDA)$_2$] 31

TMEDA (*ca.* 2 mL containing silicon grease fragments) was added to the complex [{Li$_2$(ONDIPP)}$_2$(THF)$_4$] **12** (20 mg, 2.3x10^{-2} mmol) in a Young's capped NMR tube and heated at 70 °C overnight resulting in a small number of thin colourless crystals growing approximately 1 cm above the solution. A portion of these crystals were washed into the solution and the solution was left to stand overnight at room temperature resulting in a good crop of well-formed colourless crystals.

^{1}H NMR (300 MHz, C_6D_6, 25 °C): δ = 0.01 (6H, s, Me_3Si), 0.57 (6H, d, $^3J_{HH}$ = 6.9 Hz, CH_3), 0.61 (6H, s, Me_3Si), 1.41 (6H, d, $^3J_{HH}$ = 6.9 Hz, CH_3), 1.47, (6H, d, $^3J_{HH}$ = 6.9 Hz, CH_3), 1.58 (6H, d, $^3J_{HH}$ = 6.9 Hz, CH_3), 1.97 (32H, br, CH_2 CH_3 TMEDA), 3.45 (6H, h, $^3J_{HH}$ = 7.2 Hz, C*H*(CH_3)), 3.85 (6H, h, $^3J_{HH}$ = 7.2 Hz, C*H*(CH_3)), 4.05 (6H, d, $^3J_{HH}$ = 12.9 Hz, CH_2), 5.28 (6H, d, $^3J_{HH}$ = 12.9 Hz, CH_2), 6.27-7.22 (14H, m, Ar).

^{13}C NMR (75 MHz, C_6D_6, 25 °C): δ = 2.3 (Me_3Si), 2.5 (Me_3Si), 23.2 (CH_3), 25.3 (CH_3), 25.6 (2xCH_3), 28.2 (*C*H(CH_3)), 29.3 (*C*H(CH_3)), 45.8 (CH_3 TMEDA), 48.8 (CH_2), 57.9 (CH_2 TMEDA), 115.4 (Ar), 119.9 (Ar), 123.7 (Ar), 124.6 (Ar), 125.5 (Ar), 128.6 (Ar), 129.6 (Ar), 132.4 (Ar), 144.0 (Ar), 147.8 (Ar), 149.2 (Ar), 164.2 (Ar).

Anal. Calculated: C, 66.78; H, 9.34; N, 8.65; ($C_{27}H_{45}Li_2N_3O_2Si$)

Found: C, 67.11; H, 9.33; N, 8.62

Chapter 6

Conclusion

6.1. Concluding remarks

This thesis describes studies into the synthesis, reactivity and solid state structures of organolithium complexes containing tethered mixed anionic centres within *ortho*-phenylene based ligand scaffolds. These complexes were designed and prepared to facilitate a systematic investigation into the effect that incorporation different preferred aggregation modes into a single molecular unit had on the aggregation of organolithium complexes. Each of the lithium complexes prepared within this thesis, with the exception of the proposed veratrole adducts $[\{Li_2(ONPh)\}_2(o\text{-}MeO(C_6H_4)OMe)_2]$ and $[\{Li_2(ONDIPP)\}_2(o\text{-}MeO(C_6H_4)OMe)_2]$, were characterised by X-ray crystal structure determination.

Chapter 2 detailed the synthesis of the mixed phenoxide/amide (O/N) anion ligands, which contribute to the lithiated complexes reported in Chapter 2, Chapter 3, and Chapter 5. The ligand scaffold was designed to allow for variability of bulk at the nitrogen anion centre, as well as providing a semi-rigid spacer between the two anion centres to prevent the prevalence of double butterfly aggregation of the lithium centres to make the findings more general. The ligands were prepared via an imine condensation of salicylaldehyde with either aniline, 2,6-diisopropylaniline or *t*-butyl amine yielding, respectively, ON=PhH **1**, ON=DIPPH **2**, and ON=*t*BuH **3**. These imines were subsequently reduced with sodium borohydride yielding the secondary amine mixed O/N ligands $ONPhH_2$ **4**, $ONDIPPH_2$ **5**, and $ONtBuH_2$ **6**, respectively. The ligands were also designed to promote simple and accessible synthesis. Of the

variations pursued, the ligands reported here were found to be the best candidates for this criterion. Other variations on the O/N ligands that were initially trialled included a methylated version starting with 2'-hydroxyacetophenone rather than salicylaldehyde. This would potentially allow direct metallation of the imine substrates with MeLi via a carbolithiation reaction. This would prevent problematic crystallisations of the complexes from a racemic reaction mixture that would occur as a result of the stereogenic centre created by 1,2-carbolithiation of the imines derived from salicylaldehyde. This modification to the structure would potentially have a dramatic affect on the way the dilithiated complexes interacted with chelating Lewis basic donors.

Chapter 2 also reported the *O*-monolithiated complexes and the THF, TMEDA and DME solvated dilithiated complexes of the *N*-phenyl and *N*-2,6-diisopropylphenyl substituted O/N ligands. It was observed that the monolithiated complexes exclusively adopt tetrameric aggregates with a cubic Li_4O_4 core. In the less bulky *N*-phenyl substituted monolithiated complex [{Li(ONPhH)}$_4$] **7** the core is sufficiently exposed to allow solvation with THF, forming the adduct [{Li(ONPhH)}$_4$(THF)$_3$] **8**, while the bulkier *N*-2,6-diisopropylphenyl substituted monolithiated complex remains unsolvated from a variety of solvents, as the complex [{Li(ONDIPPH)}$_4$] **9**. The dilithiated complexes were observed to preferentially adopt dimeric aggregated structures, with a $Li_4O_2N_2$ four-rung ladder core consisting of a central Li_2O_2 ring, and two Li_2ON rings extending off opposite edges of the central ring in an *anti* arrangement. The dilithiated O/N ligands were observed to be incorporated into the dimers preferentially in an edge-strapping arrangement and in these cases were exclusively observed to bridge a distance of three rungs. The bulk at the nitrogen centre of the dilithiated ligands affects these complexes by restricting the observed degree of solvation by Lewis basic interactions

from six in the complexes of the *N*-phenyl substituted ligand, to four for the complexes of the bulkier *N*-2,6-diisopropylphenyl substituted ligand. The dilithiated THF adducts $[\{Li_2(ONPh)\}_2(THF)_6]$ **11** and $[\{Li_2(ONDIPP)\}_2(THF)_4]$ **12** were prepared via lithiation with *n*-BuLi in THF, while alternate Lewis basic solvated complexes were prepared via simple solvent exchange reactions from the THF adducts. A tetrameric dilithiated complex $[\{Li_2(ONPh)\}_4(THF)_4]$ **13** was observed to form upon heating of **11** in benzene. This was the only tetrameric complex of a dilithiated ligand observed in this study; the core of the complex is comprised of a central Li_4O_4 cubic stack, akin to that observed for the monolithiated complexes, with four Li_2ON laddering rings extending from it. In a non-mechanistically implied manner, the four laddering rings appear in such a way as if the central part of the core was arranged with four monolithiated O/N ligand molecules arranged parallel to each other, as observed in complex $[\{Li(ON{=}DIPPH)\}_4]$ **10**, and have then been deprotonated to give the amide centres forming two pairs of laddering rings extending off alternate, opposite pairs of edges on opposite faces of the cubic core.

The binding of different chelating Lewis basic solvents was observed to have mixed effects on the dilithiated complexes. While the number of Lewis basic interactions in each dimeric $Li_4O_2N_2$ unit is maintained in all cases (six for the less bulky complexes, and four for the bulky complexes), DME forms complexes with both dilithiated ligands yielding $[\{[Li_2(ONPh)]_2(DME)_3\}_\infty]$ **16** and $[\{Li_2(ONDIPP)\}_2(DME)_2]$ **17**. For the dilithiated *N*-phenyl substituted ligand, an intermediate ligand exchange complex $[\{Li_2(ONPh)\}_2(DME)_2(THF)_2]$ **18** was also isolated on one occasion. In each DME solvated complex the initially observed $Li_4O_2N_2$ four-rung ladder core is maintained. In contrast, the bulkier chelating Lewis base TMEDA forms the complexes $[\{Li_2(ONPh)\}_2(TMEDA)_3]$ **14** and $[\{Li_2(ONDIPP)\}_2(TMEDA)_2]$ **15** and induces a change in the core of the dimeric

aggregate in both cases, producing a novel $Li_4O_2N_2$ 'grafted' four-rung ladder core for the less bulky ligand complex **14** and a four-rung ladder core of a different nature with chelated terminal lithium centres for the bulkier ligand complex **15**. While the 'grafted' core maintains the 'edge-strapping' arrangement of the dilithiated ligand, the core of the bulkier complex includes the dilithiated ligand in a 'face-bridging' arrangement.

Chapter 3 describes further dilithiated complexes of the O/N ligands closely related to those discussed in Chapter 2. These are the asymmetrical $MeOCH_2CH_2Ot$-Bu DME analogue solvated complexes $[\{Li_2(ONPh)\}_2(MeOCH_2CH_2Ot\text{-}Bu)_2(THF)_2]$ **19** and $[\{Li_2(ONDIPP)\}_2(MeOCH_2CH_2Ot\text{-}Bu)_2]$ **20**, as well as the 1,4-dioxane solvated complex of the bulkier *N*-2,6-diisopropylphenyl substituted ligand $[\{[Li_2(ONDIPP)]_2(1,4\text{-dioxane})(THF)\}_\infty]$ **21**. These three complexes were prepared via ligand exchange reactions from the THF adducts, and it was correctly predicted that each complex maintains the $Li_4O_2N_2$ four-rung ladder core of the precursor complexes. Complexes **19** and **20** containing the asymmetrically substituted dialkyl diether molecule $MeOCH_2CH_2Ot$-Bu maintain the chelation and arrangement of bridging Lewis base centres as observed for the analogous DME complexes **16** and **17**. The *t*-Bu substituent was observed to adopt opposite positions between the *N*-phenyl and *N*-2,6-diisopropylphenyl substituted complexes, with the bulky *t*-Bu group of the $MeOCH_2CH_2Ot$-Bu ligand orientated away from the centre of the core in the bulkier complex **20** and positioned towards the centre of the complex in the less bulky complex **19**. While the 1,4-dioxane complex containing those Lewis basic donor interactions at opposite ends of the molecule, forms a polymeric chain by interacting with adjacent $Li_4O_2N_2$ dimeric units. Presumably 1,4-dioxane cannot bridge/chelate in an analogous manner to DME leading to this structural change.

Chapter 3 also discusses the observed novel reactivity of the dimeric dilithiated complexes towards various ether type Lewis basic solvents. When reacted with the dilithiated complex [{Li_2(ONDIPP)}$_2$(THF)$_4$] **12** solvent attack resulting in fragmentation occurring with each of the solvents diethyl ether, DME, $MeOCH_2CH_2O$*t*-Bu, veratrole and 1,2,4-trimethoxy benzene. This reactivity is thought to be linked to the observed change in the CH_2 positioning within the dilithiated ligand due to the increased bulk of the *N*-2,6-diisopropylphenyl substituent. Where internal O-CH_2 protons (α- to the heteroatom) were available the fragmentation resulted in cleavage of an internal O-C bond. In the cases where no internal α-protons were available, the fragmentation resulted in a removal of the group attached to the external site of the ether group (*O*-demethylation). Both of these types of reactivity, when occurring in a chelating ligand substrate, were observed to show specificity related to the proximity of steric bulk within the substrate. The substituted DME analogue $MeOCH_2CH_2O$*t*-Bu gave exclusively vinyl methyl ether and *t*-BuOH upon workup, consistent with the orientation observed in the crystal structure. Reactivity was only observed with methoxy benzene substrates where a chelation interaction was possible. Less facile reactivity of the dilithiated complex [{Li_2(ONPh)}$_2$(THF)$_6$] **11** with veratrole was also observed, yielding the modified O/N ligand monolithiated complex [{Li(ON(Me)Ph)}$_4$] **22** which incorporates the methyl group lost from the veratrole as a new substituent on the nitrogen centre.

A theoretical investigation was also undertaken to explore the potential mechanism by which the solvent fragmentation occurs for DME based on the observed fragmentation products for $MeOCH_2CH_2O$*t*-Bu. The modelled reaction pathway proposes that a nitrogen centre in the $Li_4O_2N_2$ core abstracts one of the internal α-protons of the coordinated solvent molecule, resulting in the observed

fragmentation. Within the bounds of the model, this provides strong evidence that this pathway is energetically plausible.

The observation of the dilithiated O/N complexes displaying reactivity towards a variety of ether type Lewis basic solvents is highly significant. The formal Brønsted basicity of each of the anions in the dilithiated O/N complexes is far less than other chemical systems observed to display similar reactivity. It may be reasonably concluded that the driving force for this observed reactivity is linked to the mixing of anion types of the two organolithium centres. Further to this, the observation of regioselectivity in some of the reactions has allowed the rationalisation of this reactivity in terms of a hypothesised structure property relationship for the complexes. The proposed mechanism is supported by experimental evidence, as well the computational model.

Chapter 4 details the synthesis of mixed amido/alkyl (N/C) anion ligands and their resulting lithiated complexes. These ligands were designed around a similar *ortho*-xylene backbone to the O/N ligands, using an alkyl bromide as a precursor to react with various primary amines to produce the variability at the secondary amine functionality. The potential carbanion centre position was stabilised by the incorporation of a trimethylsilyl group attached to the benzylic carbon. The experimental conditions required for the conversion of the alkyl bromide to the desired secondary amine were established, yielding ligand scaffolds based on the *N*-phenyl substituted ligand $NCPhH_2$ **23**, and the *N*-2,6-diisopropylphenyl substituted ligand $NCDIPPH_2$ **24**.

An attempt was made to prepare and isolate analogous mono- and dilithiated complexes as described in Chapters 2 and 3, however only two lithium complexes were obtained and characterised; a monolithiated complex

[{[Li(NCPhH)]$_2$(NC=PhH)}$_2$] **25** incorporating an imine ligand by-product impurity, as well as a monolithiated complex of the partially fragmented ligand NCDIPPH$_2$ **24**, [(2,6-*i*Pr$_2$C$_6$H$_3$)N(SiMe$_3$)Li(THF)$_3$] **26**. These complexes do not contribute significantly to the overall structural discussion of lithium aggregates within this thesis.

Chapter 5 presents some serendipitous molecular fragment incorporated compounds characterised by X-ray crystal structure determination isolated during this work. These complexes feature unexpected molecular fragments incorporated into either the aggregated complex, into the O/N ligand scaffold itself, or in some cases both.

The reaction of the *N*-*t*-Bu substituted ligand ON*t*BuH$_2$ **6** with *n*-BuLi in diethyl ether yielded the complex [{Li$_2$(ON*t*Bu)}$_3$Li(OEt)(Et$_2$O)$_3$] **27**, which is a trimer based on the dilithiated ligand, incorporating an ethoxide fragment. This structure relates to the work presented in Chapter 3 involving solvent attack with a serendipitously incorporated a diethyl ether derived fragment presumed to have been produced via attack of the solvent. A related structure was obtained from the reaction of ONDIPPH$_2$ **5** with *n*-BuLi in diethyl ether. This observed complex [{Li$_2$(OODIPPSi)}$_2${Li(OEt)}$_2$(Et$_2$O)$_2$] **28** incorporates two ethoxide fragments in the aggregate, however the aggregate itself is based on the dimerisation of a modified O/O ligand OODIPPSiMe$_2$H$_2$ which incorporates a monomer of silicon grease, -Si(Me$_2$)O-, covalently bound to the nitrogen atom by insertion into the N-Li bond. This larger dilithiated ligand scaffold aggregates with the ethoxide to produce a hexameric prism, typical of lithium alkoxide and phenoxide complexes. Also observed to have incorporated various silicon grease fragments into the ligand scaffold and/or into the aggregated core were the complexes [{Li$_2$(OODIPPSi$_2$)}$_2$(DME)$_2$] **29**,

$[K_2\{Li_2(OODIPPSi)\}_2\{Li(ONDIPPH)\}_2\{LiOSi(Me)_2O\}_2(DME)_4]$ **30**, and $[\{Li_2(OODIPPSi)\}_2(TMEDA)_2]$ **31**.

It is important to note that the source of the silicon grease fragments appears to be a combination of contaminated solvent, in the case of complexes **29-31**, as well as direct attack of the grease by the dilithiated complex, in the case of **27**.

The complexes presented in Chapter 5, though serendipitous in their observation, help to emphasise the enhanced reactivity of the O/N mixed anion lithium aggregates prepared in this thesis and support the central hypothesis of a mixing of aggregation mode types of the organolithium components leading to unique structural features that is potentially linked to the properties of superbasic reagents.

This work has shown a variety of novel structures in the area of mixed anion lithium chemistry. By adopting a systematic approach to varying the Lewis basic solvation of these complexes some of the preferred trends in their aggregation have been established. In one particular case it has been possible to understand the structure property relationship within the complex providing a rationalisation of specific and unexpected reactivity observed towards chelating Lewis basic ether ligands. In the short term this work would benefit from some further NMR investigations, particularly into the solution behaviour of complexes $[\{Li_2(ONPh)\}_2(THF)_6]$ **11** and $[\{Li_2(ONDIPP)\}_2(THF)_4]$ **12** with variable temperature and NOESY experiments. Further experiments that would be of interest and relevance to the work presented in this thesis include the preparation and lithiation of O/N ligands with intermediate bulk to that of the phenyl substituted ligand ONPhH2 4 and the 2,6-diisopropylphenyl substituted ligand ONDIPPH2 5 such as a 2,4,6-trimethylphenyl substituted ligand. Such a ligand would further test the hypotheses generated from this work regarding retainment of the dimeric $Li_4O_2N_2$

four-rung ladder core and the behaviour towards Lewis basic solvents upon its dilithiation. In particular however, if the characteristics of the dilithiated complex remain similar to those observed in this thesis it would be of significant interest to examine the behaviour of the dilithiated complex containing intermediate bulk on the nitrogen anionic centre towards ether-type solvents as the limit of the driving force for this behaviour is not yet known. It would also be on interest to extend the investigation of the demethylation reaction observed for complex $[\{Li_2(ONDIPP)\}_2(THF)_4]$ **12** into examining its behaviour towards natural product substrates such as those mentioned in Section 3.1.

In a longer term continuation of the project, investigations might include pursuing carbolithiation reactions of methylated variants of the O/N imine ligands formed by starting with 2'-hydroxyacetophenone rather than salicylaldehyde as mentioned earlier in this chapter. Further to this, the intended investigation comprising Chapter 4 of this thesis offers a significant area for further work. Complexes containing mixed alkyl/amido anionic centres offer a closer approximation of the original superbases, and as they contain anions with higher formal Brønsted basicity it is reasonable to expect that further reactivity investigations would be able to be undertaken on a wider range of substrates to further expand the structure-property relationships observed within this thesis. It would also be of interest to investigate the behaviour of mixed anion lithium complexes containing anion types that share preferred aggregation modes, e.g. alkyls and alkoxides that stack.

Much remains to explore the full structural features of this overall class of mixed anion alkali metal complexes and develop an advanced understanding of their chemical behaviours to enable the rational and tailored design of novel reagents for chemical synthesis.

APPENDIX

Experimental Procedures

Supplementary electronic files are included on a CD-ROM attached with this thesis. Included are all crystallographic information files (cif) and XYZ data files associated with the structures reported in this thesis. Also included is a pdf with labelled ortep diagrams of the crystal structures reported in this thesis.

Unless noted otherwise, all manipulations of complexes were performed under an argon atmosphere (high purity) by using standard Schlenk techniques. Storage of complexes and preparation of samples for various analyses required the use of a dry, nitrogen atmosphere glove box. Solvents for the preparation of complexes were dried by passage through an Innovative Technologies solvent purification system and, where appropriate, stored over a sodium mirror. For the preparation of organic intermediates or ligands, solvents including methanol, ethanol, dichloromethane, toluene, hexanes and diethyl ether were used as received.

TMEDA and DME were dried over sodium using benzophenone as an indicator. DME was initially stored over a potassium mirror. Subsequent preparations were stored with no mirror. All other reagents were purchased from commercial sources and used as received.

NMR spectra were recorded in chloroform-d, DMSO-d6 or appropriately dried benzene-d6, THF-d8 and toluene-d8 and using a Varian Mercury Plus 300 operating at 299.91 MHz (^{1}H) and 75.42 MHz (^{13}C) or Varian Inova 400 operating at 399.66 MHz (^{1}H) and 100.50 MHz (^{13}C). The ^{1}H NMR spectra were referenced to the residual ^{1}H resonances of chloroform-d (7.26 ppm), DMSO-d6 (2.50 ppm),

benzene-d6 (7.15 ppm), toluene-d8 (2.09 ppm), and THF-d8 (1.73 or 3.75 ppm), and ^{13}C NMR were referenced to the 13C resonances of $CDCl_3$ (77.2 ppm), C_6D_6 (128.4 ppm), THF-d8 (67.6 or 25.4 ppm) and toluene-d8 (20.4 ppm).

IR spectra were recorded using a HITACHI 270-30 infrared spectrometer as Nujol mulls using KBr plates.

Elemental analysis, variable temperature NMR studies, GC-MS, and HRMS were performed at the Central Science Laboratory, University of Tasmania. Elemental analysis was conducted by Dr Thomas Rodemann using a ThermoFinnigan Flash EA 1112 Elemental Analyser. Variable temperature NMR studies were performed by Dr James Horne using a Varian Inova 400 NMR spectrometer. GC-MS was conducted by A/Prof. Noel Davies using a Varian 1200 triple quadrupole bench top GC-MS. HRMS was conducted by Mr Marshall Hughes using a Kratos Concept High-Resolution Mass Spectrometer with a GC inlet.

X-seed[223] and POV-Ray for Windows[224] were used for the molecular structure diagrams shown in this thesis. Stacked NMR spectra shown in this thesis were processed using MestReNova v6.0.1-5391 Mestrelab Research S.L.

Theoretical calculations were performed using Gaussian03[141] and Gaussian 09[142] on the National Computational Infrastructure (NCI) supercomputer cluster Vayu in Canberra.

Diffraction data collected at the University of Tasmania at -80 °C was obtained with an Enraf Nonius Turbo CAD4 with Mo Kα radiation (0.71073 Å) on crystals mounted on glass fibres within a preset 2θ limit of 50 ° using conventional scans. Computation for data collection, absorption correction, cell refinement, data

reduction, structure solution and refinement was carried out using CAD4 Express,[225] WinGX,[226] XCAD4[227] and PsiScans[228] program systems.

Diffraction data collected at Monash University -150 °C was obtained with a Bruker X8 Apex II CCD with Mo Kα radiation (0.71073 Å) on crystals mounted on glass fibres within a preset 2θ limit of 55 ° using psi and omega scans. Computation for data collection, absorption correction, cell refinement, data reduction, structure solution and refinement was carried out using the Bruker Apex II program suite.[229]

Data collected at the Australian Synchrotron used the MX1 or MX2 beamlines at -173 °C on crystals mounted on Hampton Scientific cryoloops (wavelength 0.70-0.74 Å) with single axis rotation scans to maximum resolution possible using the fixed detector. Computation for data collection used Blu-Ice software[230] and data was reduced using XDS.[231]

The structures were solved by direct methods with SHELXS-97, refined using full-matrix least-squares routines against F^2 with SHELXL-97,[232] and visualised using X-SEED.[223] All non-hydrogen atoms were refined anisotropically. All hydrogen atoms were placed in calculated positions and refined using a riding model with fixed C–H distances of 0.95 (sp^2-CH), 0.99 (sp^3-CH, CH_2), 0.98 Å (CH_3). The thermal parameters of all hydrogen atoms were estimated as $U_{iso}(H) = 1.2U_{eq}(C)$ except for CH_3 where $U_{iso}(H) = 1.5U_{eq}(C)$.

Variations to the above summarised methodologies are given the *refine_special_details* field of the cifs, available as an electronic resource in the enclosed CD. Refer to the fully labelled ortep representations of the crystal structures given on the CD for aid in interpreting metric parameters of the crystal structures, which appear in the cifs.

REFERENCES

[1] V. H. Gessner, C. Daeschlein, C. Ströhmann, *Chem. Eur. J.* **2009**, *15*, 3320.

[2] K. Gregory, P. v. R. Schleyer, R. Snaith, *Adv. Inorg. Chem.* **1991**, *37*, 47.

[3] R. E. Mulvey, *Chem. Soc. Rev.* **1991**, *20*, 167.

[4] E. Frankland, *Justus Liebigs Ann. Chem.* **1849**, 171.

[5] W. Schlenk, J. Appenrodt, A. Michael, A. Thal, *Ber. Dtsch. Chem. Ges.* **1914**, *47*, 473.

[6] D. Seyferth, *Organometallics* **2006**, *25*, 2.

[7] D. Seyferth, *Organometallics* **2009**, *28*, 2.

[8] M. J. Harvey, *Alkali Metals: Organometallic Chemistry. Encyclopedia of Inorganic Chemistry*, **2006**.

[9] P. Schorigin, *Ber. Dtsch. Chem. Ges.* **1908**, *41*, 2723.

[10] J. C. Stowell, *Carbanions In Organic Synthesis*, **1979**.

[11] E. Weiss, *Angew. Chem., Int. Ed. Engl.* **1993**, *32*, 1501.

[12] S. Harder, M. Lutz, *Organometallics* **1994**, *13*, 5173.

[13] V. H. Gessner, C. Strohmann, *J. Am. Chem. Soc.* **2008**, *130*, 14412.

[14] B. Walfort, L. Lameyer, W. Weiss, R. Herbst-Irmer, R. Bertermann, J. Rocha, D. Stalke, *Chem.--Eur. J.* **2001**, *7*, 1417.

[15] E. Juaristi, M. Hernández-Rodríguez, H. López-Ruiz, J. Aviña, O. Muñoz-Muñiz, M. Hayakawa, D. Seebach, *Helv. Chim. Acta* **2002**, *85*, 1999.

[16] M. Jones, *Organic Chemistry*, **2000**.

[17] A. E. H. Wheatley, *Eur. J. Inorg. Chem.* **2003**, 3291.

[18] D. Seebach, *Angew. Chem., Int. Ed. Engl.* **1988**, *27*, 1624.

[19] C. D. Broaddus, *J. Org. Chem.* **1970**, *35*, 10.

[20] H. Dietrich, *Acta Crystallogr.* **1963**, *16*, 681.

[21] A. Abou, F. Foubelo, M. Yus, *Tetrahedron* **2007**, *63*, 6625.

[22] C. Melero, A. Guijarro, V. Baumann, A. J. Perez-Jimenez, M. Yus, *Eur. J. Org. Chem.* **2007**, 5514.

[23] S. Rummel, S. M. Yunusov, E. S. Kalyuzhnaya, V. B. Shur, *J. Organomet. Chem.* **2009**, *694*, 1467.

[24] M. Schlosser, *Angew. Chem., Int. Ed.* **2005**, *44*, 376.

[25] N. S. Simpkins, *Pure Appl. Chem.* **1996**, *68*, 691.

[26] B. J. Bunn, P. J. Cox, N. S. Simpkins, *Tetrahedron* **1993**, *49*, 207.

[27] R. S. Ward, *Chemical Society Reviews* **1990**, *19*, 1.

[28] C. M. Cain, R. P. C. Cousins, G. Coumbarides, N. S. Simpkins, *Tetrahedron* **1990**, *46*, 523.

[29] P. J. Cox, A. Persad, N. S. Simpkins, *Synlett* **1992**, 194.

[30] P. J. Cox, N. S. Simpkins, *Tetrahedron: Asymmetry* **1991**, *2*, 1.

[31] T. Honda, N. Kimura, M. Tsubuki, *Tetrahedron: Asymmetry* **1993**, *4*, 21.

[32] T. Honda, N. Kimura, M. Tsubuki, *Tetrahedron: Asymmetry* **1993**, *4*, 1475.

[33] K. Aoki, H. Noguchi, K. Tomioka, K. Koga, *Tetrahedron Lett.* **1993**, *34*, 5105.

[34] K. Koga, *Pure Appl. Chem.* **1994**, *66*, 1487.

[35] Y. Fort, P. Gros, A. L. Rodriguez, *Tetrahedron: Asymmetry* **2001**, *12*, 2631.

[36] P. Gros, Y. Fort, *Eur. J. Org. Chem.* **2002**, 3375.

[37] P. Gros, S. Choppin, J. Mathieu, Y. Fort, *J. Org. Chem.* **2002**, *67*, 234.

[38] P. Gros, S. Choppin, Y. Fort, *J. Org. Chem.* **2003**, *68*, 2243.

[39] P. C. Gros, Y. Fort, *Eur. J. Org. Chem.* **2009**, 4199.

[40] M. Schlosser, F. Mongin, *Chem. Soc. Rev.* **2007**, *36*, 1161.

[41] W. N. Setzer, P. v. R. Schleyer, *Adv. Organomet. Chem.* **1985**, *24*, 353.

[42] D. R. Armstrong, D. Barr, R. Snaith, W. Clegg, R. E. Mulvey, K. Wade, D. Reed *J. Chem. Soc., Dalton Trans.* **1987**, 1071.

[43] M. Motevalli, D. Shah, A. C. Sullivan, *J. Chem. Soc., Dalton Trans.* **1993**, 2849.

[44] K. B. Aubrecht, B. L. Lucht, D. B. Collum, *Organometallics* **1999**, *18*, 2981.

[45] J. Allan, F., R. Nassar, E. Specht, A. Beatty, N. Calin, W. Henderson Kenneth, *J. Am. Chem. Soc.* **2004**, *126*, 484.

[46] H. Koester, D. Thoennes, E. Weiss, *J. Organomet. Chem.* **1978**, *160*, 1.

[47] M. F. Lappert, L. M. Engelhardt, C. L. Raston, A. H. White, *J. Chem. Soc., Chem. Commun.* **1982**, 1323.

[48] J. L. Gay-Lussac, L. J. Thenard, *Ann. Physik.* **1806**, *32*, 43.

[49] A. W. Titherley, *J. Chem. Soc., Trans.* **1894**, *65*, 504.

[50] N. D. R. Barnett, R. E. Mulvey, W. Clegg, P. A. O'Neil, *J. Am. Chem. Soc.* **1991**, *113*, 8187.

[51] M. F. Lappert, A. R. Sanger, R. C. Srivastava, P. P. Power, *Metal and Metalloid Amides: Synthesis, Structure, and Physical and Chemical Properties*, **1980**.

[52] W. Clegg, S. T. Liddle, R. E. Mulvey, A. Robertson, *Chem. Commun.* **1999**, 511.

[53] G. R. Kowach, C. J. Warren, R. C. Haushalter, F. J. DiSalvo, *Inorg. Chem.* **1998**, *37*, 156.

[54] A. R. Kennedy, R. E. Mulvey, A. Robertson, *Chem. Commun.* **1998**, 89.

[55] W. Clegg, K. W. Henderson, L. Horsburgh, F. M. Mackenzie, R. E. Mulvey, *Chem. Eur. J.* **1998**, *4*, 53.

[56] D. R. Armstrong, D. Barr, W. Clegg, R. E. Mulvey, D. Reed, R. Snaith, K. Wade, *J. Chem. Soc., Chem. Commun.* **1986**, 869.

[57] D. R. Armstrong, D. Barr, W. Clegg, S. M. Hodgson, R. E. Mulvey, D. Reed, R. Snaith, D. S. Wright, *J. Am. Chem. Soc.* **1989**, *111*, 4719.

[58] G. Boche, I. Langlotz, M. Marsch, K. Harms, N. E. S. Nudelman, *Angew. Chem.* **1992**, *104*, 1239.

[59] A. D. Bond, *Chem. Eur. J.* **2004**, *10*, 1885.

[60] A. D. Bond, *Coord. Chem. Rev.* **2005**, *249*, 2035.

[61] C. A. Brown, *J. Chem. Soc., Chem. Commun.* **1975**, 222.

[62] D. Bauer, A. Caillet, *Analusis* **1975**, *3*, 440.

[63] P. Caubère, *Chem. Rev.* **1993**, *93*, 2317.

[64] G. Wittig, R. Ludwig, R. Polster, *Chem. Ber.* **1955**, *88*, 294.

[65] R. E. Mulvey, *Chem. Soc. Rev.* **1998**, *27*, 339.

[66] A. A. Morton, G. H. Patterson, J. J. Donovan, E. L. Little, *J. Am. Chem. Soc.* **1946**, *68*, 93.

[67] A. A. Morton, M. E. T. Holden, *J. Am. Chem. Soc.* **1947**, *69*, 1675.

[68] L. Lochmann, *J. Organomet. Chem.* **1989**, *364*, 281.

[69] L. Lochmann, D. Lím, *J. Organomet. Chem.* **1971**, *28*, 153.

[70] L. Lochmann, J. Trekoval, *J. Organomet. Chem.* **1987**, *326*, 1.

[71] L. Lochmann, J. Trekoval, *J. Organomet. Chem.* **1979**, *179*, 123.

[72] L. Lochmann, J. Pospisil, J. Vodnansky, J. Trekoval, D. Lim, *Collect. Czech. Chem. Commun.* **1965**, *30*, 2187.

[73] V. Halaska, L. Lochmann, *Collect. Czech. Chem. Commun.* **1973**, *38*, 1780.

[74] M. Marsch, L. Lochmann, G. Boche, K. Harms, *Angew. Chem., Int. Ed. Engl.* **1990**, *29*, 309.

[75] R. P. Davies, P. R. Raithby, R. Snaith, *Angew. Chem., Int. Ed. Engl.* **1997**, *36*, 1215.

[76] D. Barr, W. Clegg, R. E. Mulvey, R. Snaith, *J. Chem. Soc., Chem. Commun.* **1989**, 57.

[77] S. Harder, A. Streitwieser, *Angew. Chem., Int. Ed. Engl.* **1993**, *32*, 1066.

[78] T. Kremer, S. Harder, M. Junge, P. v. R. Schleyer, *Organometallics* **1996**, *15*, 585.

[79] F. M. Mackenzie, R. E. Mulvey, W. Clegg, L. Horsburgh, *J. Am. Chem. Soc.* **1996**, *118*, 4721.

[80] M. Uchiyama, M. Koike, M. Kameda, Y. Kondo, T. Sakamoto, *J. Am. Chem. Soc.* **1996**, *118*, 8733.

[81] M. Uchiyama, M. Kameda, O. Mishima, N. Yokoyama, M. Koike, Y. Kondo, T. Sakamoto, *J. Am. Chem. Soc.* **1998**, *120*, 4934.

[82] Y. Kondo, M. Shilai, M. Uchiyama, T. Sakamoto, *J. Am. Chem. Soc.* **1999**, *121*, 3539.

[83] M. Uchiyama, T. Miyoshi, Y. Kajihara, T. Sakamoto, Y. Otani, T. Ohwada, Y. Kondo, *J. Am. Chem. Soc.* **2002**, *124*, 8514.

[84] M. Uchiyama, Y. Kobayashi, T. Furuyama, S. Nakamura, Y. Kajihara, T. Miyoshi, T. Sakamoto, Y. Kondo, K. Morokuma, *J. Am. Chem. Soc.* **2008**, *130*, 472.

[85] P. C. Andrikopoulos, D. R. Armstrong, D. V. Graham, E. Hevia, A. R. Kennedy, R. E. Mulvey, C. T. O'Hara, C. Talmard, *Angew. Chem. Int. Ed.* **2005**, *44*, 3459.

[86] E. Hevia, G. W. Honeyman, A. R. Kennedy, R. E. Mulvey, D. C. Sherrington, *Angew. Chem. Int. Ed.* **2005**, *44*, 68.

[87] H. R. L. Barley, W. Clegg, S. H. Dale, E. Hevia, G. W. Honeyman, A. R. Kennedy, R. E. Mulvey, *Angew. Chem. Int. Ed.* **2005**, *44*, 6018.

[88] G. Bentabed-Ababsa, S. Cheikh Sid Ely, S. Hesse, E. Nassar, F. Chevallier, T. T. Nguyen, A. Derdour, F. Mongin, *J. Org. Chem.* **2010**, *75*, 839.

[89] K. Snegaroff, F. Lassagne, G. Bentabed-Ababsa, E. Nassar, S. C. S. Ely, H. Stephanie, E. Perspicace, A. Derdour, F. Mongin, *Org. Biomol. Chem.* **2009**, *7*, 4782.

[90] T. T. Nguyen, F. Chevallier, V. Jouikov, F. Mongin, *Tetrahedron Lett.* **2009**, *50*, 6787.

[91] W. Clegg, S. H. Dale, A. M. Drummond, E. Hevia, G. W. Honeyman, R. E. Mulvey, *J. Am. Chem. Soc.* **2006**, *128*, 7434.

[92] R. E. Mulvey, *Organometallics* **2006**, *25*, 1060.

[93] R. E. Mulvey, *Acc. Chem. Res.* **2009**, *42*, 743.

[94] M. Schlosser, *Mod. Synth. Methods* **1992**, *6*, 227.

[95] C. Schade, P. V. R. Schleyer, *Adv. Organomet. Chem.* **1987**, *27*, 169.

[96] W. Bauer, L. Lochmann, *J. Amer. Chem. Soc.* **1992**, *114*, 7482.

[97] P. C. Andrews, P. J. Duggan, G. D. Fallon, T. D. McCarthy, A. C. Peatt, *J. Chem. Soc., Dalton Trans.* **2000**, 1937.

[98] J. L. Rutherford, D. B. Collum, *J. Am. Chem. Soc.* **1999**, *121*, 10198.

[99] J. G. Donkervoort, J. L. Vicario, E. Rijnberg, J. T. B. H. Jastrzebski, H. Kooijman, A. L. Spek, G. van Koten, *J. Organomet. Chem.* **1998**, *550*, 463.

[100] P. G. Williard, M. J. Hintze, *J. Am. Chem. Soc.* **1987**, *109*, 5539.

[101] H. Chen, R. A. Bartlett, H. V. R. Dias, M. M. Olmstead, P. P. Power, *Inorg. Chem.* **1991**, *30*, 2487.

[102] D. S. C. Black, N. E. Rothnie, *Aust. J. Chem.* **1983**, *36*, 1149.

[103] W. T. Gao, Z. Zheng, *Molecules* **2003**, *8*, 788.

[104] B. De Clercq, F. Verpoort, *J. Mol. Catal. A: Chem.* **2002**, *180*, 67.

[105] H. Keypour, S. Salehzadeh, R. V. Parish, *Molecules* **2002**, *7*, 140.

[106] J. Beretka, B. O. West, M. J. O'Connor, *Aust. J. Chem.* **1964**, *17*, 192.

[107] C. Cimarelli, G. Palmieri, M. Camalli, *Tetrahedron* **1997**, *53*, 6893.

[108] A. Filarowski, A. Koll, T. Glowiak, *Monatsh. Chem.* **1999**, *130*, 1097.

[109] F. Arod, M. Gardon, P. Pattison, G. Chapuis, *Acta Crystallogr., Sect. C: Cryst. Struct. Commun.* **2005**, *C61*, o317.

[110] Y. Qu, L.-J. Tian, J. Dong, *Acta Crystallogr., Sect. E: Struct. Rep. Online* **2007**, *E63*, o4832.

[111] F. Arod, P. Pattison, K. J. Schenk, G. Chapuis, *Cryst. Growth Des.* **2007**, *7*, 1679.

[112] O. Graalmann, U. Klingebiel, W. Clegg, M. Haase, G. M. Sheldrick, *Angew. Chem. Int. Ed.* **1984**, *23*, 891.

[113] J. Strauch, T. H. Warren, G. Erker, R. Fröhlich, P. Saarenketo, *Inorg. Chim. Acta* **2000**, *300*, 810.

[114] M. Rajeswaran, W. J. Begley, L. P. Olson, S. Huo, *Polyhedron* **2007**, *26*, 3653.

[115] J. T. B. H. Jastrzebski, G. v. Koten, M. J. N. Christophersen, C. H. Stam, *J. Organomet. Chem.* **1985**, *292*, 319.

[116] E. M. Arnett, M. A. Nichols, A. T. McPhail, *J. Am. Chem. Soc.* **1990**, *112*, 7059.

[117] M. A. Nichols, A. T. McPhail, E. M. Arnett, *J. Am. Chem. Soc.* **1991**, *113*, 6222.

[118] M. Brehon, E. K. Cope, F. S. Mair, P. Nolan, J. E. O'Brien, R. G. Pritchard, D. J. Wilcock, *J. Chem. Soc., Dalton Trans.* **1997**, 3421.

[119] D. R. Armstrong, J. E. Davies, R. P. Davies, P. R. Raithby, R. Snaith, A. E. H. Wheatley, *New J. Chem.* **1999**, *23*, 35.

[120] W. Clegg, S. T. Liddle, R. Snaith, A. E. H. Wheatley, *New J. Chem.* **1998**, *22*, 1323.

[121] W. Clegg, R. E. Mulvey, R. Snaith, G. E. Toogood, K. Wade, *J. Chem. Soc., Chem. Commun.* **1986**, 1740.

[122] N. D. R. Barnett, R. E. Mulvey, W. Clegg, P. A. O'Neil, *Polyhedron* **1992**, *11*, 2809.

[123] G. G. Briand, T. Chivers, M. Krahn, M. Parvez, *Inorg. Chem.* **2002**, *41*, 6808.

[124] N. Kuhn, U. Abram, C. Maichle-Mössmer, J. Wiethoff, *Z. Anorg. Allg. Chem.* **1997**, *623*, 1121.

[125] A. Armstrong, T. Chivers, M. Krahn, M. Parvez, G. Schatte, *Chem. Commun.* **2002**, 2332.

[126] W. Clegg, S. T. Liddle, R. E. Mulvey, A. Robertson, *Chem. Commun.* **2000**, 223.

[127] M. G. Gardiner, C. L. Raston, *Inorg. Chem.* **1996**, *35*, 4162.

[128] S. De Angelis, E. Solari, E. Gallo, C. Floriani, A. Chiesi-Villa, C. Rizzoli, *Inorg. Chem.* **1992**, *31*, 2520.

[129] F. E. Hahn, M. Keck, K. N. Raymond, *Inorg. Chem.* **1995**, *34*, 1402.

[130] G. Becker, K. Hubler, M. Niemeyer, N. Seidler, B. Thinus, *Z. Anorg. Allg. Chem.* **1996**, *622*, 197.

[131] J. Durkin, D. E. Hibbs, P. B. Hitchcock, M. B. Hursthouse, C. Jones, J. Jones, K. M. A. Malik, J. F. Nixon, G. Parry, *J. Chem. Soc., Dalton Trans.* **1996**, 3277.

[132] S. R. Boss, R. Haigh, D. J. Linton, A. E. H. Wheatley, *J. Chem. Soc., Dalton Trans.* **2002**, 3129.

[133] E. G. Lewars, *Computational Chemistry*, Kluwer Academic Publishers, **2003**.

[134] M. G. Gardiner, C. L. Raston, *Inorg. Chem.* **1995**, *34*, 4206.

[135] M. G. Gardiner, C. L. Raston, *Inorg. Chem.* **1996**, *35*, 4047.

[136] A. Abbotto, A. Streitwieser, P. v. R. Schleyer, *J. Am. Chem. Soc.* **1997**, *119*, 11255.

[137] A. Hildebrand, P. Löennecke, L. Silaghi-Dumitrescu, I. Silaghi-Dumitrescu, E. Hey-Hawkins, *Dalton Trans.* **2006**, 967.

[138] C. Strohmann, V. H. Gessner, *Angew. Chem. Int. Ed.* **2007**, *46*, 4566.

[139] Y. Kondo, J. V. Morey, J. C. Morgan, H. Naka, D. Nobuto, P. R. Raithby, M. Uchiyama, A. E. H. Wheatley, *J. Am. Chem. Soc.* **2007**, *129*, 12734.

[140] H. Naka, J. V. Morey, J. Haywood, D. J. Eisler, M. McPartlin, F. Garcia, H. Kudo, Y. Kondo, M. Uchiyama, A. E. H. Wheatley, *J. Am. Chem. Soc.* **2008**, *130*, 16193.

[141] M. J. Frisch, G. W. Trucks, H. B. Schlegel, G. E. Scuseria, M. A. Robb, J. R. Cheeseman, J. Montgomery, J. A., T. Vreven, K. N. Kudin, J. C. Burant, J. M. Millam, S. S. Iyengar, J. Tomasi, V. Barone, B. Mennucci, M. Cossi, G. Scalmani, N. Rega, G. A. Petersson, H. Nakatsuji, M. Hada, M. Ehara, K. Toyota, R. Fukuda, J. Hasegawa, M. Ishida, T. Nakajima, Y. Honda, O. Kitao, H. Nakai, M. Klene, X. Li, J. E. Knox, H. P. Hratchian, J. B. Cross, V. Bakken, C. Adamo, J. Jaramillo, R. Gomperts, R. E. Stratmann, O. Yazyev, A. J. Austin, R. Cammi, C. Pomelli, J. W. Ochterski, P. Y. Ayala, K. Morokuma, G. A. Voth, P. Salvador, J. J. Dannenberg, V. G. Zakrzewski,

S. Dapprich, A. D. Daniels, M. C. Strain, O. Farkas, D. K. Malick, A. D. Rabuck, K. Raghavachari, J. B. Foresman, J. V. Ortiz, Q. Cui, A. G. Baboul, S. Clifford, J. Cioslowski, B. B. Stefanov, G. Liu, A. Liashenko, P. Piskorz, I. Komaromi, R. L. Martin, D. J. Fox, T. Keith, M. A. Al-Laham, C. Y. Peng, A. Nanayakkara, M. Challacombe, P. M. W. Gill, B. Johnson, W. Chen, M. W. Wong, C. Gonzalez, J. A. Pople, Revision E.01 ed., Gaussian, Inc, Wallingford CT, **2004**.

[142] M. J. Frisch, G. W. Trucks, H. B. Schlegel, G. E. Scuseria, M. A. Robb, J. R. Cheeseman, G. Scalmani, V. Barone, B. Mennucci, G. A. Petersson, H. Nakatsuji, M. Caricato, X. Li, H. P. Hratchian, J. Izmaylov, J. Blonio, G. Zheng, J. L. Sonnenberg, M. Hada, M. Ehara, K. Toyota, R. Fukuda, J. Hasegawa, M. Ishida, T. Nakajima, Y. Honda, O. Kitao, H. Nakai, T. Vreven, J. Montgomery, J. A., J. E. Peralta, F. Ogliaro, M. Bearpark, J. J. Heyd, E. Brothers, K. N. Kudin, V. N. Staroverov, R. Kobayashi, J. Normand, K. Raghavachari, A. Rendell, J. C. Burant, S. S. Iyengar, J. Tomasi, M. Cossi, N. Rega, J. M. Millam, M. Klene, J. E. Enox, J. B. Cross, V. Bakken, C. Adamo, J. Jaramillo, R. Gomperts, R. E. Stratmann, O. Yazyev, A. J. Austin, R. Cammi, C. Pomelli, J. W. Ochterski, R. L. Martin, J. J. Dannenberg, V. G. Zakrzewski, G. A. Voth, P. Salvador, J. J. Dannenberg, S. Dapprich, A. D. Daniels, O. Farkas, J. B. Foresman, J. V. Ortiz, J. Cioslowski, D. J. Fox, Revision A.02 ed., Gaussian, Inc., Wallingford CT, **2009**.

[143] C. T. Lee, W. T. Yang, R. G. Parr, *Phys. Rev. B* **1988**, 785.

[144] A. D. Becke, *J. Chem. Phys.* **1993**, *98*, 5648.

[145] R. Ditchfield, W. J. Hehre, J. A. Pople, *J. Chem. Phys.* **1971**, *54*, 724.

[146] P. C. Hariharan, J. A. Pople, *Theor. Chim. Acta* **1973**, *28*, 213.

[147] A. Schepartz, R. Breslow, *J. Am. Chem. Soc.* **1987**, *109*, 1814.

[148] P. Maroni, L. Cazaux, P. Tisnes, M. Zambeti, *Bull. Soc. Chim. Fr.* **1980**, 179.

[149] S. A. Weissman, D. Zewge, *Tetrahedron* **2005**, *61*, 7833.

[150] B. C. Ranu, S. Bhar, *Org. Prep. Proced. Int.* **1996**, *28*, 371.

[151] A. Maercker, *Angew. Chem.* **1987**, *99*, 1002.

[152] M. V. Bhatt, S. U. Kulkarni, *Synthesis* **1983**, 249.

[153] R. L. Burwell, Jr., *Chem. Rev.* **1954**, *54*, 615.

[154] A. Wacek, I. Morghen, *Ber. Dtsch. Chem. Ges. B* **1937**, *70B*, 183.

[155] A. Wacek, E. David, *Ber. Dtsch. Chem. Ges. B* **1937**, *70B*, 190.

[156] A. L. Kranzfelder, J. J. Verbanc, F. J. Sowa, *J. Am. Chem. Soc.* **1937**, *59*, 1488.

[157] P. A. Sartoretto, F. J. Sowa, *J. Am. Chem. Soc.* **1937**, *59*, 603.

[158] B. Loubinoux, G. Coudert, G. Guillaumet, *Synthesis* **1980**, 638.

[159] R. Ahmad, J. M. Saá, M. P. Cava, *J. Org. Chem.* **1977**, *42*, 1228.

[160] M. G. Banwell, B. L. Flynn, S. G. Stewart, *J. Org. Chem.* **1998**, *63*, 9139.

[161] G. B. Deacon, P. C. Junk, G. J. Moxey, *Z. Anorg. Allg. Chem.* **2008**, *634*, 2789.

[162] J. E. Cosgriff, G. B. Deacon, G. D. Fallon, B. M. Gatehouse, H. Schumann, R. Weimann, *Chem. Ber.* **1996**, *129*, 953.

[163] G. B. Deacon, A. J. Koplick, T. D. Tuong, *Aust. J. Chem.* **1984**, *37*, 517.

[164] J. Hitzbleck, A. Y. O'Brien, C. M. Forsyth, G. B. Deacon, K. Ruhlandt-Senge, *Chem. Eur. J.* **2004**, *10*, 3315.

[165] D. J. Duncalf, P. B. Hitchcock, G. A. Lawless, *Chem. Commun.* **1996**, 269.

[166] S. T. Liddle, P. L. Arnold, *Dalton Trans.* **2007**, 3305.

[167] Y. K. Gun'ko, P. B. Hitchcock, M. F. Lappert, *J. Organomet. Chem.* **1995**, *499*, 213.

[168] H. H. Karsch, *Chem. Ber.* **1996**, *129*, 483.

[169] F. H. Köhler, N. Hertkorn, J. Blümel, *Chem. Ber.* **1987**, *120*, 2081.

[170] A. Maercker, W. Demuth, *Angew. Chem.* **1973**, *85*, 90.

[171] C. Strohmann, V. H. Gessner, *Angew. Chem. Int. Ed.* **2007**, *46*, 8281.

[172] X. Tian, R. Fröehlich, T. Pape, N. W. Mitzel, *Organometallics* **2005**, *24*, 5294.

[173] S. C. Honeycutt, *J. Organomet. Chem.* **1971**, *29*, 1.

[174] R. B. Bates, L. M. Kroposki, D. E. Potter, *J. Org. Chem.* **1972**, *37*, 560.

[175] A. Maercker, W. Theysohn, *Justus Liebigs Ann. Chem.* **1971**, *747*, 70.

[176] E. Bartmann, *Journal of Organometallic Chemistry* **1985**, *284*, 149.

[177] J. Corset, M. Castella-Ventura, F. Froment, T. Strzaiko, L. Wartski, *J. Raman Spectrosc.* **2002**, *33*, 652.

[178] S. Fantasia, J. M. Welch, A. Togni, *J. Org. Chem.* **2010**, *75*, 1779.

[179] K. Raghavachari, J. S. Binkley, R. Seeger, J. A. Pople, *J. Chem. Phys.* **1980**, *72*, 650.

[180] T. Clark, J. Chandrasekhar, G. W. Spitznagel, P. v. R. Schleyer, *J. Comp. Chem.* **1983**, *4*.

[181] M. J. Frisch, J. A. Pople, J. S. Binkley, *J. Chem. Phys.* **1984**, *80*, 3265.

[182] T. Ribelin, C. E. Katz, D. G. English, S. Smith, A. K. Manukyan, V. W. Day, B. Neuenswander, J. L. Poutsma, J. Aubé, *Angew. Chem. Int. Ed.* **2008**, *47*, 6233.

[183] R. T. Hobgood, G. S. Reddy, J. H. Goldstein, *J. Phys. Chem.* **1963**, *67*, 110.

[184] D. M. Wetzel, J. I. Brauman, *J. Am. Chem. Soc.* **1988**, *110*, 8333.

[185] R. Damrauer, S. R. Kass, C. H. DePuy, *Organometallics* **1988**, *7*, 637.

[186] E. A. Brinkman, S. Berger, J. I. Brauman, *J. Am. Chem. Soc.* **1994**, *116*, 8304.

[187] E. S. Petrov, M. I. Terekhova, A. I. Shatenshtein, B. A. Trofimov, R. G. Mirskov, M. G. Voronkov, *Dokl. Akad. Nauk SSSR* **1973**, *211*, 1393.

[188] E. S. Petrov, M. I. Terekhova, A. I. Shatenshtein, *Zh. Obshch. Khim.* **1974**, *44*, 1118.

[189] A. Streitwieser, L. Xie, P. Wang, S. M. Bachrach, *J. Org. Chem.* **1993**, *58*, 1778.

[190] A. Krief, *Tetrahedron* **1980**, *36*, 2531.

[191] B. D. Lenihan, H. Shechter, *J. Org. Chem.* **1998**, *63*, 2072.

[192] A. J. Blake, P. Mountford, G. I. Nikonov, *Acta Crystallogr., Sect. C: Cryst. Struct. Commun.* **1996**, *C52*, 1911.

[193] D. K. Kennepohl, S. Brooker, G. M. Sheldrick, H. W. Roesky, *Chem. Ber.* **1991**, *124*, 2223.

[194] I. Haiduc, *Organometallics* **2004**, *23*, 3.

[195] S. Caddick, F. G. N. Cloke, P. B. Hitchcock, A. K. d. K. Lewis, *Angew. Chem. Int. Ed.* **2004**, *43*, 5824.

[196] H. Braband, U. Abram, *Organometallics* **2005**, *24*, 3362.

[197] H. H. Karsch, G. Ferazin, H. Kooijman, O. Steigelmann, A. Schier, P. Bissinger, W. Hiller, *J. Organomet. Chem.* **1994**, *482*, 151.

[198] S. Harvey, M. F. Lappert, C. L. Raston, B. W. Skelton, G. Srivastava, A. H. White, *J. Chem. Soc., Chem. Commun.* **1988**, 1216.

[199] R. A. Jones, S. U. Koschmieder, J. L. Atwood, S. G. Bott, *J. Chem. Soc., Chem. Commun.* **1992**, 726.

[200] E. Iravani, D. Dashti-Mommertz, B. Neumüeller, *Z. Anorg. Allg. Chem.* **2003**, *629*, 1136.

[201] X. Zhou, W. Ma, Z. Huang, R. Cai, X. You, X. Huang, *J. Organomet. Chem.* **1997**, *545-546*, 309.

[202] X. Zhou, Z. Huang, R. Cai, L. Zhang, L. Zhang, X. Huang, *Organometallics* **1999**, *18*, 4128.

[203] X. Zhou, Z. Huang, R. Cai, L. Zhang, Y. Liu, C. Duan, *Synth. React. Inorg. Met.-Org. Chem.* **2000**, *30*, 649.

[204] A. R. Cowley, A. J. Downs, H.-J. Himmel, S. Marchant, S. Parsons, J. A. Yeoman, *Dalton Trans.* **2005**, 1591.

[205] M. Veith, P. König, A. Rammo, V. Huch, *Angew. Chem., Int. Ed.* **2005**, *44*, 5968.

[206] F. García, D. J. Linton, M. M. Partlin, A. Rothenberger, A. E. H. Wheatley, D. S. Wright, *J. Chem. Soc., Dalton Trans.* **2002**, 481.

[207] W. Uhl, M. R. Halvagar, *Angew. Chem., Int. Ed.* **2008**, *47*, 1955.

[208] R. Ahlrichs, A. Eichhöfer, D. Fenske, O. Hampe, M. M. Kappes, P. Nava, J. Olkowska-Oetzel, *Angew. Chem., Int. Ed.* **2004**, *43*, 3823.

[209] J. Olkowska-Oetzel, D. Fenske, P. Scheer, A. Eichhöfer, *Z. Anorg. Allg. Chem.* **2003**, *629*, 415.

[210] J.-X. Chen, Q.-F. Xu, Y. Zhang, Z.-N. Chen, J.-P. Lang, *J. Organomet. Chem.* **2004**, *689*, 1071.

[211] D. T. T. Tran, L. M. C. Beltran, C. M. Kowalchuk, N. R. Trefiak, N. J. Taylor, J. F. Corrigan, *Inorg. Chem.* **2002**, *41*, 5693.

[212] A. Eichhöfer, D. Fenske, *J. Chem. Soc., Dalton Trans.* **2000**, 941.

[213] A. Eichhöfer, D. Fenske, J. Olkowska-Oetzel, *Eur. J. Inorg. Chem.* **2007**, 74.

[214] T. A. Bazhenova, R. M. Lobkovskaya, R. P. Shibaeva, A. E. Shilov, A. K. Shilova, *J. Organomet. Chem.* **1987**, *330*, 9.

[215] B. Goldfuss, P. von Ragué Schleyer, F. Hampel, *J. Am. Chem. Soc.* **1996**, *118*, 12183.

[216] F. Diedrich, U. Klingebiel, F. Dall'Antonia, C. Lehmann, M. Noltemeyer, T. R. Schneider, *Organometallics* **2000**, *19*, 5376.

[217] B.-H. Huang, B.-T. Ko, T.Athar, C.-C. Lin, *Inorg. Chem.* **2006**, *45*, 7348.

[218] M. A. Nichols, C. M. Leposa, A. D. Hunter, M. Zeller, *J. Chem. Cryst.* **2007**, *37*, 825.

[219] X. Tian, M. Woski, C. Lustig, T. Pape, R. Fröhlich, D. L. Van, K. Bergander, N. W. Mitzel, *Organometallics* **2005**, *24*, 82.

[220] T. Maetzke, C. P. Hidber, D. Seebach, *J. Am. Chem. Soc.* **1990**, *112*, 8248.

[221] B.-T. Ko, C.-C. Lin, *J. Am. Chem. Soc.* **2001**, *123*, 7973.

[222] L. M. Jackman, D. Çizmeciyan, P. G. Williard, M. A. Nichols, *J. Am. Chem. Soc.* **1993**, *115*, 6262.

[223] L. J. Barbour, *J. Supramol. Chem.* **2001**, *1*, 189.

[224] C. Cason, T. Froehlich, N. Kopp, R. Parker, 3.5 ed., **2002**.

[225] *CAD4 Express Software*, Enraf-Nonius, Delft, The Netherlands, **1994**.

[226] L. J. Farrugia, *J. Appl. Crystallogr.* **1999**, *32*, 837.

[227] K. Harms, S. Wocadlo, *XCAD4, CAD4 Data Reduction*, University of Marburg, **1995**.

[228] A. C. T. North, D. C. Phillips, F. S. Mathews, *Acta. Crystallogr. Sect A* **1968**, *24*, 351.

[229] *Apex II version 2.1*, Bruker AXS Ltd:, Madison, Wisconsin.

[230] T. M. McPhillips, S. E. McPhillips, H. J. Chiu, A. E. Cohen, A. M. Deacon, P. J. Ellis, E. Garman, A. Gonzalez, N. K. Sauter, R. P. Phizackerley, S. M. Soltis, P. Kuhn, *J. Synchrotron Radiat.* **2002**, *9*, 401.

[231] W. Kabsch, *J. Appl. Crystallogr.* **1988**, *21*, 916.

[232] G. M. Sheldrick, *SHELX97, Programs for Crystal Structure Analysis*, Universität Göttingen **1998**.